NOVEL CATIONIC POLYMERS FOR USE AT BIOLOGICAL INTERFACES

KAREN ANGELA FRENCH

Doctor of Philosophy

THE UNIVERSITY OF ASTON IN BIRMINGHAM

April 1996

THE UNIVERSITY OF ASTON IN BIRMINGHAM

NOVEL CATIONIC POLYMERS FOR USE AT BIOLOGICAL INTERFACES

KAREN ANGELA FRENCH

Submitted for the Degree
of Doctor of Philosophy

April 1996

SUMMARY

One of the main problems with the use of synthetic polymers as biomaterials is the invasion of micro-organisms causing infection. A study of the properties of polymeric antibacterial agents, in particular polyhexamethylene biguanide, has revealed that the essential components for the design of a novel polymeric antibacterial are a balance between hydrophilicity and hydrophobicity coupled with sites of cationicity. The effect of cation incorporation on the physical properties of hydrogels has been investigated. Hydrogel systems copolymerised with either N-vinyl imidazole or dimethylaminoethyl methacrylate have been characterised in terms of their water binding, mechanical and surface properties. It has been concluded that the incorporation of these monomers does not adversely affect the properties of such hydrogels and that these materials are potential candidates for further development for use in biomedical applications.

It has been reported that hydrogels with ionic character may increase the deposition of biological material onto the hydrogel surface when it is in contact with body fluids. An investigation into the deposition characteristics of hydrogels containing the potentially cationic monomers has been carried out, using specific protein adsorption and *in vitro* spoilation techniques. The results suggest that at low levels of cationicity, the deposition of positively charged proteins is reduced without adversely affecting the uptake of the other proteins. The gross deposition characteristics were found to be comparable to some commercially available contact lens materials.

A preliminary investigation into the development of novel antibacterial polymers has been completed and some novel methods of bacterial inhibition discussed. These methods include development of an hydrogel whose potential application is as a catheter coating.

Keywords: **hydrogel, cations, antibacterial activity, deposition characteristics, N-vinyl imidazole, dimethylaminoethyl methacrylate**

"A scientist once trained a flea to jump whenever he rang a bell. Using a microscope, the scientist then anaesthetised one of the flea's legs and rang the bell again. The flea still jumped. He anaesthetised another leg and rang the bell once more. The flea still jumped. The scientist anaesthetised more and more legs, each time ringing the bell, and each time observing that the flea jumped. Finally, the flea had only one free leg remaining. When the scientist anaesthetised this last leg and rang the bell, he found to his astonishment that the flea no longer moved. The scientist solemnly declared his conclusion, based on irrefutable evidence - ***fleas hear through their legs!****"*

Quotation taken from 'Hyperspace', M. Kaku

ACKNOWLEDGEMENTS

I would like to take this opportunity to express my thanks to the following:

Firstly, to my supervisor Professor Brian Tighe for his advice and encouragement throughout the course of this work.

To Dr. Val Franklin for completing the in-vitro spoilation studies described in this thesis, and Dr Pari Sariri for her help with the specific protein adsorption studies.

To Dr. Sarah Tebbs of the Queen Elizabeth hospital, Birmingham and Dr. Christine Jakeman of the biology department, Aston University for carrying out the 'zone of inhibition' antibacterial testing.

To all members of the research group who have made my time at Aston so enjoyable, in particular Mark Eccleston and Fiona Lydon for their useful discussions on both academic issues and otherwise.

To EPSRC and VistaOptics for their financial support under the CASE award scheme

Finally, special thanks go to my family for their confidence in me and to Dr. Scott Summerfield for his endless patience, support and advice over the last four years.

LIST OF CONTENTS

LIST OF TABLES

LIST OF FIGURES

LIST OF ABBREVIATIONS

AMO	Acryloyl morpholine	AZBN	α-Azo-bis-isobutyronitrile
BP	Benzoyl peroxide	CHMA	Cyclohexyl methacrylate
DMAEA	Dimethylaminoethyl acrylate	DMAEMA	Dimethylaminoethyl methacrylate
DMSO	Dimethyl sulphoxide	DSC	Differential Scanning Calorimetry
E	Initial Youngs modulus	ε_b	Elongation at break
EEMA	Ethoxyethyl methacrylate	EGDM	Ethyleneglycol dimethacrylate
EWC	Equilibrium Water Content	γ_s^d	Dispersive Component of Surface Free Energy
γ_s^p	Polar Component of Surface Free Energy	γ_s^t	Total Surface Free Energy
HEMA	2-Hydroxyethyl methacrylate	Ind	Indene
MAA	Methacrylic acid	MeOH	Methanol
MMA	Methyl methacrylate	NHMA	n-Hexyl methacrylate
NNDMA	N, N-Dimethylacrylamide	NMR	Nuclear magnetic resonance
NVI	N-Vinyl imidazole	NVP	N-Vinyl pyrrolidone
PHMB	Polyhexamethylene biguanide	σ_b	Tensile strength
SPE	N-(3-sulfopropyl)-N-methacryloxyethyl-N, N-dimethylammonium betaine	THF	Tetrahydrofuran
$ZnCl_2$	Zinc chloride		

CHAPTER 1

Introduction

1.1 General Introduction

Hydrogels are most simply described as polymer networks of natural or synthetic origin that are able to imbibe large amounts of water, without dissolution. Those of particular interest are the cross-linked, covalently bonded hydrogels that have found their place in the field of biomedicine. The earliest development of synthetic hydrogels dates back to 1960 when Wichterle and Lim[1] reported the potential of hydrogel materials fabricated from poly(2-hydroxyethyl methacrylate) for use in biomedical applications. Because of the transparency and biocompatibility of these polymers, they were ideal candidates for use as soft contact lenses[2,3]. Since then many other hydrophilic polymers have been investigated for use as both soft contact lenses and other prostheses, including carriers for the release of drugs or bioactive macromolecules.

1.2 Water Structuring in Hydrogels

When a cross-linked hydrophilic polymer is placed in water it will swell, absorbing water until an equilibrium is reached between the uptake of water and the physical restrictions of the 3-dimensional polymer network. The amount of water absorbed by an hydrogel is quantitatively represented by the equilibrium water content, EWC. The EWC is the ratio of the weight of water in the hydrogel to the weight of the hydrogel at equilibrium hydration, expressed as a percentage. It is calculated as in equation 1.1.

$$EWC = \frac{\text{weight of water in the gel}}{\text{total weight of hydrated gel}} \times 100\% \quad (1.1)$$

The EWC is arguably the most significant property of an hydrogel. The mechanical properties, surface properties, permeability and behaviour at biological interfaces are all a direct consequence of the amount of water present. The value of the EWC is determined by the nature of the monomers, the density of the cross-linking and external factors like temperature, pH and tonicity of hydrating solution.

Although work in the area of water binding in synthetic hydrogels has only relatively recently attracted interest, work on the water binding of cellulose and related systems has been in progress for a considerably longer period of time and has been discussed by various authors[4,5]. Early work has also included the investigation of the water binding properties of cellulose acetate membranes for reverse osmosis applications[6-9,10]. All of these studies indicated that there are a minimum of two states of water in cellulose acetate membranes

Following work on synthetic polymer systems much evidence was presented to suggest that the water in polymers can exist in more than one state[4-30] and that the nature and relative amounts of these states will also affect the properties of hydrogels. The water exists as a continuum of states between two extremes. Water strongly associated to the polymer matrix through hydrogen bonding is often referred to as 'bound' or non-freezing water. Water not taking part in direct hydrogen bonding to the polymer has a greater degree of mobility and is often referred to as 'free' or freezing water. The properties of an hydrogel are therefore strongly influenced by both the equilibrium water content and also by the ratio of freezing to non-freezing water.

A variety of techniques exist for the study of the states of water in an hydrogel system and the ratio of the various states of water presented will depend on the experimental technique used. Thus the technique used is likely to determine the way in which the water is classified and the terms used to describe these states. Table 1.1 summarises the number of terms that have come into use to describe the various states of water.

<table>
<tr><th colspan="4">Terms Used</th><th>References</th></tr>
<tr><td colspan="2">Primary
Bound
Non-Freezing</td><td colspan="2">Secondary
Free
Freezing</td><td>12-14
15,6-8
6,9,16</td></tr>
<tr><td>Primary
bound
Bound water
which rejects
salts</td><td>Secondary
bound
Bound water
which can
contain salts
with polymer</td><td>Free

Free water
weakly
interacting</td><td>Bulk

Completely
free water</td><td>17,4

10</td></tr>
<tr><td>Bound
Bound
Non-Freezing
X
W_3</td><td colspan="2">Interfacial
Interfacial
Freezable Bound
Y
W_2</td><td>Bulk
Free
Free
Z
W_1</td><td>18,19
20,21,22
23-27
18,21,22,28
29,30</td></tr>
</table>

Table 1.1 Comparison of the terms used in water binding studies

The techniques that have been used to study water binding in hydrogel systems include ^1H nuclear magnetic resonance spectroscopy (NMR), dilatometry, specific conductivity and differential scanning calorimetry (DSC). This work favours the use of DSC, which enables a quantitative determination of the relative amounts of

freezing and non-freezing water to be made. Further information may be obtained from the fine structure of the melting endotherms, and example of which is presented in Figure 1.2.

1.3 Characterisation Techniques

1.3.1 Differential Scanning Calorimetry

When water in hydrogels is cooled to very low temperatures only part of the water in the network freezes. Several calorimetric techniques have been used to study these water binding effects in cellulose an related materials[31]. Differential Scanning Calorimetry (DSC) was developed in 1964 by Perkin Elmer and is a useful tool for calculating the ratio of freezing to non-freezing water and also for gaining information about the binding states of the water in the polymer. A schematic diagram of the instrument is drawn in Figure 1.1[32]. In conventional Differential Thermal Analysis (DTA) the difference between the sample and a reference is measured as energy is applied to the system. In contrast, in DSC the amount of energy required to maintain both the sample and the reference holder at the same temperature is measured. Energy input is increased to equilibrate the sample temperature with the reference holder for endothermic transitions and energy input is increased to the reference holder for exothermic transitions. The energy input to the sample or reference holder is then measured directly as the area under the recorded peak. A typical melting endotherm for polyHEMA is shown in Figure 1.2 and the shape of the peak enables further information to be obtained about the water binding states. Work has shown that the heat of fusion in polymers is identical to that for pure water[15,17]. This allows

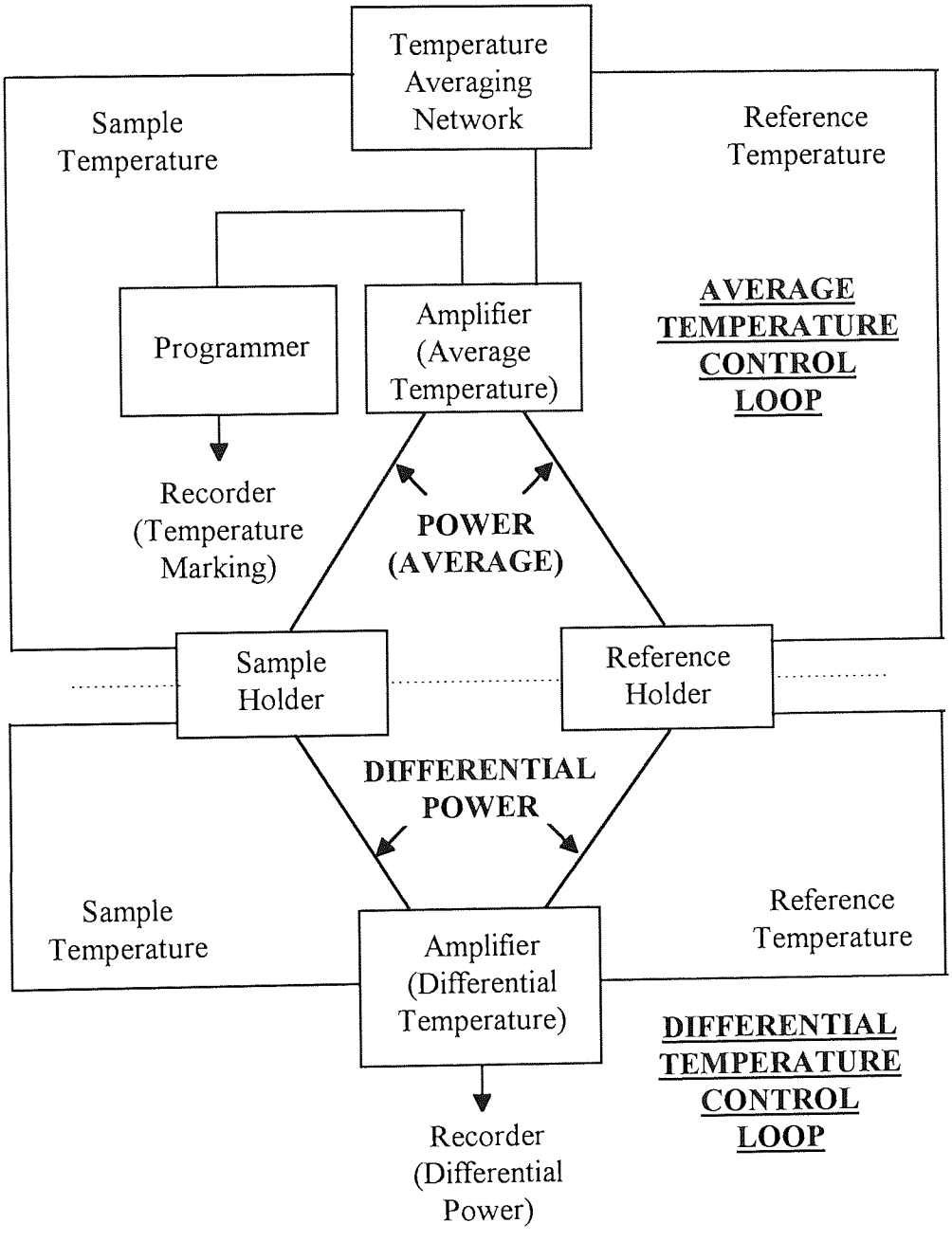

Figure 1.1 Block diagram of a Differential Scanning Calorimeter

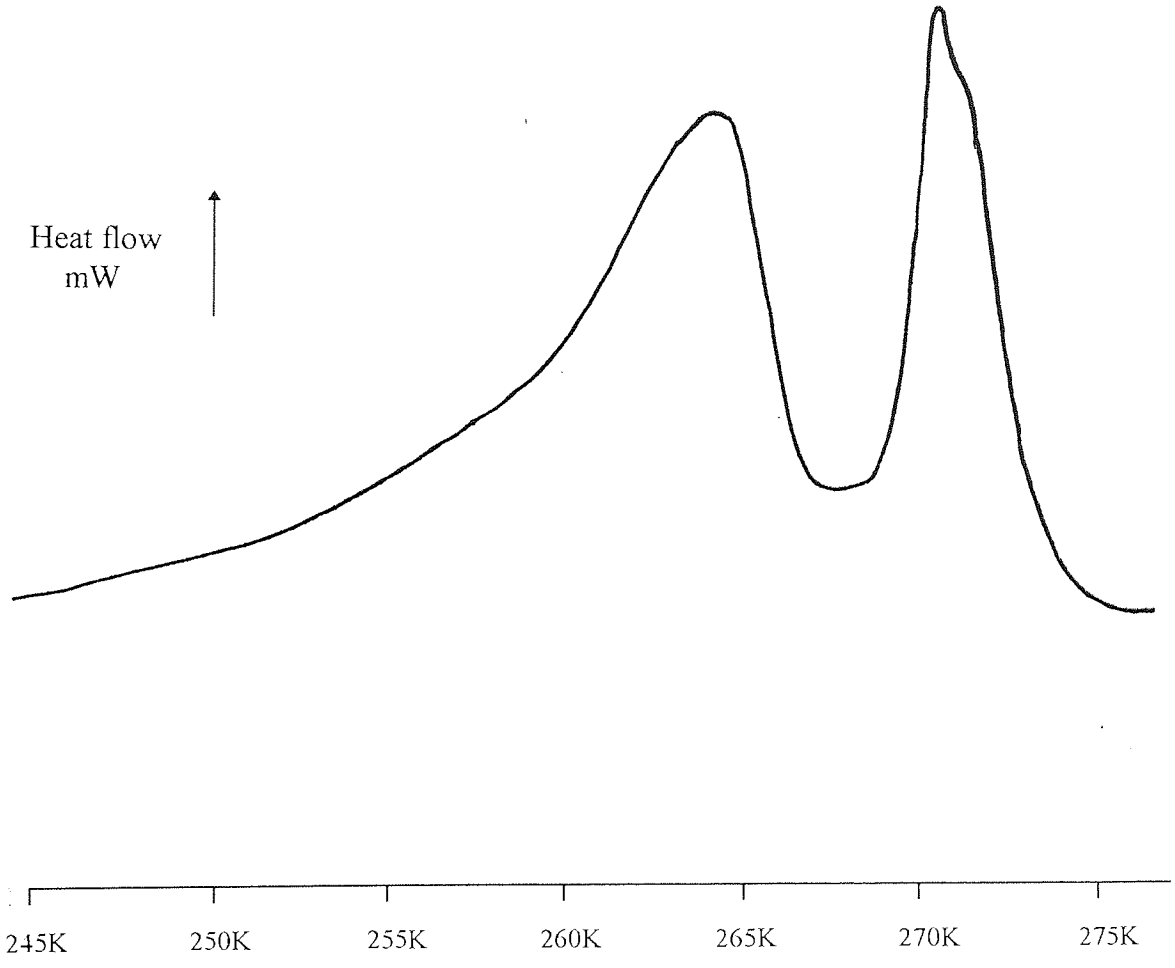

Figure 1.2 Typical melting endotherm of a polyHEMA hydrogel

the quantitative amounts of freezing and non-freezing water present in the polymer to be calculated as described in Section 2.5.

1.3.2 Mechanical Testing

In its dehydrated state poly HEMA is hard and brittle, somewhat similar to poly (methyl methacrylate). However upon immersion in water, the swollen state of polyHEMA is soft and rubber-like making it useful for consideration in biological applications. Unfortunately in its hydrated state polyHEMA and many other hydrogel polymers have very low mechanical strength limiting their range of application and their life-span as biomaterials.

Techniques for measuring mechanical properties in a reproducible and absolute fashion are difficult to set up. This is due to the inherent properties of the materials themselves and also to the loss of water that is inevitable from an hydrogel in a non-aqueous environment. Standard test conditions and specimen geometry for use with the Hounsfield tensometer have been established by Trevett and Tighe[33] although values obtained cannot be regarded as absolute values, as measured values are very sensitive to any changes in test procedures and conditions. However in this report all test conditions remained the same for each sample and the results therefore give useful and comparative information.

1.3.3 Contact Angle Measurements

Contact angle measurements provide valuable information on the interfacial properties of an hydrogel. From the values obtained for the contact angles, the surface free energy of the hydrogel can be determined both in the hydrated and the dehydrated state. Contact angle measurements rely on the resolution of the forces at a three phase interface of a drop of wetting liquid or vapour on a solid surface either immersed in liquid or in air. Several techniques have been used for the measurement of contact angles[34,35] and in this work Hamiltons method[36,37] and the captive air bubble technique[34,38] were used for hydrated hydrogels while the conventional sessile drop technique was used for dehydrated hydrogels[35].

The solid-vapour interfacial free energy, γ_{sv}, calculated from contact angle measurements can in most cases be approximated to γ_s, the surface free energy of the solid in a vacuum. This value can be split into polar (γ_s^p) and dispersive (γ_s^d) components. The biotolerence and blood compatibility of a synthetic material will be strongly influenced by its total surface free energy as well as the magnitude of the polar and dispersive components, as discussed in Section 1.4.

Consistent and accurate surface energy measurements of hydrogel materials can be very difficult to obtain particularly in the dehydrated state, where hydrophilic samples readily absorb water, altering the state of the surface and changing true readings. Contact angle hysteresis can be caused by surface rugosity or inhomogeneity[39] although it has also been suggested that gel deformation occurs under water droplets[40]. Contact angle hysteresis may also occur from polymer chain reorientation

at the hydrogel surface such that the conformation of the polymer changes to minimise the interfacial energy between itself and the adjacent phase.

1.3.3.1 Dehydrated Surfaces

In 1805 Young[41] was the first to derive Equation 1.2 by resolving the forces at a point of contact of a sessile drop and a solid, as demonstrated in Figure 1.3.

$$\gamma_{sv} = \gamma_{sl} + \gamma_{lv} \text{Cos}\theta \qquad (1.2)$$

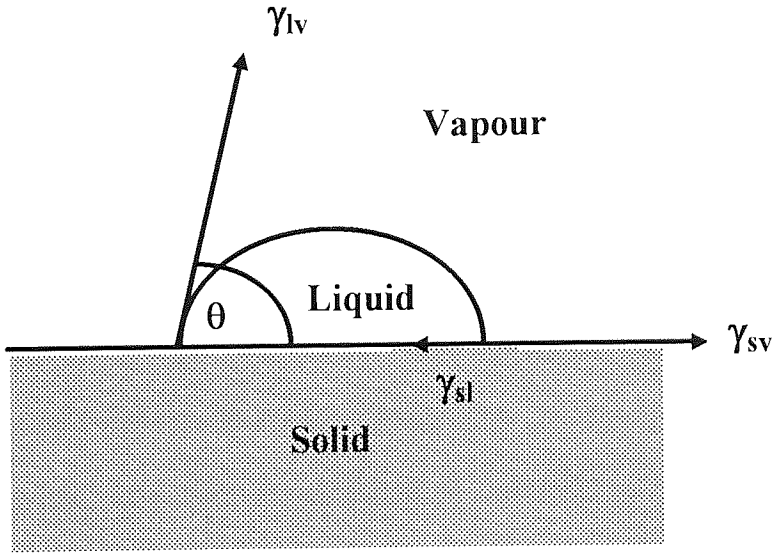

where:-

γ_{sv} = solid - vapour interfacial free energy $\approx \gamma_s$ = solid surface free energy

γ_{sl} = solid - liquid interfacial free energy

γ_{lv} = liquid - vapour interfacial free energy

Figure 1.3 Components of solid surface free energy

In 1865 Dupre[42] followed Young's work by demonstrating that the reversible work of adhesion, (W_a) of a liquid and a solid could be expressed as in Equation 1.3.

$$W_a = \gamma_s + \gamma_{lv} - \gamma_{sl} \quad (1.3)$$

Combining Equations 1.2 and 1.3 gives the Young - Dupre equation, 1.4

$$W_a = (\gamma_s - \gamma_{sv}) + \gamma_{lv}(1 + \text{Cos}\theta) \quad (1.4)$$

When a solid surface comes into contact with the saturated vapour of the wetting liquid, some of the liquid will adsorb onto the solid surface reducing the surface free energy. The difference between the surface free energy of the solid and the solid - vapour interfacial free energy is called the spreading pressure π_e[43].

$$\pi_e = \gamma_s - \gamma_{sv} \quad (1.5)$$

For solids with which the liquid form a finite contact angle, the spreading pressure has been shown to be negligible[44].

Whilst the Dupre equation was used to express the reversible work of adhesion for many years, when polar force interactions across the interface were taken into consideration this equation was found to be inadequate. Following the work of Good *et al.*[45-47] and Fowkes[48], the equation was modified and could be rewritten as

$$W_a = 2[(\gamma_1^d\gamma_2^d)^{0.5} + (\gamma_1^p\gamma_2^p)^{0.5}] \quad (1.6)$$

where γ_1^d and γ_2^d are the dispersive components and γ_1^p and γ_2^p are the polar components of the surface tensions of the two pure phases adjacent to the interface, i.e. γ_{lv} and γ_s for a solid-liquid interface. For a liquid-solid interface the work of adhesion will have a polar and dispersive component and this can be expressed as[36,39,49,50]

$$W_a = \gamma_s + \gamma_{lv} - \gamma_{sl} = 2[(\gamma_{lv}^d\gamma_s^d)^{0.5} + (\gamma_{lv}^p\gamma_s^p)^{0.5}] \quad (1.7)$$

Combining this equation with the Young equation, (1.2), gives Equation 1.8

$$1 + \text{Cos}\theta = (2 / \gamma_{lv}) [(\gamma_{lv}^d\gamma_s^d)^{0.5} + (\gamma_{lv}^p\gamma_s^p)^{0.5}] \quad (1.8)$$

This equation is often referred to the Owens and Wendt equation[39] and is used to determine the surface free energies of polymers in the dehydrated state. Two wetting liquids whose polar and dispersive components are known are used. The contact angle of each liquid on the polymer surface is measured and by solving the simultaneous equations the polar and dispersive components of the surface free energy, γ_s^p and γ_s^d, of the polymer can be determined. The two wetting liquids most commonly used are water and diiodomethane because of their high total surface free energies and their balance of polar and dispersive forces. Table 1.2 shows the surface free energies and the polar and dispersive components of several liquids that may be used[39,48,49].

Liquid	γ^d (mN/m)	γ^p (mN/m)	γ^t (mN/m)
Water	21.8	51.0	72.8
Glycerol	37.0	26.4	63.4
Formamide	39.5	18.7	58.2
Diiodomethane	48.5	2.3	50.8
n-Hexane	27.6	0.0	27.6
n-Octane	21.8	0.0	21.8

Table 1.2 Polar and dispersive components of some wetting liquids commonly used for contact angle studies

1.3.3.2 Hydrated Surfaces

There are two main problems that arise when attempting to measure contact angles on hydrated surfaces in air. The first is the lack of an efficient and reproducible way to remove the surface water from the sample. The other problem is the dehydration of

the polymer surface. Hamiltons method[36,37] and the captive air bubble technique[34,38] have been developed to help overcome these problems, allowing the surface energy of hydrogels to be measured in a fully hydrated state.

Hamilton method[36,37] involves measuring the contact angles of small n-octane droplets on solid surfaces under water. Assuming the effect of gravity on such droplets to be negligible, the polar component of the surface free energy may be calculated.

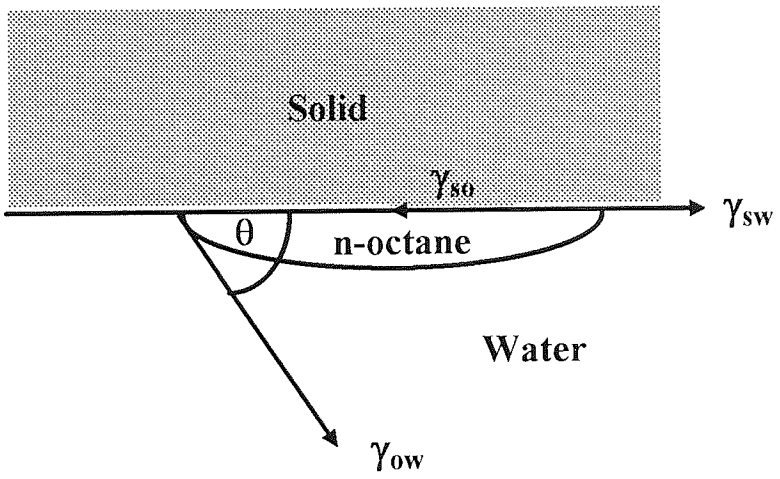

where:-

γ_{sw} = solid - water interfacial free energy

γ_{so} = solid - octane interfacial free energy

γ_{ow} = octane - water interfacial free energy

Figure 1.4 Components of surface free energy for Hamiltons method

Fowkes[121] developed an equation for the work of adhesion at a solid - liquid interface, assuming that there was no polar interaction across the surface.

$$\gamma_{sl} = \gamma_s + \gamma_{lv} - 2(\gamma_{lv}^{d}\gamma_s^{d})^{0.5} \qquad (1.9)$$

A modified form of this equation was developed by Tamai *et al.*[122] which accounted for stabilisation by non-dispersive forces.

$$\gamma_{sl} = \gamma_s + \gamma_{lv} - 2(\gamma_{lv}^d \gamma_s^d)^{0.5} - I_{sl} \qquad (1.10)$$

where:-

$$I_{sl} = 2(\gamma_{lv}^p \gamma_s^p)^{0.5} \qquad (1.11)$$

N-octane has no polar component and the dispersive components for n-octane and water are identical, thus it is possible to combine equations (1.2) and (1.10) to give an expression for I_{sw}, the polar stabilisation energy between water and the solid. The subscripts o for n-octane and w for water have been used.

$$I_{sw} = \gamma_{w'v} - \gamma_{ov} - \gamma_{ow}.\text{Cos}\theta \qquad (1.12)$$

$\gamma_{w'v}$ is the surface tension of n-octane saturated water and γ_{ov} and γ_{ow} can be determined experimentally allowing equation (1.12) to be solved. γ_s^p, the polar component of surface free energy can now be determined from equation (1.11).

A calibration curve plotting the polar component of surface free energy as a function of Hamilton contact angle shows that as the contact angle becomes larger, γ_s^p also increases.

Andrade *et al.*[39] showed that by using data from Hamiltons method and also the captive air bubble technique, it is possible to find values for γ_{sv}, γ_{sv}^p, γ_{sv}^d and γ_{sw} for the hydrogel water interface. Applying Youngs equation (1.2), with water as the liquid phase gives:

$$\gamma_{sv} - \gamma_{sw} = \gamma_{wv}\,\text{Cos}\theta' \qquad (1.13)$$

γ_{wv} is known to be 72.8 mN/m and θ' is the contact angle of the captive air bubble, measured as shown in Figure 1.5. Thus γ_{sv} - γ_{sw}, the adhesion tension can be calculated.

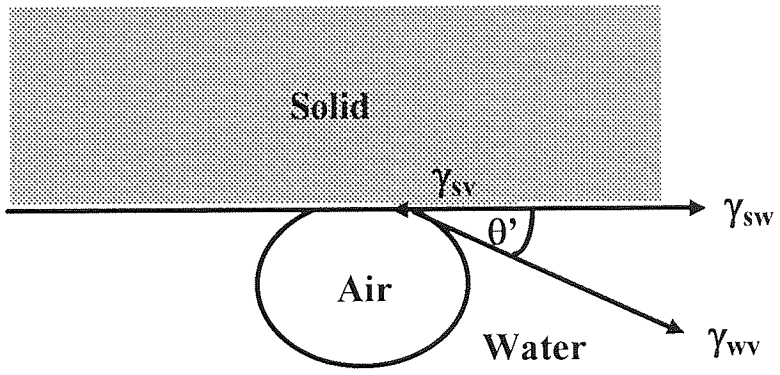

where:-

γ_{sw} = solid - water interfacial free energy

γ_{wv} = water - vapour interfacial free energy (i.e. the surface tension of water)

γ_{sv} = solid - vapour interfacial free energy $\approx \gamma_s$ = solid surface free energy

Figure 1.5 Components of surface free energy for the captive air bubble technique

An equation for the polar stabilisation parameter has already been derived (1.2)

$$I_{sw} = \gamma_{w'v} - \gamma_{ov} - \gamma_{ow}.\text{Cos}\theta' \qquad (1.12)$$

Knowing that γ_{wv} = 72.8 mN/m, γ_{ov} = 21.8 mN/m and γ_{ow} = 51.0 mN/m, this equation can be rewritten:-

$$I_{sw} = 51.0(1 - \text{Cos}\,\theta') \qquad (1.14)$$

I_{sw} can now be calculated. Combining equations (1.10) with (1.13) gives equation (1.15):-

$$(\gamma_{sv} - \gamma_{sw}) = 2(\gamma_{wv}^{d}\gamma_{sv}^{d})^{0.5} + I_{sw} - \gamma_{wv} \qquad (1.15)$$

Rearranging this equation gives an expression for the dispersive component, (γ_{sv}^{d}) of the hydrogel:-

$$\gamma_{sv}^{d} = [\{(\gamma_{sv} - \gamma_{sw}) - I_{sw} + \gamma_{wv}\} / 2(\gamma_{wv}^{d})^{0.5}]^2 \qquad (1.16)$$

The polar component, (γ_{sv}^{p}) can also be derived by rearranging equation (1.11) to give:-

$$\gamma_{sv}^{p} = I_{sw}^{2} / (4\gamma_{wv}^{p}) \qquad (1.17)$$

($\gamma_{sv} - \gamma_{sw}$), I_{sw}, γ_{sv}^{d}, γ_{sv}^{p}, γ_{sv} and γ_{sw} were all calculated using Macintosh Works™ software.

An alternative method of calculating the dispersive component was used based on the Owens and Wendt equation (1.8). The polar component is obtained by using Hamiltons method and by inserting this value into Owens and Wendt equation, together with the measured water / air contact angle, the dispersive component can be calculated. Results obtained for the dispersive component using both methods have been shown to be within 0.2 mN/m[51].

1.3.4 *In Vitro* Spoilation and Specific Protein Adsorption Techniques

In vitro spoilation gives us a guide as to the biocompatibility of a particular material, with the Aston Tear Model specifically designed to give an indication of how a material may behave in the ocular environment. Protein adsorption studies can also be used to assess biocompatibility but moreover they can also give us some idea of the surface structure of a material at a molecular level. This technique has been developed and used in our laboratory by a number of workers[52,53,54]. In the current

work specific protein adsorption studies have been used as a probe of surface charge. It has already been demonstrated that very small amounts of methacrylic acid (MAA) present in a polyHEMA material will affect the concentrations of protein adsorbed[54]. In particular it has been shown that FDA Group IV contact lens materials (high EWC, anionic), containing no more than 5% MAA increase the adsorption of the small positively charged tear protein, lysozyme, quite considerably[55]. It can be seen, therefore that this is a sensitive technique. Protein adsorption is also influenced by the EWC and nature of water structuring in copolymers, however the groups of polymers used all had similar EWCs and the effect of the charged groups should make the major contribution.

1.4 Biocompatibility

Much research has been carried out into the factors that contribute to biocompatibility in the biological environment. This has centred mainly around surface energy related phenomena, although it is also important to take into account the effect of molecular architecture and monomer sequence distribution on the surface energy of a material and the resultant effects on biocompatibility. Biocompatibility is concerned primarily with the interactions that take place between materials and the body fluids with which they are in contact, and physiological responses to these materials. The interactions that occur are dominated by initial events at a molecular level at the interface between the materials and body fluids, thus it is primarily the surface properties of a material that govern its degree of biocompatibility.

1.4.1 Materials in Blood Contact

Several theories have been proposed as to the factors which are important in rendering a material non-thrombogenic, (blood compatible). Baier and co-workers[56] suggested that materials should have a critical surface tension in the region of 20-30 mN/m. Andrade[57] proposed that a minimum interfacial tension should exist between an implant material and its environment to improve biocompatibility. Ratner *et al.*[58] reported that a balance of polar and apolar sites within a material increases blood compatibility. Extensive work on microphase separated copolymers and the effect on blood compatibility has been carried out. Regions of both hydrophilicity and hydrophobicity at a polymer surface control the composition of the adsorbed protein from the blood, which then influences platelet adhesion. Work on the protein adsorption to this system indicates that γ-globulin and fibrinogen adhere to the hydrophobic domains and albumin adheres to the hydrophilic domains[59]. The formation of ordered areas of adsorbed protein is thought to suppress platelet adhesion. Thus the composition of the copolymers which influences the morphology of the microdomains, can control the thrombogenicity of the copolymer.

1.4.2 Hydrogels in the Ocular Environment

The first hydrogels widely used as contact lens materials were based on poly(2-hydroxyethyl methacrylate), polyHEMA. Their flexibility, biocompatibility, and transparency made them good candidates for this application. Although they represent an improvement on the previous lens materials, polyHEMA lenses are not ideal. Even highly cross-linked polyHEMA has relatively poor mechanical properties. Many other monomers and monomer combinations have been investigated in an

attempt to improve the properties of hydrogel lenses, but still the major problem associated with hydrogel contact lenses is one of ocular compatibility or "spoilation". The problem of deposit formation on soft contact lenses is not unique, as the underlying processes that govern blood clotting at a foreign surface and membrane fouling in biochemical separation are other examples of the same phenomena. However these processes are most easily studied in the ocular environment which is readily accessible unlike the study of blood contacting devices requiring surgery.

The term "spoilation" includes any physical or chemical changes due to deposits which may induce discomfort, intolerance or impair the optical properties. It may refer to manifestations at the surface of the hydrogel or within the matrix. Several types of spoilation occur as a result of interaction with the tear components, including the deposition of protein and lipid films, discrete elevated deposits or 'white spot' formation and microbial spoilation. A complete review of lens spoilation has been compiled by Bowers and Tighe[60].

Any material placed into a biological environment carries a risk of infection due to invasion and contamination by micro-organisms. As far as contact lenses are concerned the surface of the lens can be expected to have traces of micro-organisms, normally harmless flora. They only become significant if their number increase due to decreased activity of tear lysozyme or if the lens is inadequately disinfected. Pathogenic species may be introduced by unclean fingers or by cosmetics. Small defects in the hydrogel surface can harbour micro-organisms which contaminate the

lens. Methods of disinfection have included boiling of lens materials or the use of chemical disinfectants like hydrogen peroxide and more recently chlorhexidine.

1.4.3 Protein Deposition on Soft Contact Lens Materials

One of the major uses of hydrogels is as extended wear contact lenses and the problem of protein adsorption contributes greatly to lens spoilation. Protein adsorption has been studied extensively on both hydrogel and non-hydrogel surfaces by several workers including Horbett[61,62] and Baker and Tighe[63].

1.5 Copolymer Sequence Distribution

Work carried out previously within this group[64,65] has shown that synthetic polymers with large irregular molecular domains in which components of the same chemical type tend to become aggregated, have a greater tendency to show non-specific protein adsorption than polymers that mimic naturally occurring polymers with regular chemical variations. The desire to produce biomimetic polymers with an approximately alternating sequence distribution has resulted in the development of a computer simulation program. This program allows the sequence distribution to be predicted for various monomers in a copolymerisation reaction, based on the concentration of monomers used and their associated reactivity ratios. Although the reactivity ratios for a pair of monomers are fixed, optimisation of the concentration of monomers of specific reactivity ratios enables copolymers with short repeat units to be produced.

1.5.1 Copolymerisation and Reactivity Ratios

Copolymerisation allows preparation of a much wider range of polymers with a better balance of properties for specific applications than would be afforded by polymerisation of a single monomer[66,67]. Copolymerisation may proceed by either chain growth (addition) polymerisation or step growth (condensation) polymerisation. The hydrogels prepared in this work are random chain growth polymers prepared by free radical polymerisation.

The terminal model for copolymerisation kinetics[68,69] assumes that the reactivity of an active centre is dependent only upon the monomer unit in the copolymer chain on which the active centre, (radical), is located. For the copolymerisation of two monomers, the growth of the polymer chain, the monomer consumption and the development of the microstructure can be given by four propagation equations:

$$RM_1^{\bullet} + M_1 \text{ ---> } RM_1M_1^{\bullet} \quad \text{rate} = k_{11}[M_1][M_1^{\bullet}] \qquad (1.18)$$

$$RM_1^{\bullet} + M_2 \text{ ---> } RM_1M_2^{\bullet} \quad \text{rate} = k_{12}[M_2][M_1^{\bullet}] \qquad (1.19)$$

$$RM_2^{\bullet} + M_1 \text{ ---> } RM_2M_1^{\bullet} \quad \text{rate} = k_{21}[M_1][M_2^{\bullet}] \qquad (1.20)$$

$$RM_2^{\bullet} + M_2 \text{ ---> } RM_2M_2^{\bullet} \quad \text{rate} = k_{22}[M_2][M_2^{\bullet}] \qquad (1.21)$$

The rate of consumption of the two monomers can be expressed as;

$$-d[M_1]/dt = k_{11}[M_1][M_1^{\bullet}] + k_{21}[M_1][M_2^{\bullet}] \qquad (1.22)$$

and

$$-d[M_2]/dt = k_{12}[M_2][M_1^{\bullet}] + k_{22}[M_2][M_2^{\bullet}] \qquad (1.23)$$

$\frac{d[M_1]/dt}{d[M_2]/dt}$ is the mole ratio of M_1 to M_2 in the copolymer and from equations (1.22) and (1.23):

$$\frac{d[M_1]/dt}{d[M_2]/dt} = \frac{k_{11}[M_1][M_1\bullet] + k_{21}[M_1][M_2\bullet]}{k_{12}[M_2][M_1\bullet] + k_{22}[M_2][M_2\bullet]} \quad (1.24)$$

If a steady state is reached instantly after polymerisation is started, the total concentrations of $M_1\bullet$ and $M_2\bullet$ will remain constant and the rate of conversion of $M_1\bullet$ to $M_2\bullet$ will equal the rate of conversion of $M_2\bullet$ to $M_1\bullet$, i.e.:

$$k_{21}[M_1][M_2\bullet] = k_{12}[M_2][M_1\bullet] \quad (1.25)$$

If k_{11}/k_{12} is defined as r_1, the reactivity ratio of monomer M_1 and k_{22}/k_{21} is defined as r_2, the reactivity ratio of monomer M_2 then equation (1.24) reduces to the copolymer equation[70]:

$$\frac{d[M_1]}{d[M_2]} = \frac{[M_1]\,(1 + r_1[M_1]/[M_2])}{[M_2]\,(r_2 + [M_1]/[M_2])} \quad (1.26)$$

The monomer reactivity ratios r_1 and r_2 are the ratios of the rate constant for a given radical adding to its own monomer, to the rate constant for its adding to the other monomer. It is a measure of the preference for its own kind of monomer to that of the other, thus if $r_1>1$, radical $M_1\bullet$ prefers to add to monomer M_1 and if $r_1<1$, radical $M_1\bullet$ prefers to add to monomer M_2.

A copolymer is said to be ideal when the two radicals show the same preference for addition of one of the monomers and $r_1r_2 = 1$. The end group on the growing chain has no influence on the rate of addition, and the two types of unit are arranged at random along the chain in the relative amounts determined by the composition of the feed and the relative reactivities of the two monomers.

When $r_1 \approx r_2 \approx 0$, each radical shows a strong preference for cross propagation. The monomers alternate regularly along the chain regardless of the composition of the monomer feed. When $r_1 \approx r_2 \approx 1$, neither radical centre shows a preference for either M_1 or M_2 and the rates of monomer consumption are determined only by the monomer concentrations in the feed mixture. If r_1 is much greater than r_2, the resulting copolymer will contain large blocks of M_1 interspersed with one or two molecules of M_2. However if r_1 and r_2 are closer in value, the copolymer tends towards alternation growing stronger as r_1 and r_2 approach 0.

1.5.2 Computer Simulation of Sequence Distribution

Computer simulation of the sequence distributions of copolymers allows an illustration of the copolymerisation process, whilst making it possible to vary the key parameters, such as monomer concentration, with ease. This enables the testing of copolymer systems for their approximate sequence distributions to be carried out swiftly, without the detailed structural analysis that would be necessary for the real system.

Computer simulation of the sequence distributions was carried out using two computer programs. The 'COPOL' program allowed simulation of the sequence distribution for a binary copolymerisation system. The 'TERPOL' program allowed simulation of the sequence distribution for a ternary copolymerisation system. Both methods are broadly based on the terminal model of copolymerisation described in Section 1.5.1 and make use of the Monte Carlo method of statistical trials[71,72].

1.5.3 The Alfrey-Price Q and e Scheme[73,74]

Large pairs of reactivity ratios are required for extensive simulation of sequence distributions using the computer programs. It is not always possible to find reference to experimentally determined reactivity ratios for certain monomer pairs. A reasonable approximation of reactivity ratios may be arrived at through the use of the Alfrey-Price Q-e scheme[73,74]. This scheme takes into account the different extents to which the polar and resonance stabilisation effects of monomers influence copolymerisation reactions. The two reactants in a radical / monomer addition were assigned e values e_1 and e_2 respectively, to represent their charges, identical charges being assumed for a monomer and its derived radical. The general reactivities of radicals and monomers was denoted by P and Q respectively. The rate of reaction was considered to be determined by the four quantities P, Q, e_1 and e_2 as indicated in equation (1.27):

$$k_{12} = P_1 Q_1 \exp(-e_1 e_2) \qquad (1.27)$$

The four equations (1.18-1.21) for each propagation step allow us to obtain equations (1.28) and (1.29):

$$r_1 = (Q_1 / Q_2) \exp [-e_1(e_1-e_2)] \qquad (1.28)$$

$$r_2 = (Q_2 / Q_1) \exp [-e_2(e_1-e_2)] \qquad (1.29)$$

Hence the Q-e scheme allows predictions to be made about reactivity ratios in systems that have not been studied experimentally.

1.6 Biomedical Applications of Hydrogels

Hydrogels are used extensively as biomaterials and their use in contact lens[75], drug delivery[76,77] and other biomedical applications[78-84] has been well documented. In particular polyHEMA is used for implants in surgery including vascular implants[85] and ureter prostheses[86]. Hydrogels have also been used therapeutically[87] for treatment of ocular complaints and as corneal implants[88]. Linear polyHEMA has been used for the surface treatment of other materials to improve compatibility e.g. the coating of surgical sutures[77] and rubber catheters[77]. One recent area of interest involves the use of hydrogels, often in the form of composites, some of which may be regarded as blends and interpenetrating networks, synthesised from hydrogels and other synthetic or naturally occurring polymers. Two specific areas in which this type of activity is apparent are those concerned with wound coverings[89,90] and synthetic articular cartilage[91-95].

1.7 Antimicrobial Activity

There are several types of antimicrobial agents in use, including antibiotics, preservatives, disinfectants and antiseptics. Of particular interest are the cationic 'membrane active' antimicrobial agents which find their use as disinfectants, especially in some contact lens cleaning regimes. The use of cationic species as antimicrobial agents is not a new phenomenon and much work has been carried out on low molecular weight quaternary ammonium salts[98,111] and biguanides such as chlorhexidine[99]. The mode of action of such species relies on the fact that the bacterial cell surface is negatively charged and there is electrostatic attraction of the cationic species toward the cell wall.

1.7.1 Structure of the Bacterial Cell[120]

The smallest and simplest cells are called prokaryotes and they consist of different families of unicellular micro-organisms which we know as bacteria. Every cell has a thin surrounding membrane called the cytoplasmic membrane. It is selectively permeable, allowing necessary nutrients and salts to pass into the cell and waste products to leave, whilst excluding the entry of unneeded substances from its environment. The molecular architecture of the cytoplasmic membrane consists of a mixed lipid bilayer comprising neutral phospholipids such as phosphatidylcholine (PC) and phosphatidylethanolamine (PE) and acidic phospholipids such as phosphatidylglycerol (PG). In this lipid bilayer a variety of specialised proteins are embedded. Some of these membrane proteins are enzymes and others can bind nutrients from the environment and transport them into the cell. Within the cell there is the cytoplasm and the nucleus. Figure 1.6 shows a generalised structure of a bacterial cell.

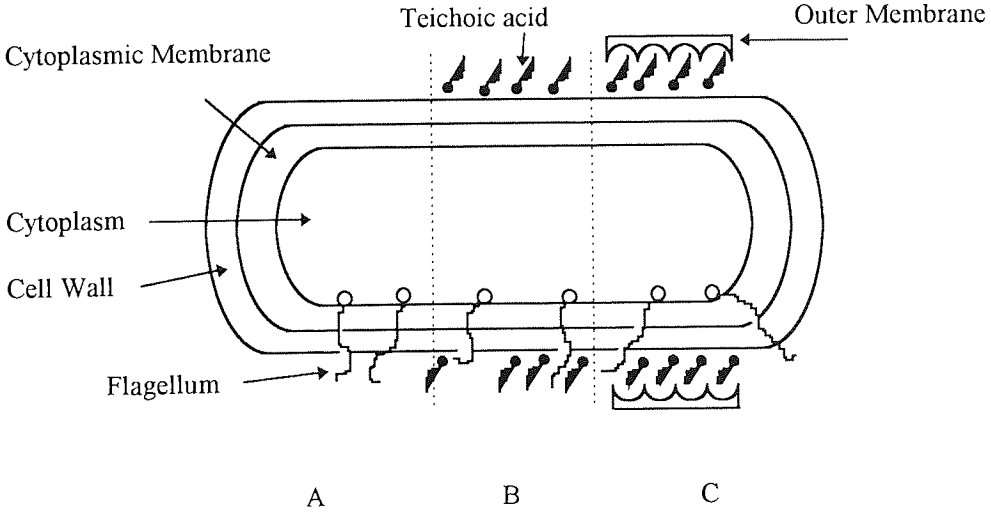

A: Generalised structure; B: Gram positive structure; C: Gram negative structure

Figure 1.6 Schematic diagram of the bacterial cell (reproduced from ref. 98)

There are two different types of bacterial cell, gram positive and gram negative. The former cells have a simple cell wall structure in which outside the cytoplasmic membrane there is only a rigid peptidoglycan layer. This layer is composed of a network of pores allowing foreign molecules to come into and out of the cell without difficulty. On the other hand, gram negative bacteria have more complicated cell walls. There is another membrane outside the peptidoglycan layer, which is called the outer membrane and has a similar structure to the cytoplasmic membrane[99,111].

1.7.2 Low Molecular Weight 'Membrane Active' Agents

The term 'membrane active' agent refers to the fact that the target site for this type of antimicrobial agent is the cytoplasmic membrane. Several such compounds exist including phenols and alcohols as well as the cationic species of particular interest in the context of this report, such as quaternary ammonium compounds (QACs) and biguanides, both of which are positively charged at physiological pH.

Quaternary ammonium compounds used for disinfection purposes are cationic surface active agents with a general structure illustrated by Figure 1.7. The hydrophobic asymmetry that is a feature of their surface activity is also an important factor in their activity against bacteria. The QACs with most potent antimicrobial activity are those in which one of the R groups has a chain length of C_8-C_{18}. The other important structural feature of QACs is the presence of positive charge. This enables them to interact with the negatively charged surface of the cell wall and the cytoplasmic membrane.

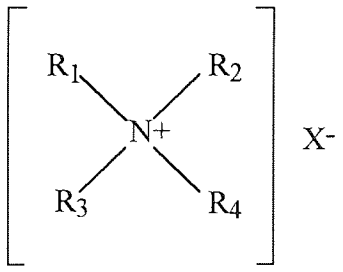

Figure 1.7 General structure of a quaternary ammonium compound

Since the early work of Rose and co-workers[96,97], low molecular weight biguanides have been employed widely as antimicrobial agents. Chlorhexidine has been one of the most popular disinfectants because of its broad spectrum of antibacterial activity, high kill rate and non-toxicity towards mammalian cells. Alexidine dihydrochloride is a similar bisbiguanide and both structures are illustrated in Figure 1.8.

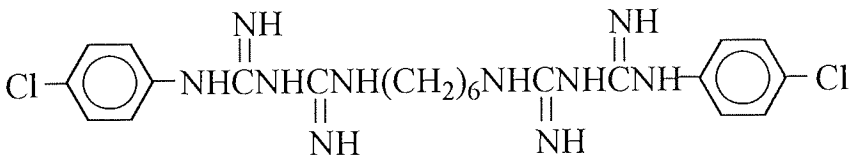

Chlorhexidine

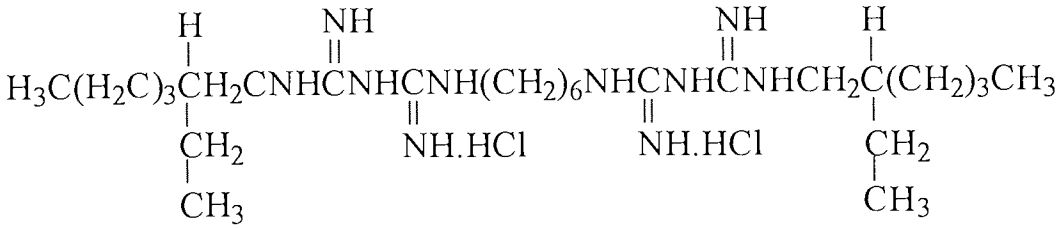

Alexidine dihydrochloride

Figure 1.8 Structures of chlorhexidine and alexidine dihydrochloride

Much work has been carried out on the mode of action of low molecular weight biguanides especially chlorhexidine[98-100]. Hugo and Longworth first showed that chlorhexidine caused a release of cytoplasmic constituents from the bacterial cells, *E. coli* and *Staph. aureus*[99] by damaging the cytoplasmic membrane. They also stated that at higher concentrations of chlorhexidine than those which caused maximum leakage from the cell, coagulation of cytoplasmic constituents took place. In 1966 Hugo and Longworth[100] proposed that the primary action of chlorhexidine consisted of an adsorption of the drug onto the negatively charged surface of the cell. The adsorption is then followed by a disorganisation of the permeability barriers of the cell. Low concentrations permit the leakage of cytoplasmic constituents; higher concentrations of chlorhexidine, which are used for antiseptic purposes and are more bactericidal, coagulate cytoplasmic constituents.

In 1969 Davies and Field[101] compared the action of some biguanides on *E. coli* and stated that bactericidal activity correlated with the ability to precipitate cytoplasm. They suggested that bactericides increased permeability and that this facilitated their own entry into the cell; once inside they kill by causing irreparable damage. Further surveys of the literature[98,104,107,113,114,119] reveal that the accepted mechanism of action of cationic disinfectants - QACs and biguanides with monomeric or dimeric forms, may be considered to consist of the following sequences of events[98]: i) adsorption onto the bacterial cell surface facilitated by the presence of the positive charge; ii) overcoming bacterial cell wall exclusion; iii) binding to the cytoplasmic membrane; iv) disruption of the cytoplasmic membrane; v) release of the cytoplasmic constituents such as K^+, RNA and DNA and death of the cell.

1.7.3 Polymeric Antibacterial Agents

Synthetic polymers with biological activity until recently received scant attention in the literature[101,102]. One reason is that bioactive groups tend to lose their activity when incorporated into polymers. The widespread use of chlorhexidine and the fact that it has been shown to have greater activity than monomeric biguanides[101], led to the development of a polymeric biguanide, polyhexamethylene biguanide, (PHMB)[101,102]. PHMB represents one of the few examples of polymeric antibacterials that have found a successful application having a broad spectrum of activity against gram positive and gram negative bacteria and low mammalian toxicity. Its structural repeat unit is shown in Figure 1.9 and it has a molecular weight of ~3000.

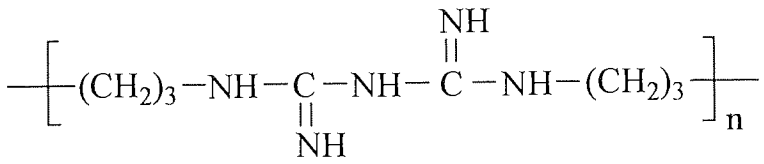

n varies with a mean of n = 5.5

Figure 1.9 Structure of polyhexamethylene biguanide

Gilbert *et al.* (1983)[105] published a study comparing the antibacterial activity of some polyhexamethylene biguanides upon *E. coli*. An amine ended dimer (n = 2), a polydisperse mixture sold by I.C.I. Limited as the active ingredient of Vantocil IB (n = 5.5) and a high molecular weight fraction of PHMB (n > 10) were used. They found that bacterial growth inhibition and bactericidal activity increased with increasing levels of biocide polymerisation. Their suggestion was that the mode of action was similar to that of the low molecular weight biguanides, i.e. irreversible

damage to the cytoplasmic membrane was initiated and completed within a short time of contact between the material and the biocide, and that death of the cells and cytoplasmic membrane damage are directly associated. However they also noted that there must be some difference in activity as the monomeric biguanide in their study was least effective in terms of bactericidal activity, failing to inhibit motility in actively growing cultures.

Ikeda *et al.*[106] also concluded that the mechanism for the action of polymeric biguanides, in particular PHMB was similar in some ways to the monomeric antibacterials and the bisbiguanides. They confirmed that the targets for the PHMB interaction were the negatively charged species in the mixed lipid bilayer of neutral and acidic phospholipids in the cytoplasmic membrane of the bacterial cell. PHMB, being a polyelectrolyte (polycation), has a much higher positive charge density than do single monomeric electrolytes. Thus the relatively stronger interaction of PHMB with negatively charged species is to be expected. Ikeda *et al.* further proposed that following the adsorption of the PHMB onto the acidic phosphatidylglycerol in the lipid bilayer, interaction of the hydrophobic hexamethylene groups with the hydrophobic interior of the bilayer occurs. This leads to disorganisation of the bilayer due to hydrophobic association, leading to higher fluidity, lateral expansion and a higher permeability of the bilayer, accompanied by loss of cellular constituents. The marked difference between polymeric and monomeric biguanides is that PHMB can induce phase separation in the mixed lipid bilayer of the cytoplasmic membrane whereas monomeric biguanides cannot.

Since the success of PHMB as the active ingredient of Vantocil IB there has been much more interest in the development of novel polymeric antibacterial agents. It is generally accepted that polycationic species will have a similar mode of action to monomeric cationic disinfectents[114]. More potent activity may result from the increased charge density leading to more sites of interaction with the cell wall and the cytoplasmic membrane. Disruption of the membrane is a consequence of interaction with the hydrophobic groups present in the cationic microbial agent. Thus one can expect that the increasing hydrophobic character shown by polycationic materials will lead to enhanced activity.

Ikeda *et al.*[107] reported the synthesis and antibacterial activity of polycations with pendant biguanide groups as opposed to backbone biguanide groups. These polymers possessed a higher level of bactericidal activity than their corresponding monomer and the proposed mode of action was similar to that of PHMB. Other classes of polycationic antibacterials include polycations with either in chain or pendant quaternary ammonium salts[108-112]. Polymers that are polyammonium salts with a positive nitrogen in the backbone are known as ionene polymers and Rembaum[108] reported their enhanced biological activity as early as 1973. Ikeda *et al.*[113] also studied this class of polymer, stating that bactericidal activity increased with the molecular weight of the polycation. Endo *et al.*[114] modified the model of using polyammonium salts and synthesised various polymeric phosphonium salts. They found that not only was the antibacterial activity of the polymer higher than that of the corresponding low molecular weight model compounds but also that the polymeric phosphonium salts exhibited a higher activity by 2 orders of magnitude than the

polymeric quaternary ammonium salt of similar structure. Allcock and co-workers[115] in 1992 discussed the antibacterial activity of water soluble phosphazene polymers and suggested that cross-linked phosphazene hydrogels may provide a long term antibacterial polymer surface, which would be impossible for a small molecule counterpart. Ferruti and his co-workers[116] synthesised several families of tertiary amino polymers - poly(amido-imine)s, a class of polymers characterised by the presence of amido and tertiary amino groups along the macromolecular chain. Additional functional groups could be introduced as side substituents. Quaternised products of these polymers[117] and cross-linked resins[118] of one of the families have been shown to be active against bacteria and are of interest as long term protective agents against infection in medical devices e.g. urinary catheters.

From the literature it is clear that in the design of a polymeric antibacterial agent, the important features are a high positive charge density available to interact with the negative charge on the cell membrane surfaces, with a balance of hydrophilic and hydrophobic character such that the hydrophobic groups can interact with the membrane interior.

1.8 Scope and Objectives of this Project

A study of the literature concerning polymeric antibacterial agents such as chlorhexidine and polyhexamethylene biguanide has led to an understanding of the mode of action of such 'membrane active' agents. This study has revealed that the essential components of a polymeric antibacterial agent include regions of hydrophilicity and hydrophobicity together with cationic sites. The present work is

concerned with an investigation into the effect of incorporating a potentially cationic monomer into an hydrogel material and the potential development of hydrogel polymers with bacterial resistance. Very little work has previously been carried out on hydrogel materials that have a positive charge, although hydrogels with a small degree of anionicity have found use in contact lens applications. The water-binding properties and the mechanical and surface properties of potentially cationic hydrogel materials have been studied.

Group IV contact lens materials which are high water content, anionic materials have been shown to increase the uptake of positively charged proteins[55]. Some workers have also suggested that charged groups in hydrogels may increase the deposition of biological materials when in contact with body fluids[78]. Specific protein deposition and *in vitro* spoilation techniques have been used to investigate the effect of cationic sites in the uptake of biological materials onto the hydrogel surface. Finally preliminary studies have been made into the potential for the development of polymers and hydrogels that show resistance to bacteria either by controlled release of an antibacterial agent or by chemical attachment of the antibacterial agent to the polymer matrix. Some novel methods for the control of bacterial infection have also been discussed with applications such as coatings for catheter materials in mind.

CHAPTER 2

Materials and Experimental Techniques

2.1 Reagents

The reagents used in this work are given in the following Tables 2.1-2.2. Structures of the reagents are shown in Figures 2.1-2.3. All monomers were purified by means of distillation at reduced pressure before use[123]. All monomers were stored in a refrigerator when not in use.

Monomer	M.Wt.	Abbreviation	Supplier
2-Hydroxyethyl methacrylate	130	HEMA	Vista
N-vinyl pyrrolidone	100	NVP	Vickers
N, N-dimethylacrylamide	99	NNDMA	Dajac
N-vinyl imidazole	94	NVI	Aldrich
Indene	116	Ind	Aldrich
Ethoxyethyl methacrylate	158	EEMA	I.C.I.
N-hexyl methacrylate	170	NHMA	Polysciences
Ethyleneglycol dimethacrylate	198	EGDMA	BDH
N-(3-sulfopropyl)-N- methacryloxyethyl-N, N-dimethylammonium betaine	250	SPE	Dajac
Acryloyl morpholine	141	AMO	Vista
Dimethylaminoethyl methacrylate	157	DMAEMA	Aldrich
Dimethylaminoethyl acrylate	143	DMAEA	Aldrich
Cyclohexyl methacrylate	168	CHMA	Aldrich

Table 2.1 Suppliers, molecular weights and abbreviations of monomers used.

Reagent	M.Wt.	Abbreviation	Supplier
α-Azo-bis-isobutyronitrile	164	AZBN	BDH
Benzoyl peroxide	242	BP	BDH
Zinc chloride	136	$ZnCl_2$	BDH
Vantocil IB	~3000	Vantocil	Zeneca Biocides
Alexidine dihydrochloride	508	Alexidine	Sigma
Methacryloyl isocyanate	111		Aldrich
Itaconyl chloride	168		Aldrich

Table 2.2 Suppliers, molecular weights and abbreviations of miscellaneous chemicals

N-vinyl pyrrolidone

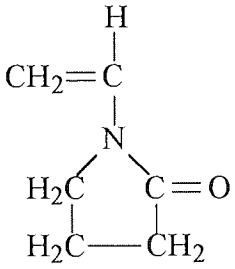

N,N-dimethylacrylamide

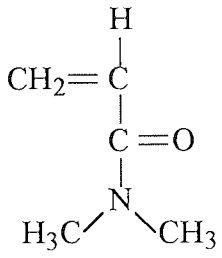

Figure 2.1 Structures of monomers used

N-vinyl imidazole

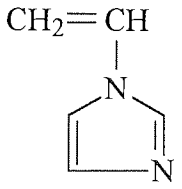

Indene

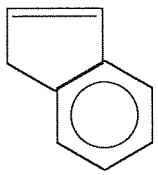

Acryloyl morpholine

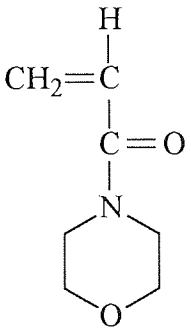

Ethyleneglycol dimethacrylate

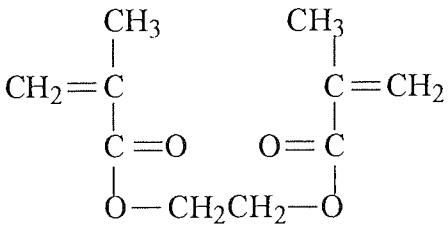

Figure 2.1 Structures of monomers used

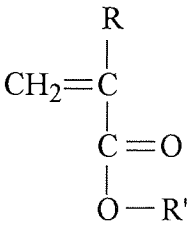

R = CH_3, R' = CH_2CH_2OH	2-Hydroxyethyl methacrylate
R = CH_3, R' = C_6H_{11}	Cyclohexyl methacrylate
R = CH_3, R' = $(CH_2)_5CH_3$	n-Hexyl methacrylate
R = CH_3, R' = $(CH_2)_2O(CH_2)_2$	Ethoxyethyl methacrylate
R = CH_3, R' = $CH_2CH_2N(CH_3)_2$	Dimethylaminoethyl methacrylate
R = H, R' = $CH_2CH_2N(CH_3)$	Dimethylaminoethyl acrylate

Figure 2.2 Structures of methacrylate monomers used

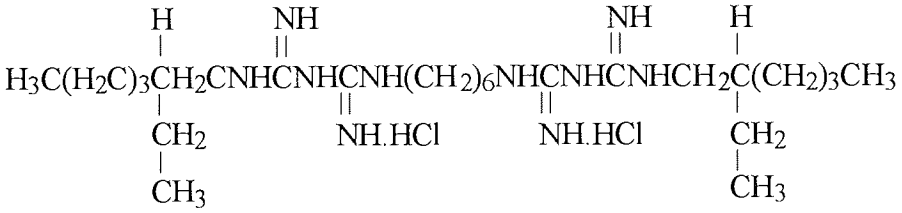

Alexidine dihydrochloride

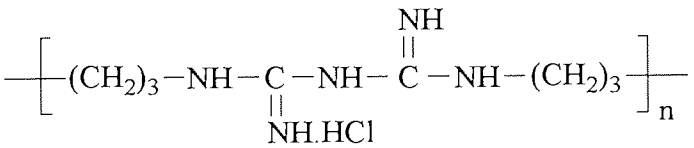

Vantocil IB

Figure 2.3 Structure of antimicrobial agents used

2.2 Polymer Synthesis

2.2.1 Membrane Preparation

Hydrogel membranes were prepared by bulk polymerisation in a glass mould. Two glass plates, (15cm x 10cm), were each mounted on one side with a sheet of "Melinex", [poly(ethylene terephthalate)], to prevent adhesion of the membrane to the glass plate. The glass plates were then placed together, with coated surfaces facing, separated by a polyethene gasket 0.2mm thick. The mould was held together using spring clips.

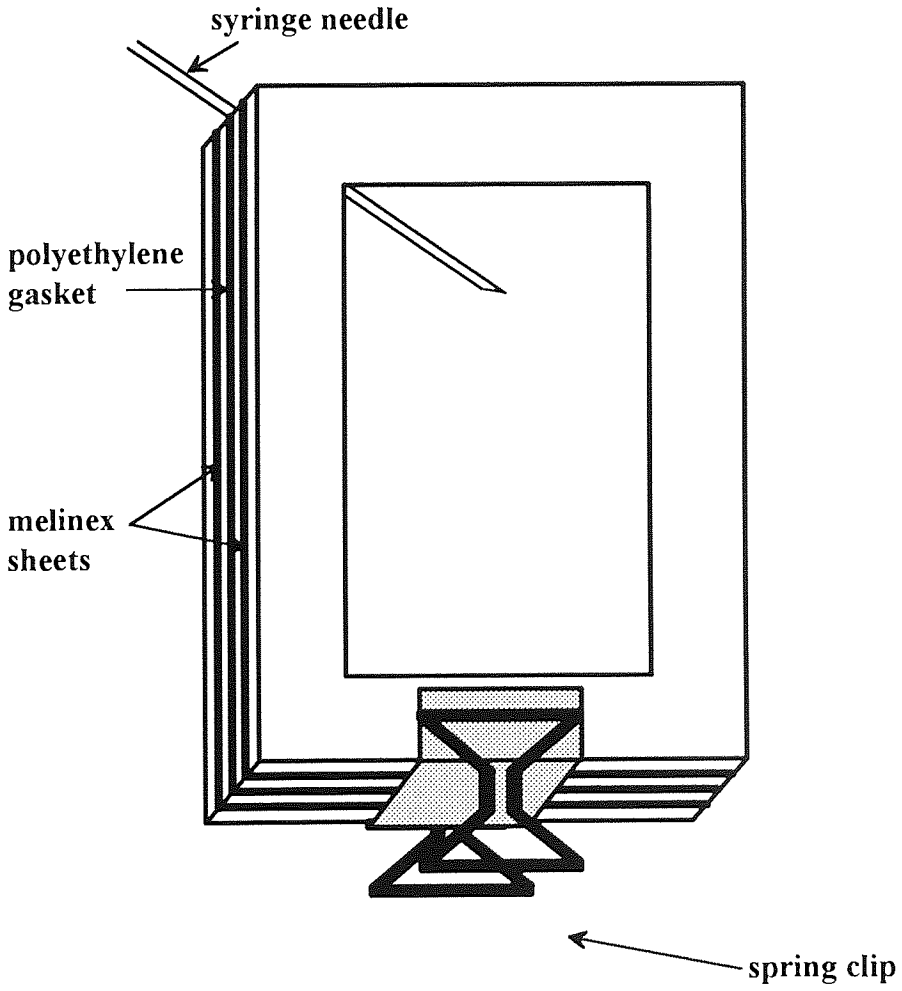

Figure 2.4 Diagram of a Membrane Mould

In a typical preparation, a 4g mix of monomer and 1%(w/w) cross linker was weighed out and degassed with nitrogen for approximately 10 minutes to remove any oxygen. 0.5%(w/w) free radical initiator was added and the mix was introduced into the mould using a syringe. The mould was placed in an oven at 60°C for 3 days to complete polymerisation, followed by a 3 hour post-cure at 90°C. Upon completion of polymerisation the membrane was removed from the mould and placed in distilled water to hydrate for a period of at least 2 weeks. During this time the water was changed regularly to ensure the removal of any residual monomer species.

Membranes prepared by photochemical initiation were injected into a mould as described, using 1%(w/w) uranyl nitrate as a catalyst. The mould was placed under a Gallenkamp UV mercury discharge lamp and polymerisation was initiated by UV light of 365nm for 2 hours.

2.2.2 Solution Polymerisation

Ultra-Violet light initiated polymerisations were carried out in the presence of a Friedel Crafts catalyst (e.g. $ZnCl_2$). In a typical experiment a 3-necked, 250ml flask was fitted with a stirrer, condenser, thermometer and a nitrogen bleed. The flask was charged with 100ml tetrahydrofuran, 13.8g (0.1M) zinc chloride, 11.6g (0.1M) indene, 9.9g (0.1M) NNDMA and 0.1g (~1%) AZBN. Polymerisation was carried out at room temperature and initiated by UV light of 365nm wavelength from a Gallenkamp UV mercury discharge lamp. After 2 hours the UV source was removed and the contents of the flask poured into 2 litres of ether cooled with solid carbon dioxide. The white precipitate obtained was filtered quickly while still cold and dried

under vacuum at 40°C. Thermally initiated polymerisations were carried out in a similar manner, heating to a temperature of 60°C in place of the UV light source, for 8 hours.

2.3 Measurement of Equilibrium Water Content

The equilibrium water content (EWC) of an hydrogel membrane is measured after allowing the membrane to hydrate for approximately 3 weeks. Not less than 3 samples were cut with a cork-borer of 1cm in diameter from the hydrated membrane. The surface water was removed from the samples with filter paper and the samples dehydrated to constant weight in a microwave oven for approximately 10 minutes. The samples were then reweighed and the EWC calculated from equation 2.1:-

$$EWC = \frac{\text{weight of hydrated sample - weight of dehydrated sample}}{\text{weight of hydrated sample}} \times 100\% \qquad (2.1)$$

The mean average of the three samples was determined.

2.4 Measurement of Mechanical Properties

The mechanical properties were investigated with the Hounsfield HTi Tensometer interfaced to an IBM 55SX computer. Samples were cut from the hydrated membrane in a dumbbell shape of 8mm length and 3.3mm width. Sample thickness was measured using a micrometer and then the test sample was clamped in the jaws of the tensometer. To maintain complete hydration (100% humidity) the samples were sprayed with distilled water before and during the test. A test speed of 20mm min^{-1} was chosen at room temperature and pressure. The program calculated values for

Youngs modulus (E), tensile strength at break (σ_b) and elongation at break (ε_b) using the following equations:

$$\text{Tensile strength } (\sigma_b) = \frac{\text{Load at break}}{\text{Cross-sectional area}} \quad (2.2)$$

$$\text{Elongation at break } (\varepsilon_b) = \frac{\text{Extension of gage length}}{\text{Original gage length}} \times 100\% \quad (2.3)$$

$$\text{Youngs modulus (E)} = \frac{\text{Stress}}{\text{Strain}} \quad (2.4)$$

where:-

Stress = Load / Cross-sectional area

Strain = Extension of gage length / Original gage length

All results quoted are the mean value of not less than 5 samples

2.5 Differential Scanning Calorimetry

Differential scanning calorimetry (DSC) was used in this instance to determine the percentage of freezing water present in an hydrated hydrogel sample.

Thermograms were obtained using a Perkin Elmer differential scanning calorimeter, DSC-7, in conjunction with a 7500 professional computer and a liquid nitrogen cooling accessory. Samples were cut from an hydrated sheet of hydrogel using a size 1 cork borer and the surface water removed using filter paper. The samples were weighed and then sealed in an aluminium pan.

Samples were cooled to 223K to ensure that any super cooled water was frozen and then allowed to reach equilibrium at this temperature. Samples were then heated to 253K at a rate of 10K min^{-1} and subsequently to ambient temperature at a rate of 5K min^{-1}.

The computer software allowed the area under the melting peaks of the hydrogel sample to be measured and ΔH to be calculated. From this information the freezing water content of the sample can be ascertained using equation 2.5.

$$\text{Freezing water content (\%)} = \frac{\Delta H \text{ calculated}}{\Delta H \text{ for pure water}} \times 100\% \qquad (2.5)$$

where:-

ΔH = area under melting peak / weight of sample

and

ΔH for pure water = 333.77 Jg^{-1}

All results quoted are the mean value of not less than 3 samples

2.6 Surface Properties

Although the experimental techniques for the measurement of contact angles on both hydrated and dehydrated samples are described in this chapter, the theory used to determine surface energies from contact angles is presented in Chapter 1.

Contact angles were measured in the hydrated state using Hamiltons method and the captive air bubble technique, and in the dehydrated state using the conventional sessile

drop technique. Samples were cleaned using 'Teepol L' detergent to remove any grease on the surface that may affect measurements and then rinsed thoroughly using distilled water. In order to remove any remaining traces of detergent the samples were soaked in distilled water for several days before testing. Using a Rame Hart goniometer the contact angle at the three phase interface was measured, with the value of the contact angle quoted being the average of the angle measured at each side of the drop / bubble. Polar, dispersive and total surface free energies were calculated from the contact angles obtained using Macintosh Works™ programmed with the relevant equations, (see Chapter 1).

2.6.1 Hamiltons Method[36]

Samples were cut from an hydrated hydrogel sheet using a size 7 cork borer. After removing the surface water from one side, the sample was glued to an electron microscope stub using super glue. The sample was then inverted and suspended in an optical cell filled with distilled water. A small drop of n-octane was placed on the surface of the sample using a specially curved G25 syringe needle. At least three measurements were made at various positions on each sample to reduce any errors arising from irregularities in surface topology.

2.6.2 Captive Air Bubble Technique

The samples were cut and mounted underwater in the same way as for Hamiltons method. In this technique however, air bubbles instead of n-octane bubbles are released onto the sample surface using a similarly curved G25 syringe needle. Using this needle allows the air bubble to be introduced at the sample surface in such a way

that a fine degree of control is maintained over the bubble size. As previously at least three measurements were made to reduce errors.

2.6.3 Sessile Drop Technique

Samples were dehydrated to constant weight in a microwave oven for approximately 10 minutes and the dehydrated sample placed on a microscope slide. This was then placed on the stainless steel support of the Rame Hart goniometer and a drop of the wetting liquid introduced onto the sample surface using a straight G25 syringe needle. The wetting liquids used here were distilled water and diiodomethane. At least three measurements were made to reduce errors.

2.7 *In Vitro* Ocular Spoilation Model

The *in vitro* ocular spoilation model has been developed at Aston in order to show the effects of lipid as well as protein deposition at an hydrogel surface. This model relies on having a suitable and stable tear substitute. The tear substitute used was based on a 1:2 (v/v) solution of foetal calf serum diluted with phosphate buffered saline as a base. This was then 'spiked' with additional components such as mucin, lactoferrin and lysozyme in order to mimic the tear composition.

The tear model enables controlled spoilation to be carried out using two forms:-

1) The 'shaker' model

2) The 'drop and dry' model

In this work the 'shaker' method has been used. A number of small glass beads were placed in a vial, in order to provide an uneven surface on which the samples could

rest, allowing contact with the air and the tear solution. The tear solution was pipetted into the vial to a level just below the top surface of the glass beads. The prepared vials were then placed on a flatbed vibrating shaker operating at 200 cycles per minute, which enhanced the air and tear solution contact with the samples. The tear solution in the vials was replaced every 24 hours to maintain a fresh supply of protein and lipid components.

The deposition of both lipids and proteins was monitored at regular intervals over a period of 28 days using fluorescence spectroscopy. An excitation wavelength of 360nm was used to record the emission spectra showing the greatest lipid sensitivity and an excitation wavelength of 280nm was used additionally to record both the protein and the lipid sensitivity.

2.8 Specific Protein Adsorption

Samples were cut from an hydrated sheet of hydrogel material using a size 6 cork borer. This gives a disk of 10mm diameter. The UV absorbance of each sample at 280nm was measured using an Hitachi UV spectrometer to give a background reading and the samples were then soaked in 2ml of each individual protein solution, ($0.5 mgml^{-1}$ concentration) for the required time period. After soaking, the UV absorbance at 280nm was remeasured. The test sample was placed right at the bottom of the UV cell filled with distilled water in order to obtain a consistent position and the absorbance was measured against distilled water. The progressive accumulation of protein on the material could then be calculated with reference to a standard Beer Lambert curve for each protein.

2.9 Surface Activity Measurement

The surface tension of linear polymers in aqueous solution was measured using a White Elec. Co digital surface balance. Measurements were carried out at a range of pH concentrations.

2.10 Analytical Techniques

FTIR spectra were obtained using a Nicolet 510 FT-IR. spectrometer interfaced to a Macintosh IIci computer

GPC analysis was carried out by analytical services at RAPRA Technology Ltd.

CHN analysis was carried out by Medac.

^{1}H and ^{13}C Nmr was carried out by Dr. M. Perry at Aston University

2.11 Measurement of the Leaching of Antibacterial Agents from Hydrogels

In a typical experiment not less than three small membranes, (5cm x 1cm), were made in the usual way incorporating 6% antibacterial agent. Before hydration the membranes were weighed. After 30 minutes hydration in distilled water the membranes were dehydrated to constant weight in a microwave oven for 10 minutes and reweighed. This procedure was repeated after every hours hydration for a subsequent four hours and then after every 24 hours for 1 week. A graph of weight loss against time was plotted to give an indication of how much antibacterial agent leached from the membrane over a period of time.

2.12 Antibacterial Testing

Antibacterial testing has been carried out by the Department of Clinical Microbiology at the Queen Elizabeth Hospital in Birmingham and also by Dr. Christine Jakeman from the Department of Pharmacy at Aston University. Zone inhibition testing was carried out by placing the sample hydrogels, containing antibacterial agent, on nutrient agar plates which had been seeded with micro-organisms. The diameter of the zone of inhibition around the material was measured after incubation for 24 hours at 37°C.

CHAPTER 3

Water Binding Studies of Hydrogels Incorporating a Basic Monomer.

3.1 Introduction

The most important property of an hydrogel is its equilibrium water content, which will have a bearing on its other physical properties. However the states of water in the gel i.e. the ratio of freezing to non-freezing water will also influence its properties.

Several techniques have been used to study the water binding properties of hydrogels, including nuclear magnetic resonance spectroscopy, differential scanning calorimetry (DSC), dilatometry and specific conductivity. For this work DSC was chosen as being the most convenient. This is because small samples are easily prepared and sealed in aluminium pans which minimises any loss of water from the sample. The ease with which the measurements are made enables results to be obtained quickly, and melt/freeze recycling can be carried out to give more detailed information on water crystallisation and structure from examination of the fine structure of the melting endotherm.

Although much work has already been published on the water structuring properties of many poly(2-hydroxyethyl methacrylate), (polyHEMA), copolymers and hydrogels synthesised from a wide range of hydrophilic and hydrophobic monomers, very little work has been carried out on the effect of incorporating a basic, potentially cationic monomer into an hydrogel copolymer. In 1991 Fushimi and his co-workers[124] studied the states of water in cationically charged poly(vinyl alcohol) membranes using both NMR spectroscopy and DSC. They state that the amounts of free and bound water depend on the mobility of the polymer chains, but they do not comment on the role of the cationic co-monomer and its effect on the states of water present.

This chapter presents the results of investigations into the water binding properties of simple polyHEMA copolymer systems containing up to 20% of a basic monomer and also more complex systems in which up to 20% of a basic monomer is incorporated into an hydrogel containing both hydrophilic and hydrophobic components. The pH of the hydration water was measured as between 7.3 and 7.6 thus making it a reasonable assumption that the basic units in the polymer will carry a degree of positive charge. All the results are illustrated in graphical form to illustrate clearly the trends associated with changing composition. However results are tabulated in Appendix 2 to show the numerical values of the equilibrium water content, freezing water and non-freezing water content.

3.2 Composition of Copolymer Hydrogels

In all the copolymer systems used in this work, there is substantially complete conversion with only trace amounts of monomer being eluted once the polymer is hydrated. Thus the composition of the copolymers is essentially as predicted from the feed ratio. This has been previously confirmed by elemental analysis and density measurements on hydrated and dehydrated polymers[51].

The sequence distributions of the copolymers prepared in this work may be predicted using the 'COPOL' and 'TERPOL' computer simulation program described in Chapter 1. In order to predict the sequence distributions of these polymers, the monomer reactivity ratios for each monomer pair is needed. Reported values for the monomer reactivity ratios of the systems used in this work are given in Table 3.1.

Monomer 1	Monomer 2	r_1	r_2	Reference
HEMA	NVI	18.12*	0.05*	125
HEMA	DMAEMA	1.86*	0.25*	126
NNDMA	CHMA	0.40	1.73	64
NNDMA	NVI	4.16	0.20	64
NNDMA	DMAEMA	0.50*	1.16*	126
AMO	CHMA	0.45*	2.05*	127
AMO	NVI	3.34*	0.17*	127
AMO	DMAEMA	0.59*	1.44*	126
CHMA	NVI	5.58	0.06	125
CHMA	DMAEMA	1.35*	0.73*	126

Table 3.1 Relative reactivity ratios for copolymer hydrogel systems studied (* values calculated from Q-e scheme)

Monomer	Q value	e value
HEMA	1.78	-0.39
NVI	0.11	-0.68
DMAEMA	0.68	0.48
CHMA	0.88	0.35
NNDMA	0.41	-0.26
AMO	0.39	0.08

Table 3.2 Q and e values for monomers used

Where no literature values have been reported for a copolymer, r_1 and r_2 were calculated from the Q-e values[128] as described in Chapter 1. Q and e values for each of the monomers used are listed in Table 3.2. In the case of cyclohexyl methacrylate, (CHMA), no Q and e values could be found in the literature. As Q and e values have been assigned based on the monomer reactivity and polarity, a reasonable approximation for the Q and e values of CHMA was given by the Q and e values of benzyl methacrylate. Examples of the sequence distributions of the copolymers prepared in this work are given in Appendix 1.

In all the sequence distributions presented in Appendix 1 it is apparent that NVI is less reactive to vinyl polymerisation than DMAEMA and DMAEMA is more readily distributed throughout the copolymer and terpolymer systems than NVI. The sequence distributions of the terpolymers containing NNDMA are very similar to those containing AMO as these monomers are very similar in their relative reactivities.

3.3 Water Binding Studies of PolyHEMA Hydrogels Copolymerised with a Basic Monomer

There is much literature available on the water binding properties of polyHEMA[13,20,21] and for this reason polyHEMA was chosen as the hydrophilic monomer with which to copolymerise either N-vinyl imidazole, (NVI) or dimethylaminoethyl methacrylate, (DMAEMA). The effects of incorporating increasing percentages of these basic co-monomers on the equilibrium water content and the ratio of freezing and non-freezing are presented in Figures 3.1 and 3.2.

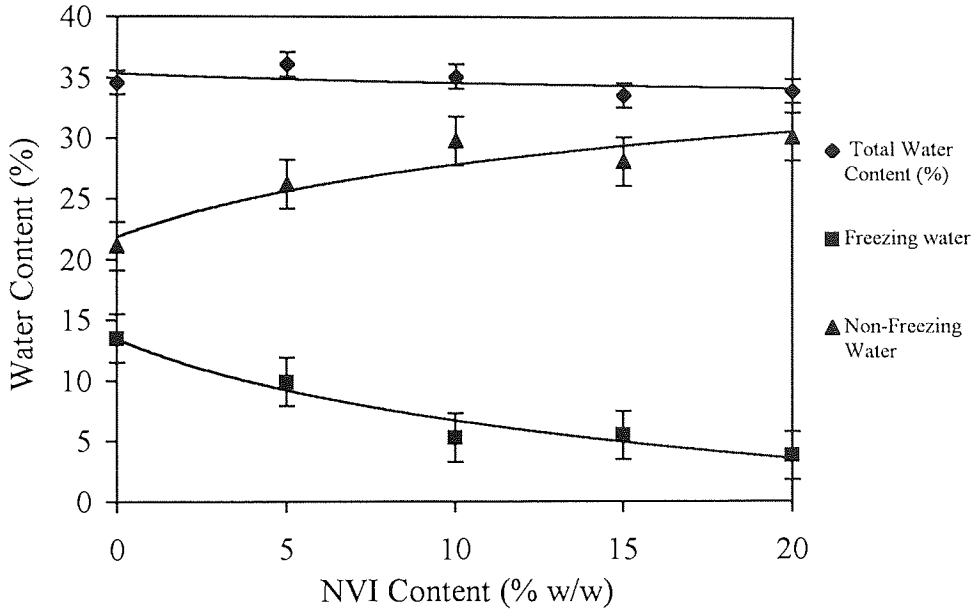

Figure 3.1 Graph to show the effect of composition on the water content of polyHEMA copolymerised with 0-20% NVI

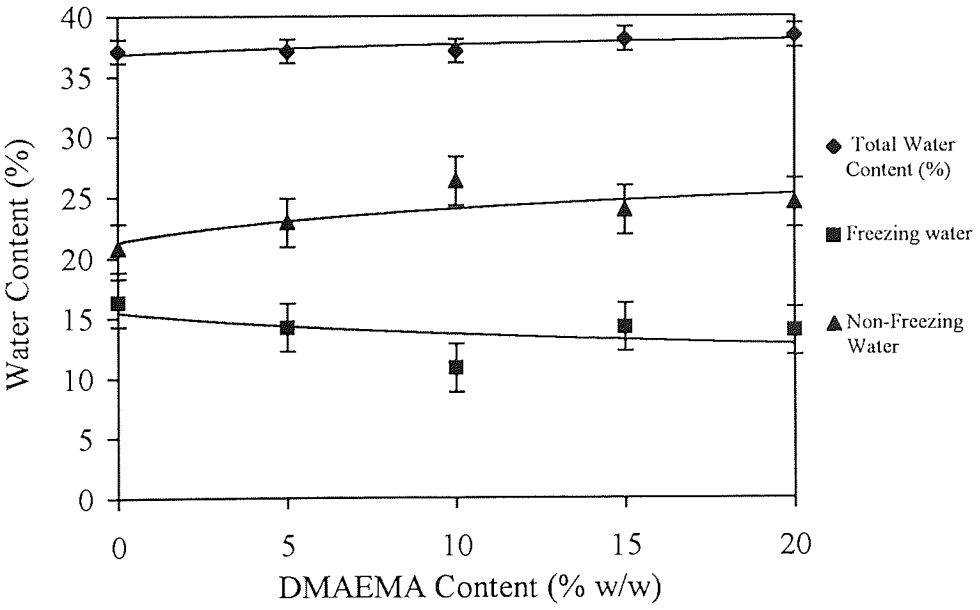

Figure 3.2 Graph to show the effect of composition on the water content of polyHEMA copolymerised with 0-20% DMAEMA

Although expressing the water contents as percentages clearly illustrates the change in total water content and freezing water content, occasionally - especially in hydrogels with a high equilibrium water content, the trend in non-freezing water can be obscured. Expressing the water content as grams of water / gram of polymer or moles of water / mole of repeat unit overcomes this problem and gives an indication of the water binding potential of a single monomer unit. Figure 3.3 and 3.4 show the results obtained when expressed in this way.

Studying Figure 3.1 it can be seen that increasing the NVI content from 0% to 20% has very little effect on the equilibrium water content. However there is a significant decrease in the freezing water content and an increase in the value of non-freezing water. The increase in non-freezing water content is also seen in Figure 3.3.

Comparing these results to those in Figures 3.2 and 3.4, where the NVI has been replaced with DMAEMA, similar trends can be observed. The equilibrium water content shows very little change while the freezing water content shows a small decrease along with a slight increase in the percentage of non-freezing water.

Although NVI is a polar, hydrophilic monomer it has a bulky ring structure as a side group. This conveys a degree of steric hindrance limiting the availability of the hydrophilic sites. DMAEMA has an additional ester group and no ring structure, but it still has a relatively bulky side group and it also has an α-methyl group limiting the mobility of the polymer chain. Thus neither monomer significantly increases the equilibrium water content as their degree of hydrophilicity is offset by steric factors.

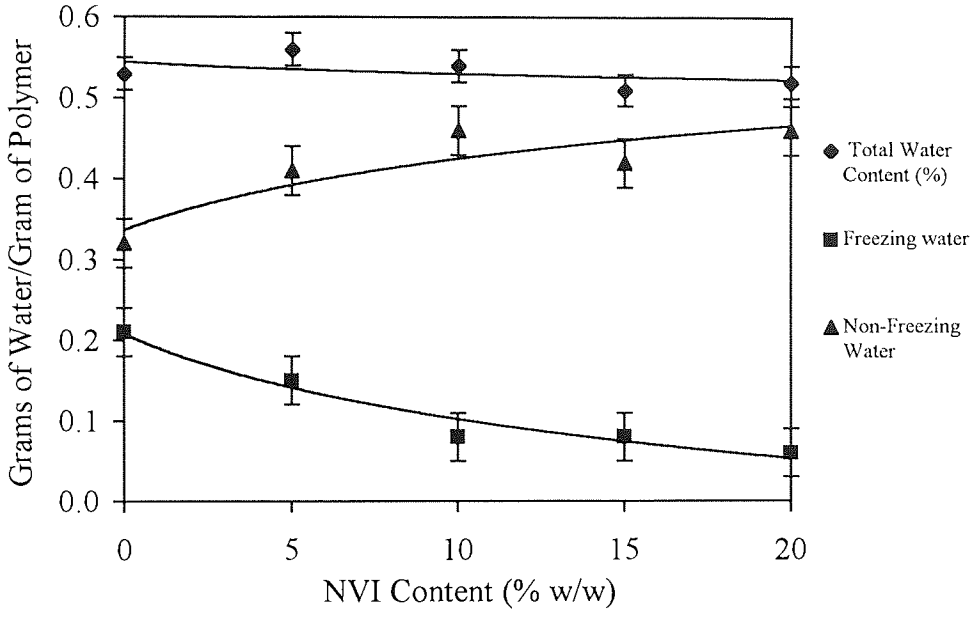

Figure 3.3 Graph to show the effect of composition on the water binding properties of polyHEMA copolymerised with 0-20% NVI

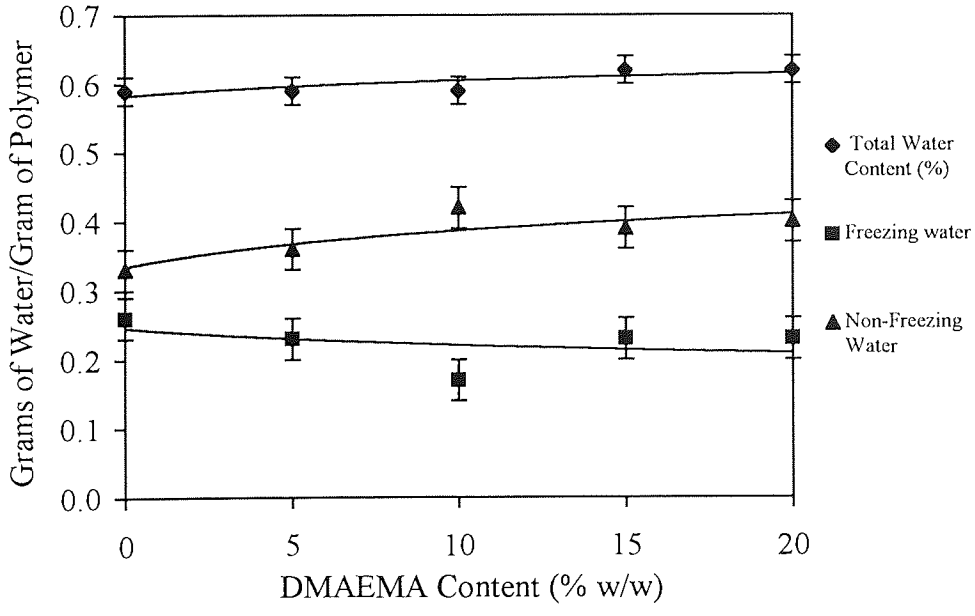

Figure 3.4 Graph to show the effect of composition on the water binding properties of polyHEMA copolymerised with 0-20% DMAEMA

The bulky ring conformation of the NVI side group may also account for the reduction in freezing water content observed when the percentage of NVI is increased, the limited mobility of the polymer leading to a reduction in the availability of hydrophilic sites. However the associated rise in non-freezing water content, (from 2.4 moles of non-freezing water per polymer repeat unit for polyHEMA to 3.1 moles for the HEMA-NVI 80:20 copolymer), suggests that as the NVI content increases a much higher proportion of the water is strongly associated with the polymer. This indicates the ability of NVI to promote hydrogen bonding of the water to the polymer chain. Incorporation of increasing percentages of DMAEMA shows a similar trend in the ratio of freezing to non-freezing water, (from 2.4 moles of non-freezing water per polymer repeat unit for polyHEMA to 2.9 moles for the HEMA-DMAEMA 80:20 copolymer), but the change is less significant. This suggests that DMAEMA is less effective in its ability to increase the proportion of water strongly associated with the polymer.

3.4 Water Binding Properties of New Materials Copolymerised with Basic Monomers

One of the broader aims of the project was to consider the design of new materials that had the ability to respond to changes in their environment e.g. pH variations and also to show increased resistance to bacterial infection by displaying antimicrobial properties. Investigations into antibacterial agents and novel polymeric antibacterials, described in more detail in Chapter 7, revealed that the criteria for the design of new polymeric antibacterial materials included regions of hydrophilicity and hydrophobicity as well as cationic sites for the interaction of the material with the negatively charged

cell walls of bacteria. This is similar to the requirements for the design of a surface active, pH responsive material. Novel hydrogel materials have been prepared using this criteria and their physical properties have been measured. The hydrophilic monomers used were either N,N'-dimethylacrylamide (NNDMA) or acryloyl morpholine (AMO). They were copolymerised with the hydrophobic component, cyclohexyl methacrylate (CHMA) and differing proportions of the potentially cationic monomers, either N-vinyl imidazole (NVI) or dimethylaminoethyl methacrylate (DMAEMA).

NNDMA was chosen as the hydrophilic monomer as it offers a potential increase in equilibrium water content over HEMA. Choosing NVP as the hydrophilic monomer would also lead to a higher potential equilibrium water content, however NVP has a low reactivity to free radical polymerisation and resulting copolymers would have a blocky sequence distribution rather than the desired alternating sequence distribution that has been demonstrated to show enhanced compatibility[129,130]. Recent work by this research group has shown AMO to have great potential for use in hydrogel systems for biomedical use. It has been shown to give copolymers with a good alternating sequence distribution and resulting hydrogels have shown acceptable equilibrium water contents and mechanical properties coupled with promising *in vitro* biocompatibility results[131]. It was hoped that indene could be used as the hydrophobic monomer as it has been shown to give linear copolymers with a reasonably alternating sequence distribution[64]. However problems occurred in the synthesis of hydrogel membranes using indene and CHMA was used in its place.

3.4.1 The Effect of Incorporating a Basic Monomer into NNDMA-CHMA 80:20 Materials

Figure 3.5 illustrates the effect on the water content, of increasing percentages of NVI when added to a copolymer of NNDMA-CHMA 80:20. This effect is also represented in terms of grams of water / gram of polymer to highlight more effectively the trend in non-freezing water, and is shown in Figure 3.7.

From these Figures, it is clear that the addition of the basic monomer, NVI causes an increase in the total water content of the system. The freezing water content also shows an increase corresponding to the increasing percentage of NVI. The trend in non-freezing water seems less apparent from Figure 3.5, but expressing the values as moles of water / mole of copolymer repeat unit, there is a marginal increase from 5.0 moles of water / mole of copolymer repeat unit for NNDMA-CHMA 80:20 to 5.5 for NNDMA-CHMA-NVI 56:24:20.

Figures 3.6 and 3.8 similarly represent the trends in total water content and the ratio of freezing to non-freezing water for NNDMA-CHMA 80:20 copolymers containing progressive incorporation of DMAEMA. From these Figures it can be seen that the effect of DMAEMA on these copolymers is not significantly different from the effect of NVI on copolymers of a similar composition.

The increase in total water content seen with the introduction of increasing percentages of either basic monomer can be attributed to an increase in the ratio of

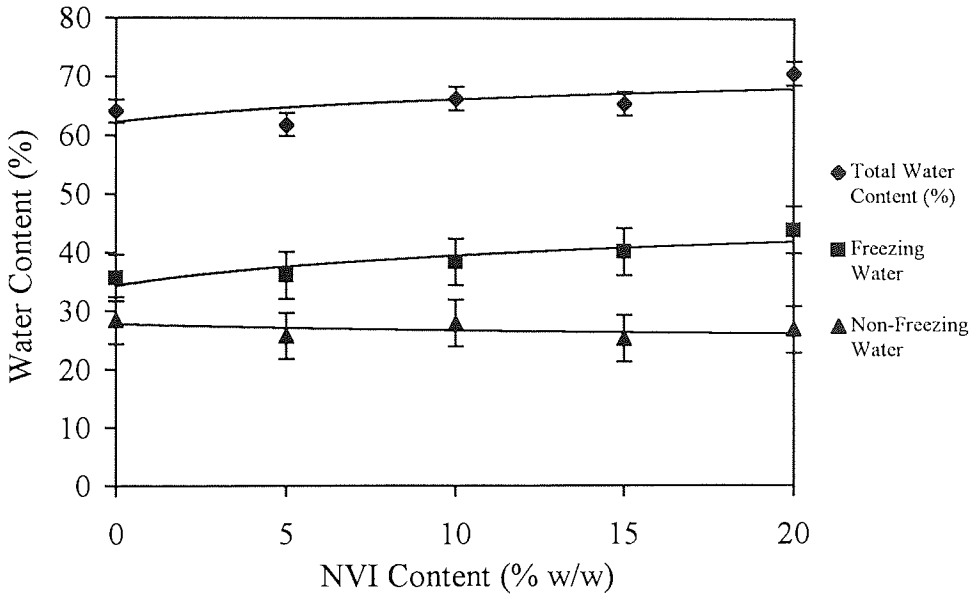

Figure 3.5 Graph to show the effect of composition on the water content of NNDMA-CHMA 80:20 materials copolymerised with 0-20% NVI

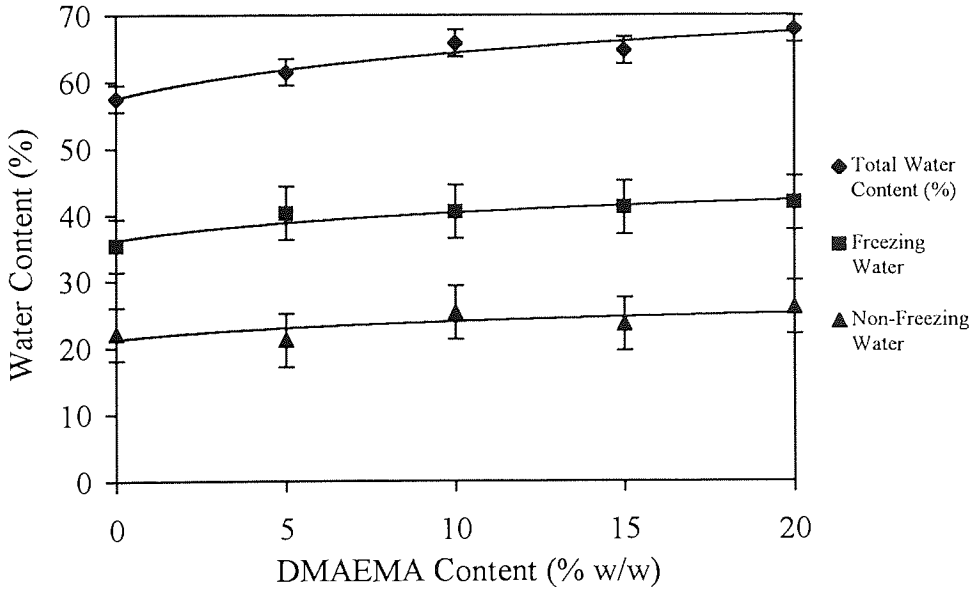

Figure 3.6 Graph to show the effect of composition on the water content of NNDMA-CHMA 80:20 materials copolymerised with 0-20% DMAEMA

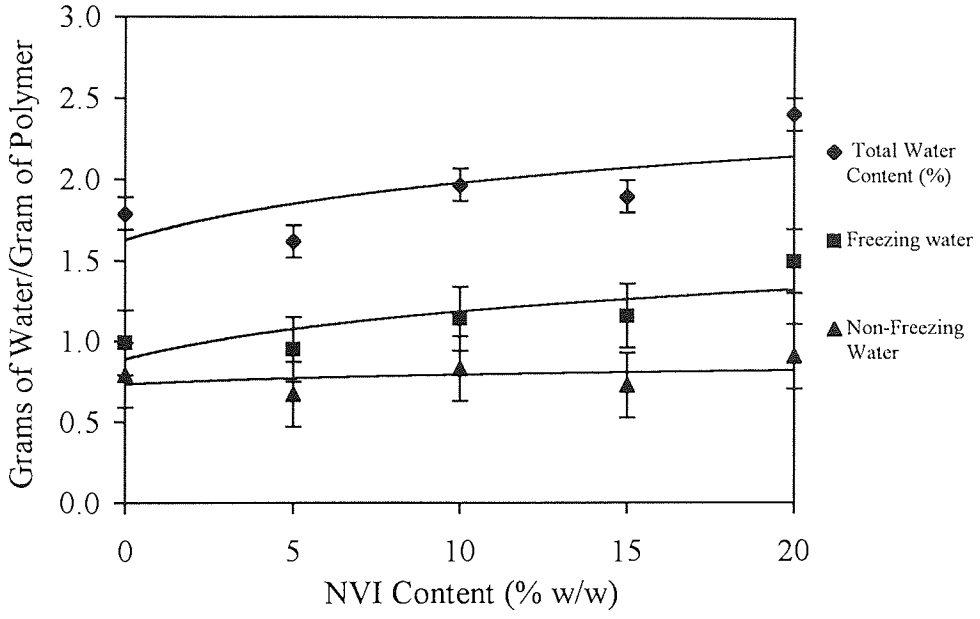

Figure 3.7 Graph to show the effect of composition on the water binding properties of NNDMA-CHMA 80:20 materials copolymerised with 0-20% NVI

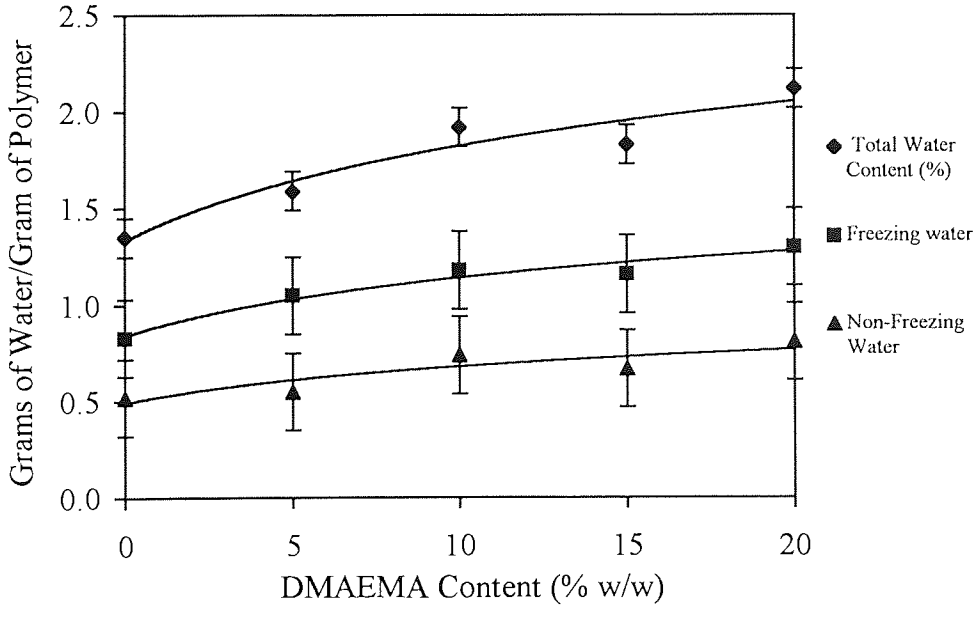

Figure 3.8 Graph to show the effect of composition on the water binding properties of NNDMA-CHMA 80:20 materials copolymerised with 0-20% DMAEMA

hydrophilic to hydrophobic monomers in the copolymer system, thus increasing the ability of the copolymer to imbibe water. The accompanying increase in freezing water would also be expected, with the progressive incorporation of an hydrophilic monomer introducing more hydrophilic sites. The trend in non-freezing water is seen more clearly from Figures 3.7 and 3.8. The small increase observed is explained by the increasing availability of hydrophilic biding sites accompanying the progressive incorporation of the hydrophilic, basic monomer. It seems that there is little difference in effect between NVI and DMAEMA. A comparison of the structures has been made in Section 3.3, where it was noted that the bulky ring side group of NVI restricted the mobility of the polymer chains, as did the α-methyl group and bulky side group of the DMAEMA. With both monomers affected by similar steric factors, it was not unexpected that they show similar effects in their contribution to the water structuring ability of the copolymer.

3.4.2 The Effect of Incorporating a Basic Monomer into NNDMA-CHMA 70:30 Materials

Figures 3.9-3.12 show the effect of the two basic monomer on the water binding properties of NNDMA-CHMA 70:30 copolymers. Thus not only is the effect of a basic centre observed but also the effect of a higher proportion of hydrophobic regions. From these Figures it can be seen that again, the incorporation of increasing percentages of either NVI or DMAEMA produces a corresponding increase in total water content and also in freezing water content. The non-freezing water content in this case does not appear to be significantly affected by higher percentages of NVI or DMAEMA.

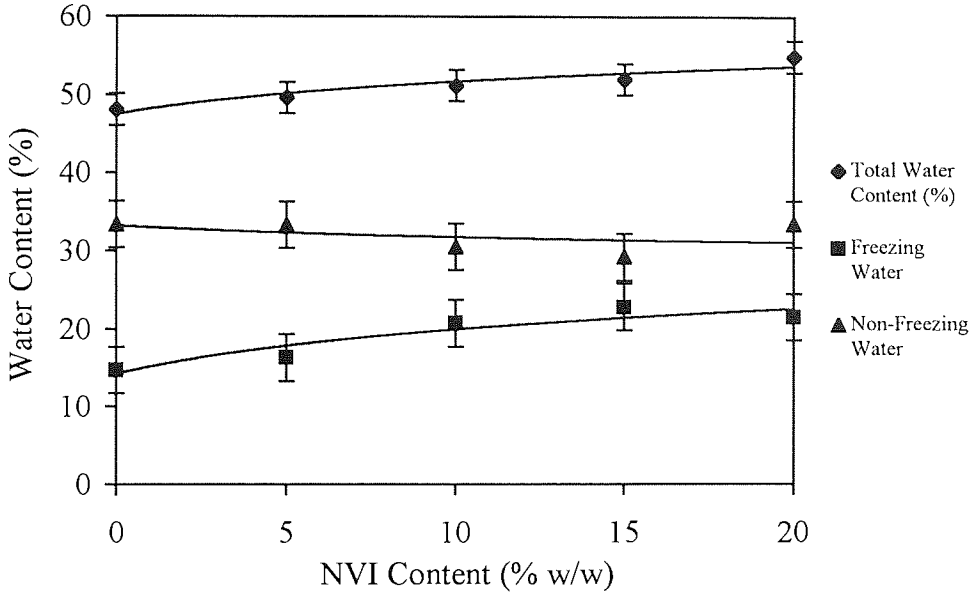

Figure 3.9 Graph to show the effect of composition on the water content of NNDMA-CHMA 70:30 materials copolymerised with 0-20% NVI

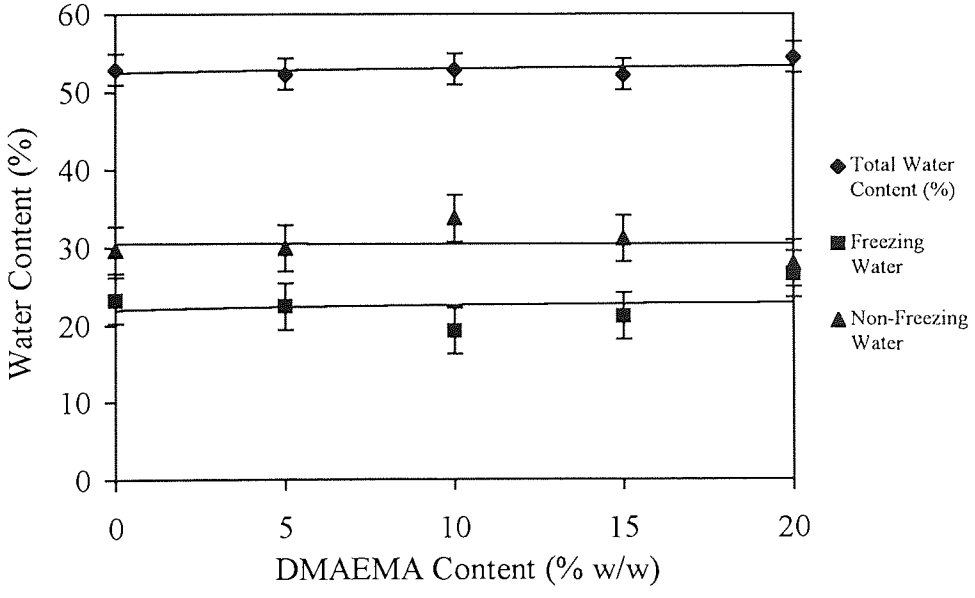

Figure 3.10 Graph to show the effect of composition on the water content of NNDMA-CHMA 70:30 materials copolymerised with 0-20% DMAEMA

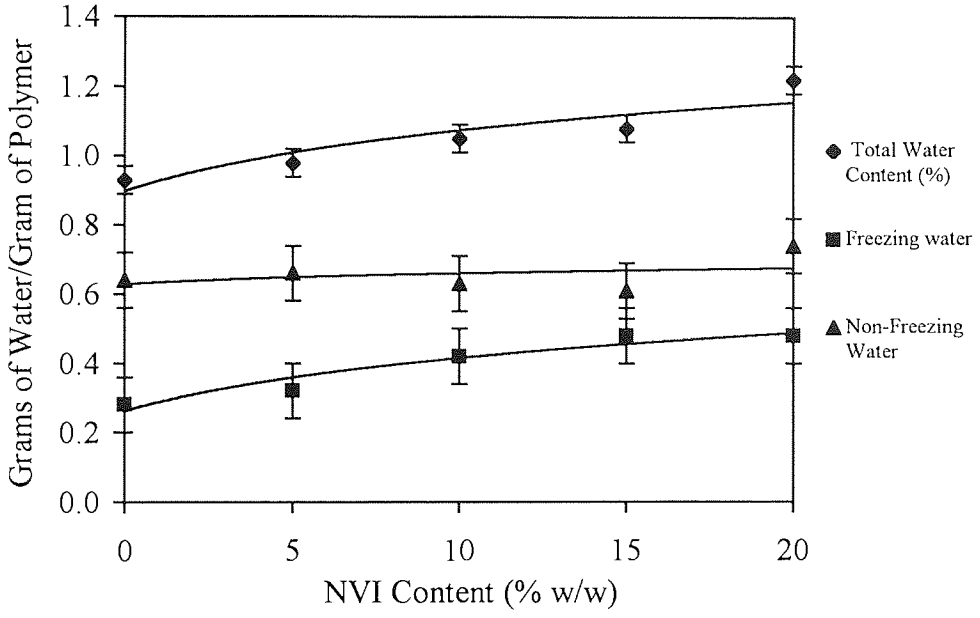

Figure 3.11 Graph to show the effect of composition on the water binding properties of NNDMA-CHMA 70:30 materials copolymerised with 0-20% NVI

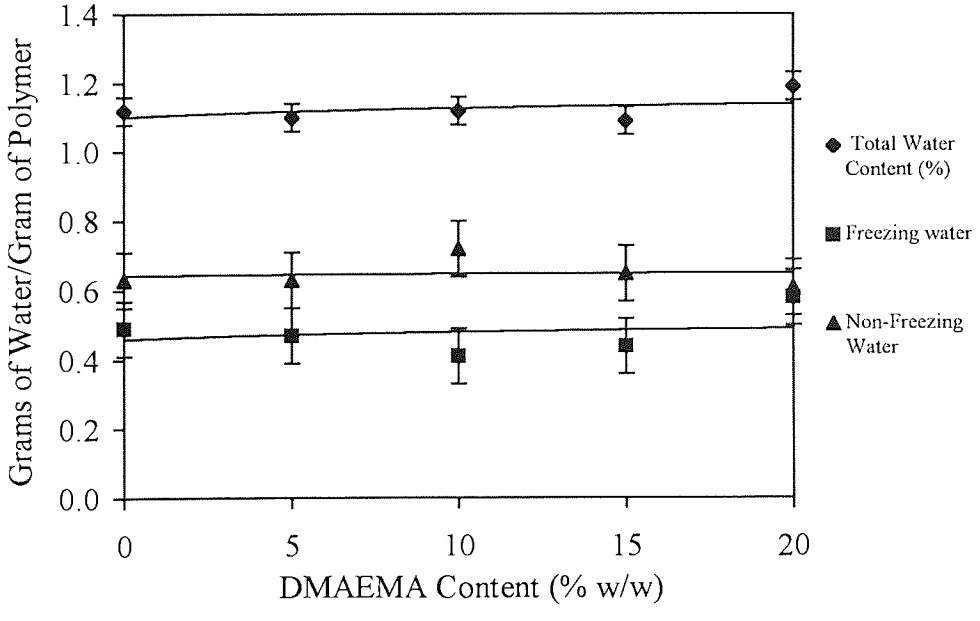

Figure 3.12 Graph to show the effect of composition on the water binding properties of NNDMA-CHMA 70:30 materials copolymerised with 0-20% DMAEMA

When comparing the results obtained here with those presented in Section 3.4.1 it can be seen that a higher proportion of hydrophobic monomer in the polymer system causes a decrease in the total water content of the hydrogel. There is also a relatively large decrease in freezing water content, whilst the value of the non-freezing water is not significantly affected. The lower values obtained for the total water contents of the NNDMA-CHMA 70:30 systems in comparison to the NNDMA-CHMA 80:20 systems is simply a consequence of an increased ratio of hydrophobic sites. The increase in CHMA percentage causes little difference in the non-freezing water content, but a large decrease in freezing water content since the introduction of a bulky hydrophobic side group decreases both the mobility and the hydrophilicity within the network. The effects of a higher concentration of hydrophobic monomer seen here are entirely consistent with results previously obtained in this group[132,133] where the introduction of increasing percentages of styrene reduced the equilibrium water content and the freezing water content of a polyHEMA hydrogel. CHMA and styrene are very similar in structure, both having sterically hindering ring side groups, and the results observed demonstrates the importance of steric effects and the availability of water binding sites within the polymer.

3.4.3 The Effect of Incorporating a Basic Monomer into AMO-CHMA 80:20 Materials

As mentioned in Section 3.4, AMO has shown potential in previous studies by this research group for incorporation into hydrogel systems for biomedical applications. Thus Sections 3.4.3-3.4.4 deal with the incorporation of basic monomers into hydrogels where the hydrophilic component NNDMA has been replaced with AMO.

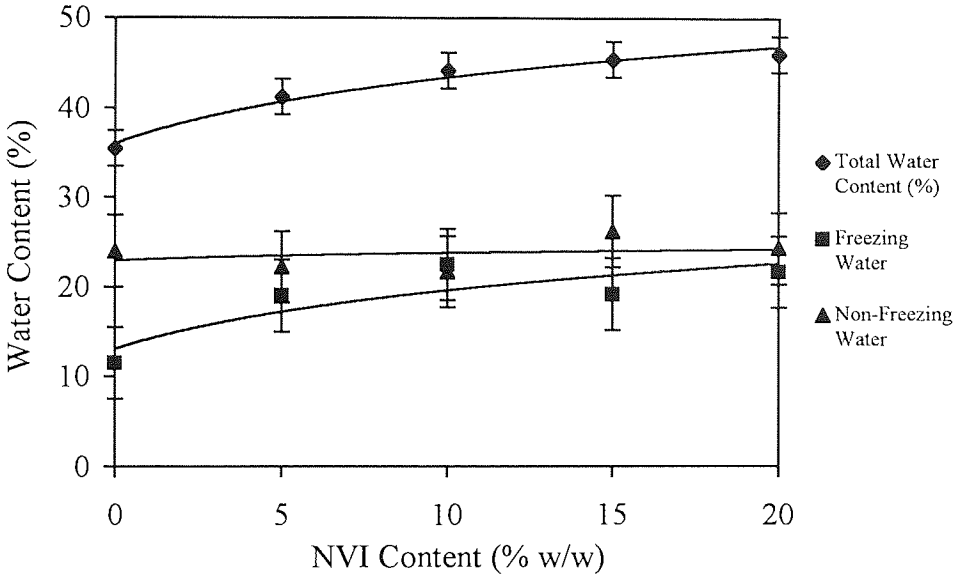

Figure 3.13 Graph to show the effect of composition on the water content of AMO-CHMA 80:20 materials copolymerised with 0-20% NVI

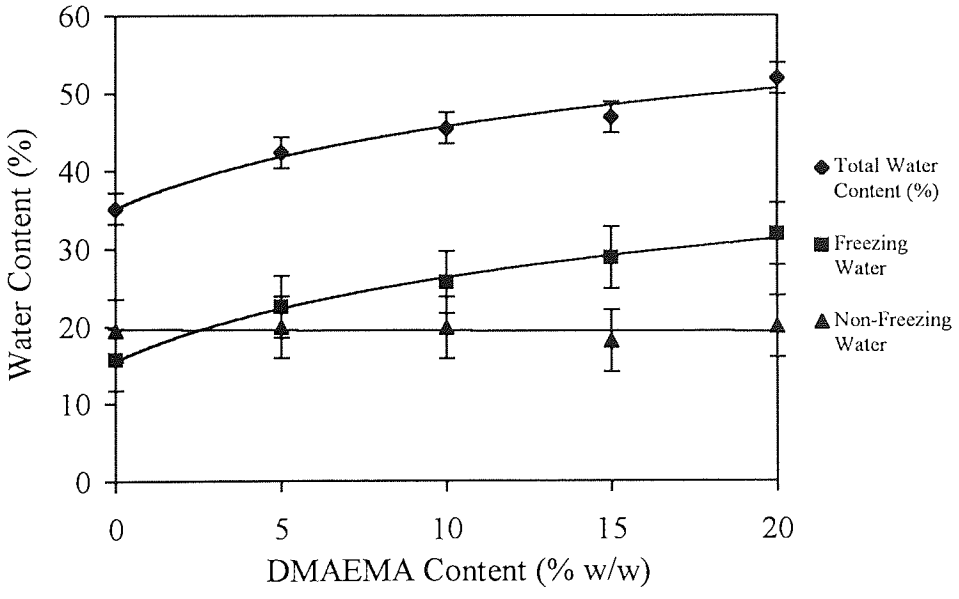

Figure 3.14 Graph to show the effect of composition on the water content of AMO-CHMA 80:20 materials copolymerised with 0-20% DMAEMA

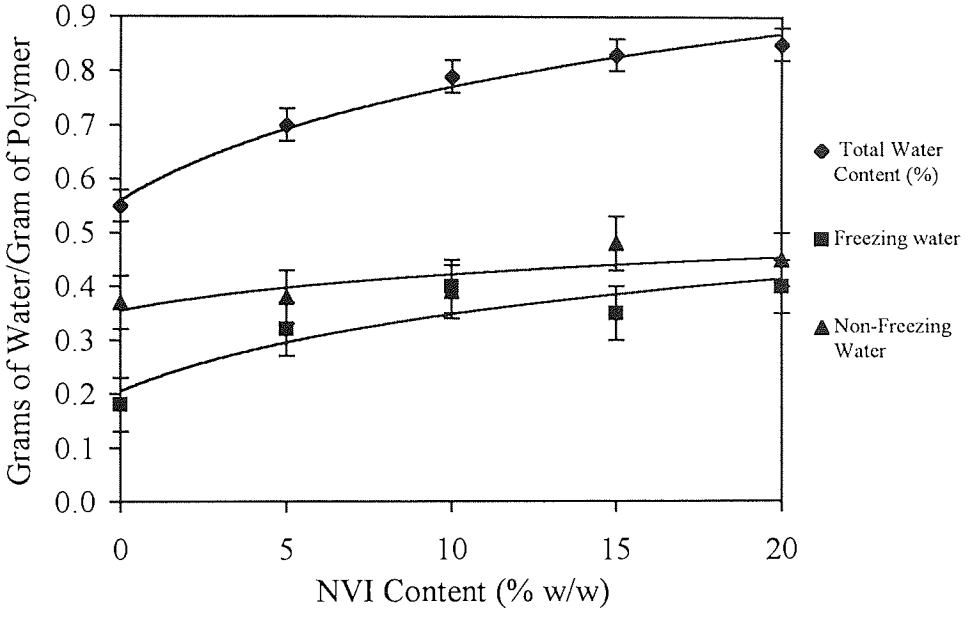

Figure 3.15 Graph to show the effect of composition on the water binding properties of AMO-CHMA 80:20 materials copolymerised with 0-20% NVI

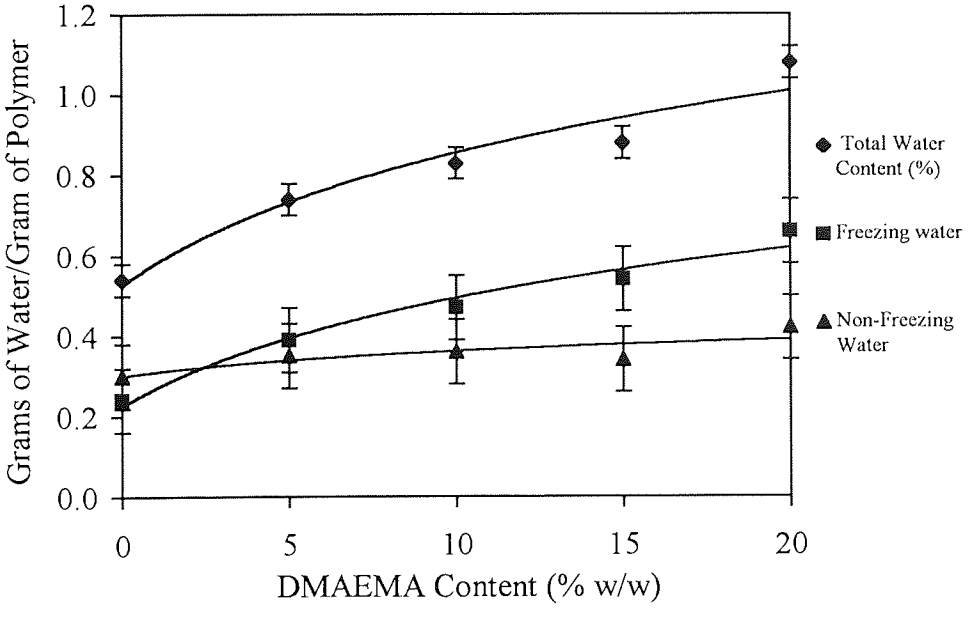

Figure 3.16 Graph to show the effect of composition on the water binding properties of AMO-CHMA 80:20 materials copolymerised with 0-20% DMAEMA

Figures 3.13-3.16 show the effect of the two basic monomers on the water binding properties of AMO-CHMA 80:20 copolymers, both in terms of percentages and in terms of grams of water / gram of polymer. As with NNDMA-CHMA hydrogel systems, incorporation of progressive amounts of either NVI or DMAEMA serves to increase the total water content. An increase in freezing water content is also observed coupled with a marginal increase in non-freezing water. If Figures 3.13-3.16 are compared to Figures 3.5-3.8 it can be seen that substituting AMO for NNDMA in these systems gives rise to a decrease in the total water content and also for the freezing and non-freezing water values.

Once again the effect of the basic monomer is to increase the proportion of hydrophilic monomer and thus increase the amount of water binding sites leading to higher values of freezing water content as well as total water content. The observed effect of replacing NNDMA with AMO leads to the conclusion that AMO is less hydrophilic than NNDMA and the ring structure of the AMO side group restricts the mobility of the polymer network thus reducing the amount of available water binding sites.

3.4.4 The Effect of Incorporating a Basic Monomer into AMO-CHMA 70:30 Materials

Figures 3.17-3.20 show the effect of the two basic monomer on the water binding properties of AMO-CHMA 70:30 copolymers, both in terms of percentages and in terms of grams of water / gram of polymer.

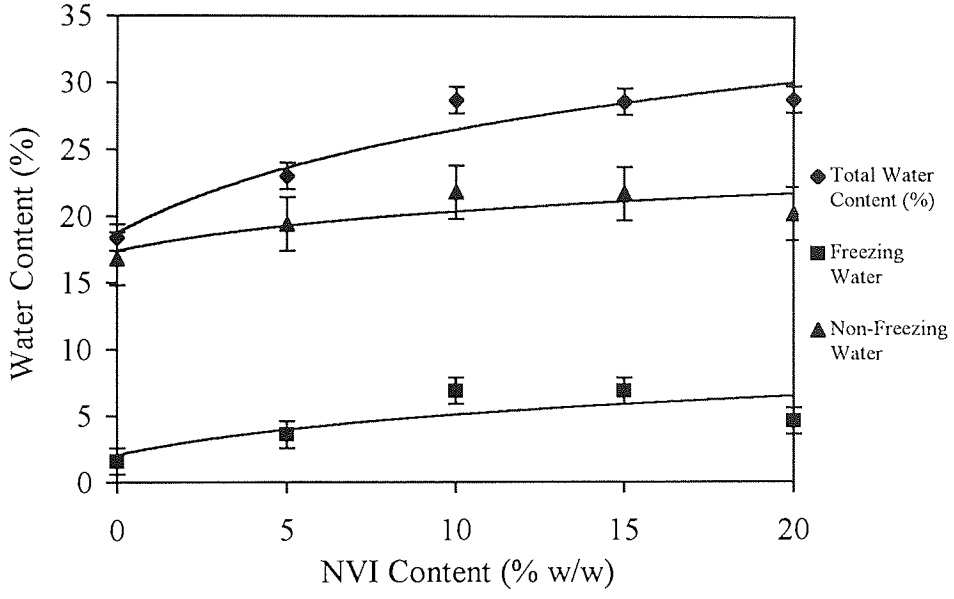

Figure 3.17 Graph to show the effect of composition on the water content of AMO-CHMA 70:30 materials copolymerised with 0-20% NVI

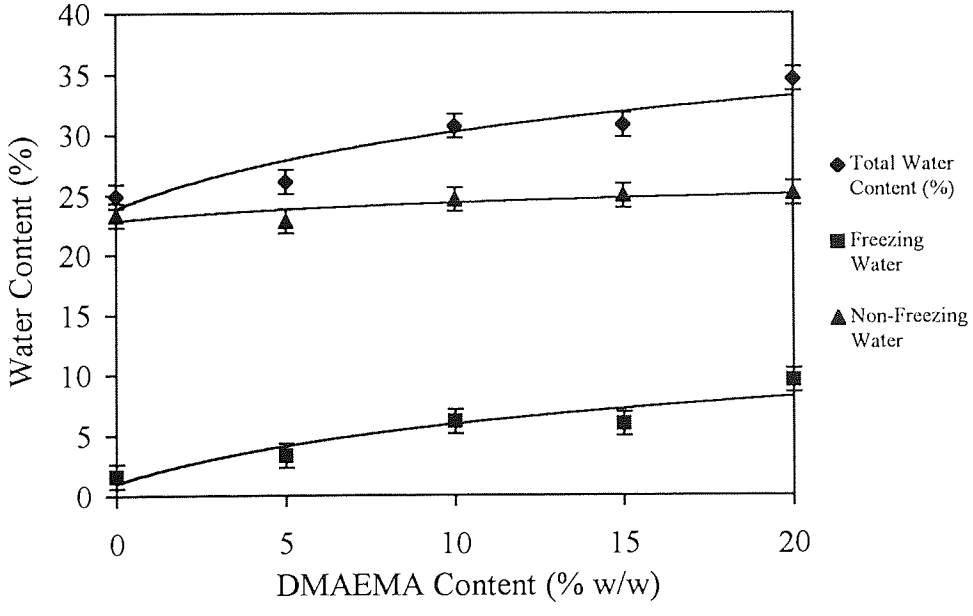

Figure 3.18 Graph to show the effect of composition on the water content of AMO-CHMA 70:30 materials copolymerised with 0-20% DMAEMA

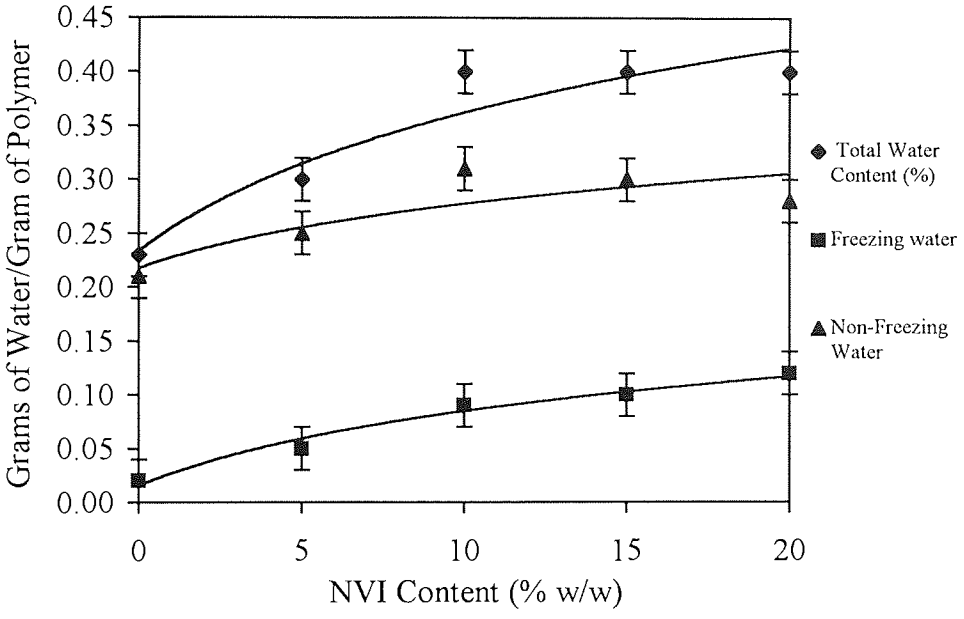

Figure 3.19 Graph to show the effect of composition on the water binding properties of AMO-CHMA 70:30 materials copolymerised with 0-20% NVI

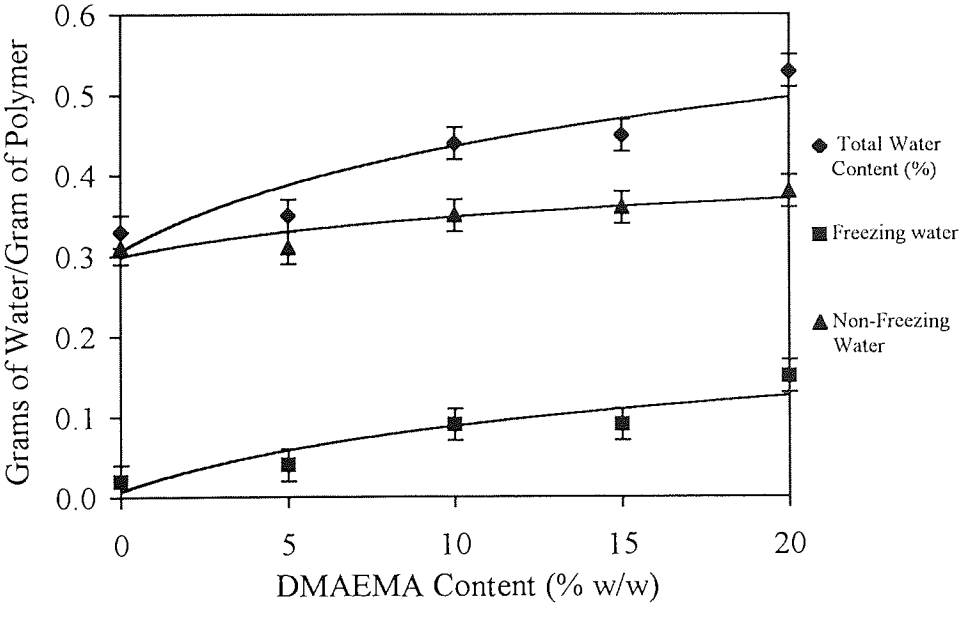

Figure 3.20 Graph to show the effect of composition on the water binding properties of AMO-CHMA 70:30 materials copolymerised with 0-20% DMAEMA

These results are consistent with the other results presented in this chapter in that addition of increasing percentages of either NVI or DMAEMA give rise to increases in total and freezing water contents together with a marginal increase in non-freezing water content. The effect of replacing NNDMA with AMO observed here is similar to that observed in Section 3.4.3 i.e. the values of total water content are lower, as are the values of freezing and non-freezing water. Finally the effect of a higher proportion of hydrophobic monomer, CHMA, is similar to that observed for NNDMA-CHMA hydrogel systems, serving to reduce the total water content and the freezing water content while the non-freezing water content remains relatively unaffected.

3.5 The Effect of Composition on the Structure of the Melting Endotherms.

The total freezing water content of an hydrogel is obtained from the area under the DSC melting curve. Further information about the states of water can also be obtained from the fine structure of the melting endotherm. Figures 3.21 and 3.22 show the melting endotherms obtained for copolymers of HEMA with 0-20% NVI and DMAEMA respectively. The melting endotherms for the HEMA-DMAEMA copolymers are all similar regardless of the percentage of basic monomer present. There are 2 distinct peaks, 1 at 274K and a broader peak at approximately 263K. The melting endotherms for the HEMA-NVI copolymers however show a clear trend with increasing NVI incorporation. There is a peak at 274K and a further peak at 263K in polyHEMA with no NVI but this peak at 263K decreases with progressive incorporation of NVI until at 20% NVI only the 274K peak remains.

The presence of two peaks in the melting endotherm suggests that there is some freezing water that has a lower melting temperature than that of pure water. Water unaffected by its polymeric environment will melt at a temperature similar to that of pure water i.e. 274K. The remaining water is somewhat affected by the polymer environment and will therefore melt at a lower temperature. Thus these results demonstrate that not all the freezing water in these samples is unaffected by the polymeric environment, and the fact that a significant proportion of the freezing water crystallises and remelts at a lower temperature than that of pure water provides evidence that water exists in a continuum of states between the two extremes of freezing and non-freezing water.

Incorporation of NVI leads to a decrease in the water that is affected by the polymeric environment until at a level of 20%, the freezing water in the sample melts at a temperature approaching the equivalent of pure water.

Examples of the trend in the melting endotherm for the series of hydrogel systems NNDMA-CHMA and AMO-CHMA with 0-20% NVI or DMAEMA are shown in Figures 3.23 and 3.24 respectively. All of the melting endotherms obtained for these series of hydrogel systems show similar features and there was no apparent trend corresponding to an increase in basic monomer. Once again two peaks are observed, one at 274K and a smaller, broader peak at 269K. These results also demonstrate that not all of the freezing water present in these samples remains unaffected by the polymeric environment.

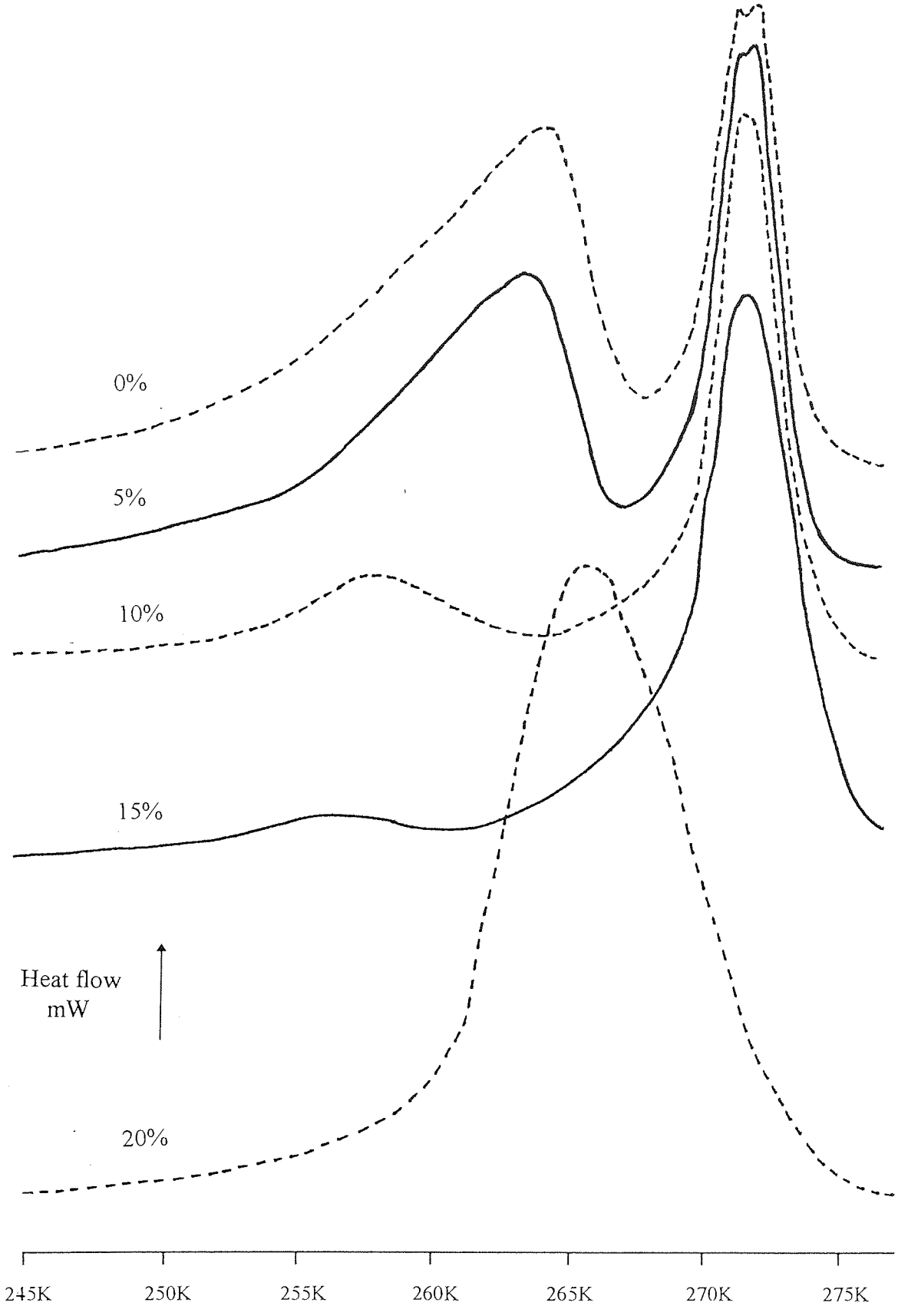

Figure 3.21 Typical melting endotherm of polyHEMA copolymerised with 0-20% NVI

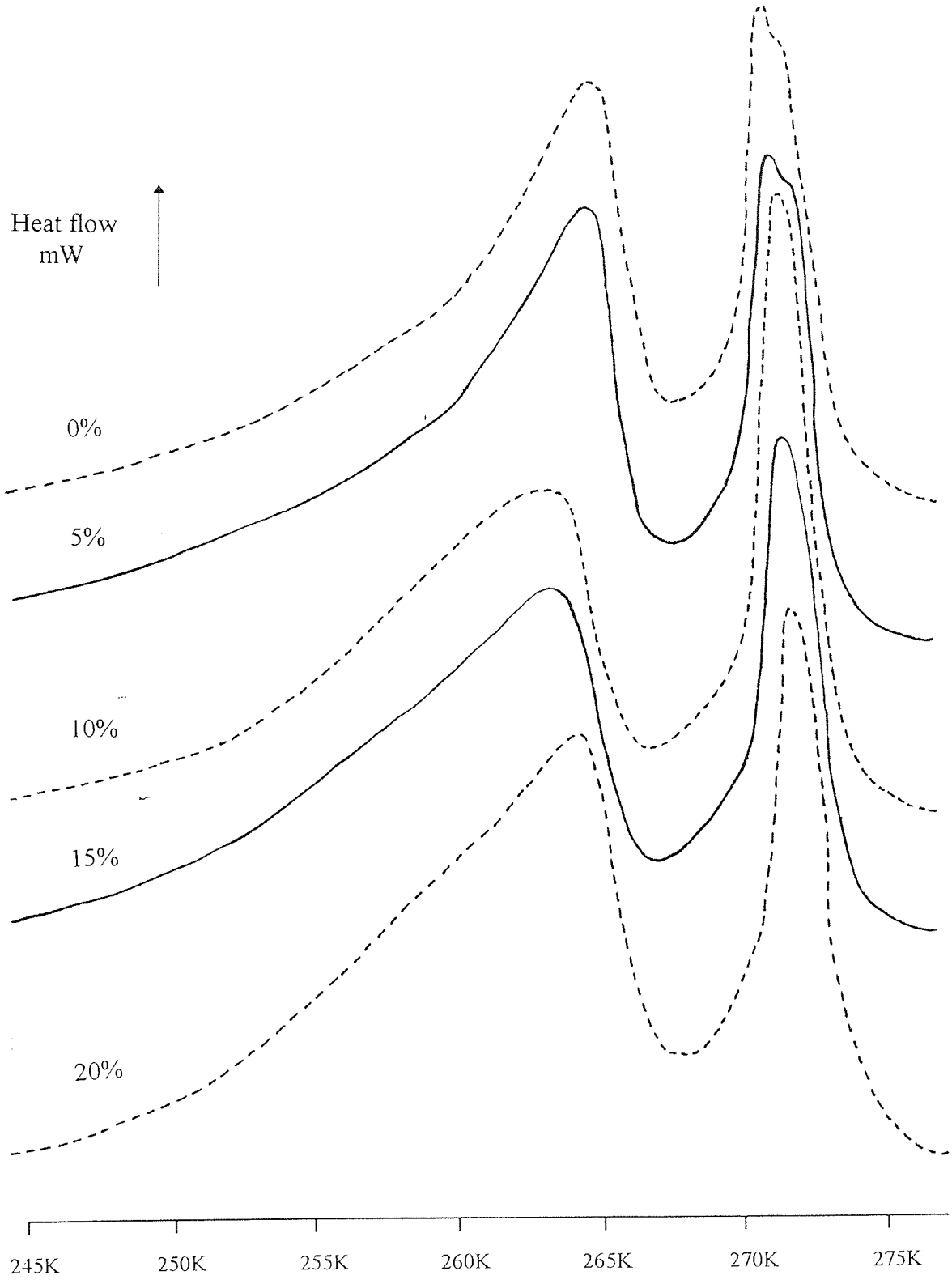

Figure 3.22 Typical melting endotherm of polyHEMA copolymerised with 0-20% DMAEMA

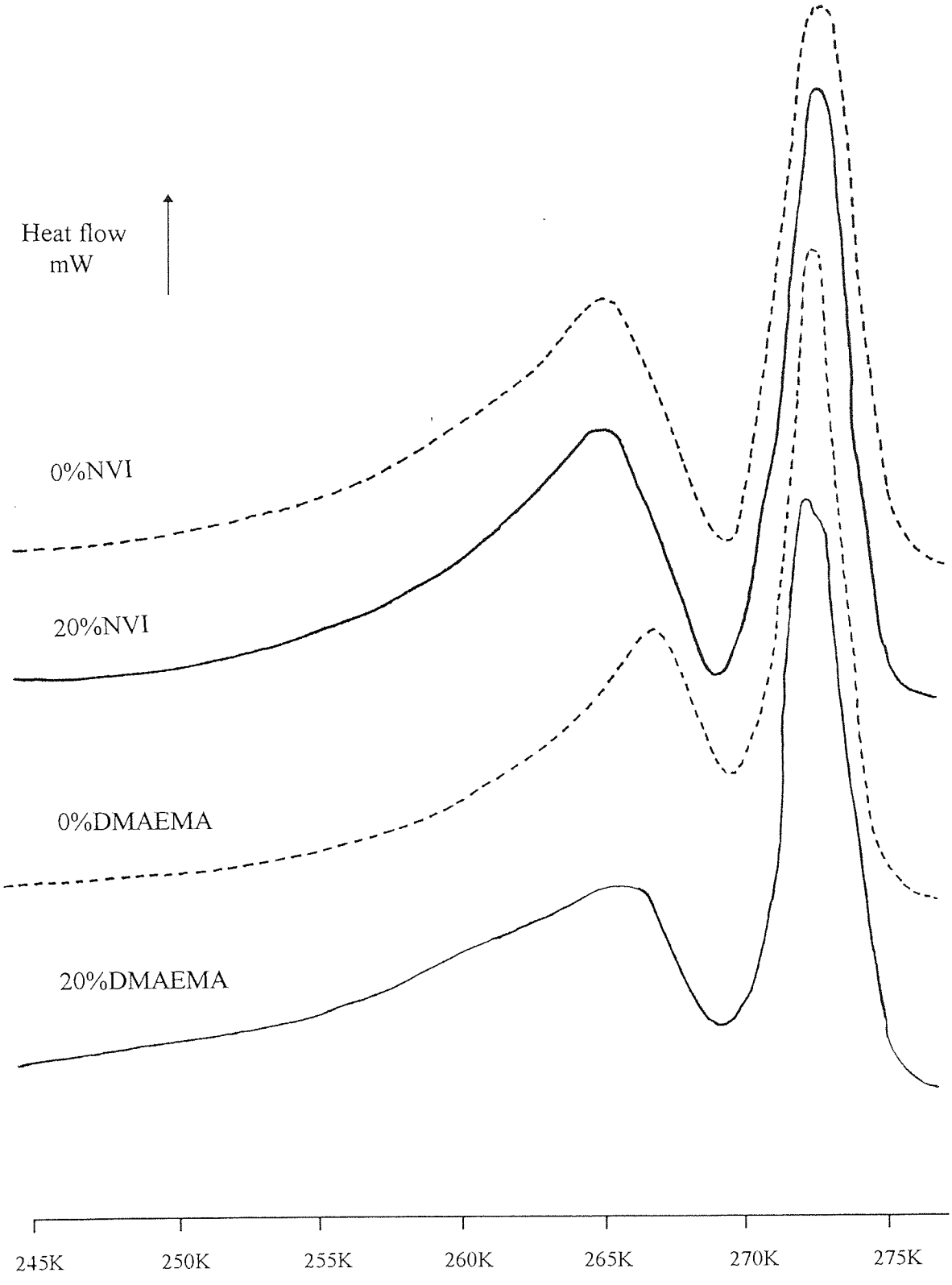

Figure 3.23 An example of the trend in melting endotherm of NNDMA-CHMA copolymerised with a)0% NVI, b)20% NVI, c)0% DMAEMA, d)20% DMAEMA

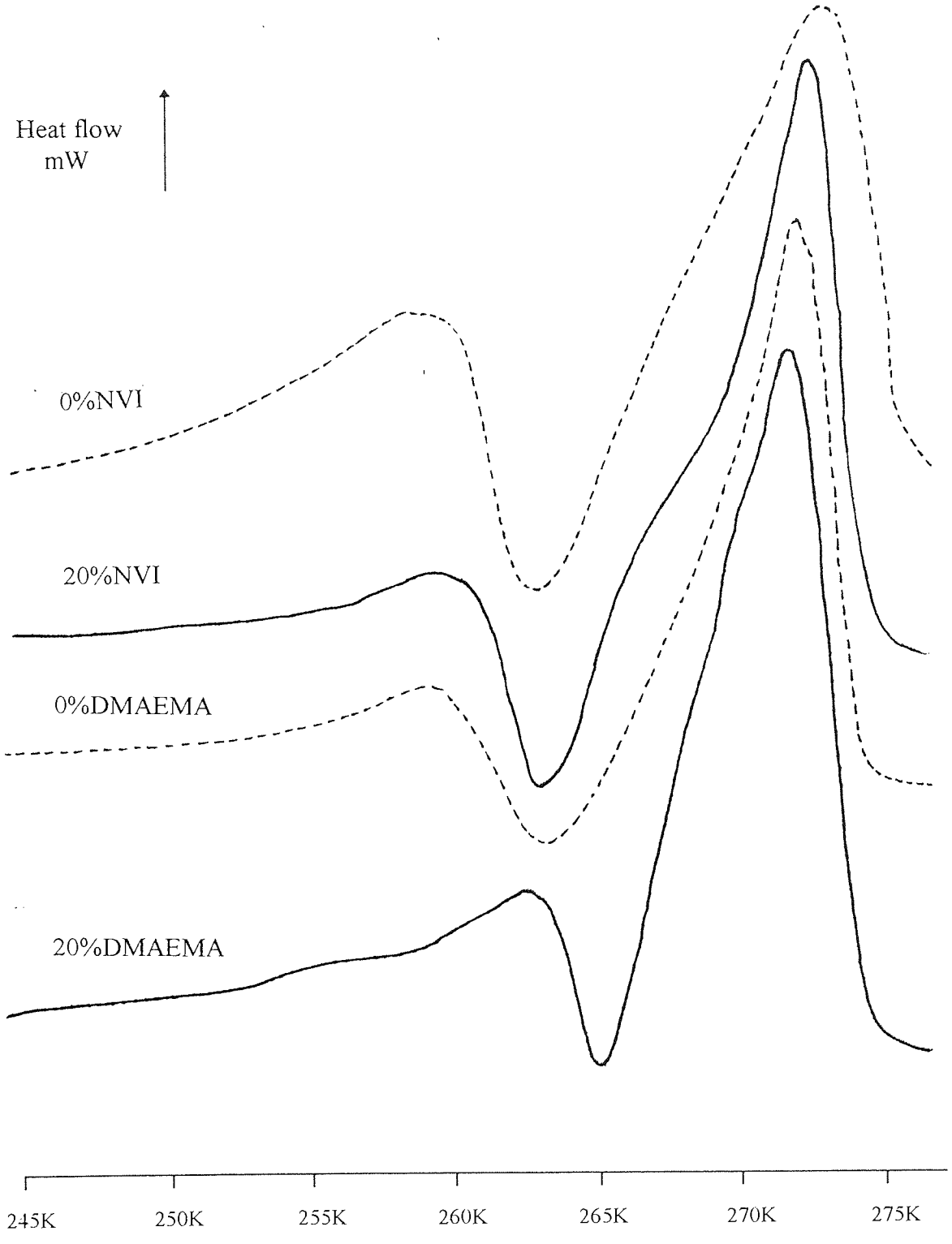

Figure 3.24 An example of the trend in melting endotherm of AMO-CHMA copolymerised with a)0% NVI, b)20% NVI, c)0% DMAEMA, d)20% DMAEMA

Temperature cycling of all of the samples shows an increase in the peak at 274K and a decrease in the other peak. Pedley and Tighe[134] and Corkhill *et al.*[132] have reported similar effects with hydrogel copolymers and have explained this increase in the peak at 274K with temperature cycling in terms of a move towards more ideal crystallisation behaviour.

3.6 Conclusions.

Water binding properties of a range of copolymers containing basic centres have been examined. The observations concerning the equilibrium water content and to the relation of freezing and non-freezing water are related to the balance of hydrophilicity and hydrophobicity in the copolymers together with the steric contributions of the monomers.

Values for the equilibrium water content, and the freezing and non-freezing water contents of polyHEMA with progressive incorporation of NVI and DMAEMA have been determined. In each case the EWC is relatively unaffected but the proportion of non-freezing water increases with a corresponding decrease in freezing water. The effect is more apparent in those samples containing NVI and appears to relate to the greater ability of NVI over DMAEMA to promote the hydrogen bonding of water to the polymer within the HEMA-NVI network.

Novel polymeric materials were prepared bearing in mind the criteria required for the ability to respond to changes in their environment. The EWCs and the freezing and

non-freezing water contents were determined. Addition of a basic monomer, be it either NVI or DMAEMA increases the water content slightly in all cases, due to the increase in the ratio of hydrophilic to hydrophobic sites within the polymer. This also accounts for the increase in freezing water content, although the non-freezing water content shows only a marginal increase. There appears to be no apparent difference in effects between NVI and DMAEMA, both having structural properties that contain a degree of steric hindrance.

Increasing the proportion of CHMA in these hydrogel systems lowers the value of the EWC as would be expected, and also lowers the value of the freezing water content. In this case however the non-freezing water content remains relatively unaffected and the results demonstrate the importance of steric effects and the availability of water binding sites within the polymer.

Substituting NNDMA with AMO lowers the EWC of the hydrogel samples and indicates the lower relative hydrophilicity of AMO in comparison with NNDMA. Reductions in the values of freezing and non-freezing water are also seen.

The fine structure of the DSC melting endotherm provides valuable information on the water structuring observed. The melting endotherms of all the hydrogel systems examined showed two peaks, indicating that not all the freezing water is entirely unaffected by the polymeric environment. The series of HEMA-NVI copolymers was the only series that showed a trend with increasing basic monomer content. The melting endotherm shows a move towards a single peak at 274K indicating the

freezing water in the polymer is less affected by the polymeric environment with increasing NVI content. One final point to note is that the complexity of the melting endotherms support the hypothesis that the water in hydrogels exists in a continuum of states.

CHAPTER 4

Mechanical Properties of Hydrogels Incorporating a Basic Monomer

4.1 Introduction

One of the limiting factors for the use of hydrogels as biomaterials has been the often very poor mechanical properties displayed by these materials. A good example of this is the poor tear strength of some contact lens materials as reported in the literature[33,53,84,135]. It is not unexpected that with higher equilibrium water contents, mechanical properties will suffer, but although water content has a marked effect on mechanical strength, the chemical structure of the polymer can also play a large part in determining its value. The elastic behaviour and rigidity of the materials will be governed by monomer structure and cross-link density, not just covalent but ionic, polar and steric interchain forces. The major factors contributing to the control of mechanical strength are the water binding properties.

Very little previous work has been carried out on the effect of basic monomers on the mechanical properties of hydrogels and this chapter describes the results of investigations into the mechanical properties of polyHEMA copolymer systems in which up to 20% of a basic monomer is incorporated. It also looks at more complex hydrogel systems in which up to 20% of a basic monomer is incorporated into a material containing both hydrophilic and hydrophobic components. Results for tensile strength (σ_b), Young's modulus (E) and elongation to break (ε_b) of each series of hydrogels are illustrated graphically and numerical values are presented in Appendix 3. As was the case for the water binding studies the pH of the hydration water was measured as between 7.3 and 7.6 thus making it a reasonable assumption that the basic units in the polymer will carry a degree of positive charge.

4.2 Mechanical Properties of PolyHEMA Hydrogels Copolymerised with a Basic Monomer

The effect of the incorporation of the basic monomers NVI or DMAEMA on the mechanical properties of polyHEMA are shown in Figures 4.1-4.3. Both of these basic monomers serve to increase the tensile strength of the polymers. The values obtained for the tensile strength of polyHEMA in this work were 0.615MPa and 0.625MPa. A range of other values for the tensile strength of polyHEMA have been reported; 0.402MPa[136], 0.318MPa[137], 0.495MPa[51], 1.19MPa[138] and 1.09MPa[138].

Reference to Figures 3.1-3.4 in Chapter 3 shows that while the equilibrium water content of these systems remains relatively unchanged, there is an increase in the non-freezing water content along with a decrease in the freezing water content.

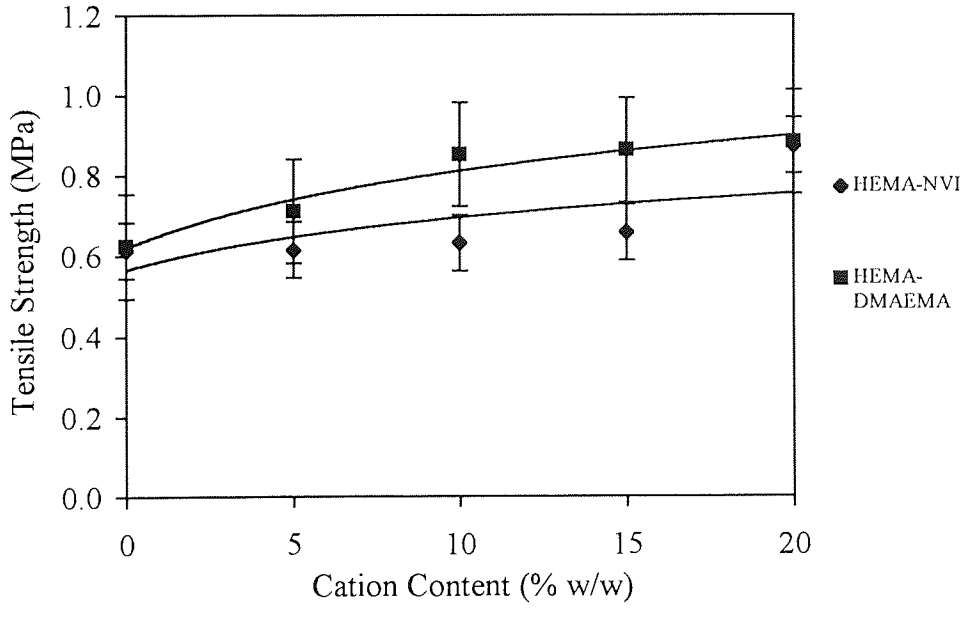

Figure 4.1 Effect of cation content on the tensile strength of HEMA-NVI and HEMA-DMAEMA copolymers

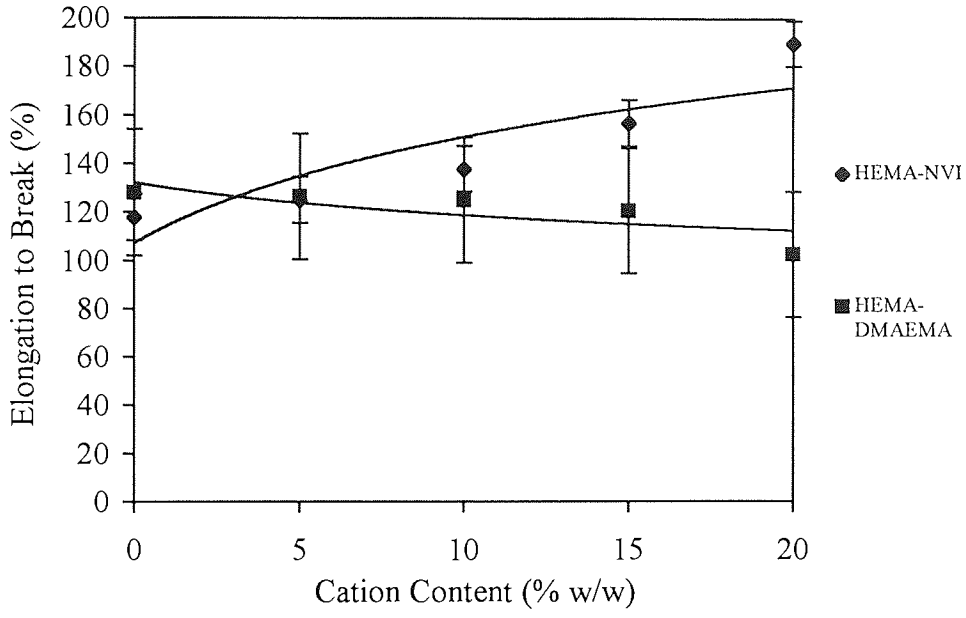

Figure 4.2 Effect of cation content on the elongation to break of HEMA-NVI and HEMA-DMAEMA copolymers

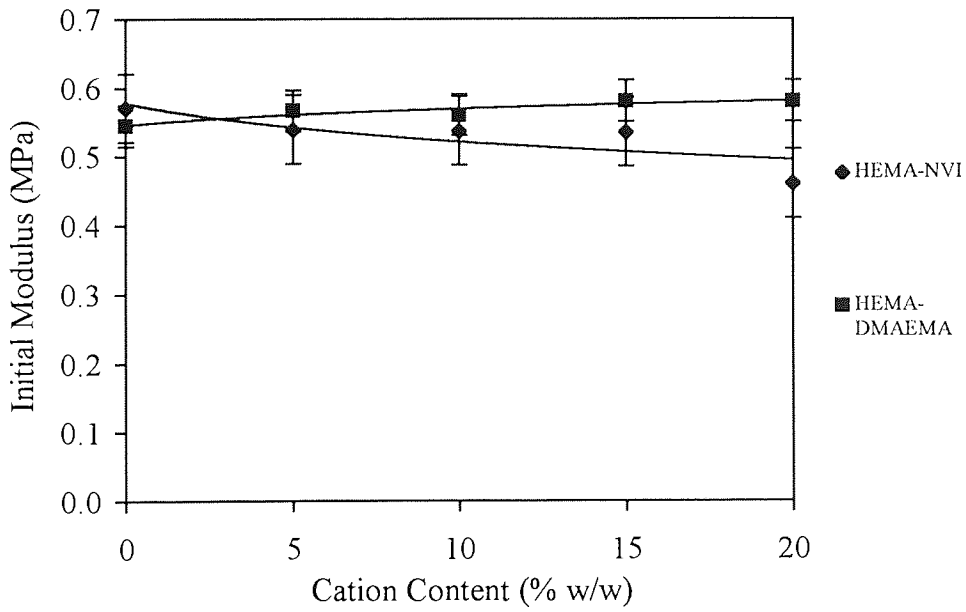

Figure 4.3 Effect of cation content on the initial modulus of HEMA-NVI and HEMA-DMAEMA copolymers

The effect is more apparent in the sample containing NVI. It has previously been noted that a decrease in freezing water will bring about a reduction in the flexibility of materials[51,132]. Freezing water can be regarded as plasticising water due to its greater relative effect on chain mobility, thus it follows that a large volume of freezing water will produce a flexible polymer, reflected in an increased elongation to break. With polyHEMA materials copolymerised with either NVI or DMAEMA, it would be expected that a decrease in the elongation to break would be seen with increasing co-monomer content, corresponding to the increase in non-freezing water. This is indeed true for the HEMA-DMAEMA copolymers as illustrated in Figure 4.2, and an increase in Youngs modulus is also seen from Figure 4.3. However for the HEMA-NVI copolymer series, increasing NVI content gives rise to an increase in ε_b accompanied by a decrease in Youngs modulus. Bearing in mind the ratio of freezing to non-freezing water in these samples, the results presented in Figures 4.2 and 4.3 were somewhat unexpected. Results obtained in the investigation of mechanical properties are not entirely free from inaccuracies or inconsistencies. For example different samples of polyHEMA can have different values for the tensile strength, elongation to break and initial modulus. The more cross-links a given polymer contains, the stiffer and less elastic it becomes. If two samples are similar in stiffness but one has a lower elongation at break, this is generally a sign that the polymer network contains imperfections. Imperfections in the polymer network are most likely to cause variations in the values of tensile strength and elongation to break. The distortion of the network due to the applied load is small at the time at which the initial modulus is calculated. Thus the error associated with the initial modulus is likely to be less than the error associated with tensile strength and elongation to break.

With this in mind, the information presented in Figure 4.3 suggests that addition of either NVI or DMAEMA to polyHEMA materials does not adversely affect the stiffness of these materials.

The HEMA-DMAEMA copolymers seem to show slightly greater σ_b values than the HEMA-NVI copolymers, although when the degree of error is taken into consideration, the differences in the values obtained for each series of copolymers were not significant. The main difference between the effect of NVI and DMAEMA is seen in the differing trends in ε_b and E.

4.3 Mechanical Properties of New Hydrogel Materials

4.3.1 The Effect of Incorporating a Basic Monomer into NNDMA-CHMA 80:20 Materials

The effects of increasing proportions of either NVI or DMAEMA on the mechanical properties of NNDMA-CHMA 80:20 hydrogels are shown in Figures 4.4-4.6. The trend in tensile strength seen from Figure 4.4 is clearly decreasing with the increase in hydrophilic, basic monomer. It has been established from Figures 3.7 and 3.8 in Chapter 3 that increasing the amount of either NVI or DMAEMA incorporated into the polymers increases the value of EWC and both the freezing and the non-freezing water content. The decrease in σ_b can thus be related to the increased presence of water in the polymer systems. Figure 4.6 illustrates the decrease in Youngs modulus, indicating a decrease in rigidity. This is expected from samples containing increasing percentages of freezing or plasticising water.

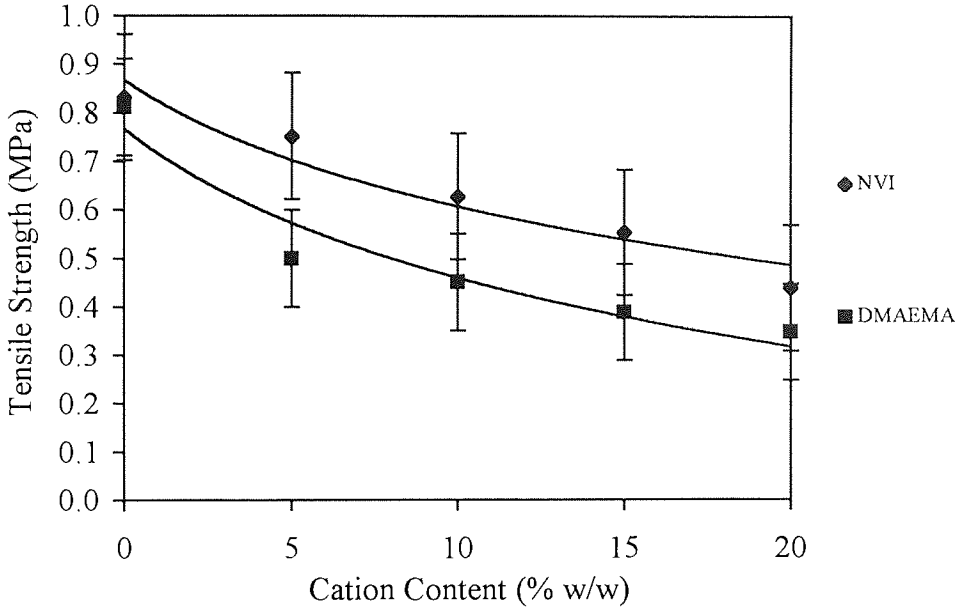

Figure 4.4 Effect of cation content on the tensile strength of NNDMA-CHMA 80:20 copolymers

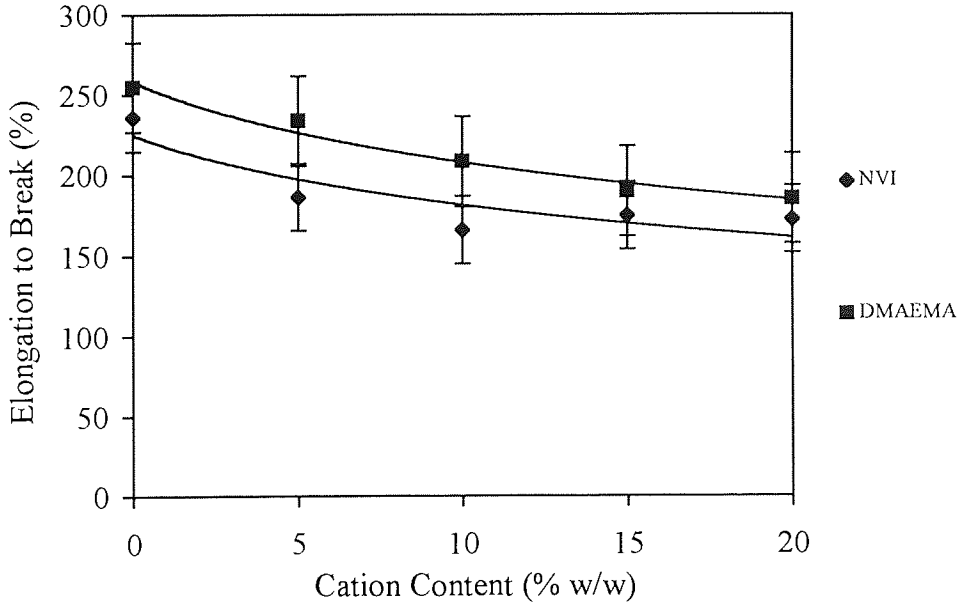

Figure 4.5 Effect of cation content on the elongation to break of NNDMA-CHMA 80:20 copolymers

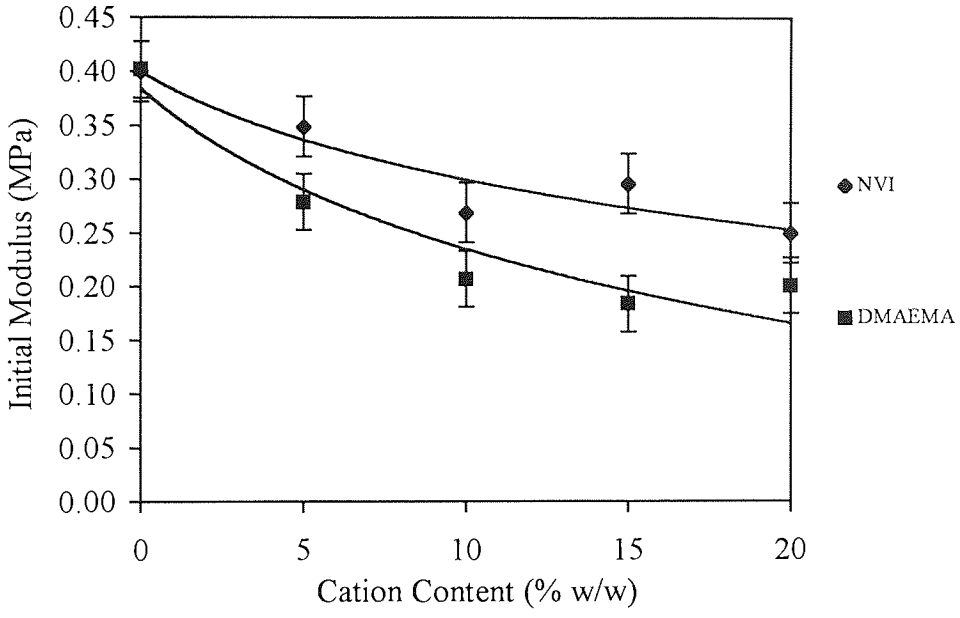

Figure 4.6 Effect of cation content on the initial modulus of NNDMA-CHMA 80:20 copolymers

It may also be expected that this decrease in rigidity would give rise to an increase in ε_b. Reference to Figure 4.5 shows that this is not the case and that the decreasing trend in ε_b seems to reflect that of the decrease in σ_b.

4.3.2 The Effect of Incorporating a Basic Monomer into NNDMA-CHMA 70:30 Materials

Figures 4.7-4.9 show not only the effect of progressive incorporation of either NVI or DMAEMA but also the effect of increasing the hydrophobic content on the mechanical properties of NNDMA-CHMA materials.

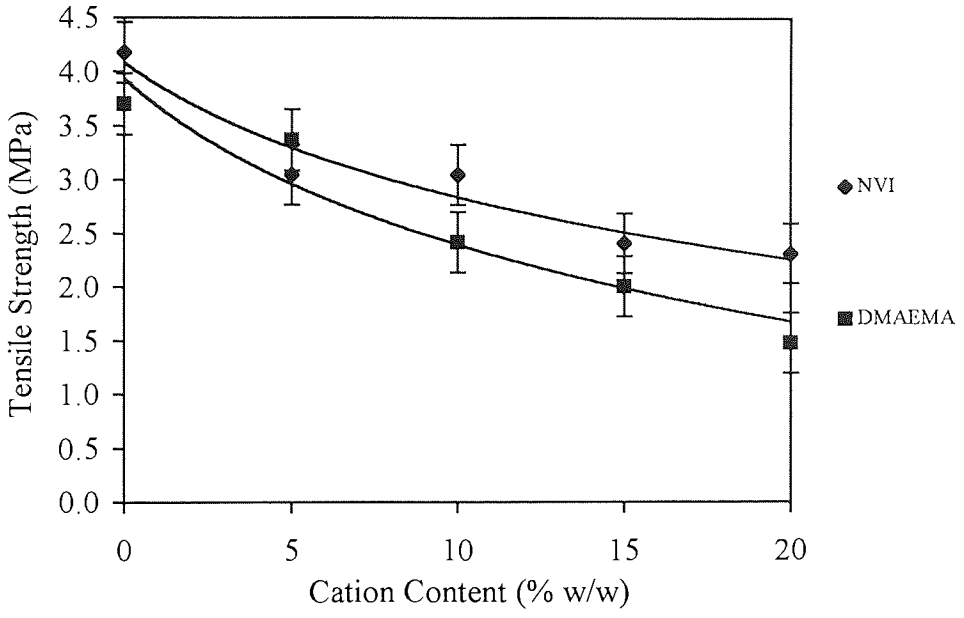

Figure 4.7 Effect of cation content on the tensile strength of NNDMA-CHMA 70:30 copolymers

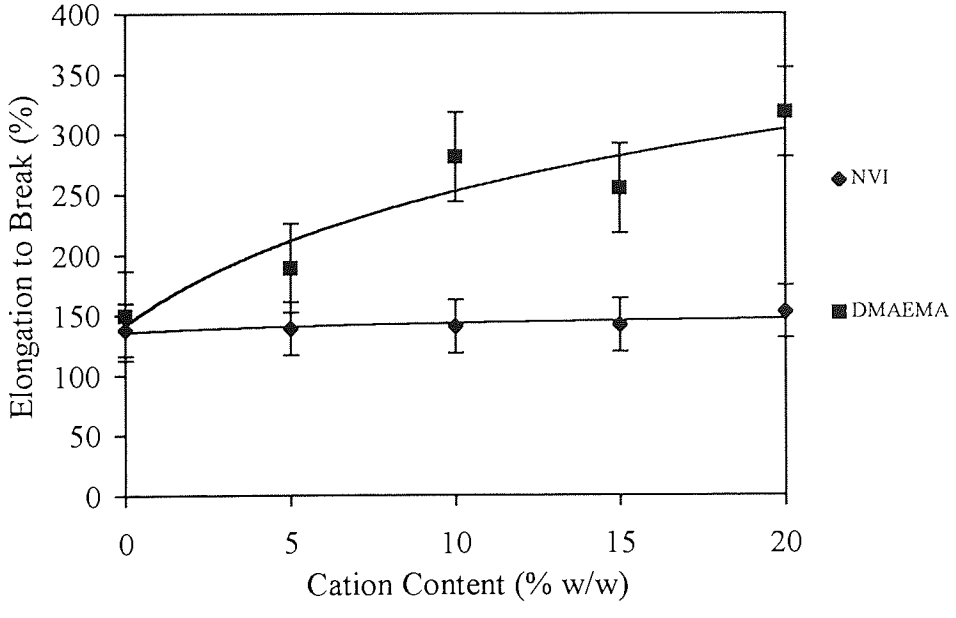

Figure 4.8 Effect of cation content on the elongation to break of NNDMA-CHMA 70:30 copolymers

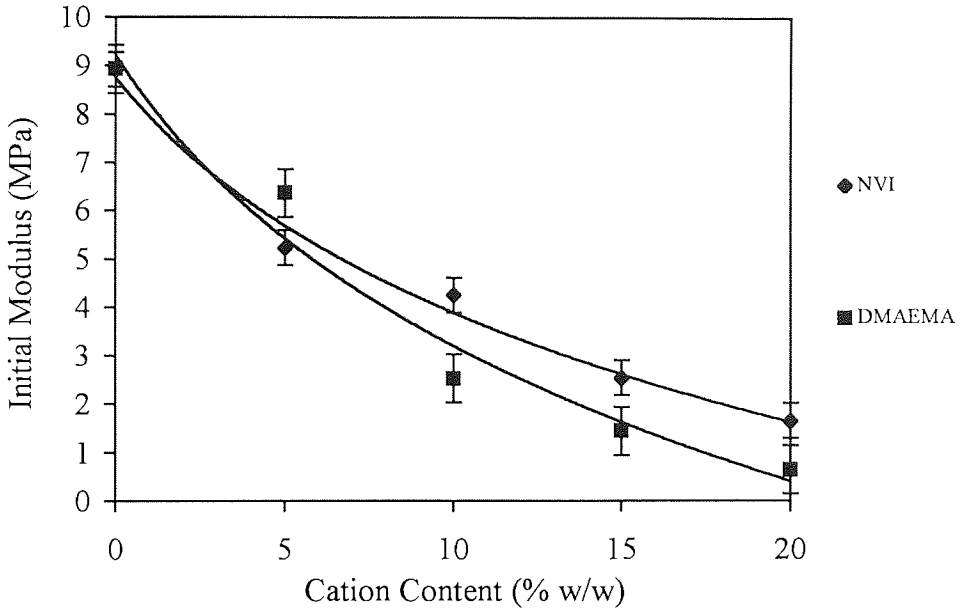

Figure 4.9 Effect of cation content on the initial modulus of NNDMA-CHMA 70:30 copolymers

From Figure 4.7 it can be seen that adding increasing proportions of either of the basic monomers reduces the tensile strength of these materials, although the overall values of σ_b obtained are significantly higher than those obtained for the NNDMA-CHMA 80:20 samples.

Figure 4.9 illustrates a significant decrease in Youngs modulus as either NVI or DMAEMA are introduced into NNDMA-CHMA 70:30 materials and as with the tensile strength, the values obtained are much higher than the values of E for NNDMA-CHMA 80:20 materials. It has already been recorded that CHMA increases the σ_b and E of hydrogel systems[91]. The limited freedom of rotation of the hydrophobic ring structure around the polymer backbone is responsible for the increase in stiffness observed. However increasing the CHMA component in these

NNDMA-CHMA systems results in materials that are much more brittle. This is reflected in the much lower values of elongation to break of NNDMA copolymers containing 30% CHMA than those containing 20% CHMA. There is a difference in trend between the NNDMA-CHMA 80:20 copolymers and the NNDMA-CHMA 70:30 copolymers upon incorporation of a basic monomer. Unlike the 80:20 copolymers which show a reduction in ε_b with increasing NVI or DMAEMA incorporation, the 70:30 copolymers show a marked increase in ε_b with NVI content. Progressive DMAEMA incorporation also gives rise to an increase in ε_b although the changes are much smaller. This increase in ε_b can be related to an increase in the freezing water content of these systems as seen in Figures 3.11 and 3.12 in Chapter 3.

4.3.3 The Effect of Incorporating a Basic Monomer into AMO-CHMA 80:20 and AMO-CHMA 70:30 Materials

The effects of replacing NNDMA with AMO on the mechanical properties of these systems are shown in Figures 4.10-4.15. The tensile strengths of both the 80:20 and the 70:30 series of polymers show a decrease with increasing NVI or DMAEMA content, which is similar to the trend shown by the series of polymers containing NNDMA. However the actual values of σ_b obtained for materials containing AMO are significantly higher than those containing NNDMA. This reflects the fact that the values for the EWC of the AMO polymers were found to be less than the NNDMA polymers in this work, as highlighted in Chapter 3. It is also an understandable result when considering the restriction in the freedom of rotation of the ring structure of AMO around the polymer backbone.

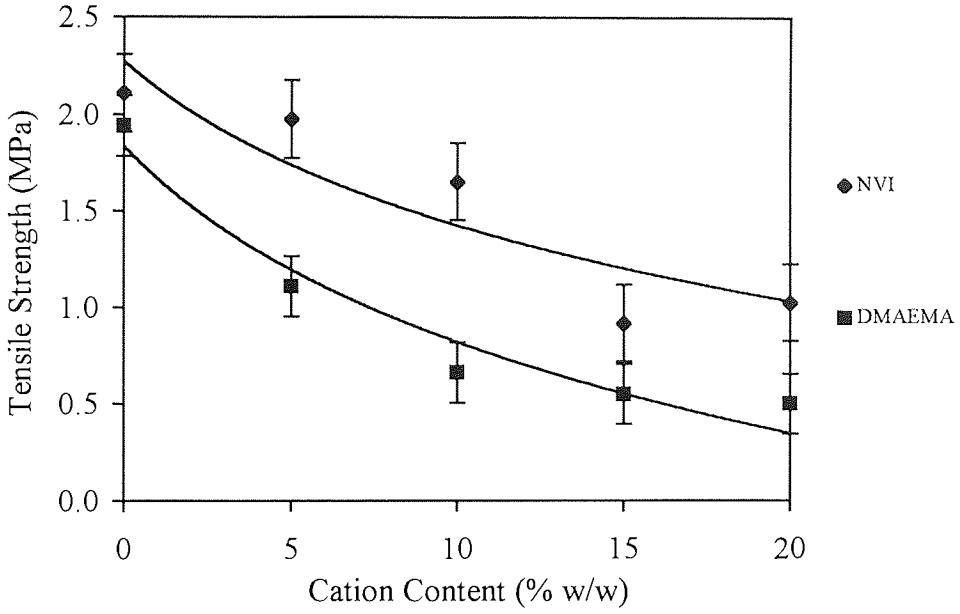

Figure 4.10 Effect of cation content on the tensile strength of AMO-CHMA 80:20 copolymers

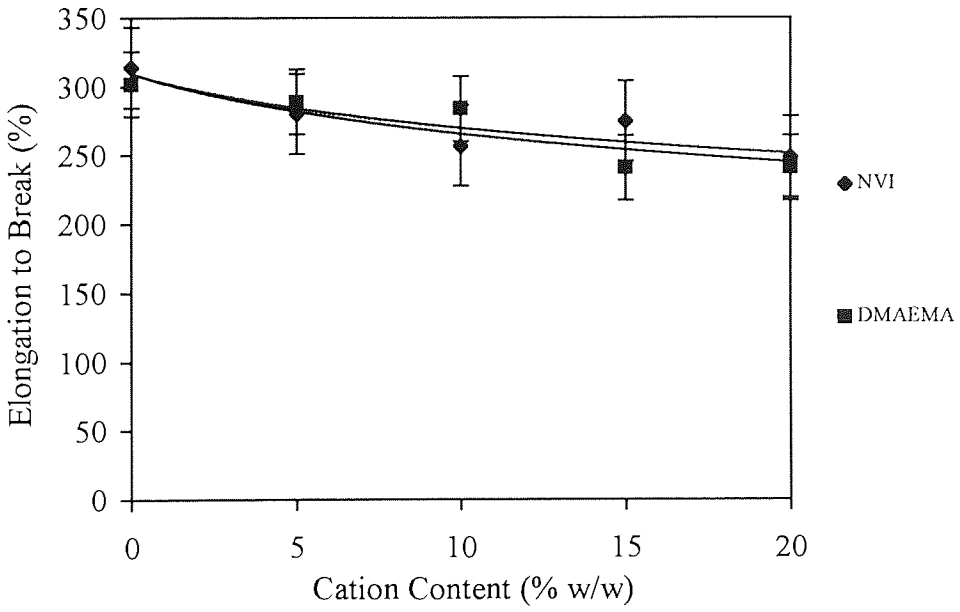

Figure 4.11 Effect of cation content on the elongation to break of AMO-CHMA 80:20 copolymers

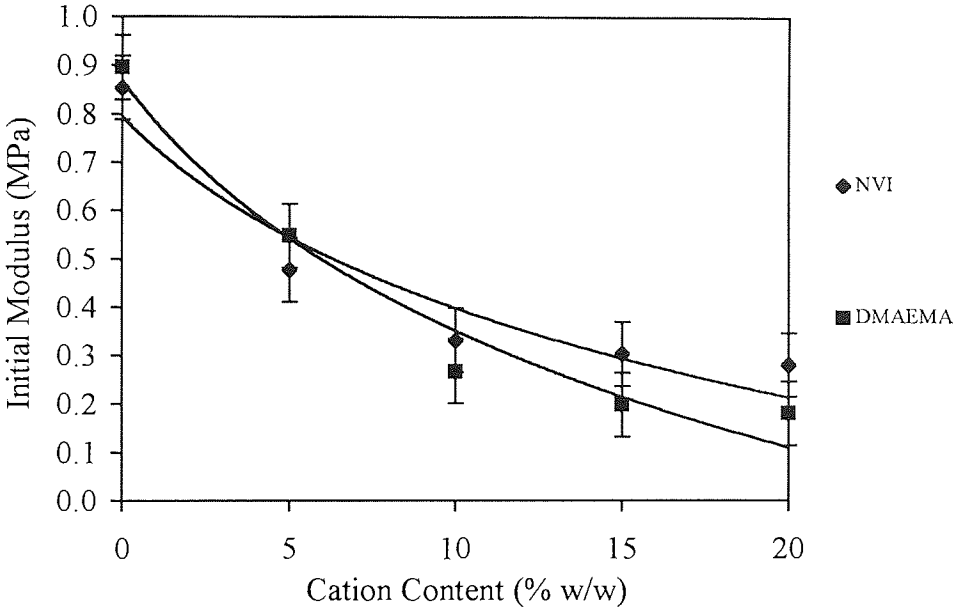

Figure 4.12 Effect of cation content on the initial modulus of AMO-CHMA 80:20 copolymers

Another contributing factor may come from the fact that NNDMA contains readily abstractable hydrogens on the methyl groups which can cause chain transfer during polymerisation, producing polymers with a lower tear strength.

The decrease in σ_b for AMO-CHMA 80:20 copolymers with increasing NVI or DMAEMA content is accompanied by a decrease in Youngs modulus as seen from Figure 4.12. This is comparable to similar materials containing NNDMA, as is the reduction in elongation to break. The freezing water content of AMO-CHMA 80:20 copolymers increases as the proportion of basic monomer increases and it might have been expected that the increased flexibility as a result of the plasticising water would be reflected in an increasing trend in ε_b. However as with NNDMA-CHMA 80:20

copolymers, Figure 4.11 illustrates that this is not the case and the decreasing trend in ε_b seems to reflect that of the decrease in σ_b.

Once again by increasing the proportion of CHMA in the hydrogel system, similar trends are observed for the AMO-CHMA polymers to those seen with the NNDMA-CHMA polymers. The tensile strength and Youngs modulus of the AMO-CHMA 70:30 copolymer increases in comparison to the AMO-CHMA 80:20 copolymer, but the introduction of a basic monomer results in decreasing σ_b, and a decrease in E as seen in Figures 4.13 and 4.15 respectively.

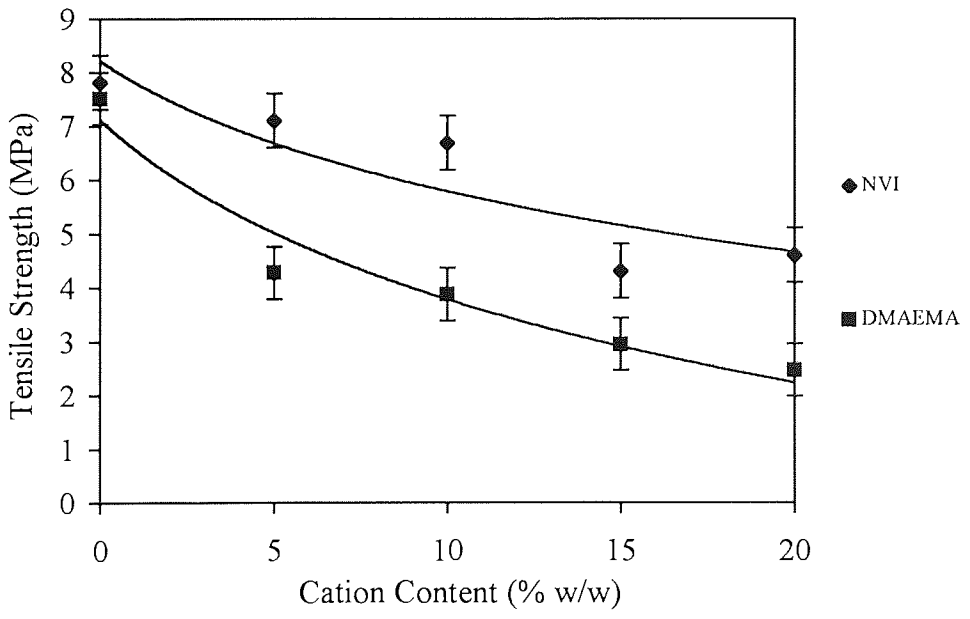

Figure 4.13 Effect of cation content on the tensile strength of AMO-CHMA 70:30 copolymers

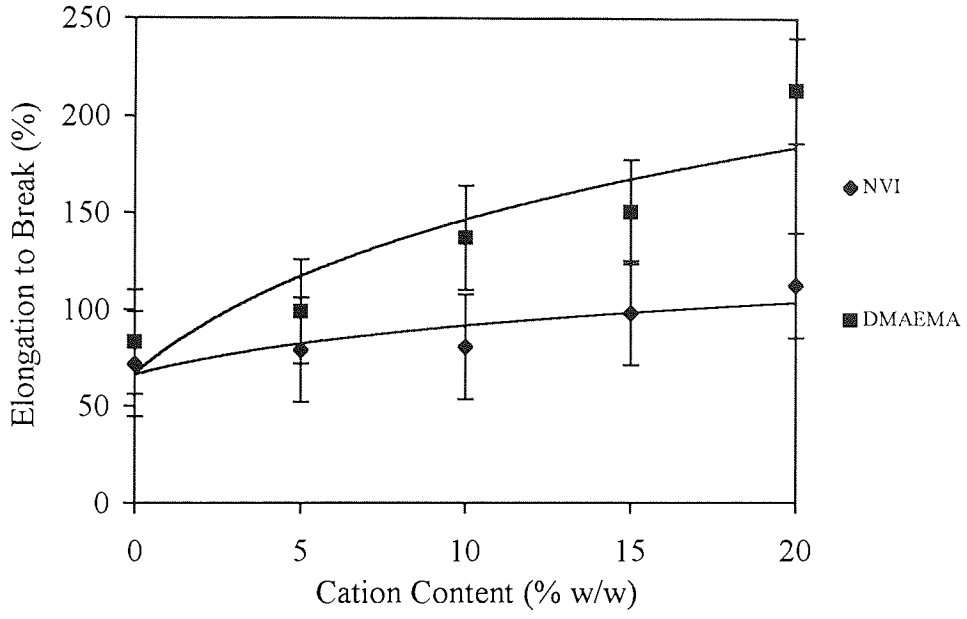

Figure 4.14 Effect of cation content on the elongation to break of AMO-CHMA 70:30 copolymers

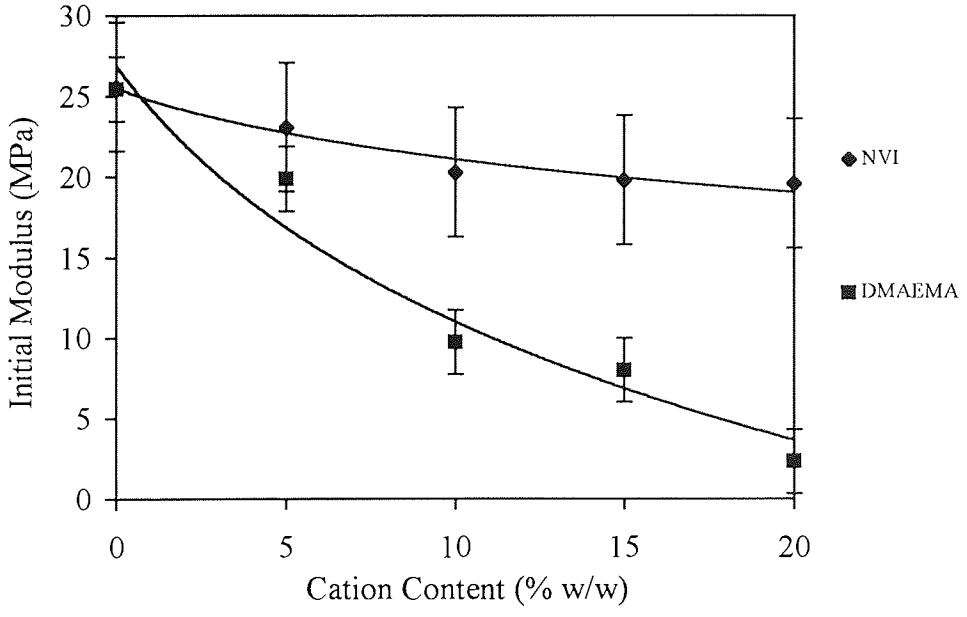

Figure 4.15 Effect of cation content on the initial modulus of AMO-CHMA 70:30 copolymers

The elongation to break of these AMO-CHMA 70:30 samples increases with progressive incorporation of NVI or DMAEMA, which might be attributed to an increasing percentage of freezing water in the samples demonstrated in Figures 3.19 and 3.20 in Chapter 3.

Throughout each of the new materials in Section 4.3.1-4.3.3 the differences between the effects of NVI and DMAEMA on these polymers have been consistent, if small. In all cases incorporation of NVI produces materials with a marginally higher tensile strength and Youngs modulus but with a lower elongation to break. The cyclic nature of NVI is important in its ability to increase the σ_b and E by restricting the freedom of rotation around the polymer backbone. Although DMAEMA has the α-methyl group which also restricts the freedom of rotation of the polymer, its slightly longer more flexible side chain plays a part in its ability to provide more flexible materials. The ratios of freezing to non-freezing water in these samples are similar regardless of which basic monomer is incorporated, and therefore the structures of the monomers themselves, rather than the water binding properties, are more likely to be responsible for differences seen in the mechanical properties.

The effect of equilibrium water content on the mechanical properties of the hydrogel copolymers studied is shown in Figures 4.16-4.18. The general trend is that a rise in equilibrium water content sees a fall in tensile strength. It is important to remember that the copolymer structure will also have a part to play in determining the tensile strength.

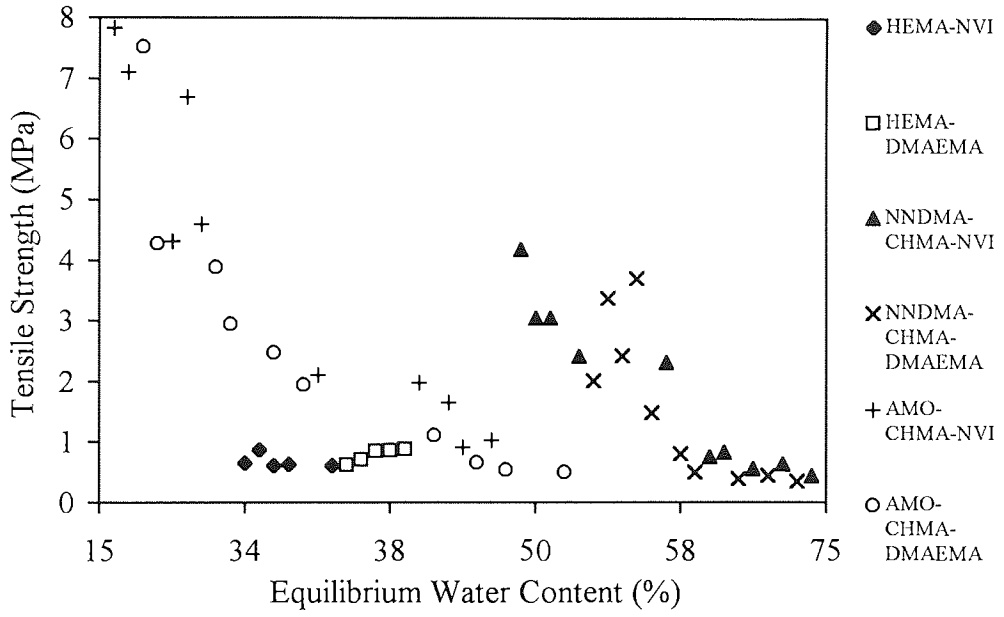

Figure 4.16 Variation in tensile strength with equilibrium water content for copolymer hydrogels

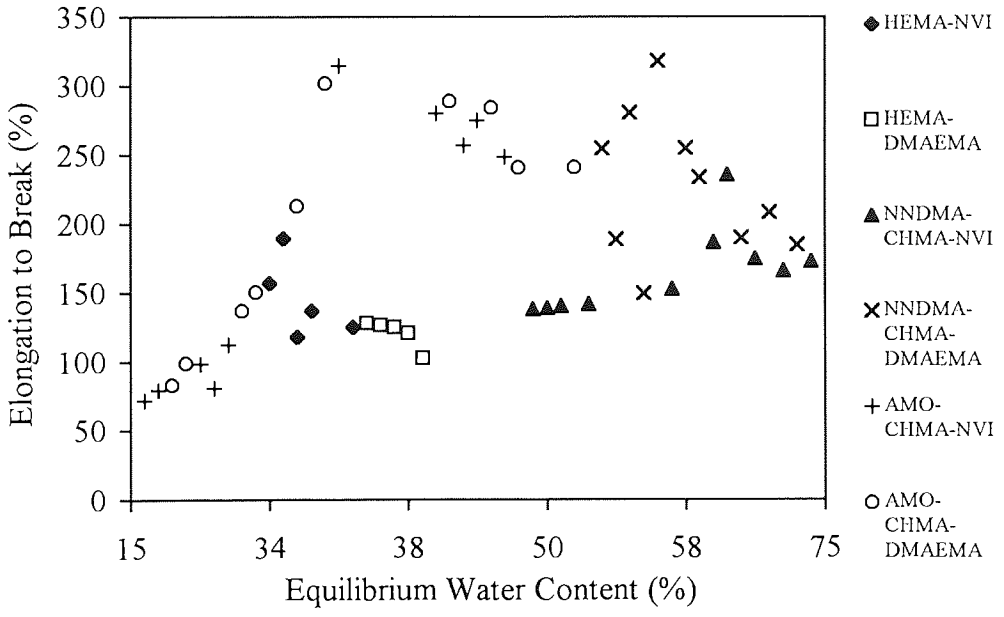

Figure 4.17 Variation in elongation to break with equilibrium water content for copolymer hydrogels

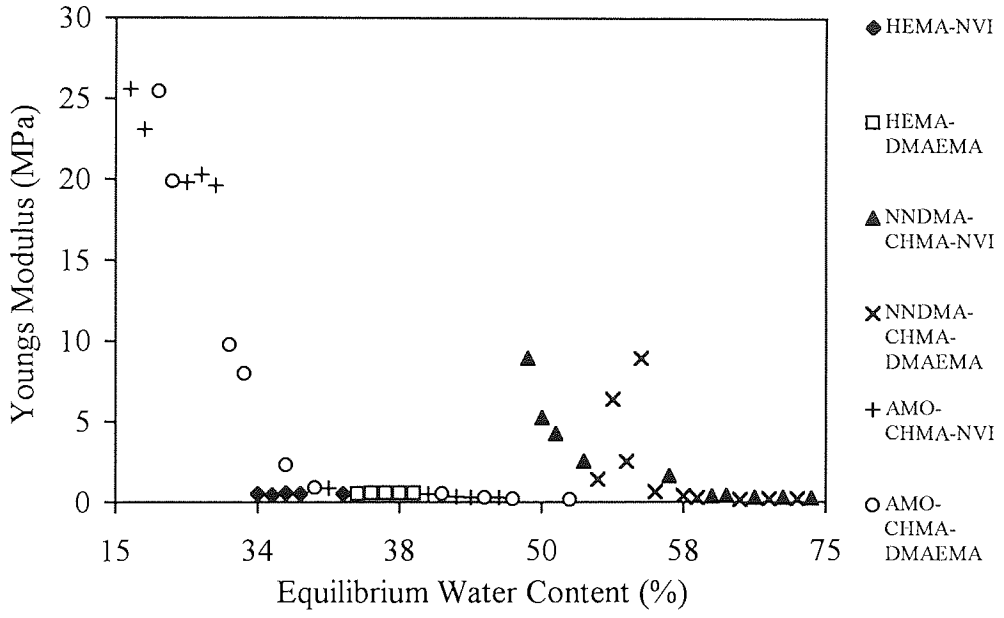

Figure 4.18 Variation in Youngs modulus with equilibrium water content for copolymer hydrogels

Thus copolymers of NNDMA-CHMA with either NVI or DMAEMA have higher tensile strengths than might be expected from their EWCs due to the presence of CHMA. Copolymer structure appears to be more important than EWC in determining the elongation to break and in some of the hydrogels studied ε_b increases with water content and in other cases the reverse is true. The effect of EWC on the initial modulus of copolymer hydrogels is illustrated in Figure 4.18. In general there is a decrease in E with increasing EWC although copolymer structure will once again have some contribution in determining the value.

4.4 Conclusions

The effect of incorporating a basic monomer on the mechanical properties of polyHEMA was investigated. The tensile strength of polyHEMA was found to

increase with either NVI or DMAEMA incorporation, and the values obtained were similar regardless of whether NVI or DMAEMA was used. For HEMA-DMAEMA copolymers, an increasing proportion of DMAEMA brought about an increase in Youngs modulus and a decrease in elongation to break. HEMA-NVI copolymers showed a differing trend in E and ε_b. A higher percentage of NVI resulted in a slight decrease in E and an increase in ε_b. This result was unexpected as the freezing water content of HEMA-NVI copolymers has been shown to reduce with progressive NVI incorporation, and thus a more inflexible stiff material may have been expected.

The σ_b of the new polymeric materials prepared using NNDMA or AMO with CHMA showed a decrease with increasing percentages of either NVI or DMAEMA. The NNDMA-CHMA 80:20 samples also showed a decrease in E with increased NVI or DMAEMA content, as do the AMO-CHMA 80:20 samples. The decreasing trend in ε_b, seen for both these sets of samples surprisingly did not reflect the fact that the freezing water of these samples increased with increasing NVI or DMAEMA content.

The NNDMA-CHMA 70:30 samples and also the AMO-CHMA 70:30 samples have higher values of σ_b than the 80:20 samples due to the higher percentage of CHMA in the system reducing the EWC. The trend in E and ε_b in these systems differs from the 80:20 samples, with E decreasing but ε_b increasing with increased percentages of NVI or DMAEMA

AMO gives rise to materials with higher tensile strengths than NNDMA and increasing the percentage of CHMA also produces materials with a higher tensile

strength. These effects have been observed by previous workers in this research group[131,91]. Looking at the results of the mechanical properties in light of the water binding properties presented in Chapter 3, and also Figures 4.16-4.18, it can be seen that although the EWC of a material has an important influence on its mechanical properties, copolymer composition and structure also plays an important role.

CHAPTER 5

Surface Properties of Hydrogels Incorporating a Basic Monomer

5.1 Introduction

The major application of hydrogel materials is in the field of biomaterials and as such hydrogel surfaces are often in intimate contact with biological fluids or tissue. It has been suggested by some workers[56,57,139] that the surface free energy of an hydrogel is an important property in determining the biotolerence of the material.

Very little previous work has been carried out on the effect of basic monomers on the surface properties of hydrogels and this chapter describes the results of investigations into the surface properties of polyHEMA copolymer systems in which up to 20% of a basic monomer is incorporated. It also looks at more complex hydrogel systems in which up to 20% of a basic monomer is incorporated into a material containing both hydrophilic and hydrophobic components. Surface energy measurements have been made in the hydrated and dehydrated state. Results for the total surface free energy (γ_s^t), dispersive component (γ_s^d) and polar component (γ_s^p) of each series of hydrogels are illustrated graphically and numerical values are presented in Appendix 4. As was the case for the water binding studies the pH of the hydration water was measured as between 7.3 and 7.6 thus making it a reasonable assumption that the basic units in the polymer will carry a degree of positive charge.

5.2 Surface Properties of Dehydrated Hydrogels

The measured surface energies are a function of the interactions that take place in the bulk polymer and at the surface of the polymer. The orientation of the groups at the polymer surface, which may be affected by the polarity of the adjacent phase, will have a bearing on the values obtained for the surface free energy. Testing of

dehydrated materials, especially those which are extremely hydrophilic, is not without its problems in terms of producing accurate and consistent results. Rapid hydration in air and the interaction with the water used as a wetting liquid in the sessile drop technique is the major cause of inaccuracies.

5.2.1 Surface Properties of Dehydrated PolyHEMA Hydrogels Copolymerised with a Basic Monomer

The effect of incorporating either of the basic monomers NVI or DMAEMA on the total surface energy of dehydrated polyHEMA, as well as the polar and dispersive components of the surface free energy, is illustrated in Figures 5.1 and 5.2.

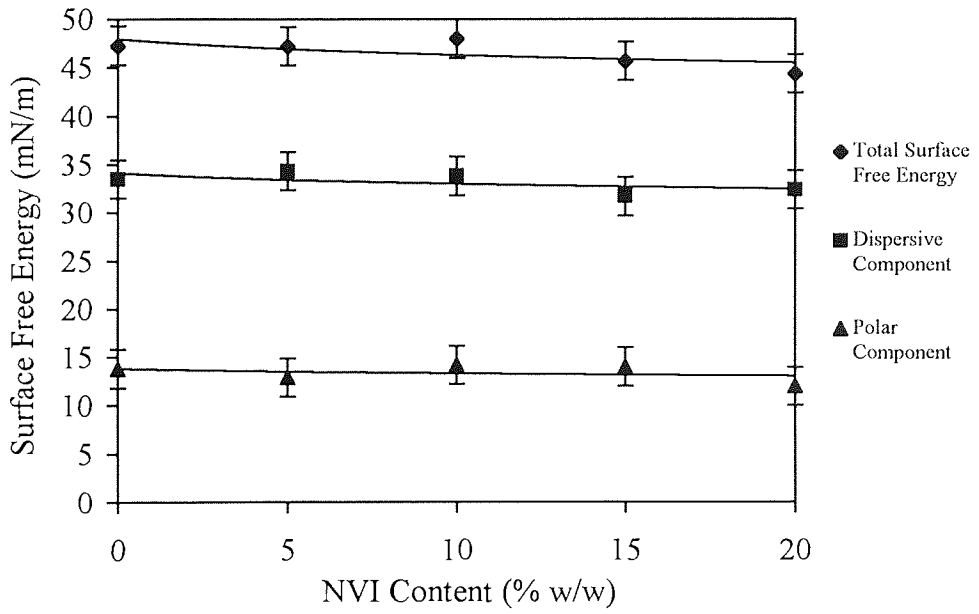

Figure 5.1 Graph to show the effect of composition on the surface properties of dehydrated polyHEMA materials copolymerised with 0-20% NVI

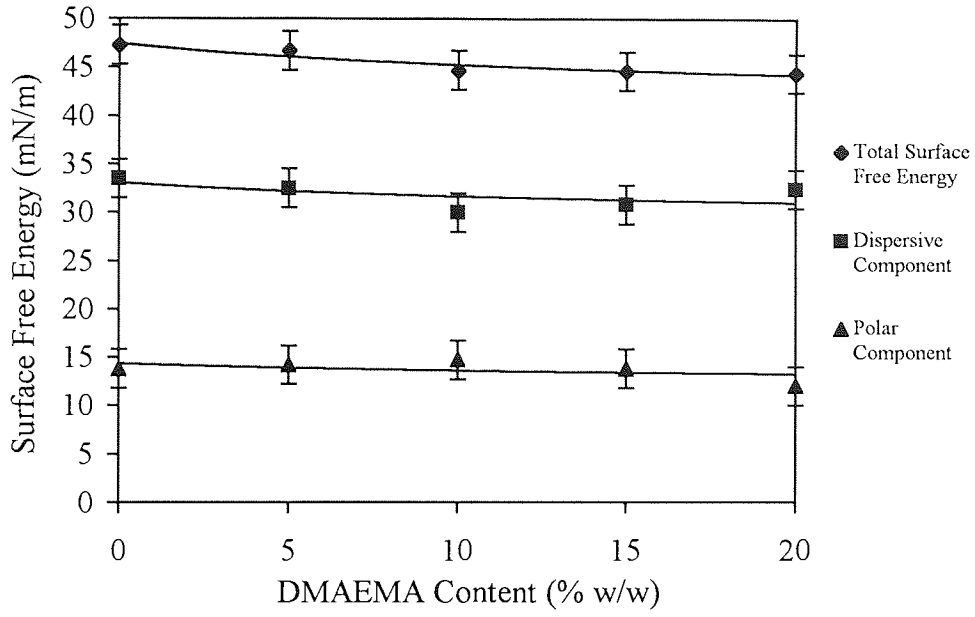

Figure 5.2 Graph to show the effect of composition on the surface properties of dehydrated polyHEMA materials copolymerised with 0-20% DMAEMA

It was noted from the results obtained that they were not dissimilar to surface energies of conventional vinyl and acrylic polymers such as polystyrene and polymethyl methacrylate, all falling in the range 42-51mN/m. Regardless of whether NVI or DMAEMA is used, incorporation of a basic monomer has very little effect on the total surface energy of these hydrogels, in the dehydrated state. Reference to Chapter 3 shows that there is very little change in equilibrium water content for similar materials and thus it is perhaps not surprising to find so little change in total surface energy. The polar and dispersive components of free energy also show very little change in value upon addition of the basic monomers.

It was noted that the dispersive component was the dominant component both in the HEMA-NVI and the HEMA-DMAEMA materials. This may be explained in terms of

the polar groups being less likely to express themselves at the surface of the polymer, with the surface instead being dominated by the hydrophobic α-methyl groups of the HEMA.

5.2.2 Surface Properties of New Materials in their Dehydrated State, Copolymerised with a Basic Monomer

The effect of incorporating either of the basic monomers NVI or DMAEMA on the total surface energy of dehydrated NNDMA-CHMA materials, as well as the polar and dispersive components of the surface free energy, is illustrated in Figures 5.3 - 5.6.

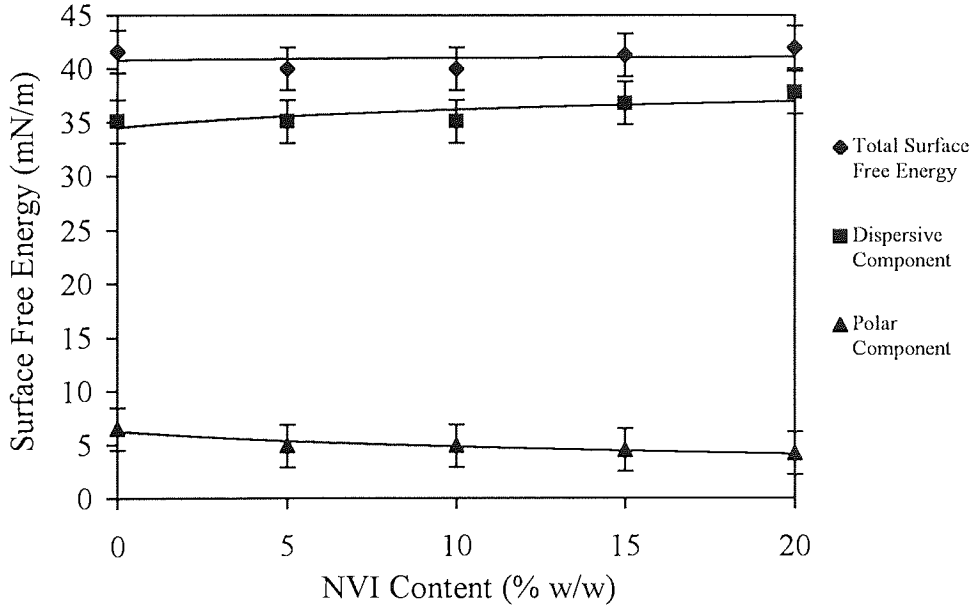

Figure 5.3 Graph to show the effect of composition on the surface properties of dehydrated NNDMA-CHMA 80:20 materials copolymerised with 0-20% NVI

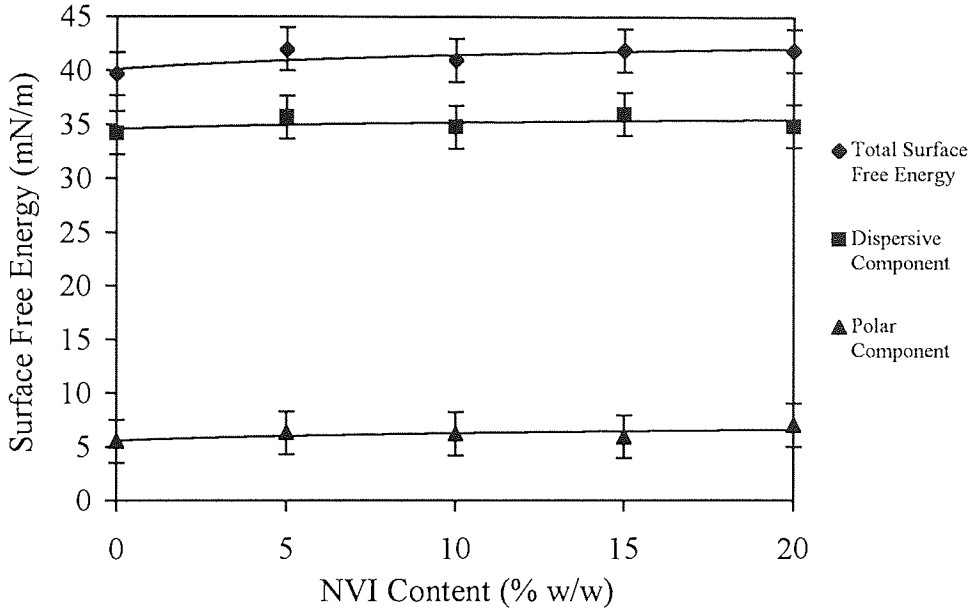

Figure 5.4 Graph to show the effect of composition on the surface properties of dehydrated NNDMA-CHMA 70:30 materials copolymerised with 0-20% NVI

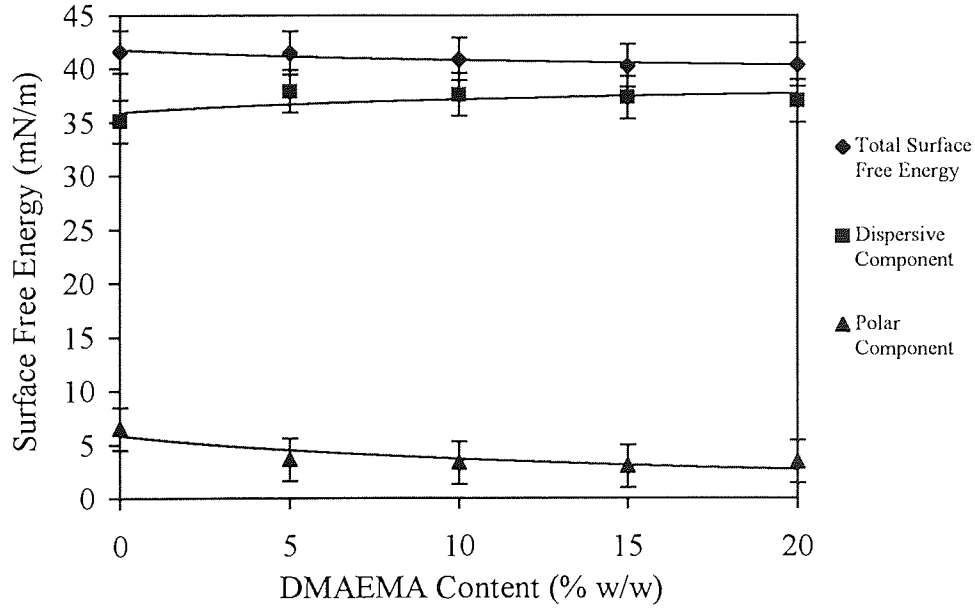

Figure 5.5 Graph to show the effect of composition on the surface properties of dehydrated NNDMA-CHMA 80:20 materials copolymerised with 0-20% DMAEMA

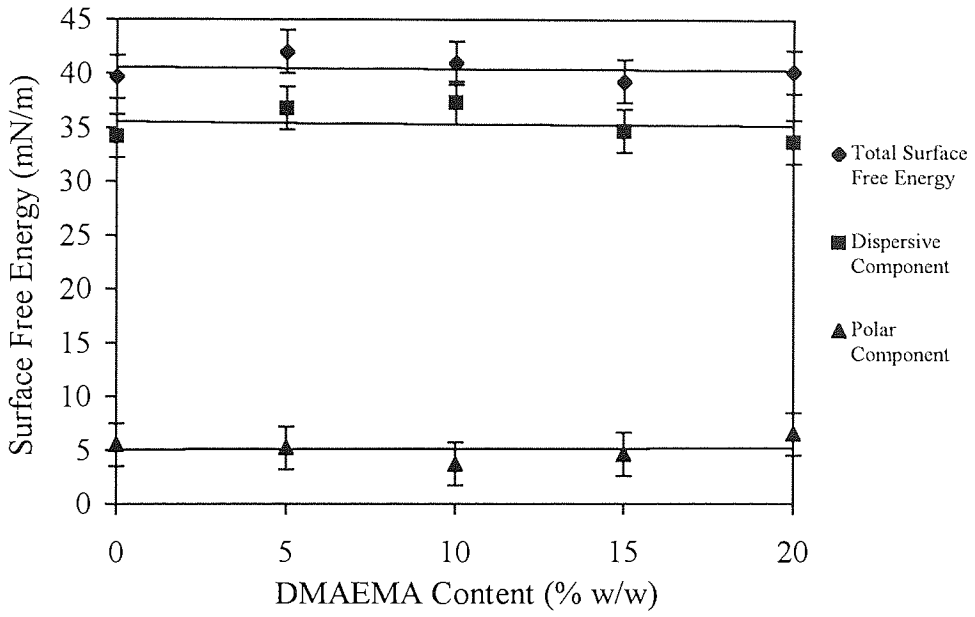

Figure 5.6 Graph to show the effect of composition on the surface properties of dehydrated NNDMA-CHMA 70:30 materials copolymerised with 0-20% DMAEMA

From Figures 5.3-5.6 it can be seen that introduction of a basic monomer, either NVI or DMAEMA, has very little effect on the total surface free energy of these copolymer systems. It can also be seen that the polar and dispersive components of the surface energy remain unaffected.

Once again it can be seen that results for the total surface free energy fall in a range that might be expected for acrylic polymers. However it can also be seen that the values obtained for total surface free energy in Figures 5.3 - 5.6 are less than those obtained for the polyHEMA materials copolymerised with NVI or DMAEMA. This is due to the introduction of the hydrophobic monomer, CHMA. Indeed, by comparing Figures 5.4 and 5.6 with Figures 5.3 and 5.5, it can be seen that increasing

the CHMA content by 10% brings about a further small reduction in total surface free energy.

The polar component of surface free energy is drastically reduced upon introduction of CHMA although the dispersive component remains similar. In fact the dispersive component makes up a large fraction of the total surface energy, (~0.8) and it may be concluded that the surface of these hydrogel materials is totally dominated by the hydrophobic CHMA.

The effect of incorporating either of the basic monomers NVI or DMAEMA on the total surface energy of dehydrated AMO-CHMA materials, as well as the polar and dispersive components of the surface free energy, is illustrated in Figures 5.7 - 5.10.

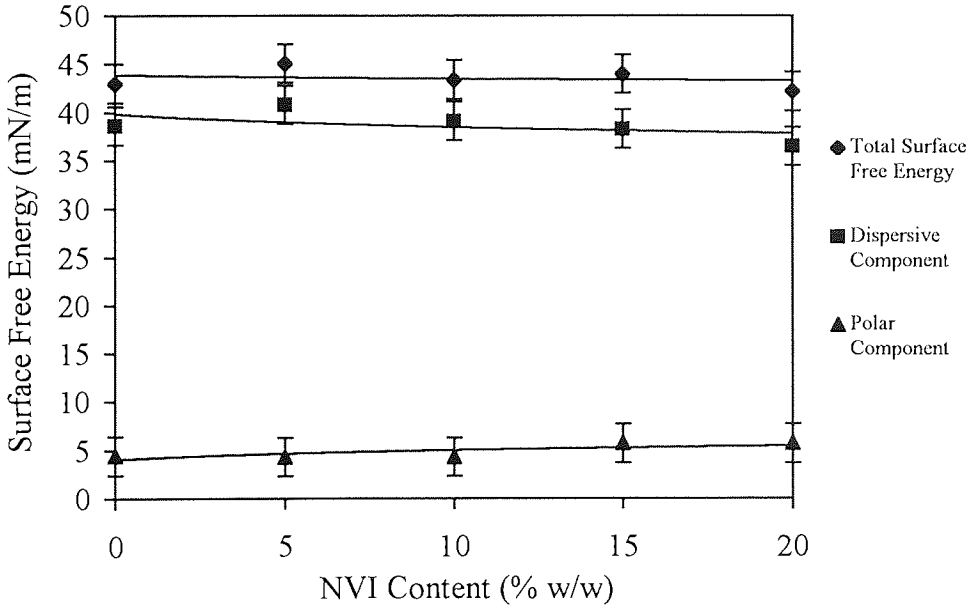

Figure 5.7 Graph to show the effect of composition on the surface properties of dehydrated AMO-CHMA 80:20 materials copolymerised with 0-20% NVI

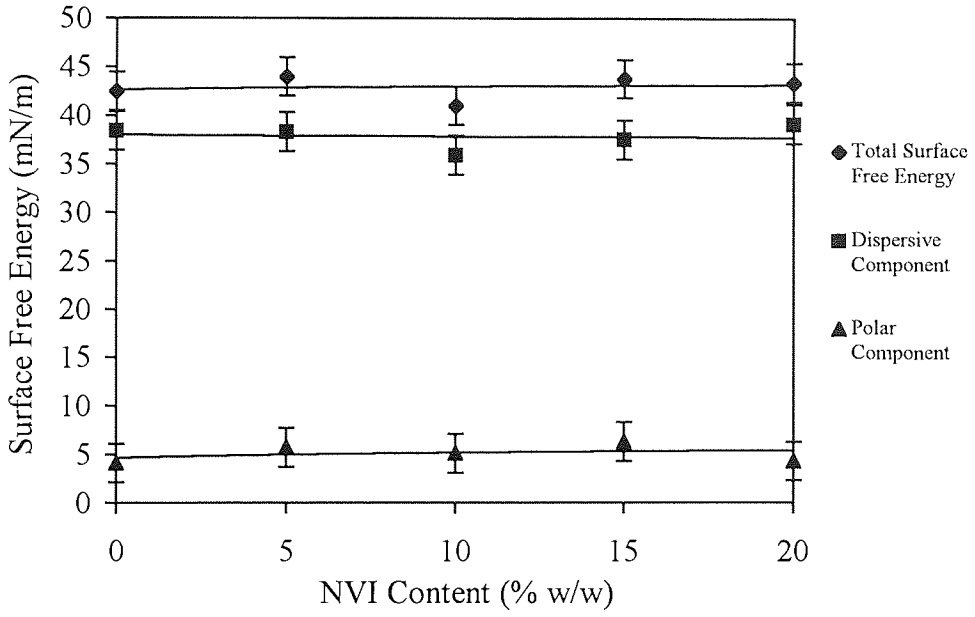

Figure 5.8 Graph to show the effect of composition on the surface properties of dehydrated AMO-CHMA 70:30 materials copolymerised with 0-20% NVI

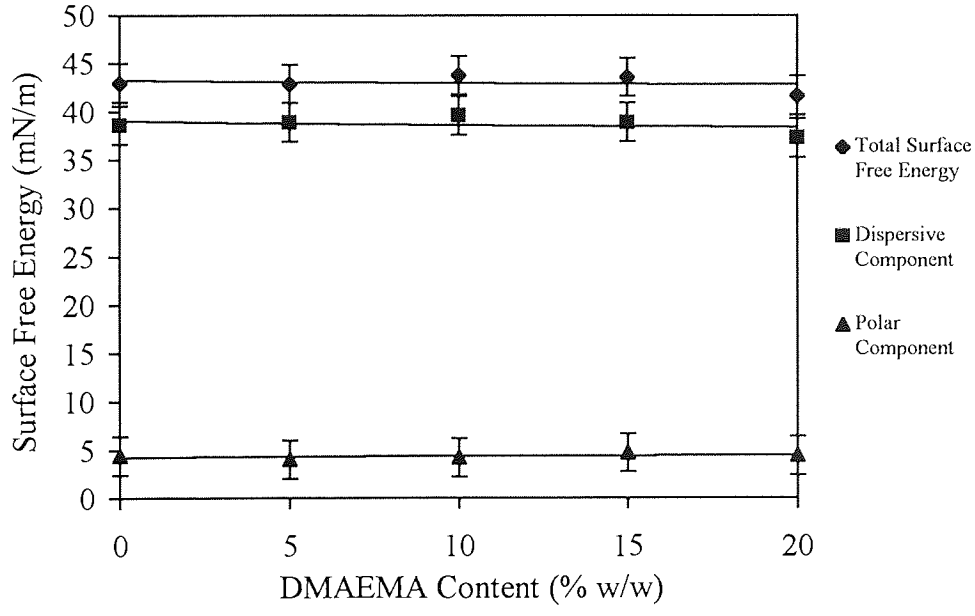

Figure 5.9 Graph to show the effect of composition on the surface properties of dehydrated AMO-CHMA 80:20 materials copolymerised with 0-20% DMAEMA

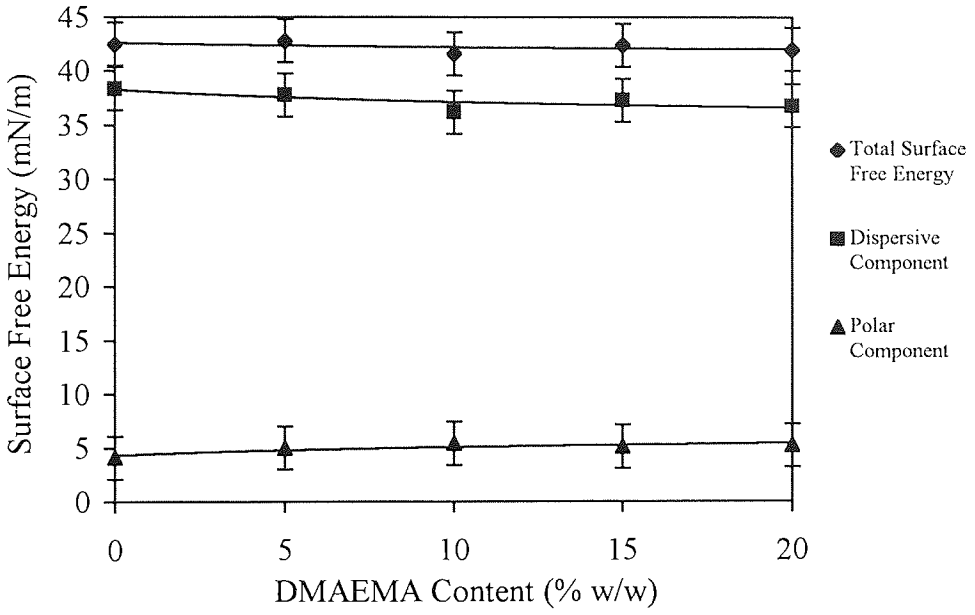

Figure 5.10 Graph to show the effect of composition on the surface properties of dehydrated AMO-CHMA 70:30 materials copolymerised with 0-20% DMAEMA

Again from Figures 5.7-5.10 it can be seen that introduction of either NVI or DMAEMA as the basic monomer has very little effect on the total surface free energy of these copolymer systems. It can also be seen that the polar and dispersive components of the surface energy remain unaffected.

Replacing NNDMA with AMO as the hydrophilic monomer produces no variation in the results. As previously suggested this is likely to be due to the domination of the surface by the hydrophobic CHMA masking any contribution from the other monomers.

5.3 Surface Properties of Hydrated Hydrogels

The best method of overcoming problems associated with surface energy measurements on dehydrated hydrogels is to carry out the measurements on the hydrogels in their hydrated form. Using Hamiltons method in conjunction with the captive air bubble technique, it is possible to gain some understanding of the factors involved in the control of surface properties.

These inverted droplet methods solve the problem of dealing with hydrated materials, but as with the dehydrated samples, inaccuracies and inconsistencies can arise in measurements. The interfacial angles are difficult to measure precisely and deformation of the bubble leads to variations in values obtained for similar materials. Furthermore there is the suspicion that the measurements are dominated by interfacial adsorbed water layers. Using water as the immersion liquid maintains the surface of the hydrogel in an hydrated state but it is difficult for the inverted droplet to displace all of the adsorbed water layers. Hence the results may be affected by this water layer.

5.3.1 Surface Properties of Hydrated PolyHEMA Hydrogels Copolymerised with a Basic Monomer

The effect of incorporating either of the basic monomers NVI or DMAEMA on the total surface energy of polyHEMA, as well as the polar and dispersive components of the surface free energy, is illustrated in Figures 5.11 and 5.12.

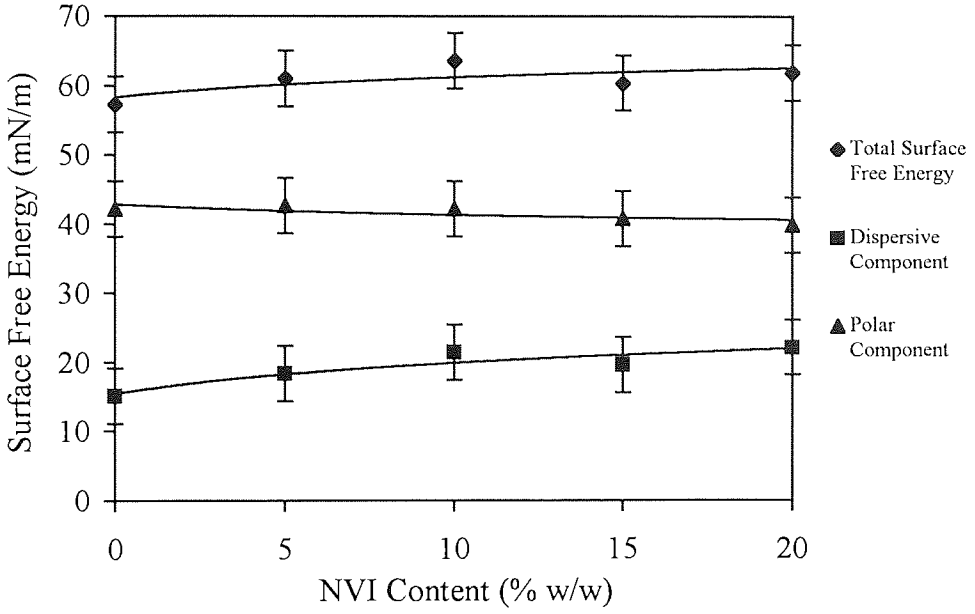

Figure 5.11 Graph to show the effect of composition on the surface properties of hydrated polyHEMA materials copolymerised with 0-20% NVI

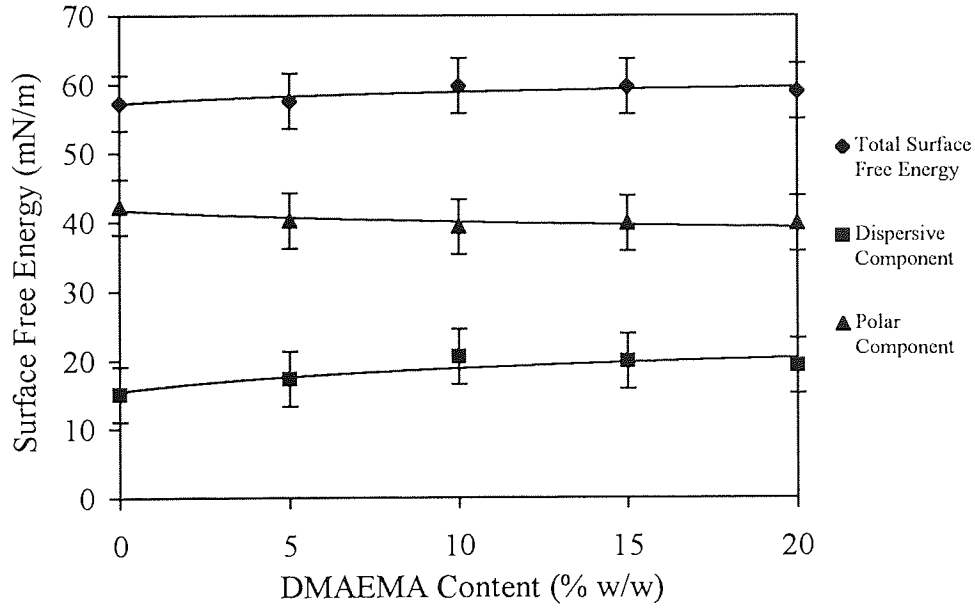

Figure 5.12 Graph to show the effect of composition on the surface properties of hydrated polyHEMA materials copolymerised with 0-20% DMAEMA

It can be seen from these Figures that addition of a basic monomer, either NVI or DMAEMA, does not produce a significant change in the total surface free energy of the hydrated polyHEMA materials. The polar and dispersive components also remain relatively unaffected.

The measured surface energies of the hydrated hydrogels used in this work are all higher than the values obtained from the same hydrogels in the dehydrated state. This phenomenon has been reported by other workers[51,140,141] and is not surprising as the surface energy of water at 72.8 mN/m is much higher than those of polymers. In addition there is a considerable increase of the polar component of surface free energy accompanied by a decrease in the dispersive component. This reflects the direct consequence of incorporating water whose polar component is significantly enhanced.

5.3.2 Surface Properties of New Materials in their Hydrated state, Copolymerised with a Basic Monomer

The effect of incorporating either of the basic monomers NVI or DMAEMA on the total surface energy of hydrated NNDMA-CHMA materials, as well as the polar and dispersive components of the surface free energy, is illustrated in Figures 5.13 - 5.16.

From these Figures it can be seen that addition of NVI or DMAEMA to these materials brings about no change in the value of the total surface free energy of the materials. Similarly the polar and dispersive components remain unaffected. Introduction of the hydrophobic monomer, CHMA does not produce a large change

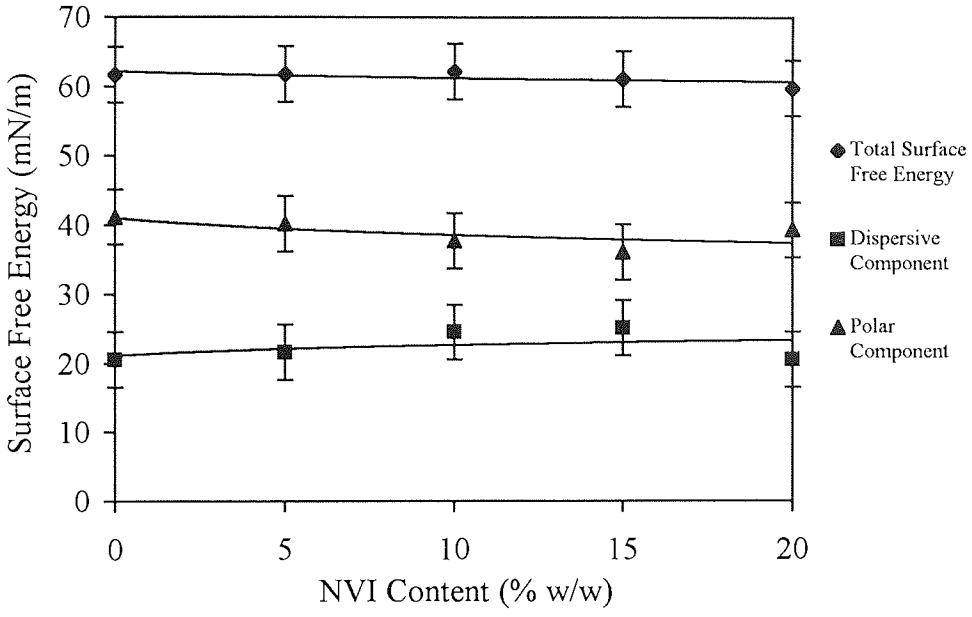

Figure 5.13 Graph to show the effect of composition on the surface properties of hydrated NNDMA-CHMA 80:20 materials copolymerised with 0-20% NVI

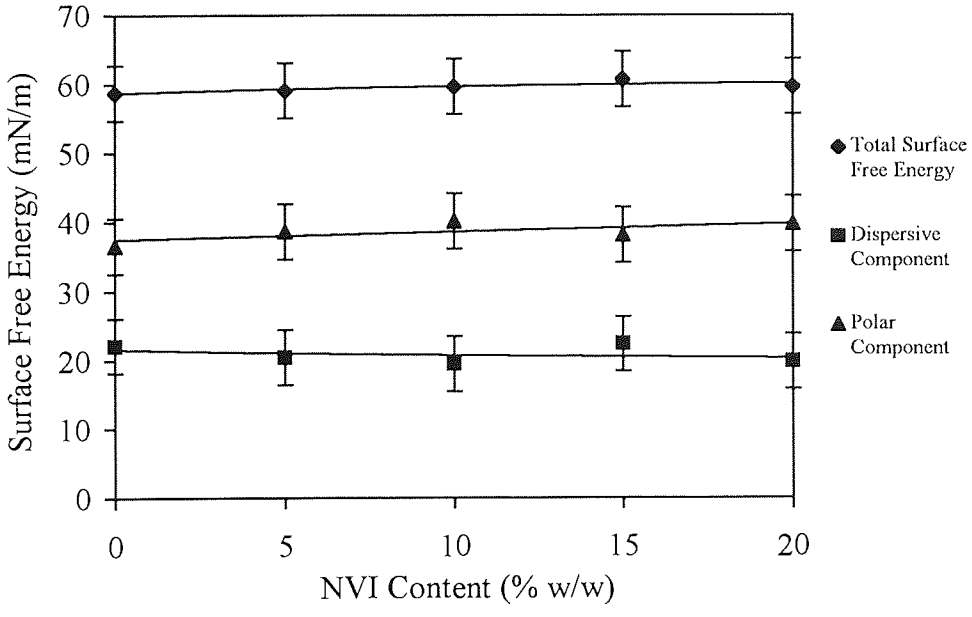

Figure 5.14 Graph to show the effect of composition on the surface properties of hydrated NNDMA-CHMA 70:30 materials copolymerised with 0-20% NVI

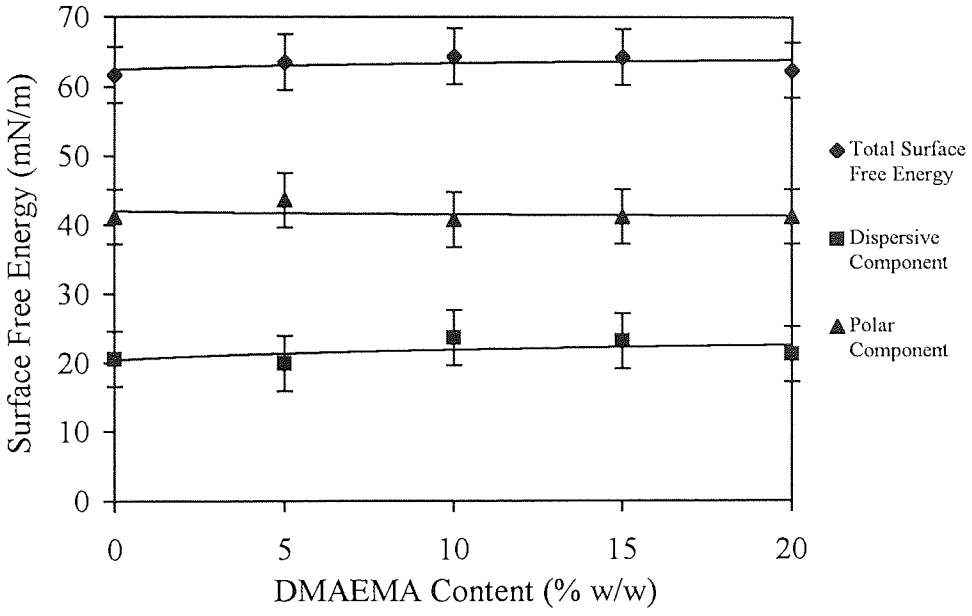

Figure 5.15 Graph to show the effect of composition on the surface properties of hydrated NNDMA-CHMA 80:20 materials copolymerised with 0-20% DMAEMA

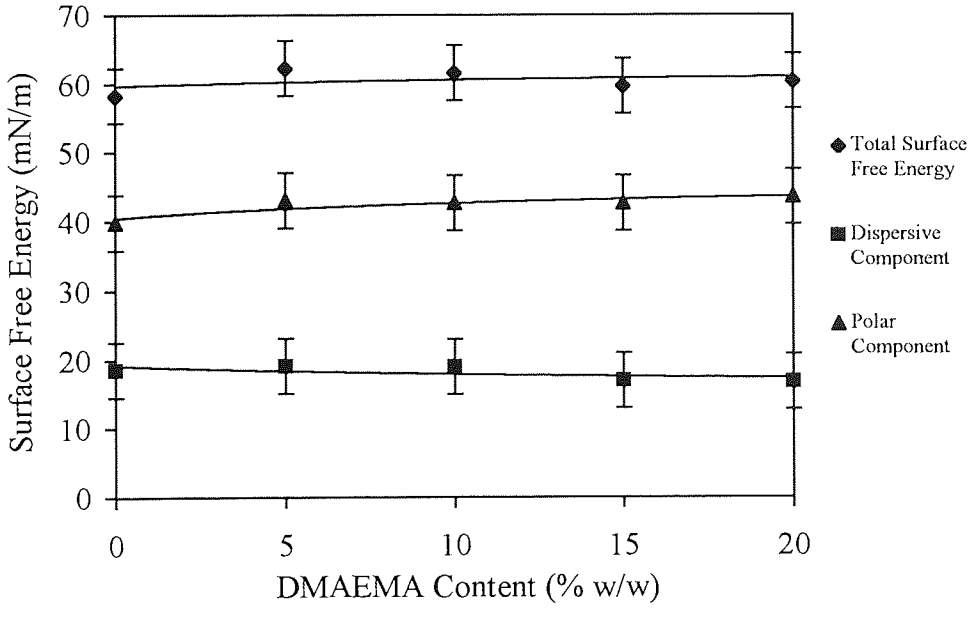

Figure 5.16 Graph to show the effect of composition on the surface properties of hydrated NNDMA-CHMA 70:30 materials copolymerised with 0-20% DMAEMA

in the total surface free energy of the materials, however the polar component is marginally reduced accompanied by an increase in the dispersive component.

Addition of a further 10% of CHMA brings about a further reduction in the polar component and a rise in the dispersive component, as demonstrated by Figures 5.14 and 5.16.

The effect of incorporating either of the basic monomers NVI or DMAEMA on the total surface energy of hydrated AMO-CHMA materials, as well as the polar and dispersive components of the surface free energy, is illustrated in Figures 5.17 - 5.20.

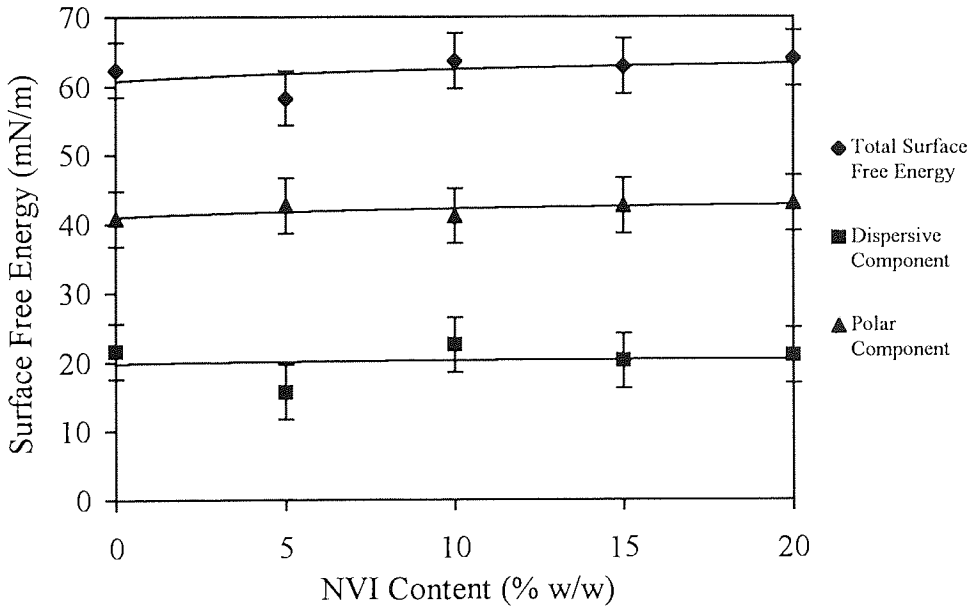

Figure 5.17 Graph to show the effect of composition on the surface properties of hydrated AMO-CHMA 80:20 materials copolymerised with 0-20% NVI

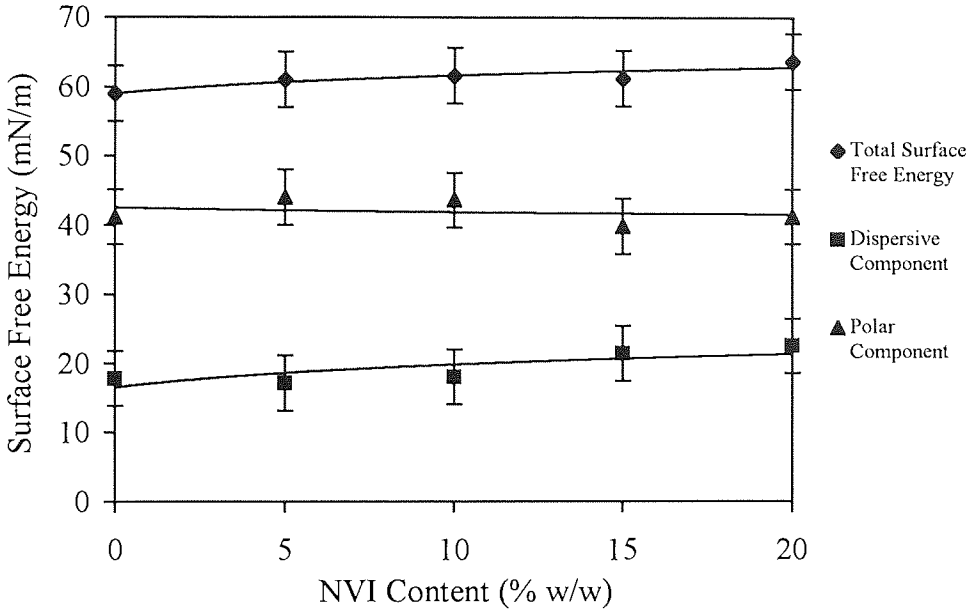

Figure 5.18 Graph to show the effect of composition on the surface properties of hydrated AMO-CHMA 70:30 materials copolymerised with 0-20% NVI

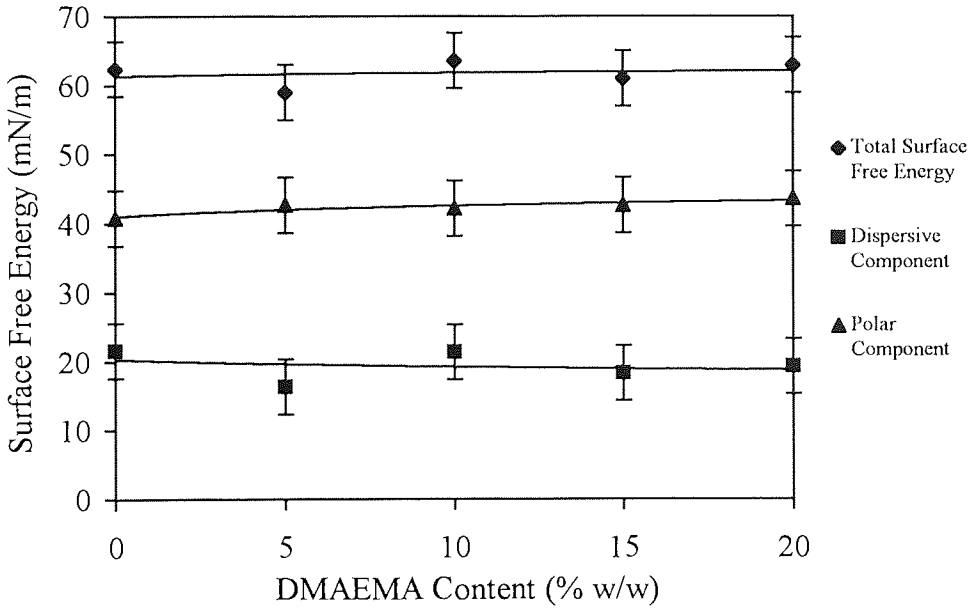

Figure 5.19 Graph to show the effect of composition on the surface properties of hydrated AMO-CHMA 80:20 materials copolymerised with 0-20% DMAEMA

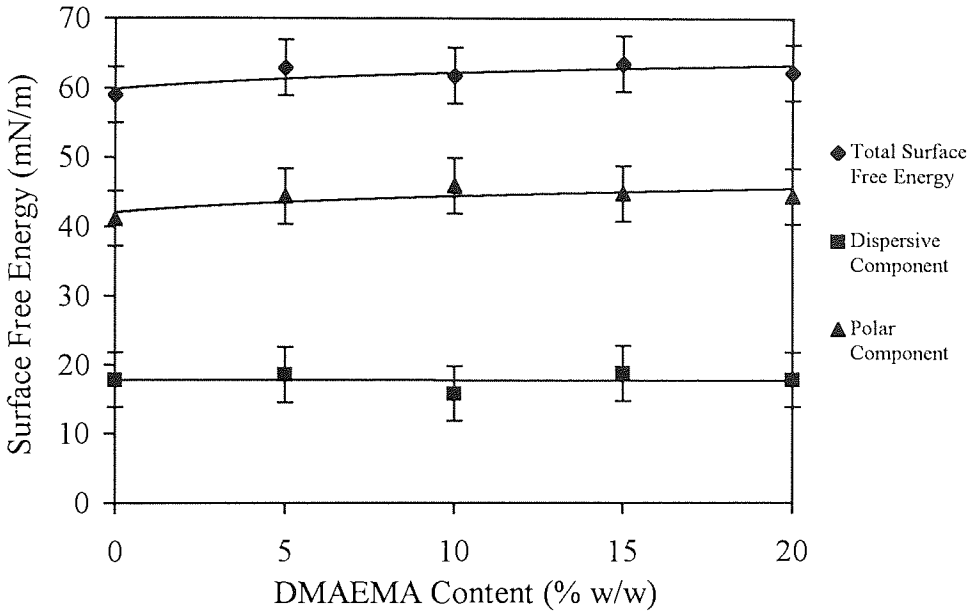

Figure 5.20 Graph to show the effect of composition on the surface properties of hydrated AMO-CHMA 70:30 materials copolymerised with 0-20% DMAEMA

It can be seen once again from these Figures that progressive incorporation of either NVI or DMAEMA does not significantly affect the total surface free energy of the AMO-CHMA materials. Neither does the incorporation of these monomers affect the contribution of the polar or dispersive components of the surface free energy. It is perhaps somewhat surprising to see so little variation in the surface properties for these materials as their water contents are not all the same and thus the contribution of the γ^t of the water to the γ_s^t of the material may be expected to vary. It has been noted already that the surface of the materials seems to be dominated by the hydrophobic CHMA. The monomers used in this work, in particular CHMA, NVI, AMO and DMAEMA all have either a ring structure or an α-methyl group, (or both in the case of CHMA). These structural features restrict the freedom of rotation around the backbone of the polymer. Thus in the hydrated state it may be the case

that the surface of the material remains dominated by the hydrophobic groups as opposed to any polar groups being expressed at the surface.

5.4 Conclusions

The surface free energies of hydrogel materials can be measured in both the hydrated and the dehydrated state using the sessile drop technique or using Hamiltons method in conjunction with the captive air bubble technique. None of the methods were without inaccuracies. In the dehydrated state rapid hydration in air and the interaction with the water used as a wetting liquid in the sessile drop technique is a major cause of inaccuracies as is orientation of the groups at the polymer surface, which may be affected by the polarity of the adjacent phase. In the hydrated state precise measurement of the interfacial angles is difficult and deformation of the bubble leads to variations in values obtained for similar materials. There is also the suspicion that the measurements are dominated by interfacial adsorbed water layers. Despite these problems useful information may be gained about the surface properties of hydrogel materials.

Incorporation of either basic monomer, NVI or DMAEMA, causes very little change in the total surface energies, or the contribution of the polar and dispersive components of the materials studied, whether in the hydrated or dehydrated state. The measured surface energies of the hydrated materials are higher than those for the dehydrated materials and the contribution of the polar component is greater. This is due to the presence of water with a high polar component of surface free energy, (51.0 mN/m) and a higher total surface free energy, (72.8 mN/m), than polymers.

Introduction of the hydrophobic monomer, CHMA increases the dispersive component of surface free energy in all of the materials studied and in the materials where CHMA is present it appears to make a major contribution to the surface of the material.

CHAPTER 6

Deposition Characteristics of Novel Ionic Materials

6.1 Introduction

The main problem associated with any synthetic material introduced at a biological interface, whether in the eye or in contact with any other body fluid, is one of biocompatibility. In many situations where a lack of biotolerence is observed e.g. clotting of the blood at foreign surfaces, marine fouling and spoilation of contact lens materials, the underlying process is the same - the adsorption of proteins at solid surfaces. Protein deposition occurs rapidly as a material is brought into contact with a protein-containing solution and in natural systems this protein film provides a convenient surface for the build up of other components such as lipids and micro-organisms.

There are several factors which affect protein adsorption at a solid surface. The surface character of the material itself plays a vital role i.e. the surface energy and surface charge of the material and the interfacial energy that exists between the material and the body fluid with which it is in contact. Castillo *et al.*[142] suggested that hydrophobic surfaces interact with proteins more strongly than hydrophilic surfaces, following their work on albumin adsorption on 2-hydroxyethyl methacrylate, (HEMA) and HEMA-co-methacrylic acid, (MAA) contact lens surfaces. However previous work carried out on protein deposition on high water content HEMA-co-N-vinyl pyrrolidone, (NVP) lens materials[143] recorded that this deposition was identical to that on a HEMA lenses. It has also been shown that deposits often occur around defects in lens surfaces[142,143]. The nature of the proteins themselves will of course affect their degree of adsorption onto synthetic surfaces. The tertiary structure of proteins renders their surface complex with various degrees of hydrophilicity and charge,

making the prediction of how specific proteins will behave at a surface less than straightforward. In the case of contact lens wear, a primary factor affecting the amounts of protein adsorbed is the individual wearing the lens. The method of manufacture and the lens composition will also be important[144], with HEMA-MAA lenses adsorbing significantly more than HEMA lenses, whilst lathe cut lenses adsorb more than spin cast lenses.

Introduction of basic monomers into a hydrogel design will create potential cationic sites at the surface of the material, and this chapter looks at the effect this has on the spoilation characteristics of such hydrogel materials. A technique whereby the interactions of specific individual proteins are studied with respect to their behaviour at a potentially positively charged surface has been employed. An *in vitro* spoilation model which has been developed at Aston[145] and provides the potential to show significant effects on lipid as well as protein deposition at the hydrogel surface has also been used.

If we are to use the ocular environment as a model to assess the level of deposition on new materials it is essential that we have an understanding of the nature and composition of the tear fluid itself. Although the tears are easily accessible, the small volumes available for study mean that the reports on the components of tears are quite diverse and dependent on the techniques used for their collection and analysis. Table 6.1 lists the major tear components relying on a survey of the literature[146]. Some of these tear components, such as lysozyme, have been well studied with

several sources on which to base an average. For others, it is necessary to rely on single reported measurements.

Component	Average Conc.	Max. Value Quoted	Min. Value Quoted	No. of Ref. Sources
Total Protein	735	800	652	3
Lysozyme	220	330	65	9
Albumin	152	390	4.2	7
Tear-specific Prealbumin	108	168	52	4
Lactoferrin	184	286	81	5
IgA	39	85	7.0	12
IgG	16	79	trace	9
IgM	0.27	0.56	0	7
IgE	0.01	0.02	0.003	2
Total Lipid	218	240	196	1
Cholesterol	105	203	8.0	4
Glucose	5.2	61.8	0	6
Ascorbic Acid	6.8	23	0.14	2
Chloride	469.6	512.9	85	6
Sodium	337.7	354	326.6	5
Calcium	3.6	8.0	1.2	6
Potassium	82.7	137	58.7	9

Table 6.1 The concentrations of some major tear components, (mg/100ml), (reproduced from ref. 55)

Of course not all biological fluids are identical in their composition and blood is the only one with a clotting mechanism designed to make sure it does not leave the body. The composition of tears might be thought of as being simpler than that of blood plasma, although each has its own elements of complexity along with certain similarities. The protein content of tears differs in several respects to that of blood plasma, despite the fact that albumin represents over 30% of the total protein in tears as it does in plasma. The remainder is principally divided between lactoferrin and lysozyme fractions together with the globulins.

The tear film is not homogeneous but consists of several phases, a superficial lipid layer, the aqueous layer comprising about 98% of the total film thickness and a mucoid layer, although it has been suggested that this is not a separate layer at all but is in fact part of the aqueous layer[147]. The protein components of tears are found chiefly in the middle aqueous layer. In addition to the proteinaceous constituents, which include the immunoglobulins and enzymes, the aqueous tear fluid also contains salts, urea, glucose, leukocytes and tissue debris. The electrolyte content resembles that of blood serum or bile and normal tears have a pH of 7.4. The superficial lipid layer is secreted by the meibomian glands and the glands of Moll and Zeis. Chromatographic analysis has shown the presence of all lipid classes in the meibomian secretion - hydrocarbons, wax esters, cholesterol esters, triglycerides and in smaller amounts diglycerides, monoglycerides, fatty acids, cholesterol and phospholipids.

6.2 The Effect of Small Percentages of Cationic Substrate on the Adsorption of Specific Proteins

Existing contact lens materials such as Etafilcon A belong to the FDA Group IV. They have a high equilibrium water content typically in the region of 58% and are ionic in nature. This is due to the presence of the anionic component methacrylic acid (MAA). The disinfecting regimes recommended with this type of lens often involve the use of recently introduced multi-purpose care solutions such as ReNu™ (Bausch and Lomb). These multi-purpose care solutions contain polycationic antibacterial agents - the nature of which are described in detail in Chapter 1. The positive charge density of the polycationic antibacterials make it reasonable to assume that they will be adsorbed at the lens surface, subsequently modifying that surface. This has been demonstrated to occur by Wall[148]. Bearing this in mind, it has been recognised that there is a need to investigate the role of cationic substrates in lens spoilation and the behaviour of specific proteins.

Very little work has been carried out in this area and the literature available mainly concerns the role of charge density in blood - hydrogel interactions. There has been some reluctance to use cationically modified hydrogel materials in the biological environment and particularly at the blood - hydrogel interface. This stems from the knowledge that the blood vessel walls and the blood cells have a negative surface charge under normal conditions and would so be expected to interact strongly with any positively charged surface that may be implanted. Ratner *et al.*[78] have summarised some of the literature available and suggest that it is generally thought that negatively charged surfaces are less thrombogenic than those which are positively

charged. Experiments have been carried out which support this[149], however there is also experimental evidence that suggests that it is not such a straightforward matter[150,151]. Ratner concludes that the importance of charge density in blood - hydrogel interactions or *in vivo* healing processes is not at all clear. The interaction of polycationic species with negatively charged body materials has been made use of in cosmetic preparations such as hair conditioners. These polycationic preparations have a relatively high charge density for the specific application of adhering strongly to the hair shaft.

In this work the interaction of specific proteins with poly(2-hydroxyethyl methacrylate), (polyHEMA), materials copolymerised with small percentages of cationic monomer is looked at. Characteristics of the proteins used are displayed in Table 6.2. These results are compared with the interaction of the same proteins with unmodified polyHEMA. The aim has been to study the effect of incorporating basic centres into polyHEMA at levels similar to the concentration of anionic centres in existing lens materials. These lens materials contain no more than 5% of the anionic component and have been shown to increase the uptake of positively charge proteins, in particular lysozyme[55]. The results of this work are seen as important both in the design of new contact lens materials and in assessing the likely role of polycationic antibacterials, absorbed at the surface of existing commercial lens materials, in modifying protein related spoilation behaviour.

Name	Source	Molecular Weight	Relative Charge
Lysozyme	Chicken Egg	12600	(+++)
Albumin	Human Serum	65000	(- - -)
Lactoferrin	Bovine Colostrum	74000	(++)
Insulin	Bovine Pancreas	6000	(0)
Ferredoxin	Spinach	12000	(- - -)

Table 6.2 Characteristics of some proteins used in this work

The effect of the cationic modification of a simple hydrogel substrate on the adsorption of the three main tear proteins was determined by measuring the uptake of lysozyme, lactoferrin and albumin over a period of 14 days. Copolymer samples of 95%(w/w) HEMA with either 5%(w/w) N-vinyl imidazole (NVI) or 5%(w/w) dimethylaminoethyl methacrylate (DMAEMA) were used for this work. Samples cut from the hydrated hydrogel membrane were discs with a surface area of 75mm^2. The results are represented graphically in Figures 6.1 and 6.2 and are compared with the uptake of the proteins on unmodified polyHEMA shown in Figure 6.3. It should be noted that in this section the results presented are the mean of at least three measurements and the error associated with each result is ±2μg/sample.

From Figures 6.1 and 6.2 the trend seems quite clear. Albumin is deposited on the sample surfaces to a greater extent than lysozyme, which in turn is deposited to a greater extent than lactoferrin.

Time (Days)	Concentration of Protein (mg/sample) (±0.002)		
	Lysozyme	Albumin	Lactoferrin
1	0.001	0.003	0.001
2	0.007	0.009	0.003
3	0.009	0.012	0.006
6	0.015	0.023	0.009
7	0.019	0.026	0.010
9	0.023	0.031	0.010
14	0.027	0.034	0.010

Table 6.3 The concentrations of the three main tear proteins on a HEMA substrate modified with 5% NVI, over a period of 14 days

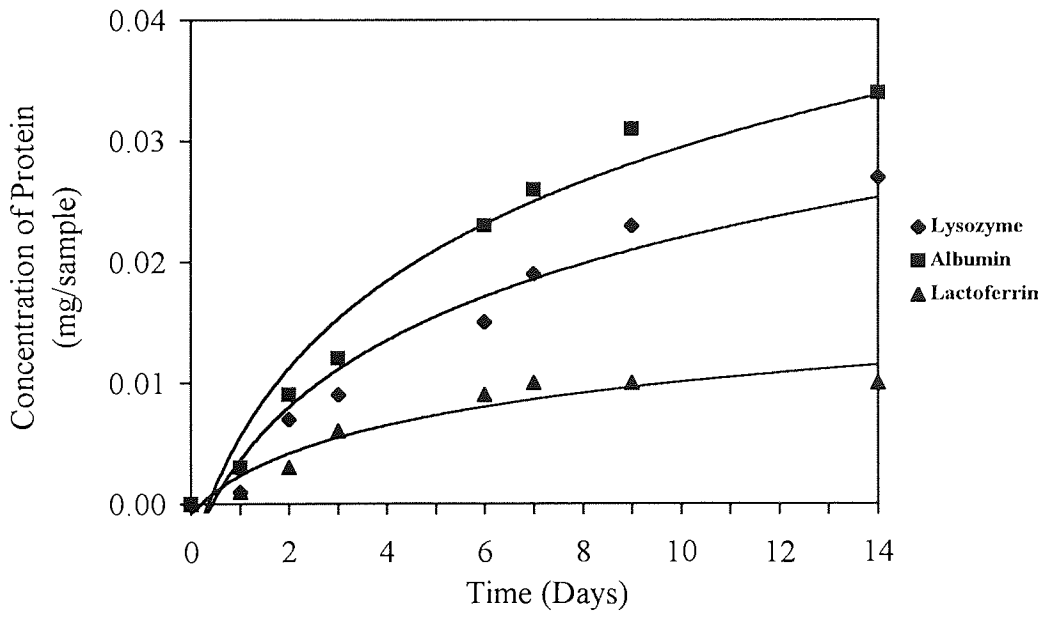

Figure 6.1 Graph to demonstrate the uptake of the three main tear proteins as a function of time on a HEMA substrate modified with 5% NVI

Time (Days)	Concentration of Protein (mg/sample) (±0.002)		
	Lysozyme	Albumin	Lactoferrin
1	0.016	0.005	0.004
2	0.019	0.010	0.005
3	0.022	0.017	0.006
6	0.023	0.026	0.011
7	0.024	0.032	0.012
9	0.025	0.039	0.012
14	0.026	0.041	0.014

Table 6.4 The concentrations of the three main tear proteins on a HEMA substrate modified with 5% DMAEMA, over a period of 14 days

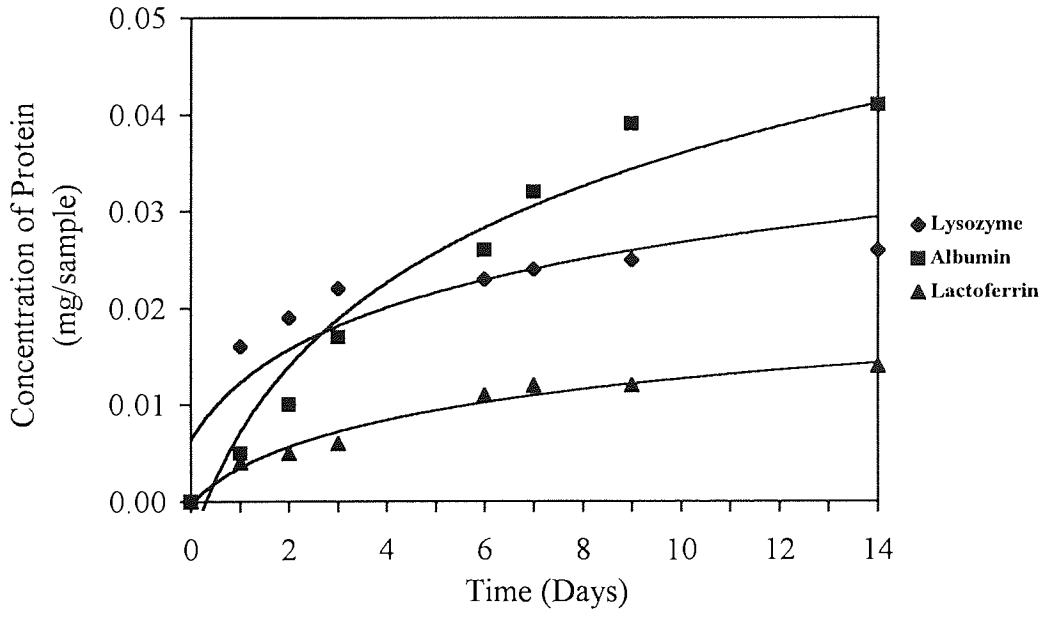

Figure 6.2 Graph to demonstrate the uptake of the three main tear proteins as a function of time on a HEMA substrate modified with 5% DMAEMA

Time (Days)	Concentration of Protein (mg/sample) (±0.002)		
	Lysozyme	Albumin	Lactoferrin
1	0.043	0.008	0.005
2	0.056	0.013	0.006
3	0.061	0.013	0.007
6	0.087	0.014	0.011
7	0.094	0.016	0.013
9	0.106	0.016	0.016
14	0.108	0.024	0.020

Table 6.5 The concentrations of the three main tear proteins on an unmodified HEMA substrate over a period of 14 days

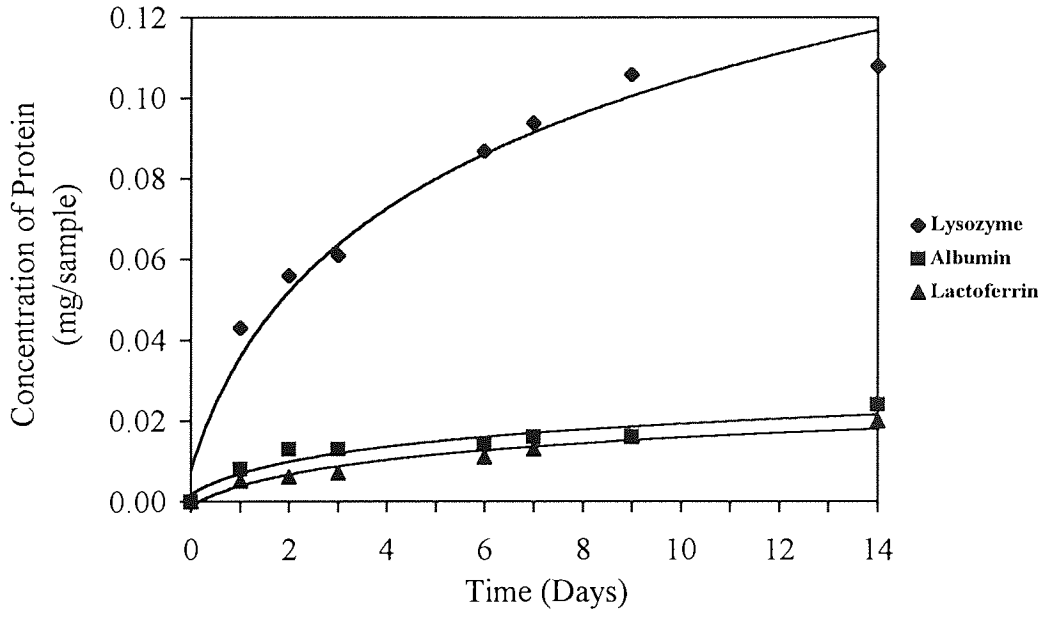

Figure 6.3 Graph to demonstrate the uptake of the three main tear proteins as a function of time on an unmodified HEMA substrate

The actual value of the lysozyme uptake varies little between samples containing either 5% NVI or 5% DMAEMA although the concentration of lactoferrin and in particular albumin shows a slight increase on the samples made using 5% DMAEMA over those containing 5% NVI. Comparing Figures 6.1 and 6.2 with Figure 6.3 it can be seen that the addition of 5% of a cationic centre significantly reduces the uptake of lysozyme. After 14 days the reduction is as much as 80%. The concentration of lactoferrin is also reduced although the degree of reduction is not as marked. In contrast, the concentration of albumin rises by somewhere in the region of 30 - 40% depending on the cationic component used.

Lysozyme has the smallest size of these three tear proteins and is an extremely compact molecule with an isoelectric point of 11.1. Under these experimental conditions, operating at pH 7.4, lysozyme has a high positive charge density. As such it is not surprising that lysozyme shows a reduced adsorption onto the more cationic hydrogel surfaces. The uptake of lactoferrin is less than that for lysozyme on both of the cationic materials. It is larger in size and, with an isoelectric point of 9.6, it has a lower charge density than lysozyme. Albumin also has larger size than lysozyme, but with an isoelectric point of 4.9, under these operating conditions it will have a negative charge density. The concentration of albumin on the cationic materials is greater than that of both lactoferrin and lysozyme, which is logically attributable to the attraction of the negative charge to the cationic surface of the material.

In order to investigate closer the relation between the charge of the protein and its association with a hydrogel that has been modified with a basic centre and to reduce

the effect of differing protein sizes, the uptake of lysozyme, ferredoxin and insulin on further samples of HEMA copolymerised with either 5% NVI or 5% DMAEMA was studied. Lysozyme and ferredoxin from spinach have very similar sizes, however they have opposite net charges. Insulin is also a small protein but has no overall charge. These results are illustrated in Figures 6.4 and 6.5 and are compared to the uptake of these proteins on an unmodified HEMA substrate, (Figure 6.6).

A reduction in the concentration of lysozyme is seen on both of the cationically modified hydrogels in comparison to the concentration on unmodified polyHEMA, although as previously there is little difference between the values obtained for samples containing either 5% NVI or 5% DMAEMA. The concentration of ferredoxin shows a significant increase of approximately 40% for those samples containing 5% NVI and almost 60% for those samples containing 5% DMAEMA. Insulin shows perhaps the most notable change in behaviour. Addition of 5% NVI hardly increases the uptake of insulin but the addition of 5% DMAEMA increases the amount of insulin adsorbed to a very significant degree with the concentration after 14 days reaching to almost the same levels as the concentration of lysozyme on the unmodified polyHEMA samples.

As explained previously the small compact nature of lysozyme and its high positive charge density account for the reduction in lysozyme concentration on the materials containing the cationic components. Conversely, the increase in concentration of ferredoxin on these materials can be assumed to be as a result of the electrostatic

Time (Days)	Concentration of Protein (mg/sample) (±0.002)		
	Lysozyme	Ferredoxin	Insulin
1	0.001	0.004	0.000
2	0.007	0.012	0.003
3	0.009	0.016	0.005
6	0.015	0.027	0.006
7	0.019	0.033	0.007
9	0.023	0.038	0.009
14	0.027	0.042	0.010

Table 6.6 The concentrations of similar sized proteins on a HEMA substrate modified with 5% NVI over a period of 14 days

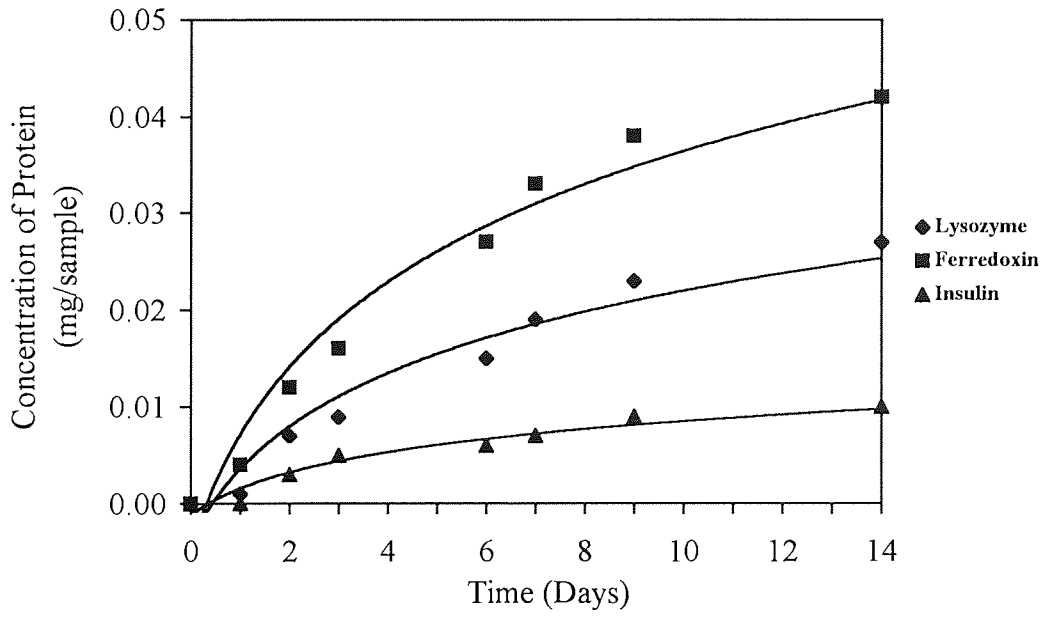

Figure 6.4 Graph to demonstrate the uptake of similar sized proteins as a function of time on a HEMA substrate modified with 5% NVI

Time (Days)	Concentration of Protein (mg/sample) (±0.002)		
	Lysozyme	Ferredoxin	Insulin
1	0.016	0.015	0.071
2	0.019	0.018	0.076
3	0.022	0.025	0.080
6	0.023	0.038	0.091
7	0.024	0.043	0.092
9	0.025	0.051	0.097
14	0.026	0.062	0.099

Table 6.7 The concentrations of similar sized proteins on a HEMA substrate modified with 5% DMAEMA over a period of 14 days

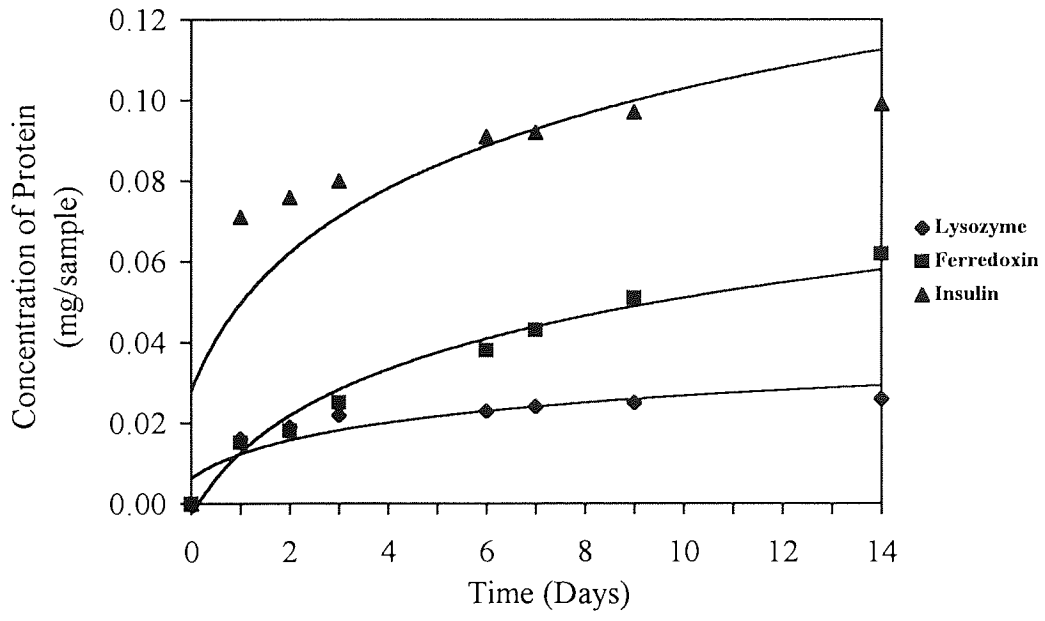

Figure 6.5 Graph to demonstrate the uptake of similar sized proteins as a function of time on a HEMA substrate modified with 5% DMAEMA

Time (Days)	Concentration of Protein (mg/sample) (±0.002)		
	Lysozyme	Ferredoxin	Insulin
1	0.043	0.003	0.000
2	0.056	0.005	0.002
3	0.061	0.008	0.004
6	0.087	0.014	0.004
7	0.094	0.015	0.006
9	0.106	0.020	0.008
14	0.108	0.024	0.009

Table 6.8 The concentrations of similar sized proteins on an unmodified HEMA substrate over a period of 14 days

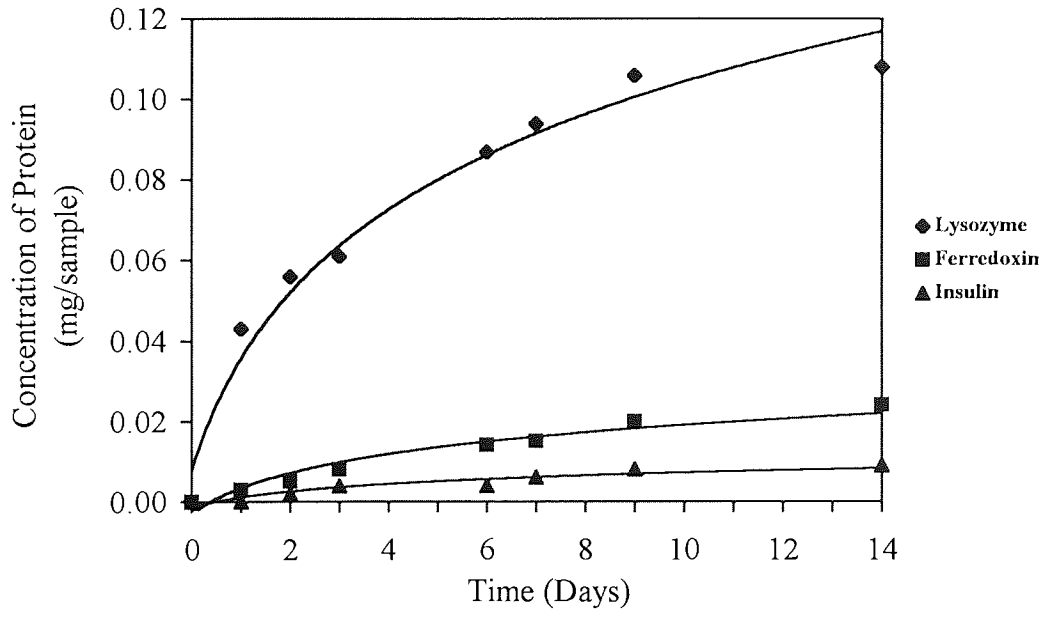

Figure 6.6 Graph to demonstrate the uptake of similar sized proteins as a function of time on an unmodified HEMA substrate

attraction that exists between the negative charge of the ferredoxin and the positive charge of the sample. Although insulin has no overall charge it shows dramatically increased adsorption on to the surface of the material containing 5% DMAEMA. Obviously the driving force for the adsorption of insulin onto this surface is not a straightforward electrostatic interaction as seems to be primarily the case with the other proteins. Although insulin shows no resultant charge, this just means that the acidic and basic residues are balanced so that the protein appears neutral. The protein sequence of bovine insulin displays regions of anionicity and cationicity as well as uncharged polar and non-polar regions with which it can interact with the hydrogel surface.

Although the adsorption of single protein solutions give useful comparative information about the behaviour of individual polymer substrates, it does not necessarily predict the more complex behaviour of mixed protein solutions in a biological fluid such as tears or blood. It is fair to say that adsorption of proteins is related to not only charge and polarity but also to size and hydrophobicity and will also be influenced by the pH and ionicity of the medium.

In order to determine whether the proteins are adsorbed reversibly onto the surface of the hydrogel, and their ease of removal, the effect of surfactant and agitation on protein removal was investigated. All of the samples were soaked in ReNu™ multipurpose cleaner (Bausch and Lomb) and placed in an ultrasonic cleaning bath for 10 minutes. The UV absorbance was measured after cleaning and the concentration of protein remaining was noted.

Protein	Concentration (mg/sample)
lysozyme	0.002±0.002
ferredoxin	0.012±0.002
insulin	0.002±0.002
lactoferrin	0.002±0.002
albumin	0.003±0.002

Table 6.9 Concentration of protein remaining after surfactant cleaning and agitation, for materials containing 5% NVI

Protein	Concentration (mg/sample)
lysozyme	0.002±0.002
ferredoxin	0.012±0.002
insulin	0.012±0.002
lactoferrin	0.002±0.002
albumin	0.003±0.002

Table 6.10 Concentration of protein remaining after surfactant cleaning and agitation, for materials containing 5% DMAEMA

From Tables 6.9 and 6.10 it can be seen that the only protein that is difficult to completely remove from both cationic materials is ferredoxin. This may be because the high negative charge density on ferredoxin enables the protein to interact more strongly with the cationic materials. Although ferredoxin is small in size it is unlikely that it has been absorbed into the bulk of the hydrogel matrix as the equilibrium content of these materials lie in the range of 38 - 40%. It can also be seen from Table

6.10 that the insulin has not been completely removed from the material containing 5% DMAEMA.

Figures 6.7 and 6.8 show the effect of adding increasing amounts of basic monomer to HEMA on the adsorption of the proteins. 0-5% of either NVI or DMAEMA was copolymerised with HEMA and samples of the materials were soaked in $0.5mgml^{-1}$ solutions of each protein for 14 days.

Figure 6.7 shows the progressive reduction in the concentration of lysozyme on the materials containing increasing percentages of NVI. Lactoferrin also shows a reduction in concentration as the NVI content increases although this effect is very slight. Albumin and ferredoxin both show an increase in concentration with increasing NVI content. Ferredoxin is slightly more affected than albumin, with its original concentration almost doubling when 5% NVI is incorporated into the polyHEMA material. Insulin shows a maximum concentration for the polyHEMA material copolymerised with 2% NVI although the variation in concentration from 0% - 5% NVI content is small.

It can be seen from Figure 6.8 that the trends are, for the most part, similar to those in Figure 6.7, although it is noted that the incorporation of DMAEMA seems to have a slightly more magnified effect on the proteins than NVI. Differences exist in the effect of DMAEMA incorporation on the adsorption of lysozyme and insulin.

% NVI (w/w)	Concentration of Protein (mg/sample) (±0.002)				
	Lysozyme	Albumin	Lactoferrin	Ferredoxin	Insulin
0	0.108	0.024	0.020	0.024	0.009
1	0.068	0.024	0.016	0.028	0.010
2	0.038	0.027	0.015	0.029	0.038
3	0.029	0.030	0.011	0.032	0.030
4	0.029	0.032	0.010	0.036	0.018
5	0.027	0.034	0.010	0.042	0.010

Table 6.11 The concentrations of proteins adsorbed after 14 days on HEMA substrates copolymerised with progressive amounts of NVI

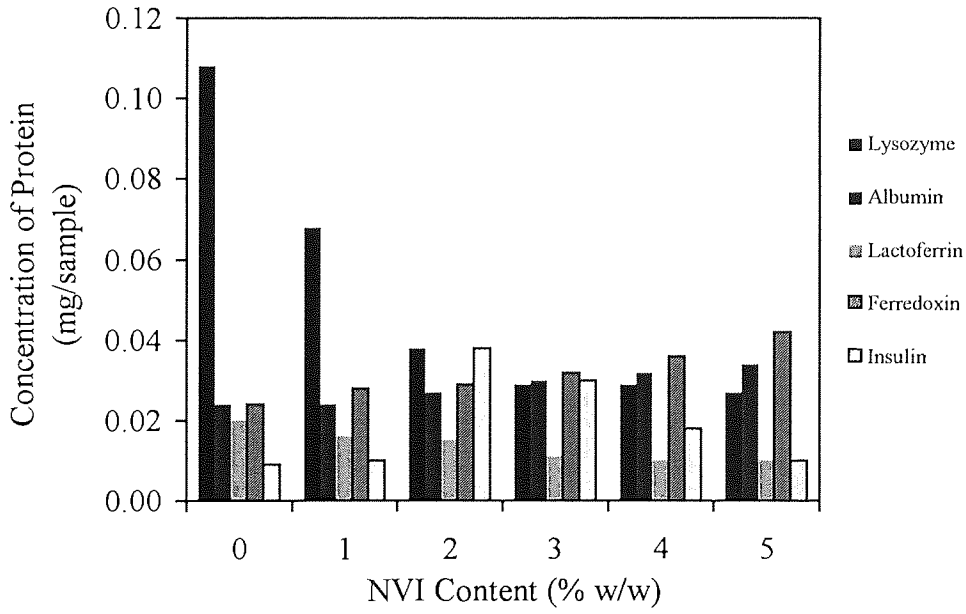

Figure 6.7 Graph to show the concentrations of proteins adsorbed after 14 days on HEMA substrates copolymerised with progressive amounts of NVI

% DMAEMA (w/w)	Concentration of Protein (mg/sample) (±0.002)				
	Lysozyme	Albumin	Lactoferrin	Ferredoxin	Insulin
0	0.108	0.024	0.020	0.024	0.009
1	0.010	0.026	0.016	0.018	0.009
2	0.011	0.031	0.015	0.028	0.020
3	0.012	0.033	0.014	0.045	0.045
4	0.018	0.036	0.010	0.053	0.055
5	0.026	0.041	0.014	0.062	0.099

Table 6.12 The concentrations of proteins adsorbed after 14 days on HEMA substrates copolymerised with progressive amounts of DMAEMA

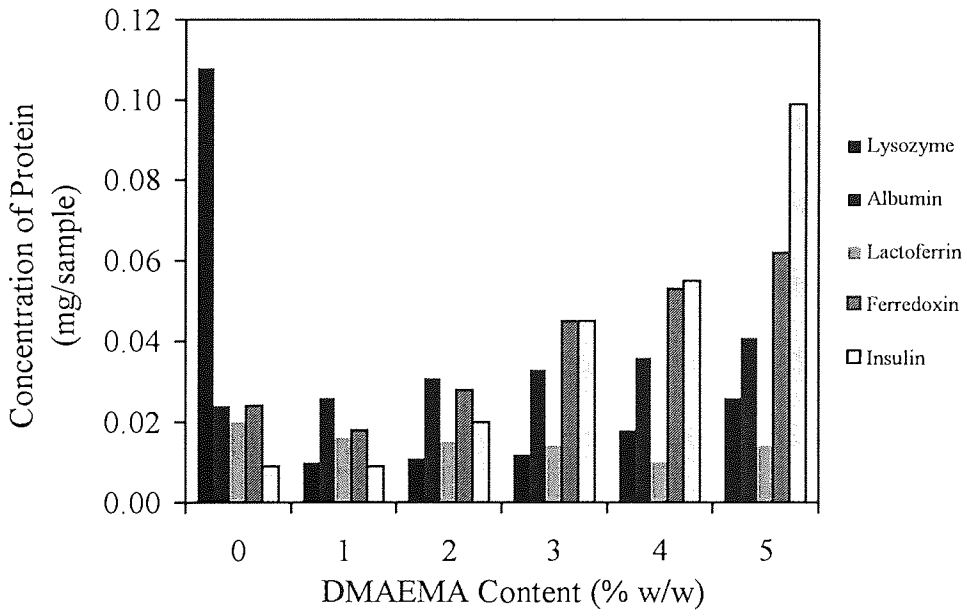

Figure 6.8 Graph to show the concentrations of proteins adsorbed after 14 days on HEMA substrates copolymerised with progressive amounts of DMAEMA

The concentration of lysozyme is reduced more dramatically when DMAEMA is introduced, but over the range of incorporation from 1% - 5% of this cation, there is a small increase in lysozyme concentration. At levels of 5% cation incorporation, the amounts of lysozyme adsorbed are similar for both NVI and DMAEMA. Insulin no longer shows a maximum at 2% DMAEMA but greatly increases over the range from 1% - 5% DMAEMA.

The trends can be explained mainly in terms of electrostatic interaction taking into account the charge and size of the individual proteins. Both albumin and ferredoxin have a negative charge and therefore would be expected to show increased adsorption with progressive incorporation of cation. But, as albumin is larger and less compact than ferredoxin, it has a lower charge density. Thus, the progressive increase in the proportion of the cationic component results in a smaller increase in the concentration of albumin than in the concentration of ferredoxin. Similarly although lysozyme and lactoferrin both have a positive charge, lysozyme is smaller and more compact than lactoferrin, with a greater charge density. Consequently a larger reduction in the concentration of lysozyme than the concentration of lactoferrin is seen with the progressive accumulation of the cationic component. The adsorption of insulin, as mentioned previously, is not driven by electrostatic attraction alone and the greatly increasing adsorption displayed on the materials containing 0% - 5% DMAEMA must be affected by other factors.

Previous values published for the concentration of lysozyme on polyHEMA materials[54] indicate that the expected concentration is in the region of 0.060 -

0.065mg/sample. It can be seen that values of 0.108mg/sample obtained in this work are somewhat higher than expected. It is well known that 2-hydroxyethyl methacrylate undergoes a disproportionation reaction, producing methacrylic acid, which in turn results in the fact that polyHEMA will possess different degrees of anionicity depending on the level of residual MAA in the monomer and the polymerisation procedure. As a result commercial polyHEMA lenses will adsorb measurably different levels of cationic proteins such as lysozyme.

The 2-hydroxyethyl methacrylate used in this study was purchased as optical monomer grade and used without further purification. The higher values of lysozyme concentration obtained suggest a degree of residual MAA in this monomer. One of the first effects of cation incorporation is to offset the resultant anionicity of the polyHEMA. Ready incorporation of DMAEMA is likely, because of the relative similarities of reactivity ratios to HEMA and MAA. Not only is NVI somewhat different in basicity, it is also quite different in reactivity and is therefore less effectively incorporated. It is believed that the difference in the progressive effect of NVI on the adsorption of lysozyme and the more abrupt effect of DMAEMA is related to a contribution of basicity of the monomer and its sequence distribution in the polymer, (illustrated in Appendix 1).

6.3 *In Vitro* Spoilation of PolyHEMA Materials Modified with a Cationic Substrate

The chemistry of tears is very complex and can vary from individual to individual. It can also be affected by external stimulation e.g. the chemistry of tears which result

from peeling onions can be very different to the unstimulated tear film. Thus it is difficult to obtain consistent results from *in vivo* ocular spoilation studies. An *in vitro* spoilation method has been developed in these laboratories[145] in order to overcome this problem. The model is used to mimic the ocular spoilation process and employs a standard artificial tear solution based on foetal calf serum and phosphate buffered saline (pH 7.4). The solution is similar to natural tears and offers opportunities to spike the system with other tear components such as mucin, lactoferrin and lysozyme. The deposition of both lipid and protein can be detected non-destructively by fluorescence spectroscopy. Since this is an *in vitro* model it allows us the opportunity to test a much wider range of materials than *in vivo* methods would allow.

The ocular spoilation model has been used here to assess whether the incorporation of a basic monomer such as NVI or DMAEMA into a hydrogel system, at very low levels, has any effect on tear film compatibility. The deposition of both lipids and proteins from artificial tear solutions was monitored at regular intervals over a period of 28 days using fluorescence spectroscopy. An excitation wavelength of 360nm was used for the emission spectra where maximum lipid sensitivity is required. An excitation wavelength of 280nm was additionally used to distinguish between the protein and lipid contributions to the deposited layer. The results are presented in numerical form in Appendix 5. The purpose of these experiments is to give a guide as to the performance of potentially cationic materials with regards to spoilation, in comparison with other materials already tested. For ease of presentation, therefore, the progressive accumulation of protein and lipid, monitored by surface fluorescence spectroscopy was compiled to give a single spoilation factor.

Figures 6.9 and 6.10 show the relative increases in spoilation factor for HEMA substrates copolymerised with either NVI or DMAEMA respectively. From these Figures it can be seen that there is a continuous increases in the spoilation factor over a period of 28 days. This is quite different from the way in which simple protein accumulation occurs, where the rapid initial deposition is followed by a plateau. It is the lipid component that causes the difference, as after a short induction period the lipid can progressively penetrate the polymer matrix of hydrogel materials.

There is no clear indication as to whether the introduction of either NVI or DMAEMA has a beneficial effect on the levels of spoilation for these polyHEMA systems. There is also no apparent difference in the spoilation factors obtained for materials containing DMAEMA in comparison with those obtained for materials containing NVI.

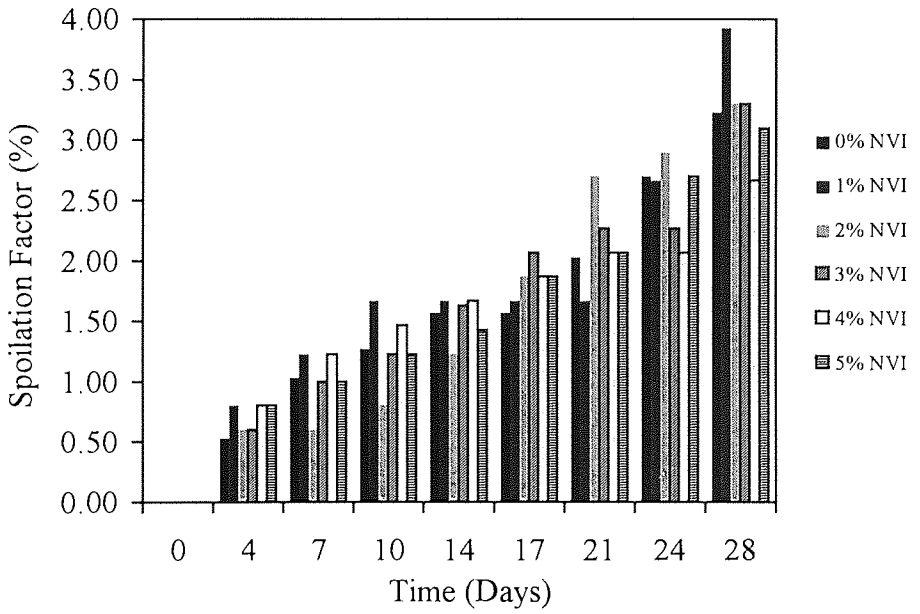

Figure 6.9 Graph to show the spoilation factors of HEMA substrates copolymerised with progressive amounts of NVI

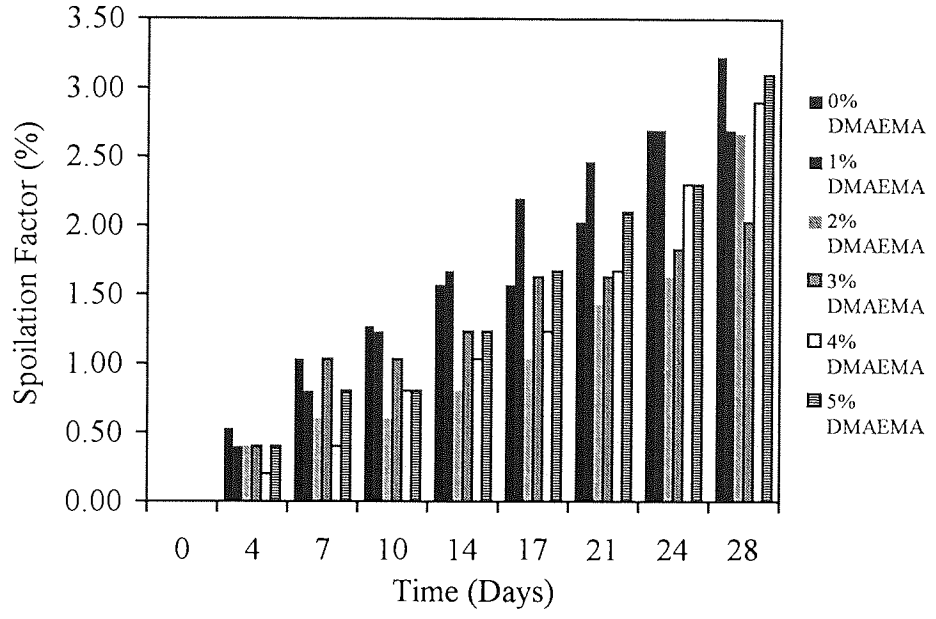

Figure 6.10 Graph to show the spoilation factors of HEMA substrates copolymerised with progressive amounts of DMAEMA

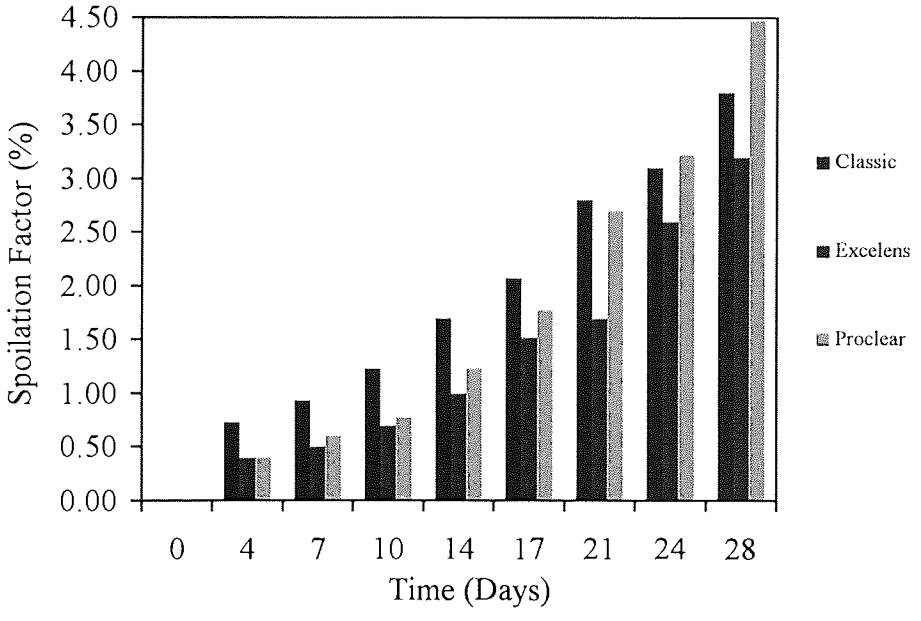

Figure 6.11 Graph to show the spoilation factors of some commercially available lenses

It can however be stated with a degree of certainty that introduction of low levels of a basic monomer does not adversely affect the levels of spoilation seen for either HEMA-NVI or HEMA-DMAEMA materials. The spoilation factors at 28 days for these materials are in the range of approximately 2.5% to 4.0% and these values compare favourably with spoilation factors of 4.5% to 8.0% for HEMA-NVP materials, 5.1% to 6.8% for HEMA-co-N,N'-dimethylacrylamide, (NNDMA), materials and are similar to the values of 2.7% to 3.5% obtained for HEMA-co-acryloyl morpholine, (AMO), materials. It is important to remember that fluorescence emission will always be greater for membrane samples than for commercial lenses, due to the surface roughness of membrane samples. However spoilation factors for some commercial lenses e.g. Proclear, Excelens, Classic, have been presented[65] and are reproduced in Figure 6.11. The results obtained for such lenses are not dissimilar to those presented for the materials in this Section.

6.4 The Effect of Combining Cationic and Anionic Substrates on the Adsorption of Specific Proteins

As stated in Section 6.2, HEMA undergoes a disproportionation reaction to form methacrylic acid and it is very hard to completely free HEMA from this side product. As a result polyHEMA materials will possess differing degrees of anionicity depending on the level of residual methacrylic acid in the monomer and the polymerisation procedure. When a basic component is polymerised with HEMA it introduces the potential for a cationic surface. If however the material already possess trace amounts of methacrylic acid, there is also the potential for anionic regions within the same material. With this in mind the following work was

undertaken to look at the effect of both basic and acidic components copolymerised with HEMA to give a potentially amphoteric material. The HEMA used was purchased as optical grade in the hope that the methacrylic acid content would be as low as possible. NVI was chosen as the basic monomer and methacrylic acid as the acidic monomer. The compositions of the materials are given in Tables 6.13 and 6.14.

Material	Monomers	% MAA (w/w)	EWC (%)
0		0	36.2
1	95% HEMA	1	40.2
2	+	2	42.4
3	5% NVI	3	42.8
4		4	43.0
5		5	42.8

Table 6.13 Compositions of materials with both basic and acidic components

Material	Monomers	% NVI (w/w)	EWC (%)
6		4	43.4
7	95% HEMA	3	41.4
8	+	2	40.4
9	5% MAA	1	38.2
10		0	67.3

Table 6.14 Compositions of materials with both basic and acidic components

These materials were soaked in individual protein solutions as described previously and the levels of protein uptake measured after 14 days. The concentration of the proteins on each material are shown in Tables 6.15 and 6.16 and the results are presented in Figures 6.12 - 6.13 along with comparative results for an unmodified polyHEMA material.

Figure 6.12 shows the effect of incorporating increasing amounts of methacrylic acid (MAA) into a HEMA material already containing 5% NVI. It was expected that the acidic component would offset the effects of the basic component on the uptake of individual proteins over a period of time. It has already been shown that the introduction of 5% NVI leads to a reduction in the amount of lysozyme adsorbed.

With the introduction of MAA even at the lowest level of 1%, it can be seen from Figure 6.12 that the concentration of lysozyme on these materials increases dramatically. A similar trend is observed for lactoferrin although to a slightly lesser effect. Incorporation of 5% NVI to HEMA materials leads to a small increase in the concentrations of albumin adsorbed onto these materials. The introduction of MAA reduces these concentrations below the levels obtained for a polyHEMA material. Increasing the percentage of MAA has little effect on the levels of ferredoxin seen on these materials, but in the case of insulin a very small increase in concentration of this protein is observed. Lysozyme and lactoferrin show greatly increased concentration levels on these materials as soon as MAA is introduced into the system. This has been attributed to the attraction between the negative charge contribution of the MAA and the positive charge of these two proteins.

The effect of MAA on positively charged proteins has been previously studied and the results presented here are consistent with those already documented[13]. The presence of NVI in these materials seems to have no counterbalancing effect.

Monomer	% MAA (w/w)	Concentration of Protein (mg/sample)				
		Lysozyme	Lactoferrin	Albumin	Ferredoxin	Insulin
	0	0.027	0.010	0.034	0.042	0.010
95%	1	0.526	0.115	0.016	0.022	0.008
HEMA	2	0.794	0.128	0.018	0.026	0.014
+	3	0.901	0.125	0.005	0.040	0.019
5%	4	0.849	0.344	0.018	0.038	0.021
NVI	5	1.025	0.672	0.008	0.026	0.025
100% HEMA		0.108	0.020	0.024	0.024	0.009

Table 6.15 The concentrations of individual proteins after 14 days on HEMA-NVI 95: 5 materials copolymerised with increasing amounts of MAA

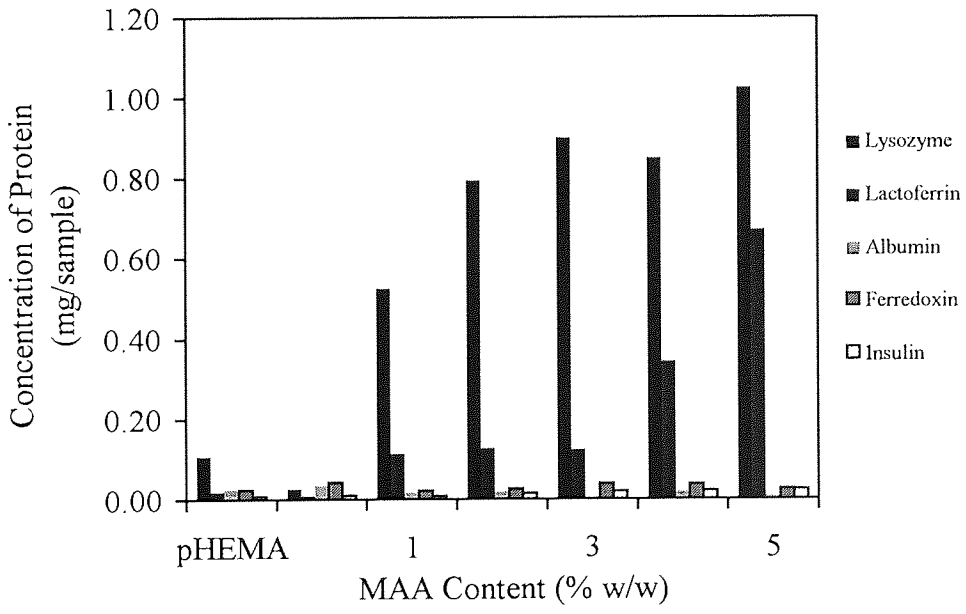

Figure 6.12 Graph to show the uptake of individual proteins after 14 days on HEMA-NVI 95:5 materials copolymerised with increasing amounts of MAA

Monomer	% NVI (w/w)	Concentration of Protein (mg/sample)				
		Lysozyme	Lactoferrin	Albumin	Ferredoxin	Insulin
	0	0.682	0.426	0.068	0.045	0.043
95%	1	0.974	0.268	0.072	0.041	0.070
HEMA	2	1.014	0.400	0.053	0.037	0.064
+	3	0.989	0.358	0.040	0.057	0.060
5%	4	1.003	0.289	0.025	0.041	0.030
MAA	5	1.025	0.672	0.008	0.026	0.025
100% HEMA		0.108	0.020	0.024	0.024	0.009

Table 6.16 The concentrations of individual proteins after 14 days on HEMA-MAA 95:5 materials copolymerised with increasing amounts of NVI

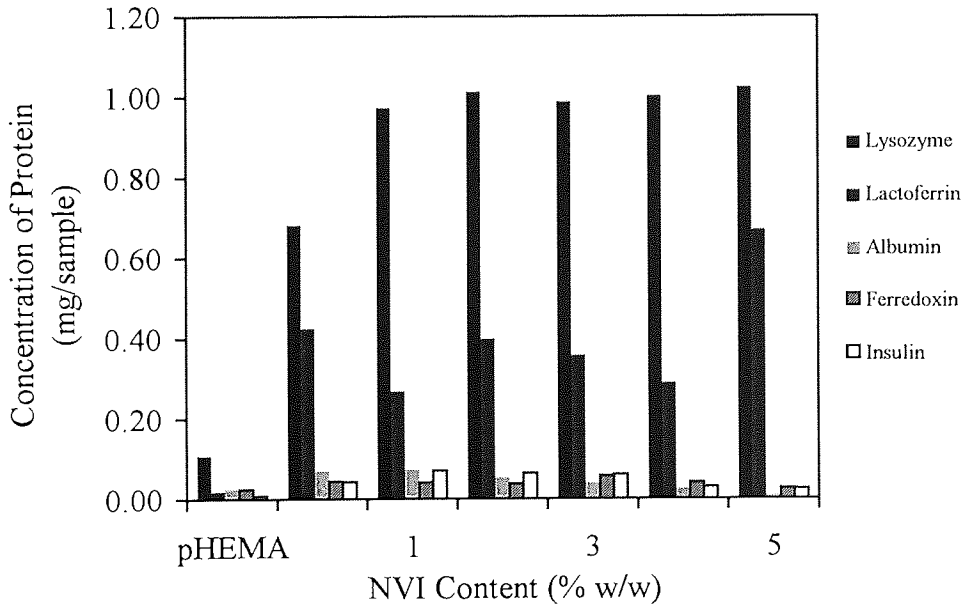

Figure 6.13 Graph to show the uptake of individual proteins after 14 days on HEMA-MAA 95:5 materials copolymerised with increasing amounts of NVI

Alongside these results, the effect of the basic and acidic components on the other negatively charged or neutral proteins is very small. The acidic MAA overrides the attraction that may exist between the positive contribution of the NVI and the other proteins.

Figure 6.13 shows the effect of incorporating increasing amounts of NVI into a HEMA material already containing 5% MAA. It was expected that the basic component would offset the effects of the acidic component on the uptake of individual proteins over a period of time. It can be seen from Figure 6.13 that the addition of 5% MAA alone increases the uptake of lysozyme significantly. Adding NVI to the materials increases the uptake of lysozyme further, although there is little change in the actual values between the material containing 1% NVI and the material containing 5% NVI. This is similarly true for the effect of NVI incorporation on the uptake of lactoferrin. Copolymerising HEMA with 5% MAA increases the concentrations of albumin adsorbed by these materials. Further adding progressive amounts of NVI serves to reduce the uptake of albumin and the material containing both 5% MAA and 5% NVI adsorbs less albumin than the original unmodified HEMA material. The concentration of ferredoxin is higher for the material containing 5% MAA than the unmodified HEMA material and the incorporation of NVI shows little change on the values of ferredoxin concentration obtained. Insulin shows an increase in concentration on the material containing 5% MAA alone. Introduction of NVI initially increases the concentration of insulin further but as the amount of NVI incorporated increases so the concentration of insulin decreases.

Once again the contribution of the MAA can be seen to have the greatest effect on the positively charged proteins masking any effect from the NVI. From the results in Figures 6.12 and 6.13 it can be seen that whilst the introduction of a basic component within a system may offset trace amounts of MAA present in a HEMA monomer as suggested in Section 6.2, as soon as MAA is introduced at levels of 1% and above it has a detrimental effect on the uptake of positively charged proteins, overriding the contribution of the NVI. The nature of the basic component in terms of its reactivity and basicity may be a factor in the results obtained. A more basic monomer may be able to balance the contribution from MAA, and a greater reactivity may lead to more efficient incorporation of the monomer within the material leading to a truer balance in the contribution from each monomer.

In order to determine whether the proteins are adsorbed reversibly onto the surface of the materials, and their ease of removal, the effect of surfactant and agitation on protein removal was investigated. All of the samples were soaked in ReNu^{TM} multipurpose cleaner (Bausch and Lomb) and placed in an ultrasonic cleaning bath for 10 minutes. The UV absorbance was measured after cleaning and the concentration of protein remaining was noted.

From Table 6.17 it can be seen that as the proportion of MAA within the material increases, the proteins are harder to remove and are irreversibly adsorbed. This is particularly evident in the case of the positively charged proteins, especially lysozyme.

Monomer	% MAA (w/w)	Concentration of Protein (mg/sample) (±0.002)				
		Lysozyme	Lactoferrin	Albumin	Ferredoxin	Insulin
	0	0.001	0.004	0.005	0.009	0.000
95%	1	0.375	0.028	0.000	0.002	0.000
HEMA	2	0.625	0.052	0.005	0.018	0.000
+	3	0.854	0.102	0.041	0.031	0.003
5%	4	0.846	0.040	0.121	0.021	0.009
NVI	5	1.005	0.053	0.128	0.032	0.014
100% HEMA		0.090	0.003	0.002	0.002	0.005

Table 6.17 The concentrations of individual proteins remaining after surfactant cleaning and agitation on HEMA-NVI 95:5 materials copolymerised with increasing amounts of MAA

Monomer	% NVI (w/w)	Concentration of Protein (mg/sample) (±0.002)				
		Lysozyme	Lactoferrin	Albumin	Ferredoxin	Insulin
	0	0.603	0.012	0.098	0.031	0.003
95%	1	0.953	0.028	0.115	0.039	0.009
HEMA	2	0.877	0.014	0.077	0.033	0.011
+	3	0.995	0.043	0.059	0.014	0.012
5%	4	1.012	0.023	0.063	0.014	0.015
MAA	5	1.005	0.053	0.128	0.032	0.014
100% HEMA		0.090	0.003	0.002	0.002	0.005

Table 6.18 The concentrations of individual proteins remaining after surfactant cleaning and agitation on HEMA-MAA 95:5 materials copolymerised with increasing amounts of NVI

From Table 6.18 it can be seen that the presence of MAA in these materials reduces the ease with which the proteins could be removed with this method of cleaning and the increasing amounts of NVI have no effect on the results.

From both Tables 6.17 and 6.18 it can be seen that the materials previously soaked in the albumin solution behave strangely during the cleaning process. The concentrations calculated based on the UV absorbance obtained, suggest that there is more protein on some of the materials after the cleaning process. Of course this cannot be the case because the materials are no longer in contact with the protein solution. The conclusion must then be drawn that elements of the cleaning solution are adsorbing to the surface of the materials rather that removing the protein, or indeed adsorbing onto the protein which is in turn adsorbed onto the material. This phenomenon is most evident for the materials with the highest concentrations of MAA. The active antibacterial agent in ReNu^{TM} is polyhexamethylene biguanide which is a positively charged polymeric antibacterial. It is feasible that the negative charge contribution of the MAA attracts the cationic antibacterial to its surface. It should also be remembered that albumin is a negatively charged protein and when adsorbed at the surface of a material will convey a negative charge to that surface again leading to greater attraction between the material and the cationic antibacterial agent.

It should be possible to determine whether the materials adsorb the cationic antibacterial from the cleaning solution and whether the albumin is responsible for increasing the potential of the cationic antibacterial to adsorb to these surfaces. This

can be achieved by cleaning unspoiled samples of these materials in ReNu™ in the same way as the spoiled samples and then noting the difference in the UV absorbance.

Monomer	% MAA (w/w)	Original UV Absorbance	UV Absorbance after cleaning	Resultant UV Absorbance
	0	0.058	0.058	0.000
95%	1	0.102	0.108	0.006
HEMA	2	0.074	0.084	0.010
+	3	0.077	0.100	0.023
5%	4	0.080	0.106	0.026
NVI	5	0.099	0.136	0.037

Table 6.19 The resultant absorbance of HEMA-NVI 95:5 materials copolymerised with increasing amounts of MAA after surfactant cleaning and agitation

From Tables 6.19 and 6.20 it can be seen that the UV absorbance of the samples increases after cleaning with ReNu™ and sonication for 10 minutes in an ultrasound bath. This can be attributed to deposition of the polycationic antibacterial agent in ReNu™ onto the surface of the materials which, by virtue of the fact that they contain MAA, will possess a degree of anionic character. The results from Tables 6.19 and 6.20 can then be explained in terms of the attraction of the negative sites to the cationic antibacterial agent in the cleaning solution, further enhanced by the presence of the negative protein, albumin.

Monomer	% NVI (w/w)	Original UV Absorbance	UV Absorbance after cleaning	Resultant UV Absorbance
	0	0.061	0.133	0.072
95%	1	0.063	0.126	0.063
HEMA	2	0.065	0.100	0.045
+	3	0.066	0.116	0.050
5%	4	0.078	0.126	0.048
MAA	5	0.099	0.136	0.037

Table 6.20 The resultant absorbance of HEMA-MAA 95:5 materials copolymerised with increasing amounts of NVI after surfactant cleaning and agitation

6.5 *In Vitro* Spoilation of PolyHEMA Materials Modified with Combined Cationic and Anionic Substrates

The *in vitro* spoilation method described in Section 6.3 has been used to investigate whether combining both cationic and anionic substrates within a HEMA material has any effect on tear film compatibility. The deposition of both lipids and proteins from artificial tear solutions was monitored at regular intervals over a period of 28 days using fluorescence spectroscopy as described in Section 6.3. The results are presented in numerical form in Appendix 5. For ease of presentation, the progressive accumulation of protein and lipid, monitored by surface fluorescence spectroscopy was compiled to give a single spoilation factor. Figures 6.14 and 6.15 show the relative increases in the spoilation factor for HEMA-NVI 95:5 substrates copolymerised with progressive amounts of MAA and HEMA-MAA 95:5 substrates copolymerised with increasing amounts of NVI respectively.

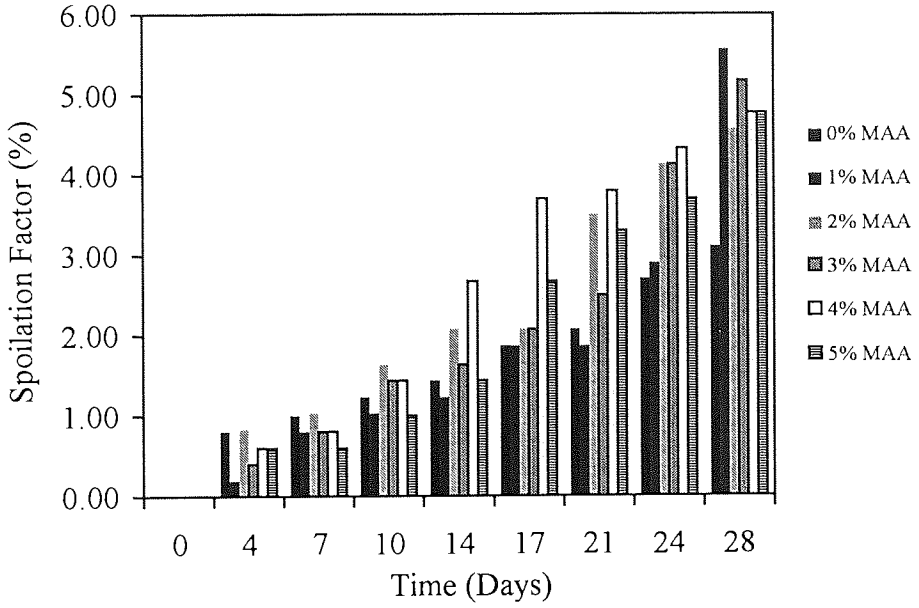

Figure 6.14 Graph to show the spoilation factors of HEMA-NVI 95:5 materials copolymerised with increasing amounts of MAA

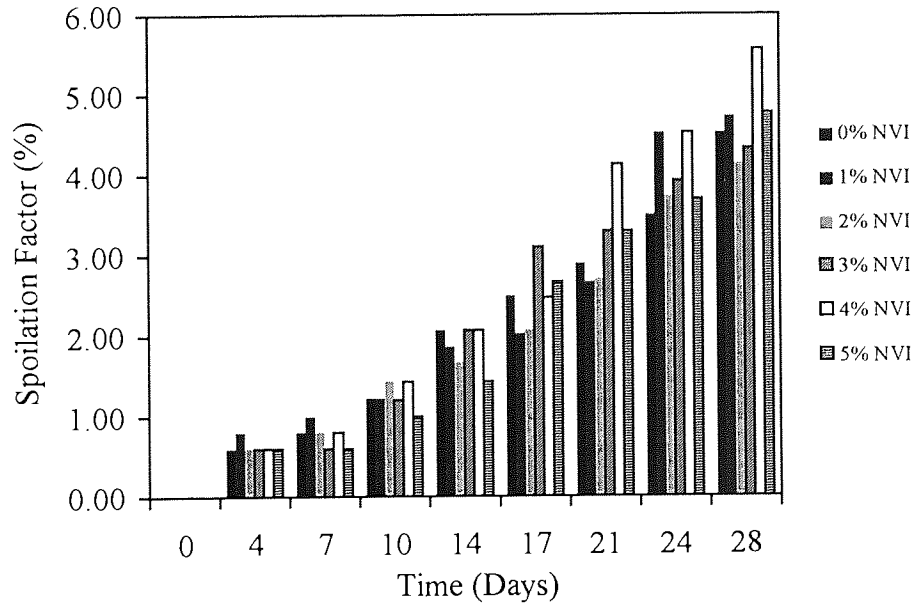

Figure 6.15 Graph to show the spoilation factors of HEMA-MAA 95:5 materials copolymerised with increasing amounts of NVI

From Figure 6.14 it can be seen that over a period of 28 days addition of a small percentage of MAA increased the levels of spoilation observed. Figure 6.15 demonstrates that for materials already containing 5% MAA, addition of NVI up to a level of 5% has little effect on the spoilation behaviour of these materials.

All HEMA materials copolymerised with MAA show greater spoilation factors than HEMA-NVI materials and 100% polyHEMA. The range of spoilation factors obtained are comparable to spoilation factors obtained for HEMA-NNDMA 80:20 hydrogels and also to HEMA-NVP 90:10 hydrogels although they are greater than spoilation factors obtained for any of the HEMA-AMO hydrogels, results of which are presented in Appendix 5.

6.6 Specific Protein Adsorption on New Cationic Materials

As stated in Chapter 3 one of the broader aims of the project was to consider the design of new materials that had the ability to respond to changes in their environment e.g. pH variations and also to show increased resistance to bacterial infection by displaying antimicrobial properties. Investigations into antibacterial agents and novel polymeric antibacterials revealed that regions of hydrophilicity and hydrophobicity as well as cationic sites for the interaction of the material with the negatively charged cell walls of bacteria were included in the criteria for the design of new polymeric antibacterial materials. This is similar to the requirements for the design of a surface active, pH responsive material. Novel hydrogel materials have been prepared using this criteria and their physical properties have been measured. The hydrophilic monomers used were either N,N'-dimethylacrylamide (NNDMA) or acryloyl

morpholine (AMO). These monomers were copolymerised with the hydrophobic component, cyclohexyl methacrylate (CHMA) and differing proportions of the potentially cationic monomers, either N-vinyl imidazole (NVI) or dimethylaminoethyl methacrylate (DMAEMA). Work on the physical properties of these materials is described in more detail in Chapters 3-5.

In order to further probe the properties of these new hydrogel materials and also to investigate the effects of incorporating higher proportions of cationic monomers than previously used, the interaction of specific protein solutions with these materials was studied. The compositions of these materials with their equilibrium water contents are given in Tables 6.21- 6.24.

% NNDMA	% CHMA	% NVI	EWC (%)
80	20	0	64.1
80	20	5	61.8
80	20	10	66.3
80	20	15	65.5
80	20	20	70.7
70	30	0	48.1
70	30	5	49.6
70	30	10	51.2
70	30	15	52.0
70	30	20	54.9

Table 6.21 Compositions and EWCs of hydrogels prepared using NNDMA, CHMA and NVI

% NNDMA	% CHMA	% DMAEMA	EWC (%)
80	20	0	57.5
80	20	5	61.5
80	20	10	65.8
80	20	15	64.7
80	20	20	67.9
70	30	0	52.9
70	30	5	52.3
70	30	10	52.9
70	30	15	52.2
70	30	20	54.4

Table 6.22 Compositions and EWCs of hydrogels prepared using NNDMA, CHMA and DMAEMA

% AMO	% CHMA	% NVI	EWC (%)
80	20	0	35.5
80	20	5	41.2
80	20	10	44.2
80	20	15	45.4
80	20	20	46.0
70	30	0	18.4
70	30	5	23.0
70	30	10	28.7
70	30	15	28.6
70	30	20	28.8

Table 6.23 Compositions and EWCs of hydrogels prepared using AMO, CHMA and NVI

% AMO	% CHMA	% DMAEMA	EWC (%)
80	20	0	35.2
80	20	5	42.4
80	20	10	45.5
80	20	15	46.9
80	20	20	51.9
70	30	0	24.9
70	30	5	26.1
70	30	10	30.7
70	30	15	30.8
70	30	20	34.6

Table 6.24 Compositions and EWCs of hydrogels prepared using AMO, CHMA and DMAEMA

The method used to study the specific protein interaction with these materials was similar to that used in previous work. Discs with a surface area of 75mm^2 were cut from hydrated membrane sheets and were soaked in 2ml of the individual protein solutions that had a concentration of 0.5mgml^{-1}. The concentration of protein adsorbed on each sample was measured after 5 days using UV spectroscopy as described previously.

The proteins used in this work were lysozyme, insulin, lactoferrin, ferredoxin and ribonuclease. The source of the ribonuclease was from bovine pancreas and it had a relative molecular mass of 13000. It has a similar size and charge to lysozyme. Characteristics of the other proteins used are described in Section 6.2. These results

are the mean value obtained for several discs of the same sample and the error associated with each reading is ±0.002mg/sample. The results are represented graphically in Figures 6.16 - 6.23.

Figures 6.16 and 6.17 show the uptake of different proteins on materials polymerised from NNDMA, CHMA and 0-20% NVI. Comparing these two Figures, it can be seen that ferredoxin shows the greatest adsorption of these proteins on each of the samples.

Monomers	NVI %	Concentration of Protein (mg/sample) (±0.002)				
	(w/w)	Lysozyme	Insulin	Lactoferrin	Ferredoxin	Ribonuclease
80%	0	0.051	0.030	0.039	0.037	0.052
NNDMA	5	0.051	0.034	0.031	0.088	0.047
+	10	0.039	0.024	0.035	0.066	0.038
20%	15	0.025	0.016	0.022	0.072	0.021
CHMA	20	0.043	0.048	0.043	0.071	0.042
70%	0	0.011	0.005	0.008	0.032	0.010
NNDMA	5	0.013	0.007	0.009	0.039	0.012
+	10	0.016	0.008	0.010	0.046	0.013
30%	15	0.019	0.009	0.011	0.052	0.015
CHMA	20	0.021	0.010	0.012	0.063	0.018

Table 6.25 Concentration of different proteins after 5 days on NNDMA-CHMA materials copolymerised with 0-20% NVI

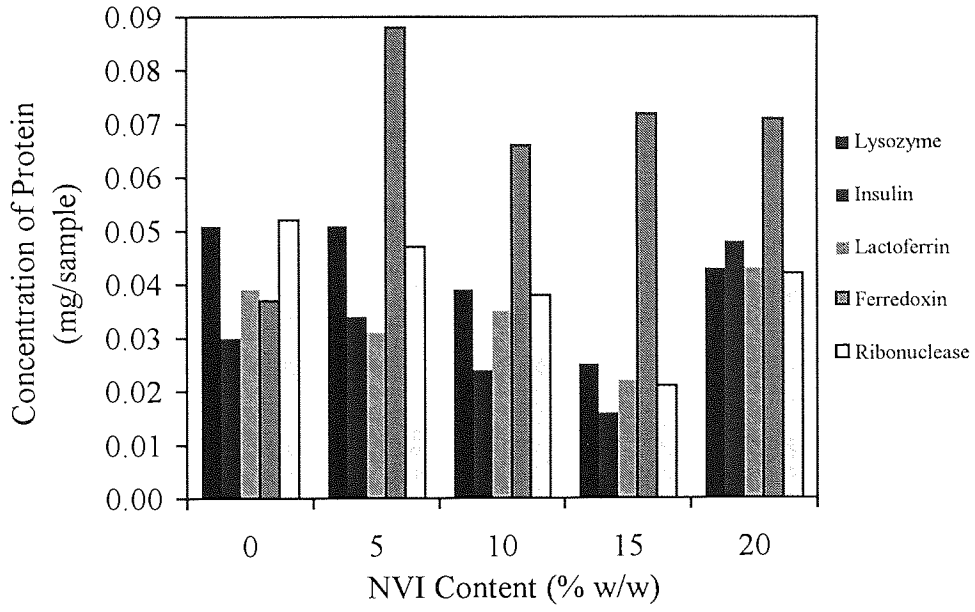

Figure 6.16 Graph to show the uptake of different proteins after 5 days on NNDMA-CHMA 80:20 materials copolymerised with 0-20% NVI

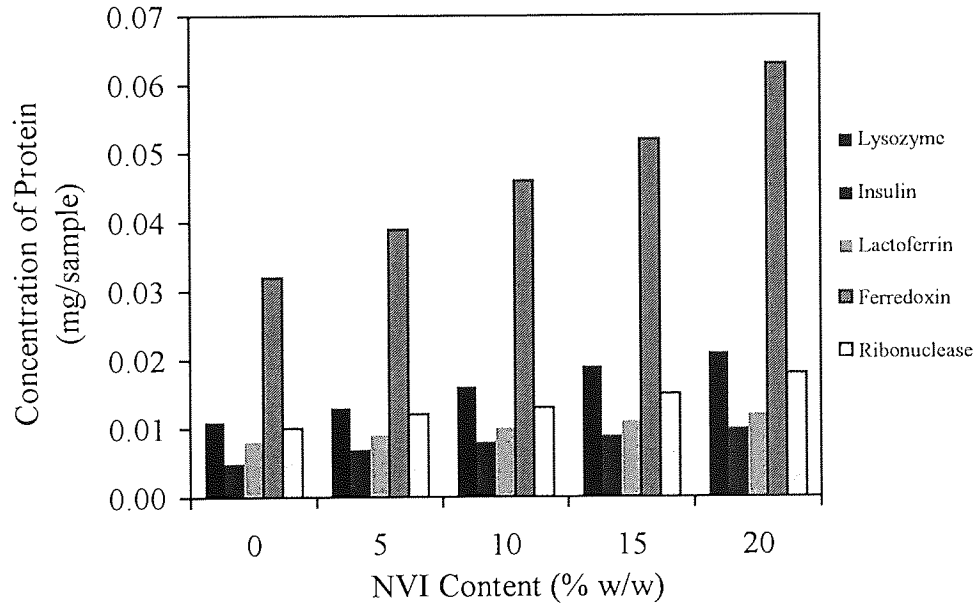

Figure 6.17 Graph to show the uptake of different proteins after 5 days on NNDMA -CHMA 70:30 materials copolymerised with 0-20% NVI

This can be attributed to the influence of the cationic component of these materials on the ferredoxin which has a high negative charge density. Reducing the hydrophilic component from 80% to 70% and in turn increasing the hydrophobic content of these materials lowers the equilibrium water content. The lower water content of these materials account for the lower values of protein adsorption seen in Figure 6.17. The lower water content also seems to override any effects of the cationic component as all of the proteins show a slight increase in concentration with the progressive incorporation of NVI, regardless of their size and charge.

Monomers	NVI %	Concentration of Protein (mg/sample) (±0.002)				
	(w/w)	Lysozyme	Insulin	Lactoferrin	Ferredoxin	Ribonuclease
80%	0	0.016	0.009	0.010	0.029	0.011
AMO	5	0.017	0.001	0.012	0.035	0.013
+	10	0.021	0.013	0.013	0.042	0.016
20%	15	0.024	0.015	0.014	0.048	0.018
CHMA	20	0.026	0.018	0.016	0.054	0.020
70%	0	0.006	0.005	0.004	0.019	0.006
AMO	5	0.007	0.005	0.004	0.021	0.007
+	10	0.007	0.006	0.006	0.029	0.008
30%	15	0.009	0.008	0.007	0.033	0.009
CHMA	20	0.012	0.009	0.008	0.038	0.010

Table 6.26 Concentration of different proteins after 5 days on NNDMA-AMO materials copolymerised with 0-20% NVI

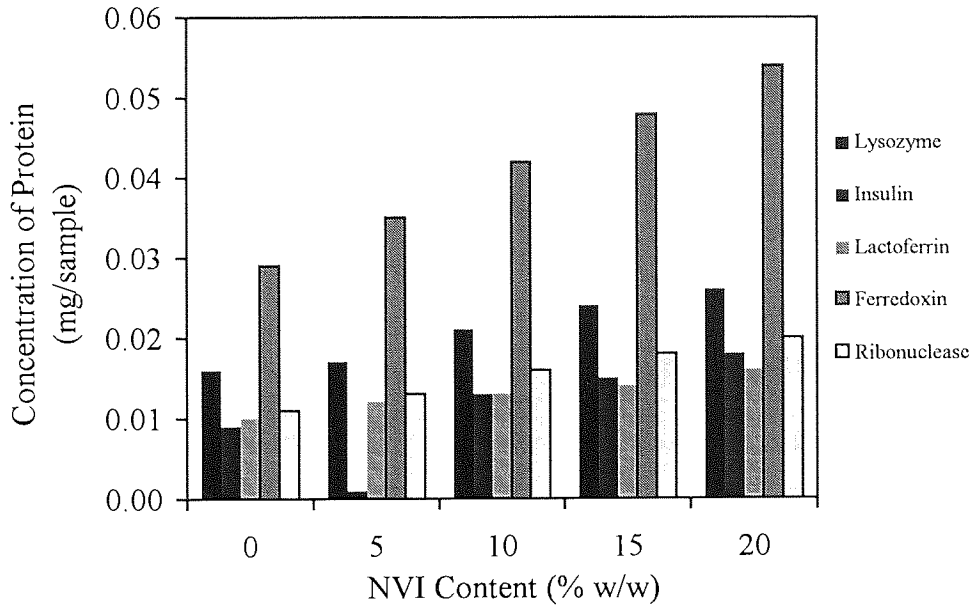

Figure 6.18 Graph to show the uptake of different proteins after 5 days on AMO-CHMA 80:20 materials copolymerised with 0-20% NVI

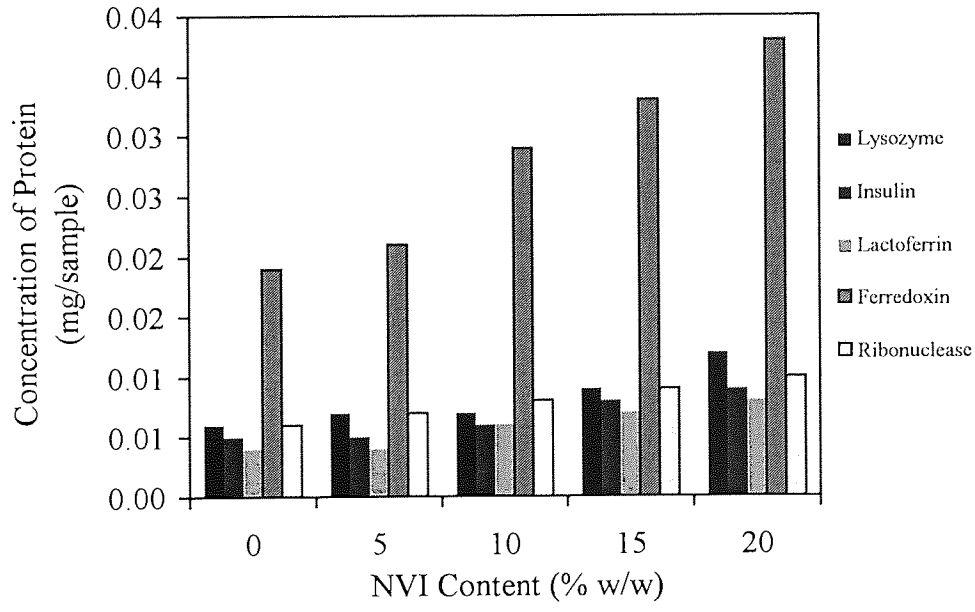

Figure 6.19 Graph to show the uptake of different proteins after 5 days on AMO-CHMA 70:30 materials copolymerised with 0-20% NVI

Figures 6.18 and 6.19 show the uptake of different proteins on materials with the hydrophilic component of NNDMA replaced with AMO. In both the 80% AMO and the 70% AMO samples the deposition of each of the proteins is less than that for the samples containing NNDMA, although ferredoxin is still the most abundant protein. AMO is slightly better suited in terms of reactivity ratios to polymerisation with CHMA and NVI, resulting in a less blocky sequence distribution than might be produced if using NNDMA. This could account for the decrease in protein deposition seen. The materials polymerised using AMO have a lower equilibrium water content than those polymerised using NNDMA. The will also be a factor in the amount of protein adsorbed by these materials.

Monomers	DMAEMA	Concentration of Protein (mg/sample) (±0.002)				
	% (w/w)	Lysozyme	Insulin	Lactoferrin	Ferredoxin	Ribonuclease
80%	0	0.020	0.013	0.014	0.033	0.015
NNDMA	5	0.020	0.013	0.014	0.031	0.014
+	10	0.019	0.012	0.016	0.028	0.014
20%	15	0.016	0.011	0.015	0.026	0.012
CHMA	20	0.014	0.009	0.014	0.022	0.011
70%	0	0.010	0.009	0.008	0.023	0.010
NNDMA	5	0.009	0.009	0.008	0.021	0.010
+	10	0.009	0.008	0.009	0.019	0.009
30%	15	0.008	0.008	0.009	0.018	0.008
CHMA	20	0.008	0.007	0.008	0.018	0.008

Table 6.27 Concentration of different proteins after 5 days on NNDMA-CHMA materials copolymerised with 0-20% DMAEMA

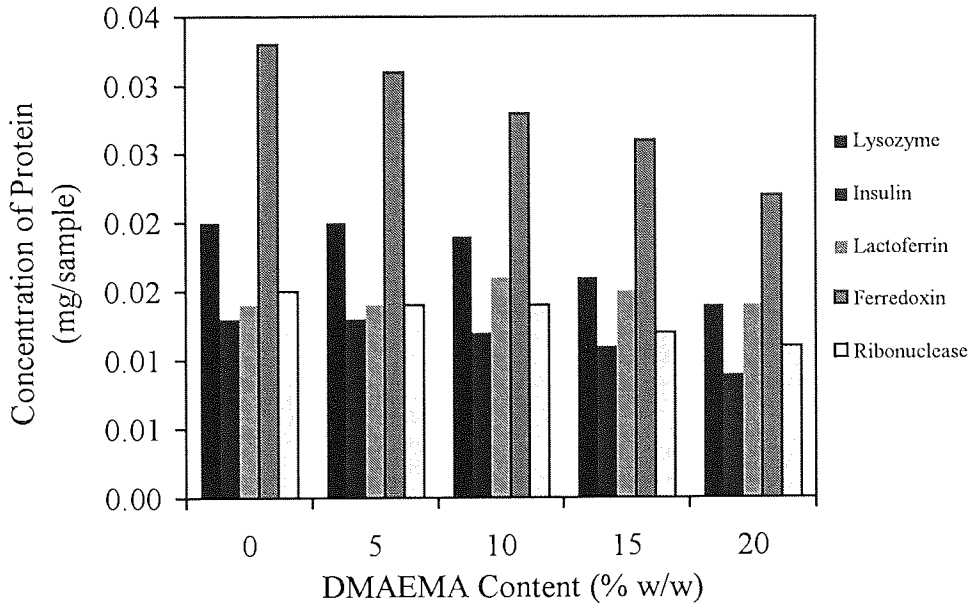

Figure 6.20 Graph to show the uptake of different proteins after 5 days on NNDMA-CHMA 80:20 materials copolymerised with 0-20% DMAEMA

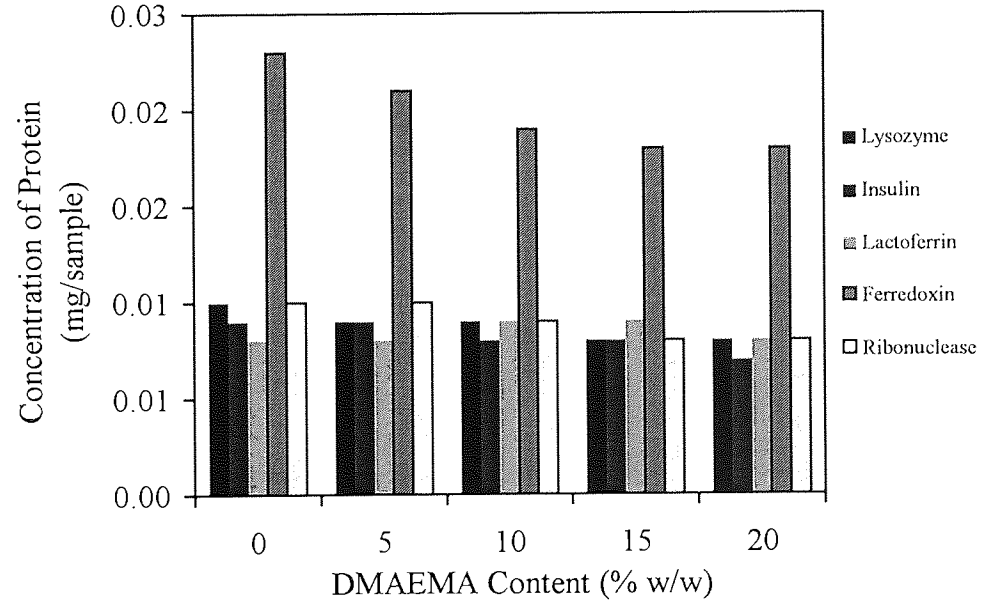

Figure 6.21 Graph to show the uptake of different proteins after 5 days on NNDMA-CHMA 70:30 materials copolymerised with 0-20% DMAEMA

Monomers	DMAEMA	Concentration of Protein (mg/sample) (±0.002)				
	% (w/w)	Lysozyme	Insulin	Lactoferrin	Ferredoxin	Ribonuclease
80%	0	0.019	0.012	0.013	0.032	0.014
AMO	5	0.018	0.011	0.012	0.029	0.013
+	10	0.016	0.011	0.011	0.025	0.012
20%	15	0.013	0.010	0.010	0.023	0.011
CHMA	20	0.013	0.008	0.010	0.022	0.010
70%	0	0.009	0.008	0.007	0.021	0.009
AMO	5	0.009	0.008	0.007	0.020	0.009
+	10	0.008	0.009	0.006	0.018	0.010
30%	15	0.009	0.009	0.005	0.017	0.007
CHMA	20	0.008	0.008	0.005	0.014	0.007

Table 6.28 Concentration of different proteins after 5 days on NNDMA-AMO materials copolymerised with 0-20% DMAEMA

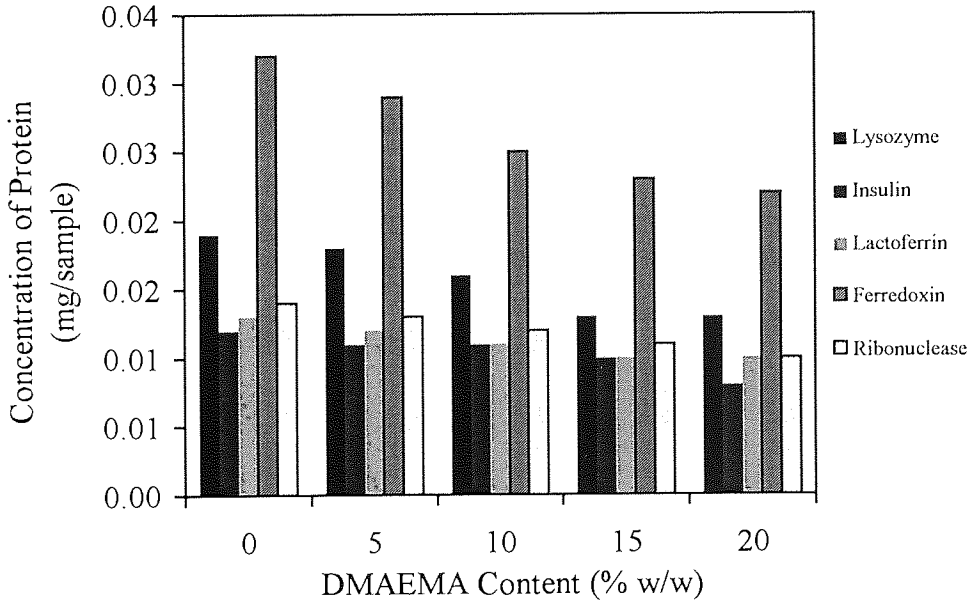

Figure 6.22 Graph to show the uptake of different proteins after 5 days on AMO-CHMA 80:20 materials copolymerised with 0-20% DMAEMA

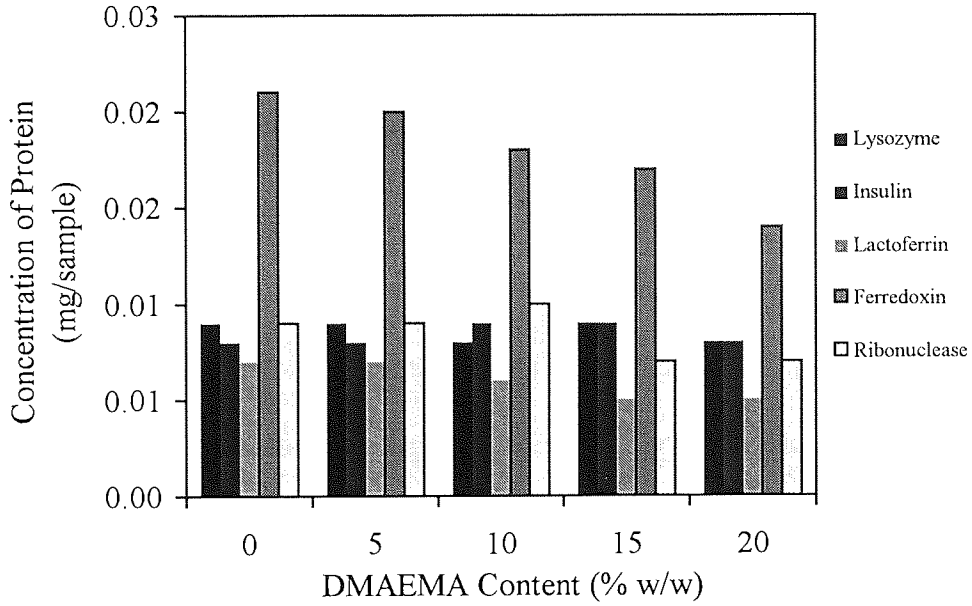

Figure 6.23 Graph to show the uptake of different proteins after 5 days on AMO-CHMA 70:30 materials copolymerised with 0-20% DMAEMA

Figures 6.20 - 6.23 show the concentrations of the different proteins on materials polymerised using NNDMA and CHMA, or AMO and CHMA with DMAEMA as the cationic component. All of these samples show low levels of protein adsorption regardless of whether the hydrophilic component is NNDMA or AMO. Once again ferredoxin is the most abundant of the proteins. The fact that there is little effect in replacing NNDMA with AMO when DMAEMA is the cationic component may be explained in terms of which of the groups are expressed at the surface of the material. If the hydrophobic CHMA dominates the surface, as stated in Chapter 5, the effect of the hydrophilic or charged groups will be less apparent.

6.7 *In Vitro* Spoilation of New Cationic Materials

The *in vitro* tear model has been used to assess the tear film compatibility of the new materials described in Section 6.6. The compositions of the materials are given in Tables 6.21 - 6.24. These new materials possess higher percentages of basic monomer than those previously studied using this technique and also have lower equilibrium water contents due to the introduction of the hydrophobic monomer, cyclohexyl methacrylate. The deposition of both lipids and proteins from artificial tear solutions was monitored at regular intervals over a period of 28 days using fluorescence spectroscopy as described in Section 6.3. The results are presented in numerical form in Appendix 5. As on previous occasions the progressive accumulation of protein and lipid, monitored by surface fluorescence spectroscopy was compiled to give a single spoilation factor. Figures 6.24 to 6.31 show the relative increases in spoilation factor for these new materials.

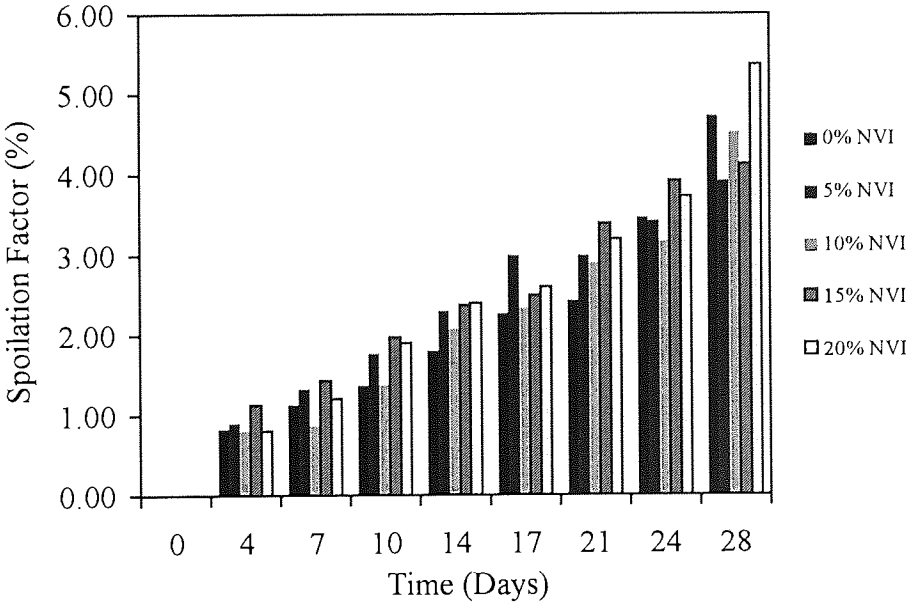

Figure 6.24 Graph to show the spoilation factors for NNDMA-CHMA 80:20 materials copolymerised with 0-20% NVI

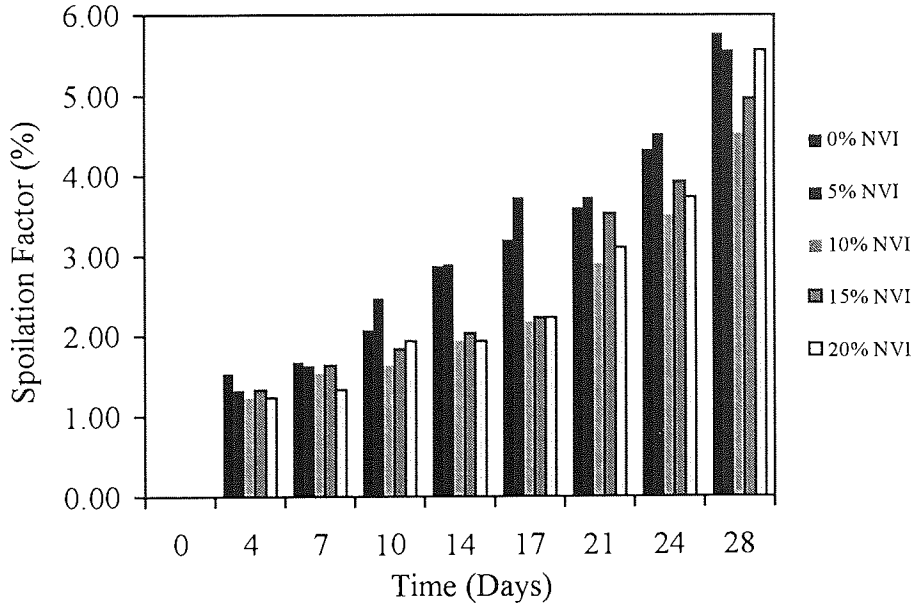

Figure 6.25 Graph to show the spoilation factors for NNDMA-CHMA 70:30 materials copolymerised with 0-20% NVI

Figures 6.24 and 6.25 illustrate the spoilation factors for NNDMA-CHMA 80:20 and NNDMA-CHMA 70:30 materials copolymerised with progressive amounts of NVI. It can be seen from these graphs that over a 28 day period the addition of NVI has very little difference on the spoilation levels observed for these materials. The values obtained for the spoilation factors of these materials range from 4.0% to 5.7% indicating higher levels of spoilation on these materials than the HEMA-NVI and HEMA-DMAEMA materials.

Figures 6.26 and 6.27 show the spoilation factors for AMO-CHMA 80:20 and AMO-CHMA 70:30 materials copolymerised with progressive amounts of NVI. It would seem that introduction of 15% NVI into the AMO-CHMA 80:20 materials gives rise

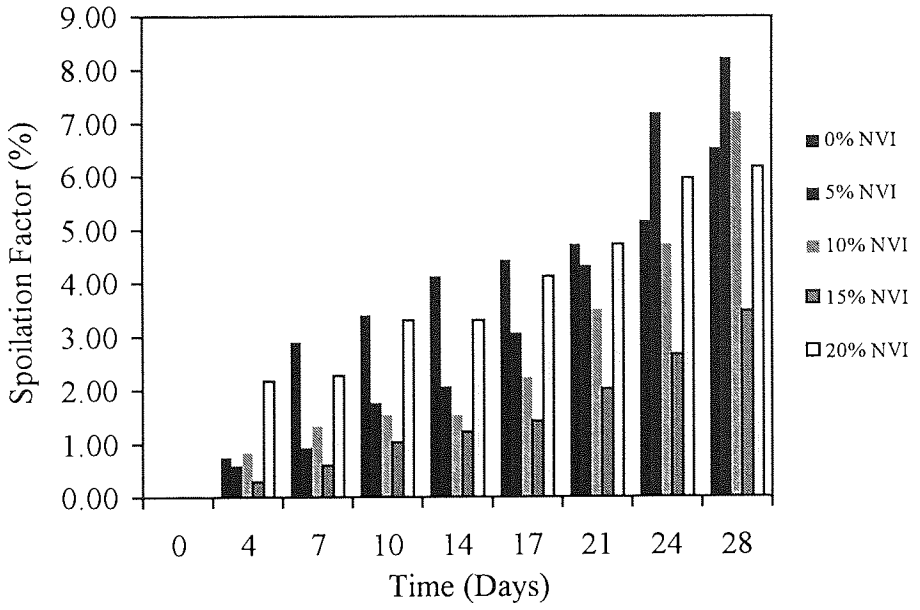

Figure 6.26 Graph to show the spoilation factors for AMO-CHMA 80:20 materials copolymerised with 0-20% NVI

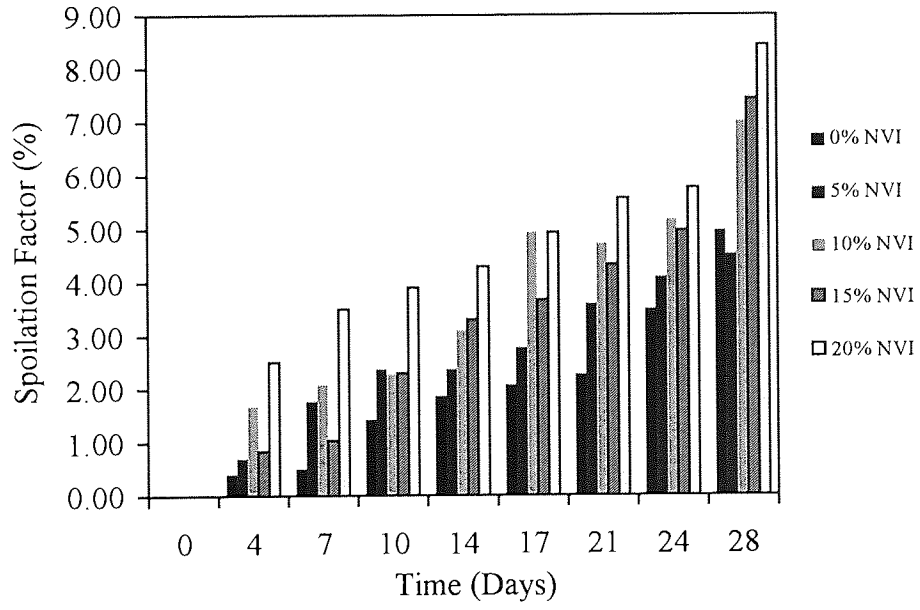

Figure 6.27 Graph to show the spoilation factors for AMO-CHMA 70:30 materials copolymerised with 0-20% NVI

to a reduction in the levels of spoilation observed. Addition of NVI at any other level up to and including 20% fails to bring about a similar reduction in spoilation levels. In fact the spoilation factors obtained for these materials are marginally higher than the spoilation factors obtained for similar materials containing NNDMA. This is somewhat surprising since previous workers[131] have obtained reduced levels of spoilation for materials employing AMO. In addition results in Appendix 5 show that HEMA-AMO hydrogels show lower levels of spoilation than HEMA-NNDMA hydrogels. Spoilation factors obtained for AMO-CHMA 70:30 materials demonstrate that in this instance addition of NVI gives rise to a small increase in spoilation levels, and again the spoilation factors of these materials are slightly higher than for similar materials containing NNDMA.

Figures 6.28 and 6.29 illustrate the spoilation factors for NNDMA-CHMA 80:20 and NNDMA-CHMA 70:30 materials copolymerised with progressive amounts of DMAEMA. The levels of spoilation seen for the NNDMA-CHMA 80:20 materials over the 28 day period are very similar to those seen with previous materials with progressive NVI incorporation. However the NNDMA-CHMA 70:30 materials seem to exhibit reduced levels of spoilation upon addition of DMAEMA.

Figures 6.30 and 6.31 illustrate the spoilation factors for AMO-CHMA 80:20 and AMO-CHMA 70:30 materials copolymerised with progressive amounts of DMAEMA. In this instance the AMO-CHMA 80:20 materials show a slight decrease in spoilation levels with the addition of DMAEMA whilst the AMO-CHMA 70:30 materials seem unaffected.

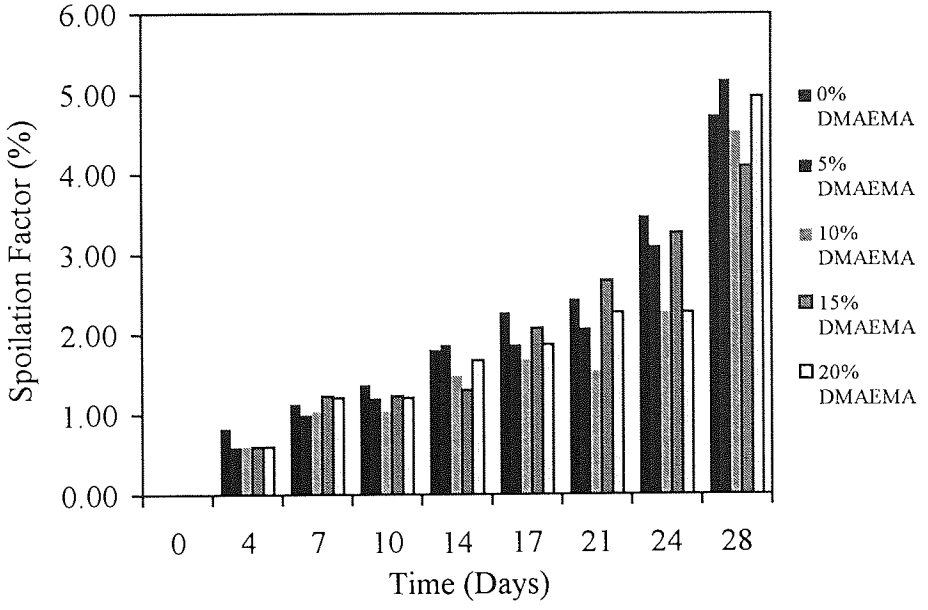

Figure 6.28 Graph to show the spoilation factors for NNDMA-CHMA 80:20 materials copolymerised with 0-20% DMAEMA

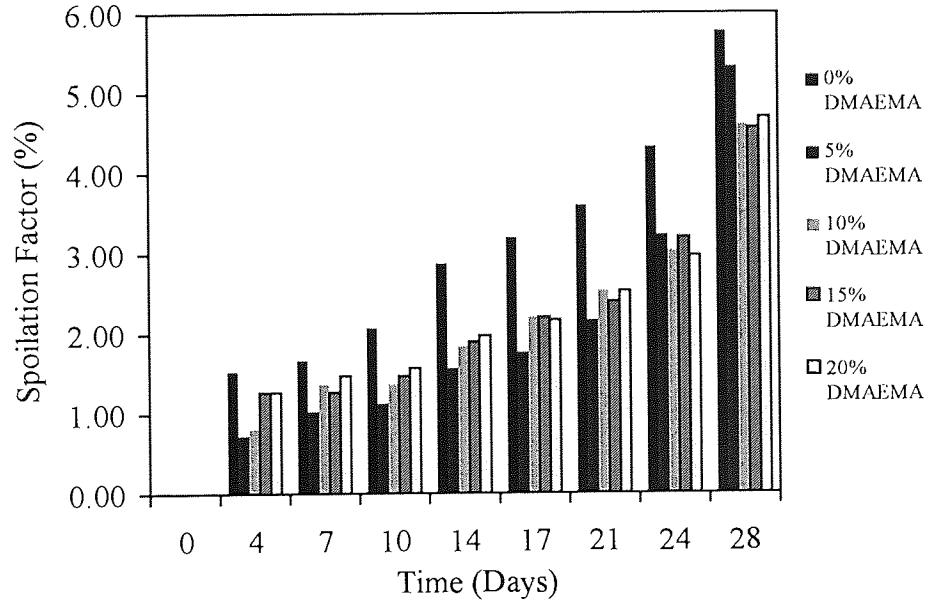

Figure 6.29 Graph to show the spoilation factors for NNDMA-CHMA 70:30 materials copolymerised with 0-20% DMAEMA

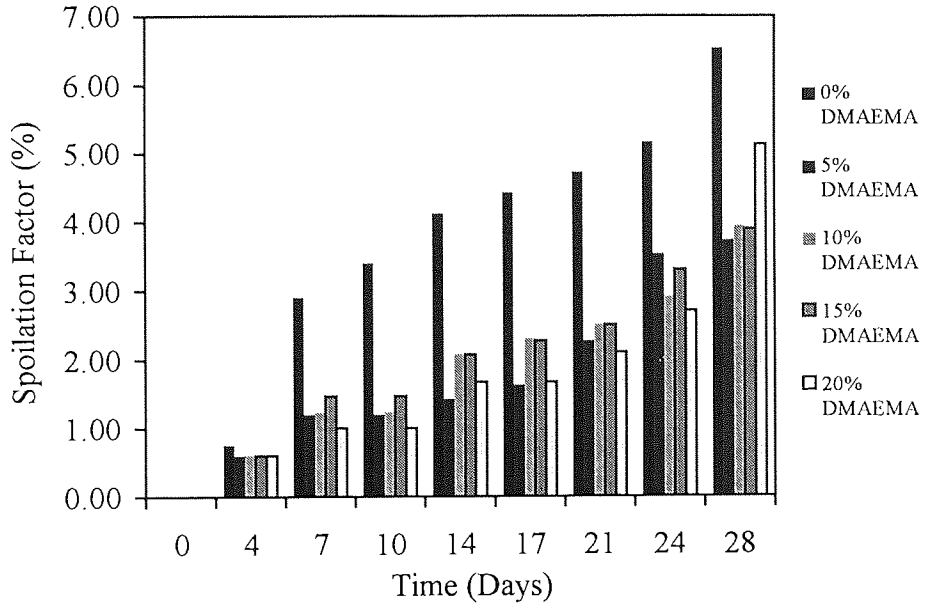

Figure 6.30 Graph to show the spoilation factors for AMO-CHMA 80:20 materials copolymerised with 0-20% DMAEMA

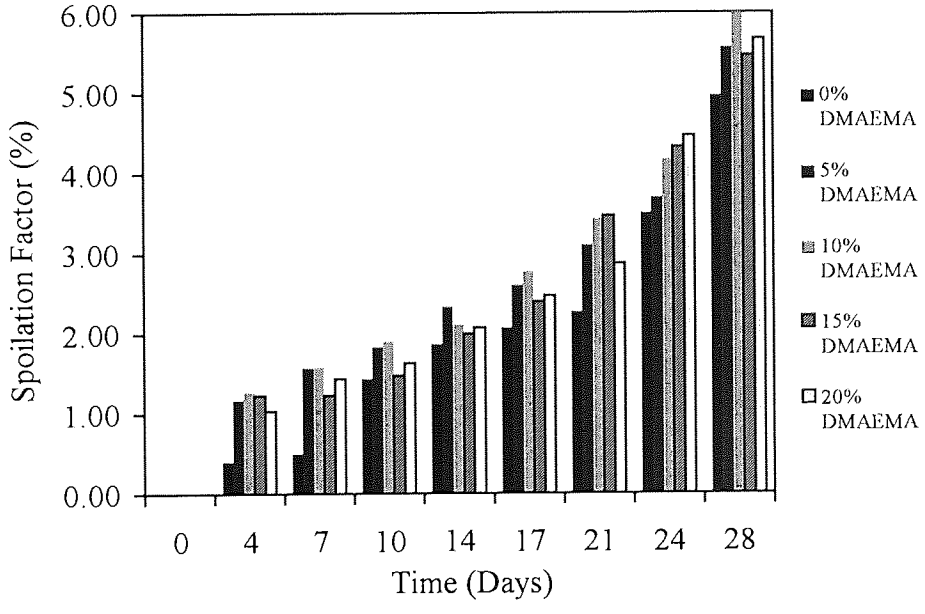

Figure 6.31 Graph to show the spoilation factors for AMO-CHMA 70:30 materials copolymerised with 0-20% DMAEMA

As previously observed the values obtained for the spoilation factors of the materials containing AMO are higher than those obtained for the similar materials containing NNDMA.

From the *in vitro* spoilation studies of all these new materials, it is hard to establish the effect of addition of a basic monomer i.e. NVI or DMAEMA. It must be remembered that the spoilation characteristics of hydrogel materials are governed by several factors and the contribution of surface charge plays only a small part. The composition of the hydrogel in terms of its sequence distribution will have an important bearing on the spoilation characteristics. An hydrogel whose sequence distribution gives rise to large irregular molecular domains in which components of the same chemical type become aggregated tend to show much greater levels of spoilation than hydrogels whose sequence distributions mimic natural cell structures that have short, regular repeat units. Hydrophobic clusters on the surface of an hydrogel material and monomers with methyl side groups also increase the potential spoilation levels by providing an area capable of docking proteins and adsorbing lipids. Although it might be suggested that ionic materials would present the greatest problems of protein deposition, it is important to remember that interactions between ionic polymers and charged proteins are easier to dissociate in an aqueous system than the interaction between hydrophobic groups on a polymer surface and a protein.

Differences in surface rugosity may lead to inconsistent results and a perfect optical surface would enable a more thorough examination of the spoilation characteristics of these materials. It was also noted that protein preferentially adsorbs on to the

primarily adsorbed lipid layer, thus if the lipid spoilation levels are great then values obtained for protein spoilation will also be higher.

None of the materials used in this experiments were examined after cleaning, due to constraints of time. However cleaning the samples with a contact lens cleaner should remove approximately 90% of adsorbed material. It may have proved useful to measure the level of spoilation remaining after cleaning to obtain an estimate of the proteins and lipid strongly associated with the hydrogel surface, that may be due to surface charge.

6.8 Conclusions

There has been some reluctance to use cationic monomers in the development of novel biomaterials, in particular in the contact lens field, because of the idea that there is increased adsorption of biological materials to cationic surfaces. This may be based on the knowledge that many cosmetic preparations, in particular hair conditioners, are strongly cationic in nature with the specific target of binding to the negative surface of biological materials. It is well known that the widely used anionic FDA Group IV contact lens materials (e.g. Etafilcon and Vifilcon) contain no more than 5% of the anionic component, and have been shown to increase the uptake of lysozyme[6].

Incorporating a cationic component at the same low levels as in these Group IV materials was found to reduce the concentration of lysozyme adsorbed onto the surface of the hydrogel without detrimentally affecting the uptake of the other major tear proteins. Similarly, although the adsorption of the polycationic antibacterials can

be demonstrated to occur[8], the results presented in this Chapter suggested that this is unlikely to adversely affect protein adsorption of the consequently modified lenses. Results from the experiments using the *in vitro* spoilation model also suggested that the bulk deposition of lipid and protein on materials containing a low level of cationic component is no greater than results obtained for polyHEMA hydrogels. This is despite suggestions by some authors that the introduction of ionic components may increase deposition[9-12], although the context of the work published has been almost exclusively on blood contacting materials.

As it is very difficult to obtain 100% pure HEMA, because of the disproportionation reaction resulting in MAA as a side product, experiments were carried out to determine the deposition characteristics of a polyHEMA hydrogel copolymerised with both MAA and either NVI or DMAEMA. Materials containing MAA at any level showed increased deposition of lysozyme and lactoferrin due to the electrostatic attraction between the anionic sites in the polymer and the positively charged proteins.

Cleaning of the samples combining anionic and cationic sites with ReNu™ showed that the proteins were irreversibly adsorbed onto materials containing higher proportions of MAA. This was particularly evident in the case of lysozyme. Some of the results obtained suggested, misleadingly, that the levels of protein after cleaning were higher than before cleaning. Further experimental work showed that the positively charged antibacterial agent in the cleaning solution was deposited onto the surface of the hydrogel samples, due to electrostatic attraction to the anionic sites.

This led to higher UV absorbance readings implying a higher level of protein deposition.

Results from the *in vitro* spoilation model showed a greater degree of spoilation on hydrogels combining cationic and anionic sites than for samples copolymerised with just a basic component. Spoilation factors in the region of 5% were obtained in comparison to spoilation factors of approximately 3.5% for HEMA-NVI or HEMA-DMAEMA.

The new materials designed with antibacterial activity in mind showed low levels of lysozyme deposition, with concentrations lying in a similar region to HEMA-NVI 95:5 and HEMA-DMAEMA 95:5 hydrogel samples. The ferredoxin adsorption was comparatively higher than any of the other proteins studied, as would be expected with the increased attraction of the negatively charged protein to the potentially positively charged surface. *In vitro* spoilation studies of these materials showed that they exhibited higher levels of spoilation than HEMA-NVI or HEMA-DMAEMA samples. However it was hard to establish exactly the effect of the addition of a basic monomer, due to the fact that several factors govern the spoilation characteristics of hydrogel materials. These factors include the sequence distribution of the monomers in the hydrogel and also the presence of hydrophobic regions clustered on the surface of the hydrogel capable of docking proteins and adsorbing lipids.

CHAPTER 7

Preliminary Steps Towards

New Antibacterial Biomaterials

7.1 Introduction

One of the major problems associated with using polymers at biological interfaces is the invasion of micro-organisms causing local and systemic infection. It is a problem that is common in all fields of biomedicine, in particular in the ocular environment with the use of contact lenses. Corneal infection is the most serious complication of contact lens wear and is most frequently associated with hydrogel lenses, especially those used on an overnight basis[152]. Bacteria, particularly *Pseudomonas aeruginosa*, are often implicated in these infections[153,154]. Organisms may be carried via the contact lens from contaminated lens cases to the ocular surface[155], or may have been transferred manually to the lens. The predominant method of growth for bacteria in nature is within glycocalyx-enclosed microcolonies, forming a biofilm on surfaces[156]. This mode of growth affords the organism protection from antimicrobial agents[157,158]. Glycocalyx-enclosed microcolonies on lenses or in lens storage cases may be similarly protected from antimicrobial agents in lens care systems[159].

Vascular catheters have similar problems with infection. Of all the patients for which a central vascular catheter is used whilst in hospital, approximately 5% develop serious infections and a further 5-10% develop minor infections. Infections will occur when organisms from the patients natural skin flora or from the hands and skin of the attendants colonise at the site of insertion and travel either along the external or internal surface of the catheter[160], where firmly attached microcolonies can form, which may be subsequently covered in glycocalyx[161].

All too often disinfectant cleaning systems and topically applied antiseptics fail to eliminate bacterial colonisation and lead to infection which can be difficult to control[162]. It may be suggested then that prevention of these infections is preferable to cure[163]. There have been several approaches to solving the problem of bacterial infection particularly in the area of catheter use[164-166], and this chapter discusses some of those methods. It also presents the results of some preliminary investigations into ways in which bacterial infection may be controlled by development of antibacterial polymers.

7.2 Bacterial Inhibition by an Electric Current[167]

Elliott and his co-workers at the Queen Elizabeth hospital in Birmingham have developed a novel approach to solving the problem of catheter infection. A polyetherurethane catheter material was impregnated with 15% carbon which enabled it to carry an electric current.

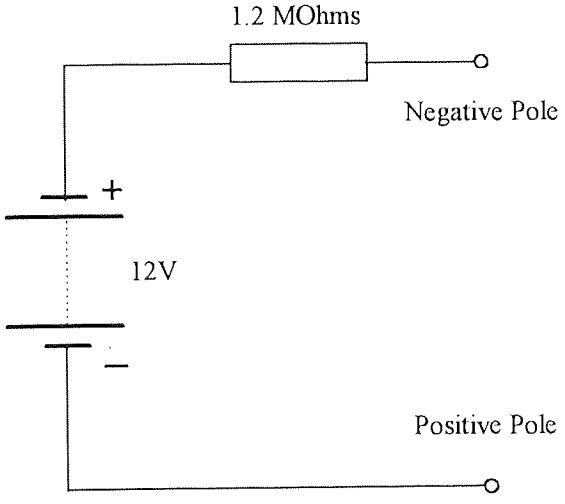

Figure 7.1 Schematic drawing of the current generating device.

A constant current generator was constructed with a 12V miniature alkaline battery in series with a 1.2 MOhm resistor. This current generating device is illustrated in Figure 7.1.

The negative pole was connected to the catheter material and the positive pole was connected to a steel needle acting as the ground return electrode. The current flow generated a negatively charged surface to the catheter. The bacteria, with their negatively charged cell walls, (as described in detail in Section 1.7.2), are thus repelled away from the catheter preventing colonisation.

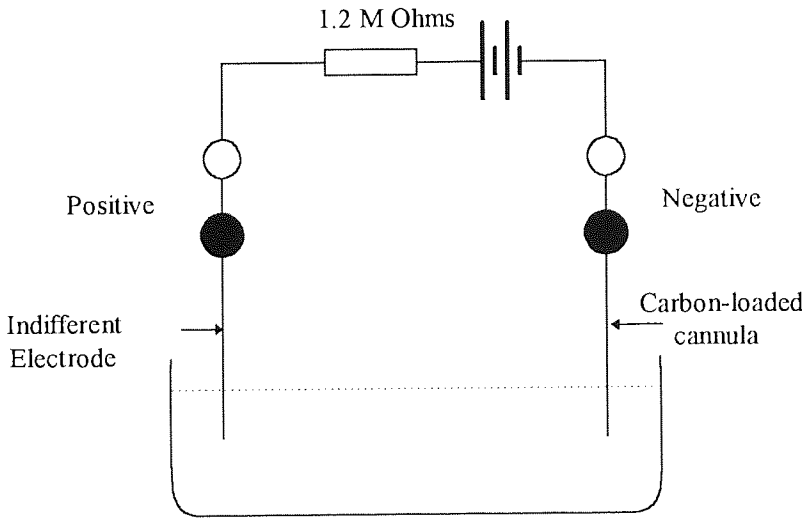

Figure 7.2 The electrical circuit in the 'zone of inhibition' model

Various *in vitro* models were used to demonstrate the effect of the electric current on bacterial inhibition. The 'zone of inhibition' model was developed to detect repulsion of micro-organisms growing on an agar surface, from the current carrying catheter. A broth culture of micro-organisms was plated out on nutrient agar. The carbon loaded

catheter and a steel needle acting as the other electrode were individually placed perpendicularly to the agar surface. The negative pole of the current generating device was connected to the catheter and the positive pole was attached to the needle. This arrangement is illustrated in Figure 7.2.

The carbon-impregnated catheter was protected by current of 2, 10 or 50μA and it was found that a circular, sharp-edged zone of inhibition was formed around the current carrying catheter depending on the magnitude of the current. Catheters not protected by a current did not produce a zone. Figure 7.3 shows a schematic illustration of the well defined zone of inhibition around the site of a current carrying catheter.

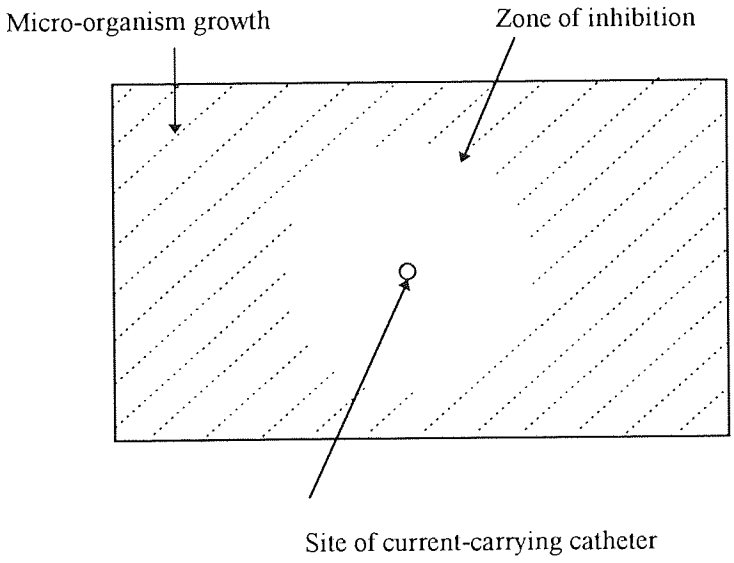

Figure 7.3 Schematic diagram of the zone of inhibition around a current carrying catheter.

It can be seen from Table 7.1 that the greater the current, the larger the zone of inhibition. The method seems to be most effective against the gram positive *S. epidermidis* bacteria and least effective against *C. albicans*. This method of bacterial protection offers some advantages over an intrinsically negatively charged catheter surface, which might repel micro-organisms for a limited period of time, but would lose its antibacterial properties as cations adsorb and eventually neutralise the surface charge. In comparison the catheter with a driven electric current will not be neutralised by free ions or positively charged bodies, thereby offering continuous protection.

BACTERIA	CURRENT	ZONE OF INHIBITION
S. epidermidis	2μA	4.0±1.2mm
	10μA	10.0±2.4mm
	50μA	14.0±2.8mm
S. aureas	10μA	8.0±1.8mm
C. albicans	10μA	1.0±0.0mm

Table 7.1 Variation of zone size with current applied to catheter material

However carbon impregnation of a polyurethane material is not without disadvantage because the physical properties of the material will be altered and it may become more difficult to process. Conduction of an electrical current may also be possible if a thin metal coating is applied to the surface of the catheter material. To investigate the

potential of this technique the coating of the catheter material with a thin layer of silver using the 'silver mirror' technique was attempted.

The antibacterial activity of silver has long been known and has found a variety of applications[182-184] because its toxicity to human cells is considerably lower than to bacteria. Clement has presented a summary of the uses of silver and silver ions[185] which include therapeutic applications and water sterilisation and also discusses possible bacterial resistance mechanisms. Beard *et al.*[186] have reported the potential use of silver as a coating for medical catheter coatings relying solely on the antibacterial nature of the silver coating to provide bacterial resistance. They found that silver coated catheters produced a small zone of inhibition against *S. aureus* and *E. coli*. In this work it is hoped that passing a electrical current through a silver coated catheter will increase the zone of inhibition seen.

The 'silver mirror' technique used for the coating of the catheter materials, has been used as an elementary analysis technique to test for reducing agents, and especially, to distinguish between aldehydes and ketones. Obviously with the widespread use of spectroscopy, it is now a rarely used test. Tollen's reagent is prepared by adding ammonium hydroxide dropwise to a silver nitrate solution until the precipitate of silver oxide has almost entirely redissolved. The complex ion $[Ag(NH_3)_2]^+$ is formed. This complex ion will then oxidise a reducing agent such as formaldehyde and the Ag^+ will be reduced to silver metal, deposited in the form of a silver mirror on the surface of the reaction vessel, e.g. test tube. The reaction scheme can be seen in Equation 1.

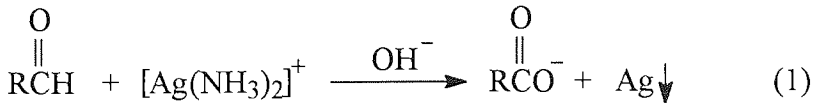

(1)

In order to coat a polyurethane catheter surface, the catheter was soaked in a small amount of formaldehyde. Tollen's reagent was added to the formaldehyde with the catheter present and the silver mirror was deposited on the catheter surface as well as the reaction vessel. Unfortunately the surface energy of the catheter was low and the silver coating was found to be inconsistent, only adhering in some places. Testing for electrical conductivity at the Queen Elizabeth hospital showed the material to be conductive in the areas where the silver metal had deposited.

Treatment of the catheter material by high energy plasma serves to increase the surface energy of the catheter material making it more receptive to silver coating by this technique. Unfortunately only small improvements were made on the effective, consistent coating of the whole catheter material. Although the possibility of conducting an electric current through a silver coated catheter has been demonstrated by this work, the practical usefulness of the technique seemed limited. It was also noted that the surface energy of a silver coated catheter which will be higher than that of the polyurethane catheter, may lead to an increased possibility of thrombus formation upon implantation into a body site. For these reasons the technique was not pursued.

7.3 Bacterial Inhibition by Controlled Release of an Antibacterial Agent

Rather than modifying the physical properties of the catheter material itself so that it can carry an electric current, the possibilities of developing a hydrogel material that

can be used as a coating for the catheter have been investigated. This hydrogel coating may serve as a slow release vehicle for an antibacterial agent.

Their permeability in aqueous systems is an important feature of hydrogels, as the imbibed water provides a medium for the transport of water soluble species through the polymer gel. In addition the comparatively good blood compatibility of hydrogels has meant that these materials are potentially useful as thromboresistant coatings for any implant or device that comes into contact with blood. These factors have led to extensive studies of the application of hydrogels in drug delivery devices[76,168-170]. Such drug delivery vehicles are often constructed from synthetic polymeric materials into which the drug is physically incorporated within the polymer matrix. Release of the agent is then controlled by its rate of diffusion from the polymer matrix.

Permeation of a drug through an hydrogel membrane can be thought of as resulting from two processes. Solubility of the drug in the polymer and diffusion which relates to the mobility of the drug within the polymer matrix. With homogeneous hydrogels it might be assumed that there are no macroscopic pores or channels, although on a molecular scale nothing can be said to be purely homogeneous, and fluctuations of the macromolecular chain segments yield a system of transient pores and channels. Pores will be neither fixed in size or location, as they may be in an heterogeneous membrane, but result from the random fluctuations of chain segments which may exhibit a high degree of mobility due to the plasticizing effect of water. It is through these pores that a water soluble drug must diffuse. The rate at which a solute will

move through the polymer matrix is governed by the chemical composition of the polymer, its water content and also by the nature of the solute itself.

7.3.1 Properties of Potential Hydrogel Coating Material

Two antibacterial agents have been considered for incorporation into an hydrogel material for controlled release, alexidine dihydrochloride and vantocil IB. Alexidine dihydrochloride is a low molecular weight bisbiguanide and vantocil IB is a polymeric biguanide, poly(hexamethylene biguanide) hydrochloride, with a relative molecular mass of approximately 3000. Structures of these antibacterial agents are given in Figure 7.4.

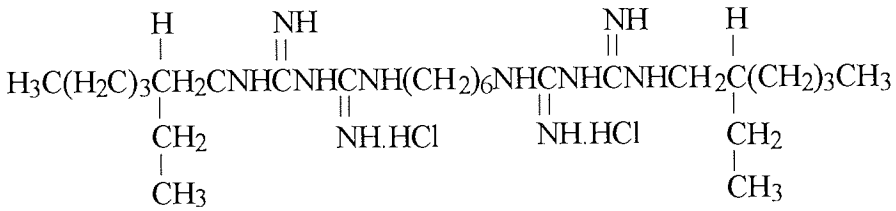

Alexidine dihydrochloride

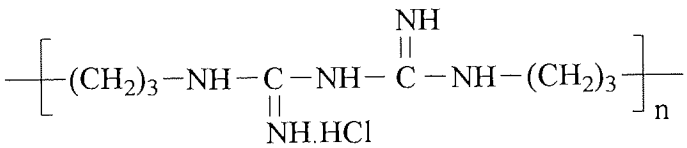

Vantocil IB

Figure 7.4 Structure of antibacterial agents used

In order to incorporate the antibacterial agents into hydrogel materials it was necessary to first dissolve them in small amounts of water. The amount of water used was kept to a minimum so as not to cause phase separation in the hydrogels upon hydration. The antibacterial agents are, however not immobilised within the network

and over a period of time will diffuse out of the hydrated membrane. The rate of diffusion of a solute species through a hydrophilic membrane is related to the equilibrium water content of the membrane. Reducing the equilibrium water content of the membrane is likely to result in a slower rate of diffusion of the antibacterial agents through the membrane. An ideal water content for this application was considered to be in the region of 25%. It is in this region that there is the transition in the water binding properties from all non-freezing water to both freezing and non-freezing water. Obviously for transport of an antibacterial agent within the polymer matrix some freezing water must be present, but too large a percentage of freezing water will cause release of the antibacterial agent to occur over too short a period of time.

If such a low water content membrane is to be used as a catheter coating it must also be sufficiently flexible. With these two requirements in mind, two series of membranes were prepared using a combination of 2-hydroxyethyl methacrylate, (HEMA) and ethoxyethyl methacrylate, (EEMA) and also a combination of HEMA with n-hexyl methacrylate (NHMA). In both series of membranes, ethylene glycol dimethacrylate (EGDM) was used as the cross-linker and α-azo-bis-isobutyronitrile was used as the initiator at a level of 0.5%(w/w). The equilibrium water contents were investigated and the results are presented in Table 7.2.

The mechanical properties of HEMA-EEMA and HEMA-NHMA membranes, cross-linked with EGDM are given in Table 7.3. Tensile strength, (σ_b), initial modulus, (E) and elongation to break, (ε_b) were measured as a function of molar feed ratio.

Monomers	Feed Ratio (%w/w)	% EGDM	EWC (%)
HEMA / EEMA	50 : 50	1%	15.5±0.4
	50 : 50	2%	16.0±0.3
	70 : 30	1%	26.9±0.3
	70 : 30	2%	25.0±0.7
	30 : 70	1%	9.2±0.3
	30 : 70	2%	8.8±0.4
HEMA / NHMA	50 : 50	1%	9.0±0.3
	60 : 40	1%	12.2±0.4
	65 : 35	1%	13.8±0.2
	70 : 30	1%	22.5±0.3

Table 7.2 Compositions and EWCs of low water content membranes for catheter coating

Monomers	Feed Ratio (%w/w)	% EGDM	σ_b (MPa)	E (MPa)	ε_b (%)
HEMA-EEMA	50 : 50	1%	2.70±0.2	0.71±0.1	401±17
	50 : 50	2%	2.94±0.3	1.51±0.3	228±19
	70 : 30	1%	1.04±0.2	0.99±0.1	179±21
	70 : 30	2%	1.45±1.6	1.11±0.3	194±21
	30 : 70	1%	4.20±0.1	6.17±1.5	366±18
	30 : 70	2%	5.45±0.4	12.61±0.4	288±19
HEMA-NHMA	50 : 50	1%	4.50±0.4	8.29±0.6	379±20
	60 : 40	1%	3.68±0.3	2.46±0.4	391±18
	65 : 35	1%	3.59±0.3	2.21±0.3	386±19
	70 : 30	1%	2.01±0.4	1.91±0.5	241±19

Table 7.3 Mechanical properties of HEMA-EEMA and HEMA-NHMA hydrogel membranes

On this basis the hydrogel with composition HEMA-EEMA 70:30 with 2% EGDM cross-linker was selected for further investigation. It has an equilibrium water content within the desired region of 25% and also has a low initial modulus which is an indication of its flexibility.

7.3.2 Incorporation of Antibacterial Agents into the Hydrogel Material

On the basis of practical information from the microbiology section at the Queen Elizabeth hospital, the hydrogel coating was required to maintain activity over a period of 7 days. A release rate of the antibacterial agent from the hydrogel catheter coating of 10μg per hour would meet this specification. This is achievable with 100mg of hydrogel coating around the catheter section with a 5-10% loading of antibacterial agent.

Detailed analysis of the kinetics involved is beyond the scope of this report, however assuming that the diffusion of the antibacterial agent follows zero-order kinetics - i.e. there is a constant release rate of the antibacterial agent from the catheter coating, then a ratio of approximately 1 : 4 antibacterial agent and diluent to monomers is required to ensure there is a sufficient reservoir of antibacterial agent to maintain this release rate over 7 days. Unfortunately neither vantocil IB or alexidine dihydrochloride are soluble in EEMA, which is a hydrophobic monomer. In order to obtain a one phase solution of all the components, a small amount of water was used as a diluent for the antibacterial agent. Care was taken that the percentage of water used did not exceed the equilibrium water content of the membrane in order to preserve the homogeneity of the membrane upon hydration.

As water soluble antibacterials agents, neither alexidine dihydrochloride nor vantocil IB were soluble in EEMA. Once again the presence of water as a diluent for the antibacterial agents was required to ensure homogeneity of the components. The most favoured compositions were as follows:-

Alexidine dihydrochloride : H_2O	40% : 60%	(I)
HEMA : EEMA	70% : 30%	(II)
(I) : (II)	1 : 4	

This gives membranes with a 8% loading of alexidine dihydrochloride

Vantocil IB : H_2O	52% : 48%	(I)
HEMA : EEMA	70% : 30%	(II)
(I) : (II)	1 : 5.5	

This gives membranes with a 8% loading of vantocil IB

These compositions gave homogeneous systems suitable for the production of hydrogel membranes for the controlled release of the antibacterial agents.

7.3.3 Release of the Antibacterial Agents from the Hydrogel Material

Experiments were carried out to compare the rates at which vantocil IB and alexidine dihydrochloride were released from the low water content hydrogel membrane to that from higher water content polyHEMA membranes. The method used was as described in Section 2.11, whereby the dry weight of the membranes was noted prior to hydration. After 30 minutes hydration in distilled water the membranes were

dehydrated to constant weight in a microwave oven for 10 minutes and reweighed. This procedure was repeated after every hours hydration for a subsequent four hours and then after every 24 hours for 1 week.

Time	Weight Loss (% w/w)					
(hrs)	pHEMA	L0	L1	L2	L3	L4
0.5	4.68	2.85	4.60	5.02	6.17	11.38
1.0	5.82	3.83	4.89	5.05	7.03	12.03
2.0	6.41	4.39	5.32	5.25	7.31	12.61
3.0	7.20	4.68	5.61	5.36	8.34	12.84
4.0	7.29	4.80	5.75	5.53	9.05	13.14
24.0	7.36	5.01	7.17	5.72	12.67	13.57
48.0	7.36	5.26	7.89	5.99	14.44	13.74
72.0	7.36	5.29	8.31	6.04	14.70	14.19
96.0	7.43	5.31	8.53	6.06	14.72	14.55

L0 = Low water content hydrogel for catheter coating

L1 = Low water content hydrogel for catheter coating + 8% alexidine dihydrochloride

L2 = Low water content hydrogel for catheter coating + 8% vantocil IB

L3 = polyHEMA + 8% alexidine dihydrochloride

L4 = polyHEMA + 8% vantocil IB

Table 7.4 Percentage weight loss from hydrogel membranes after 96 hours hydration.

Graphs of weight loss against time were plotted to give an indication of how much antibacterial agent was released from the membrane over a period of time. The results are shown in Table 7.4 and Figure 7.5.

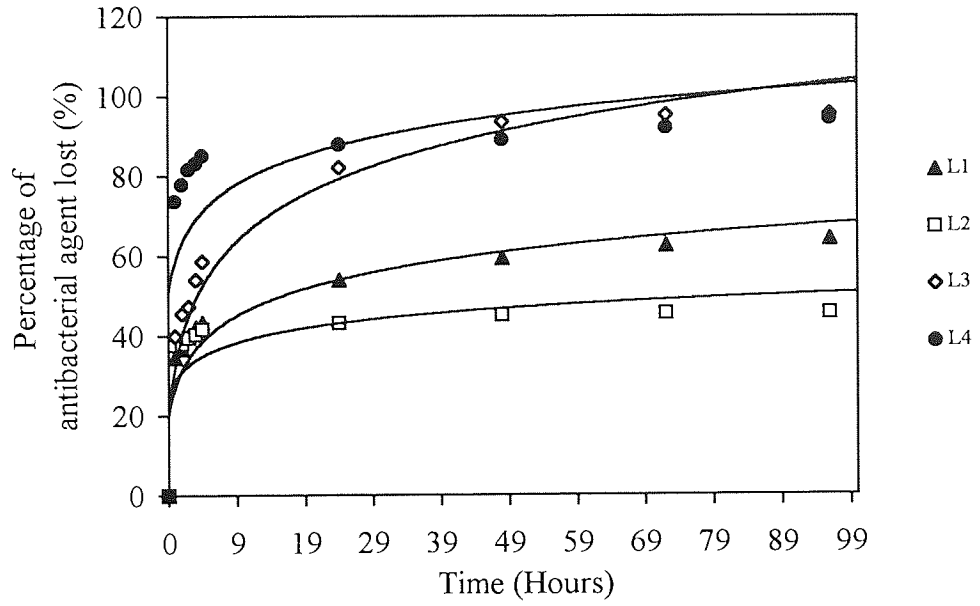

L1 = Low water content hydrogel for catheter coating + 8% alexidine dihydrochloride

L2 = Low water content hydrogel for catheter coating + 8% vantocil IB

L3 = polyHEMA + 8% alexidine dihydrochloride

L4 = polyHEMA + 8% vantocil IB

Figure 7.5 Percentage of antibacterial agent lost as a function of time

From Table 7.4 and Figure 7.5 it can be clearly seen that there is significantly greater weight loss from the polyHEMA membranes than from the HEMA-EEMA copolymer.

After 96 hours hydration it would seem that both alexidine dihydrochloride and vantocil IB have leached almost entirely from the polyHEMA membranes as illustrated in Figure 7.5 although initially, and up to 4 hours hydration, the polyHEMA membrane incorporating vantocil IB shows the greater weight loss.

Finally it can be seen that the HEMA-EEMA membranes incorporating alexidine dihydrochloride show a greater percentage weight loss after 96 hours than those incorporating vantocil IB.

The low water content material containing 8% alexidine dihydrochloride for the catheter coating was tested for antibacterial activity using the zone of inhibition testing method. These tests were carried out at the Queen Elizabeth hospital and the results are presented in Table 7.5

Organism Tested	**Zone Sizes (Diameter mm)**
S. epidermis	16, 16, 15, 15
S. epidermis 24 hour pre-leach in phosphate buffered saline	15, 15
Pseudomonas aeruginosa	11, 11

Table 7.5 Antimicrobial activity of membranes loaded with 8% alexidine dihydrochloride

From Table 7.5 it can be seen that the materials tested shows zones of inhibition even after 24 hours pre-leaching in phosphate buffered saline. The greatest zones of inhibition were shown against the *S. epidermis* bacteria.

7.3.4 Discussion

An homopolymer of polyHEMA might have been considered an ideal material in which to incorporate an antibacterial agent and to use as a catheter coating. However

it was necessary to sustain a controlled release over a period of 7 days, according to the specifications given by the Queen Elizabeth hospital. Thus a lower water content material of approximately 25% was more suitable. As stated in Section 7.3.1, it is in the region of ~20% that there is the transition in the water binding properties from all non-freezing water to both freezing and non-freezing water. Obviously for transport of an antibacterial agent within the polymer matrix some freezing water must be present, but too large a percentage of freezing water will cause release of the antibacterial agent to occur over too short a period of time. By copolymerising an hydrophobic monomer with HEMA the equilibrium water content will be reduced. However since water acts as a plasticiser within the hydrogel system, if the EWC is lowered the material may no longer be sufficiently flexible to use as a catheter coating. Therefore an ideal monomer to copolymerise with HEMA for this application will be an hydrophobic monomer with a long side chain, such as lauryl methacrylate, n-octyl methacrylate, n-hexyl methacrylate or ethoxyethyl methacrylate.

The properties of HEMA-NHMA and HEMA-EEMA materials were evaluated and from Tables 7.2 and 7.3 it can be seen that the membranes produced using NHMA in combination with HEMA were not very flexible once hydrated, as illustrated by their high initial modulii (E). This inflexibility makes them unsuitable for the application of a catheter coating. The sample with the composition: HEMA-EEMA 70:30 with 2% EGDM cross-linker had the most suitable EWC at 25% and a good flexibility, with an initial modulus of 1.11MPa. The flexibility and strength was also highlighted by an elongation to break of almost 200%. Although polyHEMA hydrogels have been shown to have an initial modulus in the region of 0.6MPa[51], indicating a greater

degree of flexibility than the HEMA-EEMA 70:30 materials, the values for the tensile strength and elongation to break of polyHEMA materials, at 0.472MPa and 71%, are significantly less than HEMA-EEMA 70:30 materials. Thus the HEMA-EEMA 70:30 materials were chosen when attempting to incorporate the antibacterial agents.

As stated in Section 7.3.2, neither alexidine dihydrochloride nor vantocil IB were soluble in EEMA because they are water soluble antibacterials agents. In order to maintain the desired ratio of HEMA and EEMA, it was necessary to dissolve the antibacterial agents in a small amount of water to ensure homogeneity. Incorporation of large amounts of water into the monomer system can result in phase separation of the membranes during polymerisation, which is undesirable. As alexidine dihydrochloride is insoluble in ethoxyethyl methacrylate, only 8%(w/w) of this antibacterial agent has thus far been incorporated into the monomer system to produce a homogeneous solution. A similar problem exists for vantocil IB, which has also been incorporated up to 8%(w/w) to produce a homogeneous solution. The weight percentage of the antibacterial agent incorporated into the hydrogel materials was calculated as a function of the monomers rather than as a function of the total hydrated gel.

From the results of the leaching experiment presented in Figure 7.5 it can be clearly seen that there is a significantly greater percentage weight loss from the polyHEMA membranes than from the HEMA-EEMA copolymer. This is to be expected because the EWC of the polyHEMA membranes, (37%), is almost twice that of the HEMA-EEMA membranes. This suggests that there is a larger free volume between the

polymer chains, facilitating the movement of the immobilised antibacterial agents through the polymer network.

After 96 hours hydration it would seem that both alexidine dihydrochloride and vantocil IB have leached almost entirely from the polyHEMA membranes as illustrated in Figure 7.5. Initially, and up to 4 hours hydration, the polyHEMA membrane incorporating vantocil IB shows the greater weight loss. This is somewhat surprising because vantocil IB is a longer chain oligomeric molecule and it would be expected that it would move through the polymer network more slowly than the lower molecular weight alexidine dihydrochloride molecule. If, however during polymerisation much of the vantocil IB accumulated at the surface of the polyHEMA membrane, this would explain the immediate weight loss upon hydration. After 24 hours the percentage weight loss from the polyHEMA membrane incorporating alexidine dihydrochloride is closer to that of the vantocil IB membranes and after 96 hours they are almost equivalent. The HEMA-EEMA membranes incorporating alexidine dihydrochloride show a greater percentage weight loss after 96 hours than those incorporating vantocil IB. This is in line with expectations, as the oligomeric vantocil IB molecules move more slowly through the polymer network than the lower molecular weight alexidine dihydrochloride.

Antibacterial testing was carried out by the microbiology department at the Queen Elizabeth hospital, Birmingham. Unfortunately only a limited number of tests could be carried out by the Queen Elizabeth hospital due to constraints of time. With this in mind HEMA-EEMA hydrogels containing alexidine dihydrochloride were selected for

antibacterial testing to determine whether the release of an antibacterial agent from a low water content hydrogel may be effective against two common microbes, *S. epidermidis* and *P. aeruginosa*. Antibacterial activity of these materials is shown by relatively large areas of inhibition, with the greater activity shown against the gram positive *S. epidermidis* bacteria. In order to determine whether the material could sustain a level of antibacterial activity over 7 days, a zone of inhibition test would need to be carried out on a sample pre-leached in phosphate buffed saline for 7 days. It can be seen from Table 7.5 that the material does retain activity after 24 hours pre-leach in phosphate buffered saline although the zone of inhibition produced is slightly less.

It is expected that the HEMA-EEMA hydrogels containing vantocil IB will also demonstrate zones of inhibition in a similar way. From Figure 7.5 it can be seen that the initial rate of release of vantocil IB from the HEMA-EEMA hydrogels is very similar to the release rate if alexidine dihydrochloride. It has been demonstrated by workers at the Queen Elizabeth hospital[189] that both antibacterial agents show similar activity against common micro-organisms and thus it would be expected that HEMA-EEMA hydrogels containing vantocil IB would show similar sized zones of inhibition. From this work it has been established that the rate of release of the antibacterial agent is dependent on both the water content of the hydrogel and the relative molecular weight of the antibacterial agent. Specifications for release rate set down by the Queen Elizabeth hospital can be met by synthesising an hydrogel with an appropriate water content by choosing relevant monomers and also by selecting an antibacterial agent of the desired relative molecular weight. It was suggested by

workers at the Queen Elizabeth hospital[189] that vantocil IB may be more suitable for incorporation into hydrogels whose potential use is as a catheter coating. This is because the activity of vantocil IB is unaffected by plasma proteins, unlike the activity of alexidine hydrochloride which is reduced. Thus the enabling technology for the production of an hydrogel catheter coating is available and awaits incorporation into a practical device. Further utilisation of this strategy depends on collaboration between the two centres involved.

This Section has outlined the potential for the development of a slow release antibacterial coating. In order to develop a long term protection device, it may be advantageous to consider the chemical bonding of an antibacterial agent to the polymer which is discussed in the following Section.

7.4 Functionalisation of Polyhexamethylene Biguanide

The possibility of incorporating an antibacterial agent such as PHMB into a low water content hydrogel for controlled release has been looked at in Section 7.3. In order to develop a long term protection device the possibility of chemically bonding the antibacterial agent within the hydrogel matrix also needs to be investigated. It is known that attachment of a drug to a polymer backbone by chemical means can result in the loss of biological activity[171] and this is a fact that must be considered when attempting to develop an hydrogel material that offers long term protection against bacterial invasion.

Polyhexamethylene biguanide, the active ingredient in vantocil IB is an oligomeric material but has an amine end group[190-192]. Reaction of this amine end group with a suitable compound containing a double bond would enable PHMB to be further polymerised. Reactions of amines with acid chlorides to produce amides are well known[172], and the reaction scheme is shown by Equation 2.

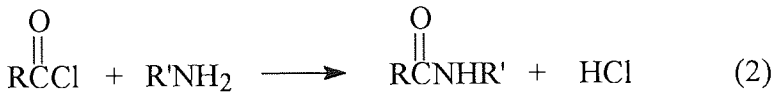

(2)

Also known are the reactions of the isocyanate group with amines to form a substituted urea. This reaction scheme is illustrated by Equation 3.

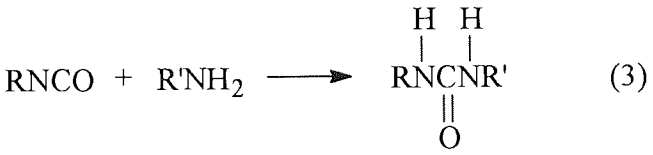

(3)

Thus reaction of methacryloyl isocyanate, which is readily available from e.g. Aldrich, with the reactive amine end group of PHMB should give a functionalised PHMB product that can be further polymerised. This reaction scheme is given by Equation 4.

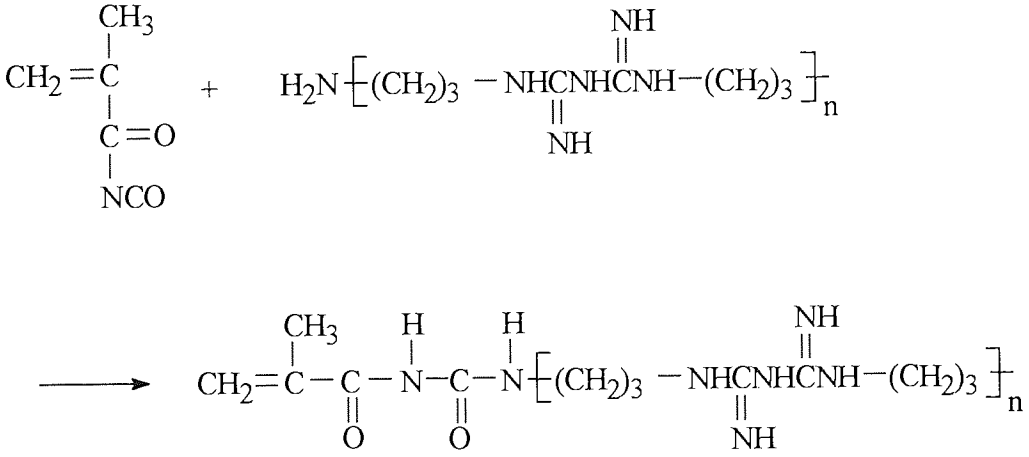

(4)

Vantocil IB is supplied from ICI Biocides as a 20% aqueous solution and the PHMB is in the form of an hydrochloride salt in order to make it water soluble. It is not advisable to add either methacryloyl isocyanate or an acid chloride directly to an aqueous solution of PHMB as the presence of water will cause hydrolysis of the reagent. Thus several preliminary experiments were carried out in order to investigate the most suitable conditions for the reaction of the PHMB end group functionality with either methacryloyl isocyanate or an acid chloride. These experiments made use of techniques and reagents readily available in the laboratory.

7.4.1 Direct Reaction of Methacryloyl Isocyanate with PHMB

Isolation of PHMB from the aqueous solution was possible by neutralising the acidic hydrochloride form with alkali and liberating the free base. It may then be possible to add methacryloyl isocyanate directly to the oily precipitate of PHMB although uncontrolled reaction of a neat base with an isocyanate would always be undesirable.

In order to control the exotherm from the reaction between methacryloyl isocyanate and PHMB, it was necessary to carry out the reaction in a common solvent. Potential solvents investigated for use in this reaction included ethyl acetate, acetone, chloroform, dichloromethane, THF, DMF and diethyl ether. Unfortunately the precipitate of PHMB only showed solubility in a weakly acidic aqueous solvent or in dimethyl sulphoxide (DMSO). As already stated carrying out the reaction in an aqueous solution was not ideal because of the potential hydrolysis of the reagent. Thus, DMSO was chosen as the common solvent for the reaction.

7.4.1.1 Results

1.48g ($8x10^{-4}$ moles) of PHMB free base, liberated from a 20% aqueous solution of vantocil IB, was dissolved in 50ml of DMSO. To this 0.09g ($8x10^{-4}$ moles) of methacryloyl isocyanate was added, with stirring, to the PHMB solution. The reaction vessel was maintained at 25°C throughout. Upon addition of the methacryloyl isocyanate there was a mild exothermic reaction accompanied by effervescence and generation of a yellow precipitate. The precipitate was isolated by vacuum filtration and dried in a vacuum oven at 30°C for 48 hours after which FTIR and ^{1}H and ^{13}C NMR spectroscopy was carried out on the product.

Analysis of the FTIR and ^{1}H and ^{13}C NMR spectra and comparison of these spectra with FTIR and ^{1}H and ^{13}C NMR spectra of the PHMB starting material, shown in Appendix 6 suggested that the isolated product was unreacted starting material and that the reaction that had taken place did not involve PHMB in any quantity. Addition of methacryloyl isocyanate to DMSO without the presence of PHMB gave rise to a similar exothermic reaction and effervescence. This led to the conclusion that the DMSO was not sufficiently dried and the presence of water brought about the hydrolysis of the methacryloyl isocyanate. The experiment was repeated and care was taken to ensure that the DMSO was dried to avoid unwanted hydrolysis of the methacryloyl isocyanate. However interpretation of the FTIR and ^{1}H and ^{13}C NMR spectra of the product once again led to the conclusion that the desired reaction had not taken place and the precipitate isolated from the reaction was unreacted starting material. The PHMB free base was isolated from an aqueous solution, but was not dried over KOH. Thus residual water associated with the amine end group of the

PHMB is likely to have been responsible for the hydrolysis of the methacryloyl isocyanate.

The direct reaction of methacryloyl isocyanate with PHMB in a common solvent has proved difficult because of the limited number of common solvents available. It was necessary to eliminate water from the reaction, to prevent hydrolysis of the methacryloyl isocyanate. For these reasons this method was not pursued and the possibility of functionalising PHMB by interfacial methods was examined

7.4.2 Functionalisation of PHMB by Interfacial Methods

Because it proved difficult to find a common solvent for both PHMB and methacryloyl isocyanate, the possibility of using an aqueous solvent for the PHMB and a water-immiscible solvent for the methacryloyl isocyanate was investigated. This type of reaction is commonly known as interfacial synthesis. Interfacial synthesis is a low temperature reaction process occurring at or near the interface of two or more distinct phases. In its simplest form the interfacial reaction takes place at or adjacent to the interface of e.g. an organic solvent and water, where the organic phase contains a diacid halide or similar reactive species and the aqueous phase contains a compound with an active hydrogen in the functional group such as the amine end group functionality of PHMB. The two phases provide a controlled delivery of reactive species to the site of reaction through diffusion[188].

Interfacial polycondensation is a technique which came into prominence in the 1950's and has proved particularly appropriate for the synthesis of polymers which are

thermally unstable, for use with unstable intermediates and for polymers with reactive functional groups[173]. Perhaps the most well known and widely demonstrated example of interfacial polycondensation is the Nylon Rope Trick[187]. In this experiment a film of polyamide is formed at the liquid-liquid interface and is removed continuously as a small flexible rope. This polymerisation system does not make use of stirring but not only does the stirring motion enhance the delivery of and removal of material to and from the reaction site but it also generates drops of one phase in the other, increasing the interfacial area where the reactions can take place[188].

One of the side reactions of interfacial synthesis is hydrolysis of the diacid chloride or other reactive species. This is particularly a problem with the lower aliphatic chlorides under C_7 where their extraction into the aqueous phase is a limiting factor in their hydrolysis. Acid chlorides with longer aliphatic chains and also less reactive aromatic acid chlorides generally give better results.

The methodology explored for the reaction of PHMB with methacryloyl isocyanate is based on techniques which have been developed for interfacial polycondensation reactions within this laboratory. The method employs a solution of methacryloyl isocyanate (or acid chloride) in a water-immiscible solvent combined with an aqueous solution of PHMB. In the instance of using an acid chloride, an inorganic base is also used.

An important variation of interfacial polycondensation is the use of wholly or partially water-miscible solvents[174-176]. The procedure has been used for several classes of

polymer including polyesters and polyamides and is particularly useful in systems where the diacid chloride component has relatively high hydrolytic stability. Examples of organic solvents are tetrahydrofuran, acetone and cyclohexanone. Advantages of this system in polycondensation reactions are accelerated reaction rates and ease of product recovery.

7.4.2.1 Results

In order to carry out the reaction to functionalise PHMB at the interface between water and a water immiscible solvent, a 30% aqueous solution of PHMB was used as supplied by ICI biocides. In a typical experiment 25cm^3 of the PHMB solution was placed in a baffled test tube (80cm^3 volume). An equimolar quantity of methacryloyl isocyanate was dissolved in 25 cm^3 carbon tetrachloride. This was added to the test tube containing the aqueous solution. A homogeniser was placed just below the interface between the two liquid phases and when switched on a dispersion was formed. The reaction was carried out for approximately 30 minutes. After this time the organic phase was removed and base was added to the aqueous layer. The yellow, oily precipitate was isolated by decanting off the aqueous phase and dried in a vacuum oven for 48 hours at 30°C.

A summary of all the experiments carried out is presented in Table 7.6.

In all but the final two experiments a yellow oily precipitate was isolated from the aqueous layer after the addition of base. After drying in a vacuum oven these products were characterised by FTIR and ^{1}H and ^{13}C NMR spectroscopy. Selected

Volume of aqueous phase	Volume and composition of organic phase	Time of reaction	Type of reactant and molar ratio of PHMB to reactant	Molar ratio of PHMB to potassium carbonate	Comments
$25cm^3$	$25cm^3$ chloroform	30 mins	methacryloyl isocyanate (1:1)	none	The emulsion formed on stirring remains when stirring ceases. Addition of base generates yellow precipitate
$25cm^3$	$25cm^3$ carbon tetrachloride	30 mins	methacryloyl isocyanate (1:1)	none	Two phases return when stirring ceases. Addition of base to the aqueous layer generates yellow precipitate
$25cm^3$	$25cm^3$ carbon tetrachloride	30 mins	methacryloyl isocyanate (1:1)	1:3	Base was added to a point just below the limit at which PHMB would precipitate out of solution. Addition of base to the aqueous layer generates yellow precipitate
$400cm^3$	$400cm^3$ carbon tetrachloride	24 hours	methacryloyl isocyanate (1:1)	1:3	A larger scale reaction was carried out in a $500cm^3$ baffled resin flask with an overhead stirrer on maximum speed. Addition of base to the aqueous layer generates yellow precipitate

Table 7.6 Summary of interfacial reactions to functionalise PHMB

Table 7.6 continued

Volume of aqueous phase	Volume and composition of organic phase	Time of reaction	Type of reactant and molar ratio of PHMB to reactant	Molar ratio of PHMB to potassium carbonate	Comments
$400cm^3$	$400cm^3$ carbon tetrachloride	24 hours	undecenyl chloride (1:1)	1:4	An acid chloride may be more reactive than methacryloyl isocyanate. In this situation excess base must be present to neutralise HCl generated from the reaction. Addition of base to the aqueous layer generates yellow precipitate
$25cm^3$	$25cm^3$ carbon tetrachloride	30 mins	undecenyl chloride (1:1)	1:4	Addition of base to the aqueous layer generates yellow precipitate
$25cm^3$	$25cm^3$ carbon tetrachloride	30 mins	itaconyl chloride (1:1)	1:5	Itaconyl chloride is a diacid chloride. It was necessary to add more base in order to ensure neutralisation of HCl generated from the reaction. Addition of base to the aqueous layer generates yellow precipitate
$25cm^3$	$25cm^3$ dry acetone	30 mins	methacryloyl isocyanate (1:1)	none	No HCl is generated in this reaction using methacryloyl isocyanate, therefore no base was added. Addition of base to the aqueous layer generates yellow precipitate

Table 7.6 continued

Volume of aqueous phase	Volume and composition of organic phase	Time of reaction	Type of reactant and molar ratio of PHMB to reactant	Molar ratio of PHMB to potassium carbonate	Comments
$25cm^3$	$25cm^3$ dry acetone	30 mins	methacryloyl isocyanate (1:1)	1:3	Sufficient base was added to neutralise the hydrochloride form of PHMB and increase the availability of the amine end group. Addition of base to the aqueous layer generates yellow precipitate
$25cm^3$	$25cm^3$ dry acetone	30 mins	itaconyl chloride (1:1)	1:5	Half of the base was added to the aqueous layer. The itaconyl chloride/acetone solution was then added to the aqueous layer with stirring, at which time the reaction turned orange in colour. Addition of the remaining base resulted in the solution becoming deep purple in colour, although as the reaction proceeded, the orange colour returned. Upon completion of the reaction a deep orange oily precipitate was isolated with no need for further additions of base.
$25cm^3$	$25cm^3$ dry acetone	30 mins	itaconyl chloride (2:1)	1:5	Itaconyl chloride is a diacid chloride and in this case 2 times the equivalent of PHMB was used. the reaction proceeded as above.

examples of the spectra are shown in Appendix 6. Analysis of the FTIR and ^{1}H and ^{13}C NMR spectra and comparison of these spectra with FTIR and ^{1}H and ^{13}C NMR spectra of the PHMB starting material, shown in Appendix 6 suggested that no reaction had taken place and that the isolated product was unreacted starting material.

Using base to isolate the PHMB products is not ideal because such basic conditions may cause hydrolysis of any product back to the starting material. To isolate the product and avoid using basic conditions the aqueous solution was evaporated using a rotary evaporator until a pale yellow product remained. Characterisation of this product proved that it had been no more successful than before. Methacryloyl isocyanate may not have been an ideal reactant. The case may also have arisen that the methacryloyl isocyanate was not sufficiently maintained in the non-aqueous phase and had undergone hydrolysis before the reaction with the PHMB could take place.

Undecenyl chloride was chosen in the place of methacryloyl isocyanate because its longer side group reduces the rate at which it undergoes hydrolysis in normal conditions. Its longer, more hydrophobic side group may also be more able to maintain its presence in the organic phase, and in this way reduce the possibility of hydrolysis before reaction could take place. The reaction was attempted in both neutral and basic conditions but did not prove successful in either.

The reaction between itaconyl chloride and PHMB using an acetone/ water system gave rise to a dark orange oily product which after drying in a vacuum oven was characterised as before. In this case the spectra of the product showed subtle

differences in comparison with the spectra of the starting material, as shown in Appendix 6.

In the ^{1}H NMR spectrum of the starting material there are two singlet peaks in the region of 1.2 - 1.4 ppm and a further singlet peak at 3.0 ppm which have been attributed to the protons on the sp^3 carbon along the backbone of the PHMB molecule. There is a broad singlet peak at 6.0 ppm which has been attributed to the protons on the nitrogen of the guanidine groups in the backbone of the PHMB molecule. The ^{1}H NMR of the product shows the three singlet peaks in a similar position and also shows a further peak at 3.5 ppm. The broad singlet peak has shifted from 6.0 to 7.2 ppm and is less well defined than in the spectrum of the starting material. The ^{13}C NMR spectrum of the starting material shows two singlet peaks in the region of 26 - 30 ppm and a further singlet peak at 41 ppm which have been attributed to the sp^3 carbon atoms along the PHMB backbone. Peaks are also seen in the 156 - 161 ppm region and these have been attributed to the carbon atoms of the guanidine groups of PHMB. The ^{13}C NMR spectrum of the product shows these peaks and also shows a further peak at 118 ppm. At first glance it appeared that the reaction had been more successful.

However, it was noted that although the use of acetone has been successfully employed as a solvent in interfacial polycondensation[174-176], its use in this situation may have led to an undesired reaction. The reaction of a primary amine with the carbonyl group of an aldehyde or some ketones gives rise to a substituted imine often referred to as a Schiff base. Although aromatic aldehydes such as benzaldehyde are

more commonly used in this reaction, ketones such as acetone are also known to react, forming an orange product. The optimum pH for the reaction is pH 3-4. Rather than the desired reaction of the acyl chloride with the PHMB end group, it would appear that the acetone solvent has reacted with the PHMB end group forming the orange Schiff base.

7.5 Incorporation of PHMB Product into a Hydrogel

The object of reacting PHMB with a reagent that had a double bond was so that the resulting product could be polymerised into either a linear copolymer or a cross-linked hydrogel system. Attempts were made to copolymerise the PHMB product with HEMA. In order to do this the PHMB product must be soluble in HEMA so that a one phase system is achieved. Unfortunately the PHMB product was only sparingly soluble in HEMA and a small quantity of acid was added to aid solubility. In this way 20%(w/w) of the PHMB product could be incorporated into the HEMA using approximately 15%(w/w) 1.022N HCl.

Experiments were carried out to compare the weight loss of the resulting membranes upon hydration with the weight loss from a polyHEMA membrane containing an equivalent amount of unreacted PHMB, (the solubility of which was also aided by approximately 15%(w/w) 1.022N HCl) and the weight loss from a straightforward polyHEMA membrane.

Time / Hours	Weight Loss (%)		
	polyHEMA	M1	M2
0.5	2.43	7.63	6.98
1.0	3.91	11.91	11.54
2.0	5.16	15.37	14.59
3.0	6.97	16.14	15.73
4.0	8.20	20.10	18.63
24.0	9.87	22.90	22.81
48.0	11.64	22.92	22.87
72.0	12.71	22.95	22.91
96.0	14.07	23.15	23.14

M1 = polyHEMA + 20%(w/w) unreacted PHMB

M2 = polyHEMA + 20%(w/w) PHMB product

Table 7.7 Percentage weight lost on hydration of polyHEMA membranes containing either unreacted PHMB or PHMB product

The membranes were prepared by the usual method, (Section 2.), using 1%(w/w) EGDM as the cross-linker and 0.5%(w/w) AZBN as the initiator. The membranes were polymerised at 60°C for 3 days and post-cured for 3 hours at 90°C. The initial dry weight of the membranes was noted prior to hydration. After 30 minutes hydration in distilled water, the membranes were dehydrated to constant weight in a microwave and reweighed. This procedure was repeated after every hours hydration for four hours and then after every 24 hours for 1 week. A graph of weight loss against time was plotted. The results are shown in Table 7.7 and Figure 7.6.

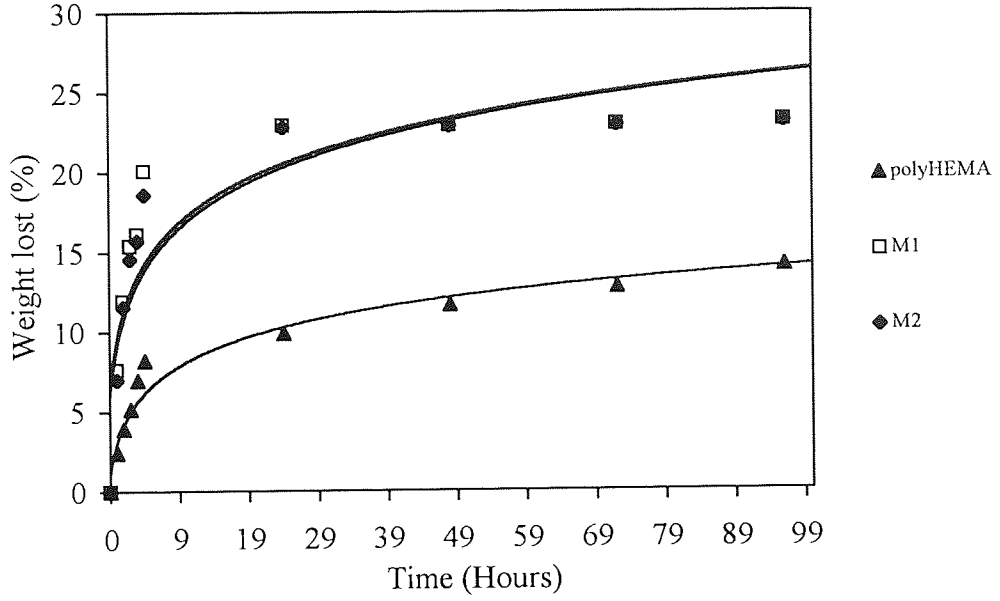

M1 = polyHEMA + 20%(w/w) unreacted PHMB

M2 = polyHEMA + 20%(w/w) PHMB product

Figure 7.6 Graph of weight loss on hydration as a function of time for polyHEMA membranes containing either unreacted PHMB or PHMB product

It can be seen from Figure 7.6 that the percentage weight loss upon hydration from the polyHEMA membrane containing 20%(w/w) unreacted PHMB after 96 hours is very similar to that of the polyHEMA membrane containing 20%(w/w) PHMB product. It might be inferred from this that the PHMB product has not copolymerised with the HEMA. It is more likely that the product does not contain the double bond desired from the reaction with acyl chloride. It can be seen as further evidence for the conclusion that a Schiff base was formed by the reaction between the acetone solvent and the PHMB amine end group.

7.6 Preparation of Novel Water Soluble Linear Polymers

The concept of hydrophobic association in conjunction with charge, the mode of action displayed by the polymeric antibacterial agents investigated in this work, is not a novel concept. It is a feature of many biological systems, in particular apoproteins present in for example lung surfactants or synovial fluid and is also a feature of the mode of action of the antibacterial tear protein, lysozyme. By mimicking the structural features of these naturally occurring systems and also bearing in mind the structure of the PHMB molecule it may be possible to synthesis a polymer that shows antibacterial activity and can respond to changes in its environment e.g. pH. Such polymers would find many applications in a biological environment with the possibility that they may be coated onto a catheter material to provide long term protection against antibacterial infection. They may also find applications in drug release systems or if cross-linked to provide a 3-dimensional network, they may provide a novel antibacterial surface.

If these polymers contain groups capable of carrying charge e.g. an amine or carboxylic acid functionality that can accept or lose a proton, they can respond to changes in the pH of the environment as well as, in the case of a cationic functionality, convey the potential for antibacterial activity. Good examples of this are the styrene-imidazole random copolymers studied by Tan *et al.*[177]. The results that they obtained suggested that the copolymers form micelle-like structures in an aqueous environment. By reducing the pH concentration of the solution, hence protonating the imidazole groups, the polymer chain can be extended, due to the electrostatic repulsion between the positive charges. Increasing the pH facilitates the formation of

hydrophobic microdomains and eventually above pH ~7.5 the imidazole groups are completely deprotonated and precipitation of the polymer occurs. This is illustrated in Figure 7.7.

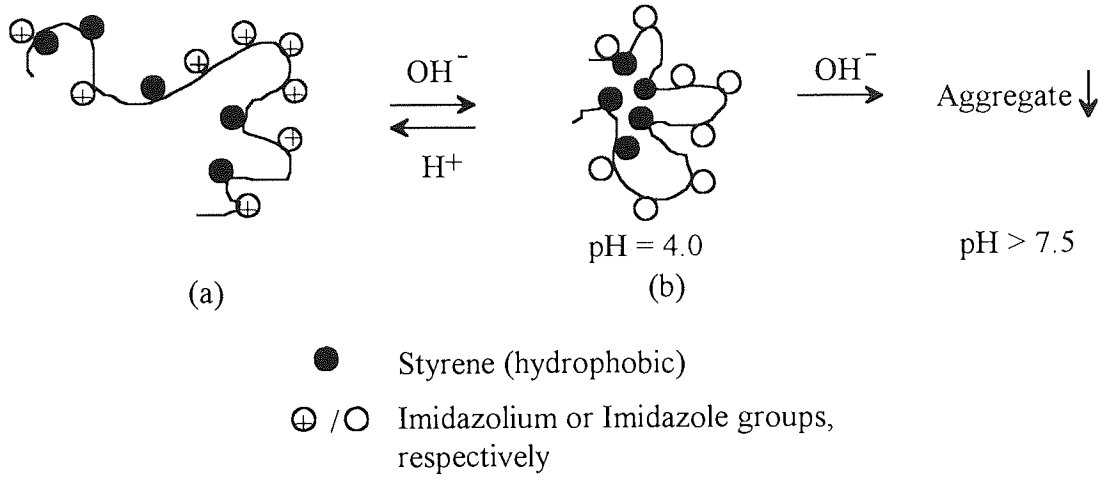

Figure 7.7 Conformational changes of a Styrene / Imidazole copolymer in aqueous solution (reproduced from reference 27).

These polymers behave in a similar way to the apoproteins in lung surfactants and synovial fluid and serve as a good model on which to base the desired novel linear polymers. Thus in order to obtain a linear co- or terpolymer that mimics the structure of the systems described it is necessary to chose a combination of monomers that have in turn hydrophilic and hydrophobic character and also a potentially cationic monomer.

A summary of all the polymerisations carried out is presented in Table 7.8.

Monomer Composition	Solvent	Catalyst System	Temperature and Time	Yield	Comments
50% Indene 50% NVP	THF	UV Light $ZnCl_2$ 1% AZBN	22°C 2 hours	32.4%	Copolymer of indene and NVP was obtained. Product was water soluble and a 5% aqueous solution showed a surface tension of 52.5 mN/m at pH 7.0
50% Indene 50% NNDMA	THF	UV Light $ZnCl_2$ 1% AZBN	22°C 2 hours	43.2%	Copolymer of indene and NNDMA was obtained. Product was water soluble and a 5% aqueous solution showed a surface tension of 47.0 mN/m at pH 7.0
50% Indene 50% NNDMA	THF	UV Light No $ZnCl_2$ 1% AZBN	22°C 2 hours	0.0%	No product was obtained on addition of the reaction contents to cold ether.
50% Indene 50% NNDMA	THF	UV Light $ZnCl_2$ No AZBN	22°C 2 hours	19.4%	Although $ZnCl_2$ will catalyse the reaction a much higher yield is obtained with the combined catalyst system of $ZnCl_2$ and AZBN
50% Indene 50% NNDMA	THF	No UV Light $ZnCl_2$ AZBN	22°C 2 hours	20.9%	Although the reaction will proceed under standard conditions, a much higher yield is obtained with the use of UV light

Monomer Composition	Solvent	Catalyst System	Temperature and Time	Yield	Comments
45% Indene 45% NNDMA 10% NVI	THF	UV Light $ZnCl_2$ AZBN	22°C 2 hours	57.4%	Analysis of product suggests that a copolymer of indene and NNDMA has been obtained. Product is water soluble.
90% Indene 10% NVI	THF	UV Light $ZnCl_2$ AZBN	22°C 2 hours	45.6%	Copolymer of indene and NVI is obtained. Product is sparingly soluble in water.
40% Indene 40% NNDMA 20% NVI	THF	UV Light $ZnCl_2$ AZBN	22°C 2 hours	59.2%	Analysis of product suggests that a copolymer of indene and NNDMA has been obtained. Product is water soluble.
45% Indene 45% NNDMA 10% SPE	THF	UV Light $ZnCl_2$ AZBN	22°C 2 hours	46.4%	Analysis of product suggests that a copolymer of indene and NNDMA has been obtained. Product is water soluble.
40% Indene 40% NNDMA 20% NVI	THF	AZBN	65°C 24 hours	30.6%	Analysis of product suggests that a copolymer of indene and NNDMA has been obtained. Product is water soluble.

Monomer Composition	Solvent	Catalyst System	Temperature and Time	Yield	Comments
40% Indene 40% NNDMA 20% SPE	THF	AZBN	65°C 24 hours	0.0%	No polymer obtained. Unreacted SPE recovered on completion of the reaction.
45% Indene 45% NNDMA 10% DMAEMA	THF	AZBN	65°C 24 hours	35.9%	Analysis of product suggests that a copolymer of indene and NNDMA has been obtained. Product is water soluble.
45% Indene 45% NNDMA 10% DMAEMA	THF	UV Light $ZnCl_2$ AZBN	22°C 2 hours	51.3%	Analysis of product suggests that a copolymer of indene and NNDMA has been obtained. Product is water soluble.
45% Indene 45% NNDMA 10% DMAEA	THF	UV Light $ZnCl_2$ AZBN	22°C 2 hours	49.8%	Analysis of product suggests that a copolymer of indene and NNDMA has been obtained. Product is water soluble.
45% Indene 45% NNDMA 10% DMAEA	THF	AZBN	65°C 24 hours	32.4%	Analysis of product suggests that a copolymer of indene and NNDMA has been obtained. Product is water soluble.

Monomer Composition	Solvent	Catalyst System	Temperature and Time	Yield	Comments
26% CHMA 45% NNDMA 28% DMAEMA	THF	UV Light $ZnCl_2$ AZBN	22°C 2 hours	81.2%	There was no need to precipitate the product in cold ether. The product was isolated directly from the reaction by vacuum filtration. Analysis of product suggests that a copolymer of CHMA and NNDMA has been obtained. Product is water soluble.
26% CHMA 45% NNDMA 28% DMAEA	THF	UV Light $ZnCl_2$ AZBN	22°C 2 hours	76.3%	There was no need to precipitate the product in cold ether. The product was isolated directly from the reaction by vacuum filtration. Analysis of product suggests that a copolymer of CHMA and NNDMA has been obtained. Product is water soluble.
26% CHMA 45% NNDMA 28% DMAEMA	THF	AZBN	65°C 24 hours	51.4%	There was no need to precipitate the product in cold ether. The product was isolated directly from the reaction by vacuum filtration. Analysis of product suggests that a copolymer of CHMA and NNDMA has been obtained. Product is water soluble.

Monomer Composition	Solvent	Catalyst System	Temperature and Time	Yield	Comments
26% CHMA 45% NNDMA 28% DMAEA	THF	AZBN	65°C 24 hours	48.9%	There was no need to precipitate the product in cold ether. The product was isolated directly from the reaction by vacuum filtration. Analysis of product suggests that a copolymer of CHMA and NNDMA has been obtained. Product is water soluble.
26% CHMA 45% NNDMA 28% DMAEMA	MeOH	UV Light $ZnCl_2$ AZBN	22°C 2 hours	61.3%	Product was isolated by precipitation in cold ether. Analysis of product suggests that a copolymer of CHMA and NNDMA has been obtained. Product is water soluble.
26% CHMA 45% NNDMA 28% DMAEA	MeOH	UV Light $ZnCl_2$ AZBN	22°C 2 hours	57.1%	Product was isolated by precipitation in cold ether. Analysis of product suggests that a copolymer of CHMA and NNDMA has been obtained. Product is water soluble.

Table 7.8 Summary of solution polymerisation reactions and conditions

Abbreviations used in Table 7.8 are as follows:-

$ZnCl_2$ = zinc chloride

NVP = N-vinyl pyrrolidone

NVI = N-vinyl imidazole

MeOH = methanol

THF = tetrahydrofuran

NNDMA = N, N-dimethyl acrylamide

DMAEMA = dimethylaminoethyl methacrylate

DMAEA = dimethylaminoethyl acrylate

CHMA = cyclohexyl methacrylate

SPE = N-(3-sulphopropyl)-N-methacryloxyethyl-N, N-dimethylammonium betaine

Two methods of polymerisation have been used, bulk free radical polymerisation and a technique patented by Serniuk *et al.*[178], for copolymerising polar and non-polar monomers. These methods are described in Section 2.2.2. Resulting polymers were characterised by FTIR and ^{1}H and ^{13}C NMR spectroscopy. Selected examples of these spectra are presented in Appendix 6.

7.6.1 Discussion

Analysis of the products of these polymerisations suggests that no terpolymers containing regions of hydrophilicity, hydrophobicity and potentially cationic sites have been prepared. Copolymers of indene with NVP, indene with NNDMA and indene with NVI were successfully prepared. The indene/NVP copolymer and the indene/NNDMA copolymers were soluble in water and showed a degree of surface activity in aqueous solution, at pH 6.8, in a similar manner to the styrene/NVI copolymers described by Tan *et al.*[177]. At pH 9.0 precipitation of the copolymers occurred due to deprotonation of the charged groups and the formation of hydrophobic microdomains.

The yield of products obtained from the reactions carried out suggest that the use of zinc chloride and AZBN as a co-catalyst system leads to higher yields of copolymer than thermally initiated bulk free radical polymerisations. This method was first used by Serniuk *et al.*[178] who successfully copolymerised methyl methacrylate and 2-methylpent-1-ene. The following mechanism has been proposed for the copolymerisation of polar and non-polar monomers by this method, based on the homopolymerisation of polar monomers in the presence of metal halides[179].

For free radical polymerisations of monomers containing polar pendant groups e.g. carbonyl groups, increased rates of polymerisation have been observed in the presence of a metal halide such as $ZnCl_2$. It has been proposed that the metal halide and the monomer form a complex via the polar pendant group. In NNDMA there is conjugation between the carbonyl function and the main chain alkene. This allows the alkene to participate in the complexation and results in a delocalised structure as shown in Figure 7.8.

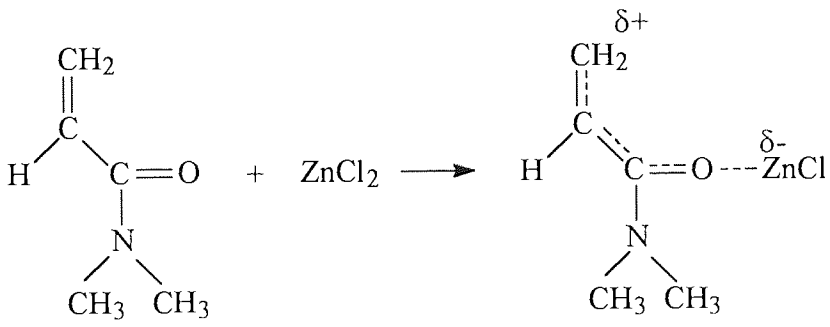

Figure 7.8 Delocalised structure of NNDMA-$ZnCl_2$ complex

Gaylord[180,181] has suggested that the polymerisation reaction occurs through a donor-acceptor charge transfer complex between the metal halide-monomer complex

(acceptor) and an uncomplexed monomer (donor). The partial positive charge that resides on the γ-carbon of the metal halide-NNDMA complex facilitates the formation of such a species. With a monomer such as indene behaving as the electron donor monomer, the charge transfer complex will be as illustrated in Figure 7.9.

Polymerisation of this charge transfer complex, either spontaneously or initiated by a free radical catalyst, will result in the formation of an alternating copolymer.

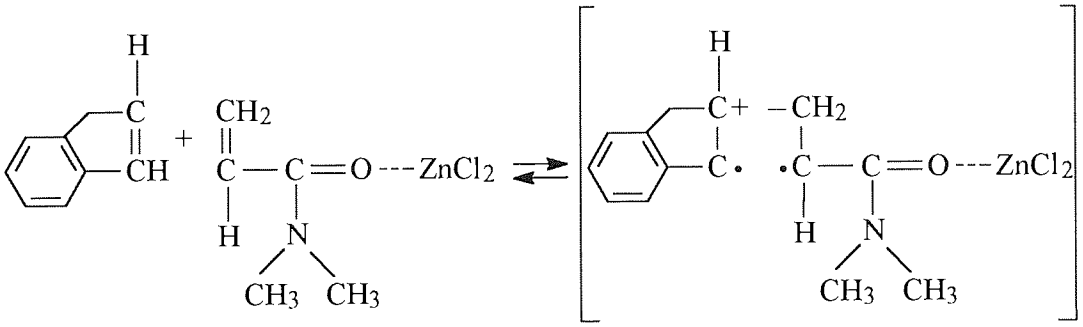

Figure 7.9 Formation of a charge transfer complex

Unsuccessful attempts to synthesise a terpolymer using this method may be explained in terms of the inability of the third monomer to form a charge transfer complex with $ZnCl_2$ hence limiting its ability to take part in the reaction. If one of the two polar monomers is better able to stabilise the charge transfer complex than the other then the reaction will take place preferentially with this monomer. Unfortunately none of the basic monomers were able to participate in the terpolymerisation reaction. Cyclohexyl methacrylate is a more reactive monomer than indene and attempts were made to form a terpolymer using this monomer in conjunction with NNDMA and either DMAEMA or DMAEA. Because CHMA is more reactive it was incorporated

into the reaction at lower percentages than indene in comparable reactions. Terpolymerisations using these monomers also proved unsuccessful.

7.7 Conclusions

One of the main problems associated with using polymers at biological interfaces is the invasion of micro-organisms causing infection. This is a particular problem both with the use of contact lenses in contact with tear fluid and with catheters in blood contact. Although infection can be controlled and minimised by the use of disinfection systems or topically applied antiseptics, it has been established that prevention of infection is preferable to cure.

Several ideas have been put forward for possible development into long term protection devices. The method of bacterial protection by an electric current, a method developed by Elliott *et al.*[167] has been discussed and has shown some success in *in vitro* tests. However limitations arise from the necessity to load the polyurethane material with carbon, making it more difficult to process and manipulate. Also this idea could not be considered for use in the contact lens field. As an alternative to carbon loading for the conduction of an electric current, silver coating was suggested using the well known 'silver mirror' technique. Unfortunately the surface energy of the material to be coated was low and silver coating proved inconsistent. Even treatment of the material with high energy plasma in order to increase its surface energy failed to improve the quality of the surface coating achieved.

Bacterial inhibition by controlled release of an antibacterial agent can be achieved by the incorporation of an antibacterial agent such as vantocil IB or alexidine dihydrochloride into an hydrogel matrix. The rate of diffusion of the antibacterial agent through the hydrogel matrix can be controlled by the incorporation of a hydrophobic monomer, such as ethoxyethyl methacrylate, thus lowering the equilibrium water content of the hydrogel. EEMA also has a long chain side group and the resulting hydrogel is sufficiently flexible to be considered as a coating for a catheter. The smaller size of alexidine dihydrochloride resulted in a faster diffusion rate from the hydrogel matrix than the higher molecular weight vantocil IB and materials containing 8% alexidine dihydrochloride were shown to be resistant to bacteria.

The problem with incorporating an antibacterial agent into an hydrogel matrix without chemical attachment is that such materials can only provide protection from bacteria for a limited period of time. The chemical attachment of polyhexamethylene biguanide to a backbone linear polymer or hydrogel system may provide an alternative long term protection device. Reaction of PHMB with methacryloyl isocyanate or an appropriate acid chloride will give PHMB the required double bond functionality such that it may be further polymerised. An interfacial synthetic method which has proved successful in interfacial polycondensation reactions, employing acetone and water as the solvent system and itaconyl chloride as the reactant, was used. Unfortunately the product from this reaction could not be polymerised into an hydrogel with HEMA. This is because rather than the PHMB amine end group reacting with the itaconyl chloride as desired, a reaction with the acetone occurred, forming a Schiff base.

Development of a new synthetic polymer that may show antibacterial activity and may also respond to changes in its environment in a similar manner to some proteins in living systems, has been investigated. Structural features of the desired polymer are regions of hydrophilicity and hydrophobicity together with potentially cationic functionalities. Thermally initiated bulk free-radical polymerisation and a novel method using a Freidel Crafts halide / free radical initiator co-catalyst system were used. Copolymers of indene and N-vinyl pyrrolidine, indene and N,N'-dimethyl acrylamide and indene and N-vinyl imidazole were prepared. However attempts to include a third monomer to give the potential cationic functionality proved unsuccessful.

CHAPTER 8

Conclusions and

Suggestions for Further Work

8.1 Conclusions

A study of the literature concerning polymeric antibacterial agents has revealed that the essential components of a polymeric antibacterial agent include regions of hydrophilicity and hydrophobicity together with cationic sites. This work has been concerned with an investigation into the effect of incorporating a potentially cationic monomer into an hydrogel material and the potential modifications that this may make to the physical properties of the hydrogel. Some workers have suggested that charged groups in hydrogels may increase the deposition of biological materials when in contact with body fluids[78]. This work has set out to study the uptake of biological materials, in particular the specific protein adsorption, of these cationically modified hydrogels. Using the knowledge gained from the study of other polymeric antibacterial agents, in particular polyhexamethylene biguanide, the potential for the development of polymers and hydrogels that show resistance to bacteria has been investigated. It was hoped that the development of such polymers would have a wide range of applications both in the optical environment and in blood contact as e.g. a catheter coating.

The effect of adding a potentially cationic monomer to two different types of hydrogel systems were investigated. In the first instance a simple polyHEMA hydrogel was modified with increasing proportions of either NVI or DMAEMA. There is much literature available on the water binding properties of polyHEMA[13,20,21] and for this reason polyHEMA was chosen as an ideal hydrophilic monomer with which to copolymerise either NVI or DMAEMA. Investigations into antibacterial agents and novel polymeric antibacterials revealed that the criteria for the design of new

polymeric antibacterial materials included regions of hydrophilicity and hydrophobicity as well as cationic sites for the interaction of the material with the negatively charged cell walls of bacteria. Novel hydrogel materials were prepared using this criteria selecting either NNDMA or AMO as the hydrophilic monomer and CHMA as the hydrophobic component. Increasing proportions of either NVI and DMAEMA were added as the potentially cationic monomer.

NNDMA was chosen as the hydrophilic monomer as it offered a potential increase in equilibrium water content over HEMA. AMO also offered some increase in equilibrium water content and recent work by this research group has shown AMO to have great potential for use in hydrogel systems for biomedical use. It was hoped that indene could be used as the hydrophobic monomer as it has been shown to give linear copolymers with a reasonably alternating sequence distribution[64]. However problems occurred in the synthesis of hydrogel membranes using indene and CHMA was used in its place.

The water binding capabilities of hydrogel systems were investigated using a gravimetric method of calculating EWC and differential scanning calorimetry. Differential scanning calorimetry allowed the percentage of freezing water to be estimated and the fine structure of the melting endotherm gave useful information as to the complex structure of water in hydrogel systems. Values obtained for the EWC, freezing and non-freezing water content of polyHEMA were 34.6%, 13.5% and 21.1% respectively. These values were in good agreement with previous values reported by this research group[51].

Progressive incorporation of either NVI or DMAEMA into a polyHEMA membrane had very little effect on the equilibrium content of the hydrogels, but a rise in the non-freezing water content was observed with a corresponding decrease in freezing water. The effect was more apparent in those samples containing NVI and appeared to relate to the greater ability of NVI over DMAEMA to promote the hydrogen bonding of water to the polymer within the HEMA-NVI network.

Determination of the EWCs, freezing and non-freezing water contents of the novel polymeric materials combining hydrophilicity and hydrophobicity with potential cationic sites was made. Results showed that an increasing proportion of either NVI or DMAEMA led to an increase in the equilibrium water content and freezing water content, due to an increasing proportion of hydrophilic sites.

Study of these materials showed that the water binding ability of an hydrogel will be modified by the steric effects and hydrophobicity of the comonomers. It also revealed that incorporation of a potentially cationic monomer such as NVI or DMAEMA does not adversely affect the water binding properties of hydrogels such that they could no longer be used in biomedical applications.

The water binding properties will have a bearing on the mechanical properties of hydrogel systems and the tensile strength, elongation at break and initial Youngs modulus of the prepared hydrogels were measured. Incorporating either NVI or DMAEMA into these hydrogel systems did not serve to reduce their strength or affect the rigidity to such an extent that they could not be used in a biomedical environment.

In fact addition of these potentially cationic monomers brought about an increase in the tensile strength whilst hardly affecting the initial Youngs modulus.

It has been suggested by some workers[56,57,139] that the surface free energy of an hydrogel is an important property in determining the biotolerence of the material. The effect of cation incorporation on the surface properties of the prepared hydrogel materials was investigated in both the dehydrated and the hydrated state using the sessile drop technique or using Hamiltons method in conjunction with the captive air bubble technique. Although inaccuracies and inconsistencies can occur using these techniques, the values obtained provide useful comparative information. It was found that incorporation of either basic monomer, NVI or DMAEMA, caused very little change in the total surface energies, or in the contribution of the polar and dispersive components of the materials studied, whether in the hydrated or dehydrated state.

There has been some reluctance to use cationic monomers in the development of novel biomaterials, in particular in the contact lens field, because of the idea that there is increased adsorption of biological materials to cationic surfaces. This work serves to illustrate that incorporating a cationic component at low concentration was found to reduce the concentration of lysozyme adsorbed onto the surface of the hydrogel without detrimentally affecting the uptake of the other major tear proteins. Results from the experiments using the *in vitro* spoilation model also suggested that the bulk deposition of lipid and protein on polyHEMA materials containing a low level of cationic component was not significantly greater than results obtained for polyHEMA hydrogels. Deposition studies on the novel hydrogels prepared showed that even with

a potential cation content of up to 20%, the levels of deposition measured were not sufficient to discount their use as biomaterials.

One of the main problems associated with using polymers at biological interfaces is the invasion of micro-organisms causing infection. Although infection can be controlled and minimised by the use of disinfection systems or topically applied antiseptics, it has been established that prevention of infection is preferable to cure. Several ideas have been put forward for possible development into long term protection devices. These include the discussion of the method of bacterial protection by an electric current developed by Elliott *et al.*[167] and possible modifications by coating the catheter with silver or developing a hydrogel coating that may have antibacterial properties.

Bacterial protection using an electric current has limitations including the processing of the material that can conduct the current. It also has little use in the context of contact lens applications. Development of an antibacterial hydrogel coating, however does not have such limitations and could find applications in a wide range of biomedical areas. Bacterial inhibition by controlled release of an antibacterial agent was demonstrated by the incorporation of an antibacterial agent such as vantocil IB or alexidine dihydrochloride into an hydrogel matrix. The rate of release of the antibacterial agents was found to be dependent on the water content of the hydrogel and also on the relative molecular weight and size of the antibacterial agent.

A preliminary investigation into the functionalisation of the end group of polyhexamethylene biguanide in order to provide a means with which this antibacterial agent could be polymerised into an hydrogel system was undertaken. Limited success was achieved using a method of interfacial synthesis with itaconyl chloride as the reactant and it is suggested that further work is under taken in this area.

Preliminary investigations were also made into the development of a new synthetic polymer that may show antibacterial activity. Desired structural features of the polymer were regions of hydrophilicity and hydrophobicity together with potentially cationic functionalities. Thermally initiated bulk free-radical polymerisation and a method using a Freidel Crafts halide / free radical initiator co-catalyst system were used. Copolymers of indene and N-vinyl pyrrolidine, indene and N,N'-dimethylacrylamide and indene and N-vinyl imidazole were prepared. Further investigation on the incorporation of a third monomer to give the potential cationic functionality is required.

8.2 Suggestions for Further Work

Investigations into simple hydrogel systems have shown that addition of the potentially cationic monomers NVI and DMAEMA do not adversely affect the physical properties of hydrogels whose potential application is in the field of biomaterials. These are only two of the potentially cationic monomers that could have been investigated and further work should be carried out using other basic monomers, including quaternary ammonium compounds. Quaternary ammonium compounds are slightly different from the basic monomers considered in that they can

form a cationic salt. The properties of hydrogel materials containing such quaternary ammonium salts may be altered significantly.

Due to the limitations on the antibacterial testing facilities, only a small number of materials were used for the 'zone of inhibition' test to demonstrate bactericidal or bacteriostatic properties. Thus further work in this area would enable the testing of a wider range of the prepared hydrogel or linear polymer materials for their antibacterial properties.

The functionalisation of polyhexamethylene biguanide, (PHMB), is an area that needs further study. The interfacial synthetic method employed has led to limited success and optimisation of reaction conditions or other synthetic methods should be considered. It may be possible to make use of the end-group functionality of PHMB by grafting the PHMB to the surface of an hydrogel material.

Further study of the ever increasing literature available on the development of novel polymeric antibacterial agents may lead to advances in the development of a linear polymer showing regions of hydrophilicity and hydrophobicity together with potentially cationic functionalities. Such a linear polymer, or perhaps existing linear polymers such as those developed by Ferruti *et al.*[116-118], could be a useful precursor to the development of a novel hydrogel material showing antibacterial activity. It may also have potential as an interpenetrant in a semi-interpenetrating hydrogel network. Finally cell adhesion studies may provide a further tool for probing the surface of potentially cationic hydrogel materials in terms of their biocompatibility.

References

REFERENCES

1. Wichterle, O. and Lim, D., Hydrophilic gels for biological use, *Nature*, **185**, 117-118, (1960)

2. Wichterle, O. and Lim, D., Process for producing shaped articles from three dimensional hydrophilic polymer networks, U.S. Patent, 2,976,576, (1961)

3. Wichterle, O. and Lim, D., Cross-linked hydrophilic polymers and articles made there from, U.S. Patent, 3,220,960, (1965)

4. Froix, M.F. and Nelson, R.A., The interaction of water with cellulose from nuclear magnetic resonance relaxation times, *Macromols.*, **8**, 726-730, (1975)

5. Bosen, C.E., Bound water, *Cellulose Chem. Technol.*, **4**, 149-164, (1970)

6. Frommer, M., Shporer, M. and Messalem, R., Water binding and irreversible dehydration processes in cellulose acetate membranes, *J. Appl. Polym. Sci.*, **17**, 2263-2276, (1973)

7. Shporer, M. and Frommer, M., Magnetic resonance studies of the water in cellulose acetate membranes, *J. Macromol. Sci., Phys.*, **B10**, 529-542, (1974)

8. Krishnamurthy, S., McIntyre, D., Santee, E.R. and Wilson, C.W., NMR of dissolved water in ultrathin and thick membranes of cellulose acetate, *J. Polym. Sci., Polym. Phys.*, **11**, 427-448, (1973)

9. Frommer, M.A. and Lancet, D., Freezing and non-freezing water in cellulose acetate membranes, *J. Appl. Polym. Sci.*, **16**, 1295-1303, (1972)

10. Tanaguchi, Y. and Horigome, S., The states of water in cellulose acetate membranes, *J. Appl. Polym. Sci.*, **19**, 2743-2748, (1975)

11. Sterling, C. and Masuzawa, M., Gel water relationships in hydrophilic polymers: Nuclear magnetic resonance, *Makromol. Chem.*, **116**, 140-145, (1965)

12. Hoffman, A.S., Modell, M. and Pan. P., Polyacrylic desalination membranes I. Synthesis and characterisation, *J. Appl. Polym. Sci.*, **13**, 2223-2234, (1969)

13. Jadwin, T.A., Hoffman, A.S. and Vieth, W.R., Cross-linked poly(hydroxyethyl methacrylate) membranes for desalination by reverse osmosis, *J. Appl. Polym. Sci.*, **14**, 1339-1359, (1970)

14. Sarbolouki, M.N., Probing the state of absorbed water by diffusion technique, *J. Appl. Polym. Sci.*, **17**, 2407-2414, (1973)

15. Yasuda, H., Olf, H.G., Christ, B., Lamaze, C.E. and Peterlin, A., Movement of water in homogeneous water swollen polymers, in *Water Structure at the Water Polymer Interface*, Ed. Jellinek, H.H.G., Plenum, New York, N.Y., 39-55, (1975)

16. Dehl, R.E., Collagen: Mobile water content of frozen fibres, *Science*, **170**, 738-739, (1970)

17. Nelson, R.A., The determination of moisture transitions in cellulosic materials using differential scanning calorimetry, *J. Appl. Polym. Sci.*, **21**, 645-654, (1977)

18. Jhon, M.S. and Andrade, J.D., Water and Hydrogels, *J. Biomed. Mater. Res.*, 7, 509-552, (1973)

19. Miller, D.R. and Peppas, N.A., Bulk characterisation and scanning electron microscopy of hydrogels of P(VA-co-NVP), *Macromols.*, **20**, 1257-1265, (1987)

20. Sung, Y.K., Gregonis, D.E., Jhon, M.S. and Andrade, J.D., Thermal and pulse NMR analysis of water in poly(2-hydroxyethyl methacrylate), *J. Appl. Polym. Sci.*, **26**, 3719-3728, (1981)

21. Kim, E.H., Jeon, S.I., Yoon, S.C. and Jhon, M.S., The nature of water in tactic poly (2-hydroxyethyl methacrylate) hydrogels, *Bull. Korean Chem. Soc.*, **2**, 60-66, (1981)

22. Kim, E.H., Moon, B.Y., Jeon, S.I. and Jhon, M.S., The nature of water in copolymer hydrogels, *Bull. Korean Chem. Soc.*, **4**, 251-256, (1983)

23. Nakamura, K., Hatakeyama, T. and Hatakeyama, H., Studies on bound water of cellulose by differential scanning calorimetry, *Textile Res. J.*, **51**, 607-613, (1981)

24. Nakamura, K., Hatakeyama, T. and Hatakeyama, H., Relationship between hydrogen bonding and bound water in polyhydroxy styrene derivatives, *Polymer*, **24**, 871-876, (1983)

25. Hatakeyama, T., Yamauchi, A. and Hatakeyama, H., Studies on bound water in poly (vinyl alcohol) hydrogel by DSC and FT-NMR, *Eur. Polym. J.*, **20**, 61-64, (1984)

26. Higuchi, A. and Iijima, T., DSC investigations of the states of water in poly (vinyl alcohol) membranes, *Polymer*, **26**, 1207-1211, (1985)

27. Higuchi, A. and Iijima, T., DSC investigations of the states of water in poly (vinyl alcohol-co-itaconic acid) membranes, *Polymer*, **26**, 1833-1837, (1985)

28. Lee, H.B., Jhon, M.S. and Andrade, J.D., Nature of water in synthetic hydrogels I. Dilatometry, specific conductivity and differential scanning calorimetry of poly hydroxyethyl methacrylate, *J. Colloid Interface Sci.*, **51**, 225-231, (1975)

29. Aizawa, M. and Suzuki, S., Properties of water in macromolecular gels III. Dilatometric studies of the properties of water in macromolecular gels, *Bull. Chem. Soc. Japan*, **44**, 2967-2971, (1971)

30. Aizawa, M., Mizuguchi, J., Suzuki, S., Hagashi, S., Suzuki, T., Mitomo, N. and Toyama, H., Properties of water in macromolecular gels IV. Proton magnetic resonance studies of the properties of water in macromolecular gels, *Bull. Chem. Soc. Japan*, **45**, 3031-3034, (1972)

31. Magne, F.C., Portas, H.J. and Wakeham, H., A calorimetric investigation of the water in textile fibres, *J. Am. Chem. Soc.*, **69**, 1896-1902, (1947)

32. Watson, L.S., O'Neil, M.J., Justin, J. and Brenner, N., A differential scanning calorimeter for quantitative differential thermal analysis, *Analytical Chem.*, **36**, 1233-1238, (1964)

33. Tighe, B.J. and Trevett, A.S., The characterisation of mechanical properties of soft contact lenses, BCLA Annual Clinical Conference, Glasgow, May 1990, reprinted in *BCLA Transactions*, **13**(2), 57-61, (1990)

34. Adamson, A.W., Physical Chemistry of Surfaces, 3rd Edn., Wiley-Interscience, New York, N.Y., (1976)

35. Owens, D.K. and Wendt, R.C., Estimation of the surface free energy of polymers, *J. Appl. Polym. Sci.*, **13**, 1741-1747, (1969)

36. Hamilton, W.C., A technique for the characterisation of hydrophilic solid surfaces, *J. Colloid Interface Sci.*, **40**, 219-222, (1972)

37. Hamilton, W.C., Measurement of the polar force contribution to adhesive bonding, *J. Colloid Interface Sci.*, **47**, 672-675, (1974)

38. Bikerman, J.J., Physical Surfaces, Academic Press, London (1970)

39. Andrade. J.D., King, R.N. and Gregonis, D.E., Probing the hydrogel-water interface, in *Hydrogels for Medical and Related Applications*, Ed. Andrade, J.D., ACS Symp. Ser. No. 31, ACS, Washington D.C., 1-76, (1976)

40. Andrade. J.D., King, R.N., Gregonis, D.E. and Coleman, D.L., Surface characterisation of poly (hydroxyethyl methacrylate) and related polymers I. Contact angle methods in water, *J. Appl. Polym. Sci., Polym. Symp.*, **66**, 313-336, (1979)

41. Young, T., On the cohesion of fluids, *Phil. Trans. Roy. Soc. (London)*, **95**, 65-87, (1805)

42. Dupré, A., Théorie méchanique de la chaleur, Gauthier Villars, Paris, 369, (1869)

43. Bangham, D.H. and Razouk, R.I., Adsorption and the wettability of solid surfaces, *Trans. Faraday Soc.*, **33**, 1459-1463, (1937)

44. Melrose, J.C., Evidence for solid-fluid interfacial tensions from contact angles, in *Contact Angles, Wettability and Adhesion*, Ed. Zisman, W.A., Advances in Chemistry Series No. 43, A.C.S., Washington D.C., 158-179, (1964)

45. Girifalco, L.A. and Good, R.J., A theory for the estimation of surface and interfacial energies I. Derivation and application to interfacial tension, *J. Phys. Chem.*, **61**, 904-909, (1957)

46. Good, R.J., Girifalco, L.A. and Kraus, G., A theory for the estimation of surface and interfacial energies II. Application to surface thermodynamics of Teflon and graphite, *J. Phys. Chem.*, **62**, 1418-1421, (1958)

47. Good, R.J. and Girifalco, L.A., A theory for the estimation of surface and interfacial energies III. Estimation of surface energies of solids from contact angles, *J. Phys. Chem.*, **64**, 561-565, (1960)

48. Fowkes, F.M., Determination of interfacial tensions, contact angles and dispersion forces in surfaces by assuming the additivity of intermolecular interactions in surfaces, *J. Phys. Chem.*, **66**, 382, (1962)

49. Kaelble, D.H., Dispersion-polar surface tension properties of organic solids, *J. Adhesion*, **2**, 66-81, (1970)

50. Panzer, J., Components of solid surface free energy from wetting measurements, *J. Colloid Interface Sci.*, **44**, 142-161, (1973)

51. Corkhill, P.H., Novel hydrogel polymers, Ph.D. thesis, Aston University, (1988)

52. Baker, D.A., Corkhill, P.H., Ng, C.O., Skelly, P.J. and Tighe, B.J., Synthetic hydrogels II: Copolymers of carboxyl, lactam and amide-containing monomers: Structure property relationships, *Polymer*, **29**, 691-700, (1988)

53. Barnes, A., Corkhill, P.H. and Tighe, B.J., Synthetic hydrogels: 3. Hydroxyalkyl acrylate and methacrylate copolymers - surface and mechanical properties, *Polymer*, **29**, 2191-2202, (1988)

54. Sariri, R., Tear protein interaction with hydrogel contact lenses, Ph.D. thesis, Aston University, (1995)

55. Sariri, R., Evans, K. and Tighe, B.J., Protein mobility and activity in hydrogel polymers, *Poster presented at 11th European Conference on Biomaterials*, Pisa, September (1994)

56. Baier, R.E., Dutton, R.C. and Gott, V.L., Surface chemical features of blood vessels walls and of synthetic materials exhibiting thromboresistance, in *Advances in Experimental Medicine*, **Vol 7**, Surface chemistry of biological surfaces, Plenum Press, New York, N.Y., 235-260, (1970)

57. Andrade, J.D., Interfacial phenomena and biomaterials, *Medical Instrumentation*, 7, 110-120, (1973)

58. Ratner. B.D., Hoffman, A.S., Hanson, S.R., Harker, S.R. and Whiffen, J.D., Blood compatibility-water content relationships for radiation grafted hydrogels, *J. Polym. Sci., Polym. Symp.*, **66**, 363-375, (1979)

59. Okano, T., Nishiyama, S., Shinohara, I., Akaike, T. and Sakurai, Y., Interaction between plasma protein and microphase separated structure of copolymers, *Polymer J. (Tokyo)*, **10**, 223-228, (1978)

60. Bowers, R.W.J. and Tighe, B.J., Studies of the ocular compatibility of hydrogels. A review of the clinical manifestations of spoilation, *Biomaterials*, **8**, 83-88, (1987)

61. Horbett, T.A., Protein adsorption on biomaterials, in *Biomaterials: Interfacial Phenomena and Applications*, Eds. Cooper, C.L. and Peppas, N.A., A.C.S. Symposium Series No. 199, A.C.S., Washington D.C., 233-244, (1982)

62. Horbett, T.A., Protein adsorption to hydrogels, in *Hydrogels in Medicine and Pharmacy*, **Vol. I**, Fundamentals, Ed. Peppas, N.A., C.R.C. Press, Boca Raton, Florida, 127-171, (1986)

63. Baker, D. and Tighe, B.J., Polymers in contact lens applications (VIII). The problem of biocompatibility, *Contact Lens J.*, **10**(3), 3-14, (1981)

64. Ashraf, N., Sequence distribution in free radical polymerisations, Ph.D. thesis, Aston University, (1995)

65. Ma, J.J., Franklin, V.J., Tonge, S.R. and Tighe, B.J., Ocular compatibility of biomimetic hydrogels, *Poster presented at BCLA 9th Annual Clinical Conference*, Torquay, May (1994)

66. Odian, G.G., Principles of polymerisation, 3rd edition, John Wiley & Sons, New York, N.Y., (1991)

67. Cowie, J.M.G., Alternating copolymers, Plenum press, New York, N.Y., (1985)

68. Mayo, F.R. and Lewis, F.M., Copolymerisation. I: A basis for comparing the behaviour of monomers in copolymerisation; The copolymerisation of styrene and methyl methacrylate, *J. Am. Chem. Soc.*, **66**, 1594-1601, (1944)

69. Alfrey, T. and Goldfinger, G., The mechanism of copolymerisation, *J. Chem. Phys.*, **12**, 205-209, (1944)

70. Billmeyer, F.W., Textbook of polymer science, 2nd edition, John Wiley & Sons, New York, N.Y., (1981)

71. Hammersley, J.M. and Handscomb, D.C., Monte Carlo methods, Methuen, London, (1964)

72. Rubinstein, R.Y., Simulation and the Monte Carlo method, John Wiley & Sons, New York, N.Y., (1981)

73. Alfrey, T. and Price, C.C., Relative reactivities in vinyl copolymerisation, *J. Polym. Sci.*, **2**, 101-106, (1947)

74. Varma, I.K. and Patnaik, S., Copolymerisation of 2-hydroxyethyl methacrylate with alkyl acrylate, *Eur. Polym. J.*, **12**, 259-261, (1976)

75. Tighe, B.J., Hydrogels as contact lens materials, in *Hydrogels in Medicine and Pharmacy*, **Vol III**, Properties and Applications, Ed. Peppas, N.A., CRC Press, Boca-Raton, Florida, 53-82, (1987)

76. Roorda, W.E., Boddé, H.E., de Boer, A.G. and Junginger, H.E., Synthetic hydrogels as drug delivery systems, *Pharm.Weekl. (Sci.)*, **8**, 165-189, (1986)

77. Levowitz, B.S., La Guerre, J.N., Calem, W.S., Gould, F.E., Scherrer, J. and Schoenfeld, H., Biologic compatibility and applications of Hydron, *Trans. Amer. Soc. Artif. Organs*, **14**, 82-87, (1968)

78. Ratner, B.D. and Hoffman, A.S., Synthetic hydrogels for biomedical applications, in *Hydrogels for Medical and Related Applications*, Ed. Andrade, J.D., ACS Symp. Ser. No. 31, ACS, Washington D.C., 1-36, (1976)

79. Wichterle, O., Hydrogels, in *Encyclopaedia of Polymer Science and Technology*, **Vol. 15**, Eds. Mark, H. and Gaylord, N., Interscience, New York, N.Y., 273-291, (1971)

80. Tighe, B.J., Biomedical applications of polymers, in *Macromolecular Chemistry*, Eds. Jenkins, A.D. and Kennedy, J.F., *Specialist Periodical Reports*, **No.17**, London: The Chemical Society, **1**, 416-428, (1980)

81. Tighe, B.J., Biomedical applications of polymers, in *Macromolecular Chemistry*, Eds. Jenkins, A.D. and Kennedy, J.F., *Specialist Periodical Reports*, **No.18**, London: The Chemical Society, **2**, 347-360, (1982)

82. Tighe, B.J., Biomedical applications of polymers, in *Macromolecular Chemistry*, Eds. Jenkins, A.D. and Kennedy, J.F., *Specialist Periodical Reports*, **No.19**, London: The Chemical Society, **3**, 375-386, (1984)

83. Ratner, B.D., Biomedical applications of hydrogels, a review and critical appraisal, in *Biocompatibility of Clinical Implant Materials*, **Vol 2**, Ed. Williams, D.F., CRC Press, Boca Raton, Florida, 145-175, (1981)

84. Pedley, D.G., Skelly, P.J. and Tighe, B.J., Hydrogels in biomedical applications, *Br. Polym. J.*, **12**, 99-110, (1980)

85. Singh, M.P., Hydron in the right atrium, *Biomed. Eng.*, **4**, 68-69, (1969)

86. Kocvara, S., Kliment, K., Kubat, J., Stol, M. and Ott, Z., Gel-fabric prostheses of the ureter, *J. Biomed. Mater. Res.*, **1**, 325-336, (1967)

87. Refojo, M.,F., A critical review of the properties and applications of soft hydrogel contact lenses, *Survey Ophthal.*, **16**(4), 233-246, (1972)

88. Refojo, M.F., Artificial membranes for corneal surgery, *J. Biomed. Mater. Res.*, **3**, 333-347, (1969)

89. Park, G.B., Burn wound coverings - A review, *Biomat. Med. Dev. Art. Org.*, **6**(1), 1-35, (1978)

90. Corkhill, P.H., Hamilton, C.J. and Tighe, B.J., Synthetic hydrogels VI: Hydrogel composites as wound dressing and implant materials, *Biomaterials*, **10**, 3-10, (1989)

91. Corkhill, P.H., Trevett A.S. and Tighe, B.J., The potential of hydrogels as synthetic articular cartilage, UK Conference 'New engineering concepts and alternative materials for prosthesis', Leeds, 1990, reprinted in *Proc. Inst. Mech. Engrs.*, **204**, 147-155, (1990)

92. Bray, J.C. and Merrell, E.W., Poly(vinyl alcohol) hydrogels for synthetic articular cartilage, *J. Biomed. Mat. Res.*, 7, 431-433, (1973)

93. Shahgaldi, B., Amis, A., Wheatley, F., McDowell, J. and Bentley, G., Repair of cartilage lesions using biological implants, *J. Bone and Joint Surgery*, **73-B**, 1, (1991)

94. Murakami, T., The lubrication in natural synovial joints and prostheses, *JSME Int. J.*, Series III, **33**(1), 465-474, (1990)

95. Noguchi, T., Yamamuro, T., Oka, M., Kumar, P., Kotoura, Y., Hyon, S. and Ikada, Y., Poly(vinyl alcohol) hydrogel as an artificial articular cartilage: Evaluation of biocompatibility, *J. Appl. Biomat.*, **2**, 101-107, (1991)

96. Curd, F.H.S. and Rose, F.L., Synthetic antimalarials. X. Some aryl-diguanide derivatives, *Journal of Chemical Society*, 729-737, (1946)

97. Rose, F.L. and Swain, G., Bisbiguanides having antibacterial activity, *Journal of Chemical Society*, 4422-4425, (1956)

98. Franklin, T. J. and Snow, G. A., Antiseptics, Antibiotics and the cell membrane, in *Biochemistry of Antimicrobial Action*, Chapman and Hall, London, 58-78, (1981)

99. Hugo, W.B. and Longworth, A.R., Some aspects of the mode of action of chlorhexidine, *J. Pharm. Pharmacol.*, **16**, 655-662, (1964)

100. Hugo, W.B. and Longworth, A.R., The effect of chlorhexidine on the electrophoretic mobility, cytoplasmic constituents, dehydrogenase activity and cell walls of E. coli and S. aureus, *J. Pharm. Pharmacol.*, **18**, 569-578, (1966)

101. Verlander, M.S., Veuter, J.C., Goodman, M., Kaplan, N.O. and Saks, B., Biological activity of catecholamines covalently linked to synthetic polymers. Proof of immobilising drug theory, *Proceedings of the National Academy of Sciences USA*, **73**, 1009-1013, (1976)

102. Vogl, O. and Tirrel, D., Functional polymers with biologically active groups, *J. Macromol. Sci; Chem.*, **A13**, 415-439, (1979)

103. Davies, A. and Field, B.S., Action of biguanides, phenols and detergents on E. coli and its spheroplasts, *J. Appl. Bact.*, **32**, 233-243, (1969)

104. Davies, A., Bentley, M. and Field, B.S., Comparison of the action of Vantocil, cetrimide and chlorhexidine on E. coli and its spheroplasts and the protoplasts of gram negative bacteria, *J. Appl. Bact.*, **31**, 448-461, (1968)

105. Gilbert, P., Broxton, P. and Woodstock, P.M., A study of the antibacterial activity of some polyhexamethylene biguanides towards E. coli, *J. Appl. Bact.*, **54**, 345-353, (1983)

106. Ikeda, T., Ledwith, A., Bamford, C.H. and Hann, R.A., Interaction of a polymeric biguanide biocide with phospholipid membranes, *Biochimica and Biophysica Acta*, **769**, 57-66, (1984)

107. Ikeda, T., Yamaguchi, H. and Tazuke, S., New polymeric biocides: Synthesis and antibacterial activities of polycations with pendant biguanide groups, *Antimicrobial Agents and Chemotherapy*, **26**(2), 139-144, (1984)

108. Rembaum, A., Biological activity of ionene polymers, *Applied Polymer Symposium*, **22**, 299-317, (1973)

109. Katchalsky, A., *Biophys. J.*, **4**, 9-41, (1964)

110. Kawabata, N. and Nishiguchi, M., Antibacterial activity of soluble pyridinium-type polymers, *Applied and Environmental Microbiology*, **Oct**., 2532-2535, (1988)

111. Ikeda, T. Suzuki, Y. and Tazuke, S., Biologically active polycations. 4. Synthesis and antimicrobial activity of poly(trialkylvinylbenzyl ammonium chloride)s, *Makromol. Chem*., **185**, 869-876, (1984)

112. Messinger, P. and Schimpke-Meier, A., Polymers with antimicrobial groups - synthesis and activity, *Arch. Pharm*., **321**, 89-92, (1988)

113. Ikeda, T., Yamaguchi, H. and Tazuke, S., Molecular weight dependence of antibacterial activity in cationic disinfectants, *Journal of Bioactive and Compatible Polymers*, **5**, 31-41, (1990)

114. Kanazawa, A., Ikeda, T. and Endo, T., Novel cationic biocides: Synthesis and anti bacterial activity of polymeric phosphonium salts, *Journal of Polymer Science: Part A: Polymer Chemistry*, **31**, 335-343, (1993)

115. Allcock, H.R., Pucher, S.R., Fitzpatrick, R.J. and Rshid, K., Antibacterial activity and mutagenicity studies of water-soluble phosphazene high polymers, *Biomaterials*, **13**(12), 857-862, (1992)

116. Ferruti, P., Marchisio, M.A. and Barbucci, R., Synthesis, physico-chemical properties and biomedical applications of poly(amido-amines)s, *Polymer*, **26**, 1336-1348, (1985)

117. Ferruti, P., Ranucci, E. and Neri, M., *Journal of Bioactive and Compatible Polymers*, **4**, 403, (1989)

118. Ferruti, P. and Ranucci, E., New functional polymers for medical applications, *Polymer Journal*, **23**(5), 541-550, (1991)

119. Ikeda, T. Suzuki, Y. and Watanabe, M., Interaction of biologically active molecules with phospholipid membranes. 1. Fluorescence depolarisation studies on the effect of polymeric biocides bearing biguanide groups in the main chain, *Biochimica and Biophysica Acta*, **735**, 380-386, (1983)

120. Lehninger, A.L., Biochemistry, Second Edition, Worth Publishers, Inc., (1975)

121. Fowkes, F.M., Additivity of intermolecular forces at interfaces I. Determination of the contribution to surface and interfacial tensions of dispersion forces in various liquids, *J. Phys. Chem*., **67**, 2538-2541, (1963)

122. Tamai, Y., Makuuchi, K. and Suzuki, M., Experimental analysis of interfacial forces at the plane surface of solids, *J. Phys. Chem*., **71**, 4176-4179, (1967)

123. Yocum, R.H. and Nyquist, E.B., (Eds), Functional Monomers, Vols 1&2, Marcel Dekker, New York, N.Y., (1973)

124. Fushimi, H., Ando, I. and Iijima, T., States of water in cationically charged poly(vinyl alcohol) membranes, *Polymer*, **32**(2), 241-248, (1991)

125. Brandrup, J. and Immergut, Polymer Handbook, Interscience Publishers, New York, N.Y., (1967)

126. Nagai, K., Fujii, I. and Kuramoto, N., Polymerisation of surface-active monomers 4. Copolymerisation of long chain alkyl salts of 2-dimethylaminoethyl methacrylate with methyl methacrylate or styrene, *Polymer*, **33**(14), 3060-3065, (1992)

127. Topping, C., Comparison of mechanical properties and correlation with structure of hydrogels made using acryloyl morpholine and N-vinyl pyrrolidone, Final Year Project submitted for the Degree of B.Sc.(Hons) Chemistry, Aston University, (1994)

128. Greenley, R.Z., Determination of Q and e values by a least squares technique, *J. Macromal. Sci. Chem.*, **A9**, 505-516, (1975)

129. Lai, Q., Protein and cell adhesion to block polymer microdomains, Conference proceedings, *Fourth World Biomaterials Congress*, Berlin, 450, (1992)

130. Minoura, N., Aiba, S., Fujiwara, Y. and Koshisaki, N., Interactions of culture cells with membranes composed of random and block copolypeptides, *J. Biomed. Mater. Res.*, **2**(2), 139-146, (1989)

131. Ma, J.J., Novel hydrogel polymers, Ph.D. thesis, Aston University, (1996)

132. Corkhill, P.H., Jolly, A.M., Ng C.O. and Tighe B.J., Synthetic hydrogels: 1. Hydroxyalkyl acrylate and methacrylate copolymers - water binding studies, *Polymer*, **28**, 1758-1766, (1987)

133. Atherton, N.D., Drug/water interactions in hydrogel matrices, Ph.D. thesis, Aston University, (1982)

134. Pedley D.G. and Tighe, B.J., Water binding properties of hydrogel polymers for reverse osmosis and related applications *Brit. Polym. J.*, **11**, 130-136, (1979)

135. Tighe, B.J., The design of polymers for contact lens applications, *Brit. Polym, J.*, **8**, 71-77, (1976)

136. Raab, M. and Janacek, J., Effect of chemical cross-links on the ultimate tensile properties of water swollen poly (2-hydroxyethyl methacrylate), *Int. J. Polymeric. Mater.*, **1**, 147-156, (1972)

137. Kolaarik, J. and Migliaresi, C., Mechanical properties of hydrophilic copolymers of 2-hydroxyethyl methacrylate with ethyl acrylate, n-butyl acrylate and dodecyl methacrylate, *J. Biomed. Mater. Res.*, **17**, 757-767, (1983)

138. Hosaka, S., Yamada, A., Tanazawa, H., Momose, T., Magatani, H. and Nakajima, A., Mechanical properties of the soft contact lens of poly (methyl methacrylate-N-vinyl pyrrolidone), *J. Biomed. Mater. Res.*, **4**, 557-566, (1980)

139. Coleman, D.L., Gregonis, D.E. and Andrade, J.D., Blood-materials interactions: The minimum interfacial free energy and the optimum polar / apolar ratio hypothesis, *J. Biomed. Mater. Res.*, **16**, 381-391, (1982)

140. Oxley, H.R., Hydrogel polymers containing linear and cyclic polyethers, Ph.D. thesis, Aston University, (1990)

141. Lydon, F.J., Novel hydrogel copolymers and semi-interpenetrating polymer networks, Ph.D. thesis, Aston University, (1996)

142. Castillo, E.J., Koenig, J.L., Anderson, J.M. and Lo, J., Characterisation of protein adsorption on soft contact lenses I. Conformational changes of adsorbed serum albumin, *Biomaterials*, **5**, 319-325, (1984)

143. Hosaka, S., Ozawa, H., Tanzawa, H., Ishida, H., Yoshimura, K., Momose, T., Magatani, H. and Nakajima, A., Analysis of biomaterials deposited on high water content contact lenses, *J. Biomed. Mater. Res.*, **17**, 261-274, (1983)

144. Castillo, E.J., Koenig, J.L., Anderson, J.M. and Lo, J., Protein adsorption of hydrogels II. Reversible and irreversible interactions between lysozyme and soft contact lens surfaces, *Biomaterials*, **6**, 338-344, (1985)

145. Franklin, V.J., Lipoidal species in ocular spoilation processes, Ph.D. thesis, Aston University, (1990)

146. Bright, A.M. and Tighe, B.J., The composition and interfacial properties of tears, *Journal of British Contact Lens Association*, **16**, 57-66, (1993)

147. Bright, A.M., Towards an improved ocular drug delivery system, Ph.D. thesis, Aston University, (1992)

148. Wall, C.A., A study of polycationic disinfectant absorption into the polymer matrix of a contact lens, Final Year Project submitted for the Degree of B.Sc.(Hons) Chemistry, Aston University, (1995)

149. Leonard F, *Trans. Amer. Soc. Artific. Int. Organs*, **15**, 15, (1969)

150. Halpern B.D., Cheng H., Kuo S. and Greenberg H., in *Artificial Heart Program Conference Proceedings*, Ed. Hegyeli R.J., U.S. Government Printing Office, Washington D.C., 87, (1969)

151. Walter C.W., Murphy W.P., Jessiman A.G. and Ahara R.M., *Surgical Forum*, **2**, 289, (1951)

152. Dart, J.K.G., Stapleton, F. and Minassian, D., Contact lenses and other risk factors in microbial keratitis, *Lancet*, **338**, 650-653, (1991)

153. Laibson, P.R. and Donnenfield, E.D., Corneal ulcers related to contact lens use, *Int. Ophthalmol. Clin.*, **26**(1), 3-14, (1986)

154. Schein, O.D., Ormerod, L.D., Barraquer, E., Alfonso, E., Egan, K.M., Paton, M.T. and Kenyon, K.R., Microbiology of contact lens-related keratitis, *Cornea*, **8**(4), 281-285, (1989)

155. Mayo, D.S., Schlitzer, R.L., Ward, M.A., Wilson, L.A. and Ahern, D.G., Association of *Pseudomonas* and *Serratia* corneal ulcers with the use of contaminated solutions, *J. Clin. Microbiol.*, **25**(8), 1398-1400, (1987)

156. Costerton, J.W. and Irvin, R.T., The bacterial glycocalyx in nature and disease, *Ann. Rev. Microbiol.*, **35**, 299-324, (1981)

157. LeChevallier, M.W., Cawthorn, C.D. and Lee, R.G., Inactivation of biofilm bacteria, *Appl. Env. Microbiol.*, **54**(10), 2492-2499, (1988)

158. Anwar, H., Dasgupta, M.K. and Costerton, J.W., Testing the susceptibility of bacteria in biofilms to antibacterial agents, *Antimicrob. Agents Chemother.*, **34**(ii), 2043-2046, (1990)

159. McCulloch, R.R., Torres, J.G., Wilhelmus, K.R. and Osato, M.S., Biofilm on contaminated hydrogel contact lenses protects adherent *Pseudomonas aeruginosa* from antibacterial therapy, ARVO abstracts., *Invest. Ophthalmol. Visual Sci.*, **11**(suppl.), 279, (1988)

160. Dickenson, G.M. and Bisno, A.L., Infections associated with indwelling devices: concepts of pathogenesis; infections associated with intravascular devices, *Antimicrob. Agents Chemother.*, **33**, 597-601, (1989)

161. Peters, G., Staphylococcal 'plastic' foreign body infections - evidence and pathogenesis, in *The Staphylococci*, Ed. Jeljaszewicz, J., Gustav Fisher, Verlag, Stuttgart, (1984)

162. Dougherty, S.H. *Staphylococcus epidermidis* - a versatile pathogen, in *Pathogenesis of wound and Biomaterial - Associated Infections*, Eds. Wadstrom, T., Eliasson, I., Holder, I., Ljungh, A., Springer - Verlag, London, 310-315, (1990)

163. Elliott, T.S.J., Intravascular-device infections, *J. Med. Microbiol.*, **27**, 161-167, (1988)

164. Elliott, T.S.J., D'Abrera, V.C.and Dutton, S., The effect of antibiotics on bacterial colonisation of vascular cannulae in a novel *in-vitro* model, *J. Med. Microbiol.*, **26**, 229-235, (1988)

165. Henry, R., Harvey, R.A. and Greco, R.S., Antibiotic bonding to vascular prostheses, *J. Thorac. Cardiovasc. Asc. Surg.*, **82**, 272-277, (1981)

166. Sherentz, R.J., Forman, D.M. and Solomon, D.D., Efficiency of dicloxacillin-coated polyurethane catheters in preventing subcutaneous *S. aureus* infection in mice, *Antimicrob. Agents Chemother.*, **33**, 1174-1178, (1989)

167. Crocker, I.C., Liu, W.K., Byrne, P.O. and Elliott T.S.J., A novel electrical method for the prevention of microbial colonisation of intravascular cannulae, *J. Hosp. Infect.*, **22**, 7-17, (1992)

168. Graham, N.B., Polymeric inserts and implants for the controlled release of drugs, *Brit. Polym. J.*, **10**, 260, (1978)

169. Tanquary, A.C. and Lacey, R.E., Eds., Controlled release of biologically active agents, in *Advances in Experimental Medicine and Biology*, Plenum Press, New York, N.Y., (1974)

170. Graham, N.B. and Wood, D.A., Hydrogels and biodegradable polymers for the controlled delivery of drugs, *Polym. News*, **8**, 230, (1982)

171. Samour, M.C., Polymeric drugs, *CHEMTECH*, **Aug.**, 494-501, (1978)

172. Fessenden, R.J. and Fessenden, J.S., Organic Chemistry, Brooks-Cole, California, (1986)

173. Morgan, P.W., Comments on the status and future of interfacial polycondensation, *J. Macromol. Sci. - Chem.*, **A15**(5), 683-699, (1981)

174. Hill, H.W., Kwolek, S.L. and Morgan, P.W., French Patent, 1,199,460 (1959) and U.S. Patent, 3,006,899 (1961)

175. Morgan, P.W., Condensation polymers by interfacial and solution methods, Interscience, New York, N.Y., 99-101, 191-192, 492-493, (1965)

176. Morgan, P.W., Kwolek, S.L. and Hill, H.W., Synthesis of condensation polymers by interfacial polymerisation in systems with high phase miscibility, *presented at the National ACS meeting*, Dallas, TX, April (1973)

177. Sutton, R.C., Thai, L., Hewitt, J.M., Voycheck, C.L. and Tan, J.S., Microdomain characterisation of styrene-imidazole copolymers, *Macromolecules*, **21**, 2432-2439, (1988)

178. Serniuk, G.E., Thomas, R. and Thomas, R.M., U.S. Patent, 3,183,217, (1965)

179. Imoto, M., Otsu, T. and Harada, Y., Vinyl polymerisation. LXVIII. The polymerisation of methyl methacrylate in the presence of zinc chloride, *Makromol. Chem.*, **65**, 180-193, (1963)

180. Gaylord, N.G. and Takahashi, A., Free-radical polymerisation of complexed monomers. I. Mechanism of metal halide activation, *J. Polym. Sci., Polymer Letters*, **6**, 743-747, (1968)

181. Gaylord, N.G. and Takahashi, A., Donor-acceptor molecular complexes in alternating copolymerisation and in the polymerisation of metal halide-complexed vinyl monomers, *Advan. Chem. Ser.*, **91**, 94-124, (1969)

182. First Intl. Conf. on Gold and Silver in Med., Bethseda, Md., (1987)

183. Spadero, J.A., Chase, S.E. and Webster, D.A., *J. Biomed. Mat. Res.*, **20**, (1986)

184. Sawyer, P.N., Ogonick, J.C. and Boddy, P.J., *Surgery*, **61**, (1967)

185. Clement, J.L. and Jarrett, P.S., Antibacterial silver, *Metal-Based Drugs*, **1**(5-6), 467-481, (1994)

186. Beard, R.B., DeLaurent, M., Pourrezaei, K. and Adrian, S., Stimulation, recording potential and antimicrobial medical catheter coatings, *Metal-Based Drugs*, **1**(5-6), 445-458, (1994)

187. Morgan, P.W. and Kwolek, S.L., *J. Chem. Ed.*, **36**, 182, (1959)

188. Rushton, J.H., Stirring in organic chemical synthesis, in *Interfacial Synthesis*, **Vol.1**, Ed. Millich, F. and Carraher, C.E., Dekker, New York, N.Y., 9-36, (1977)

189. Tebbs, S., Private communication

190. Drain, D.J. and Simmonite, D., Opthalmic compositions and contact lens disinfecting compositions, U.K. Patent, 1,432,348, (1976)

191. Ogunbiyi, L., Smith, F.X. and Riedhammer, T.M., Disinfecting and preserving systems and methods of use, U.S. Patent, 4,758,595, (1988)

192. Ogunbiyi, L., Smith, F.X. and Riedhammer, T.M., Disinfecting and preserving systems and methods of use, U.S. Patent, 4,836,986, (1989)

APPENDIX 1

Sequence Distributions of Hydrogel Polymers

1. Computer simulated sequence distribution of a HEMA-NVI 95:5 copolymer

95% of Monomer A, HEMA

5% of Monomer B, NVI

r(AB) = 18.12 r(BA) = 0.05

Polymerised to 100% conversion

In the simulated copolymer HEMA is represented by O and NVI is represented by ●:

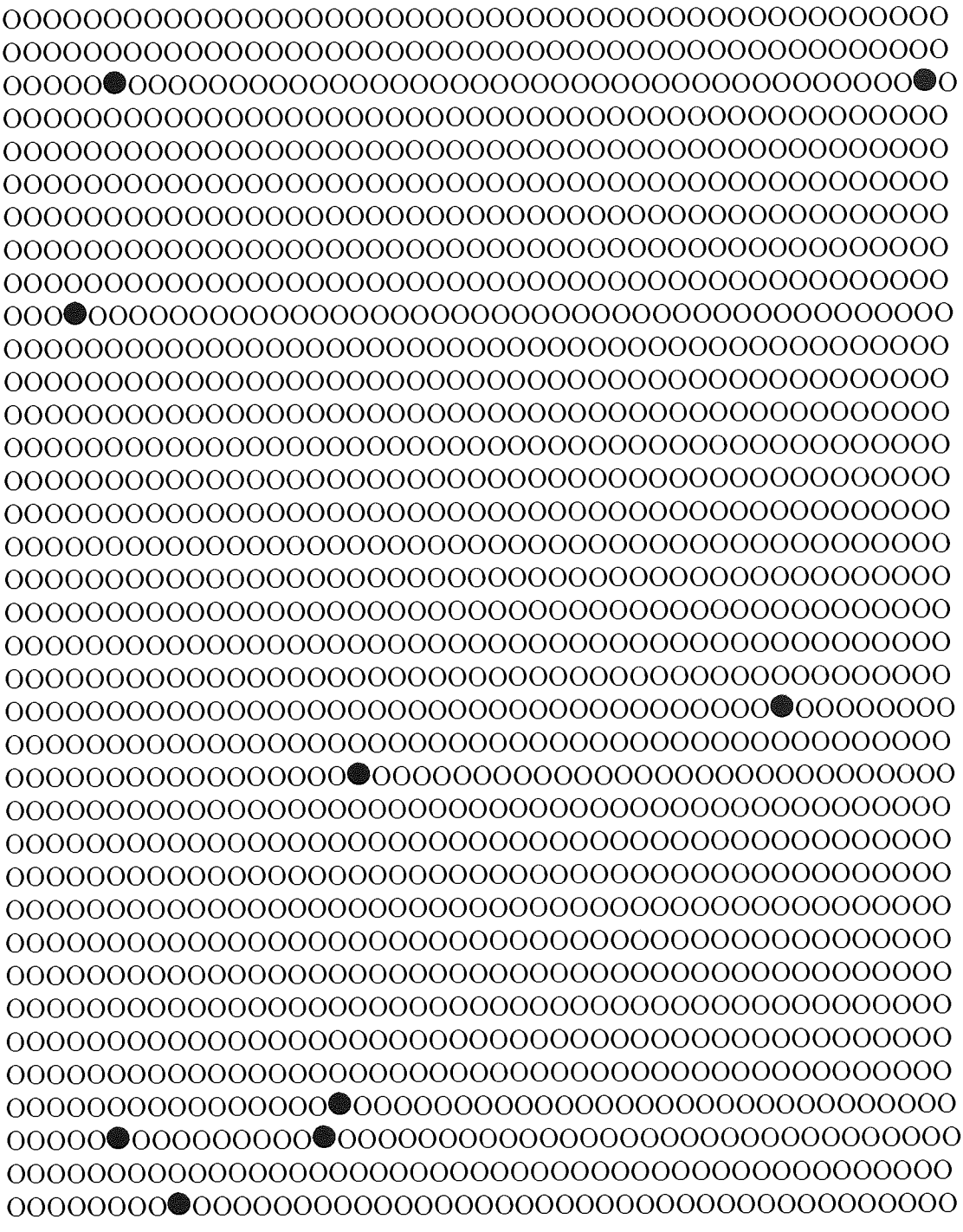

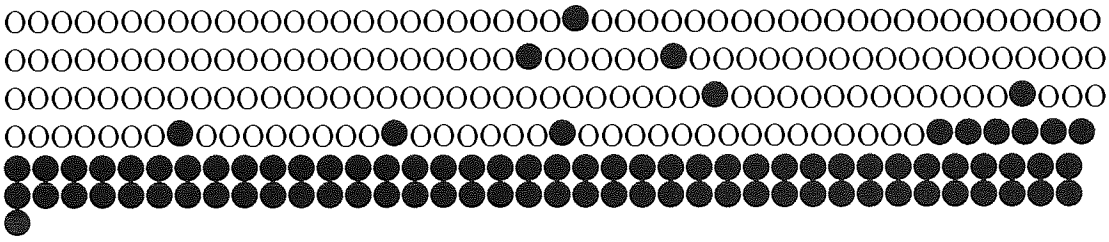

The simulated copolymer contains 1900 HEMA units and 100 NVI unit

Sequence Distributions:

Length	HEMA	NVI	Length	HEMA	NVI
1	0	17	43	1	0
5	1	0	48	1	0
6	1	0	62	1	0
8	1	0	72	1	0
9	1	0	83	0	1
10	1	0	86	1	0
12	1	0	99	1	0
15	1	0	285	1	0
35	1	0	469	1	0
39	1	0	597	1	0

2. Computer simulated sequence distribution of a HEMA-NVI 80:20 copolymer

80% of Monomer A, HEMA

20% of Monomer B, NVI

r(AB) = 18.12 r(BA) = 0.05

Polymerised to 100% conversion

In the simulated copolymer HEMA is represented by O and NVI is represented by ●:

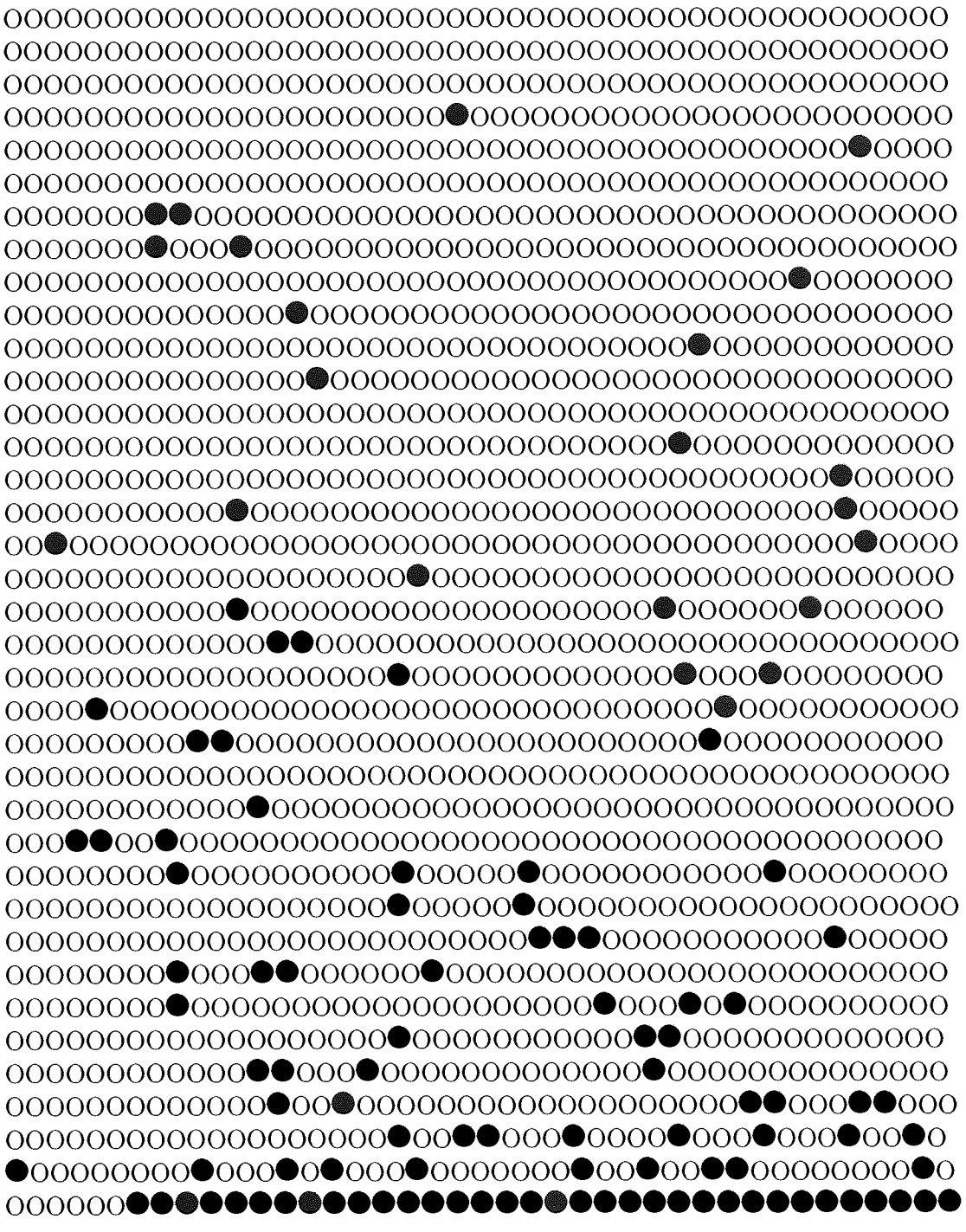

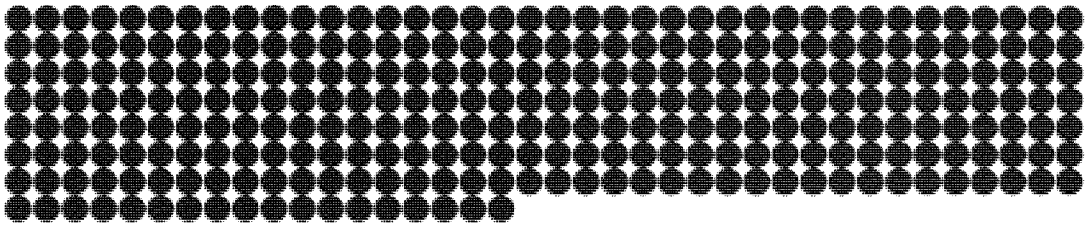

The simulated copolymer contains 1600 HEMA units and 400 NVI unit

Sequence Distributions:

Length	HEMA	NVI	Length	HEMA	NVI
1	3	58	25	1	0
2	6	11	27	3	0
3	11	1	29	2	0
4	1	0	30	1	0
5	2	0	33	1	0
6	2	0	37	2	0
7	3	0	39	1	0
8	2	0	45	1	0
10	1	0	46	1	0
11	3	0	47	1	0
12	1	0	51	1	0
13	3	0	54	1	0
16	1	0	58	1	0
19	2	0	66	2	0
20	3	0	70	1	0
21	1	0	74	1	0
22	1	0	111	1	0
23	1	0	163	1	0
24	1	0	317	0	1

3. Computer simulated sequence distribution of a HEMA-DMAEMA 95:5 copolymer

95% of Monomer A, HEMA

5% of Monomer B, DMAEMA

r(AB) = 1.86 r(BA) = 0.25

Polymerised to 100% conversion

In the simulated copolymer HEMA is represented by O and DMAEMA is represented by ●:

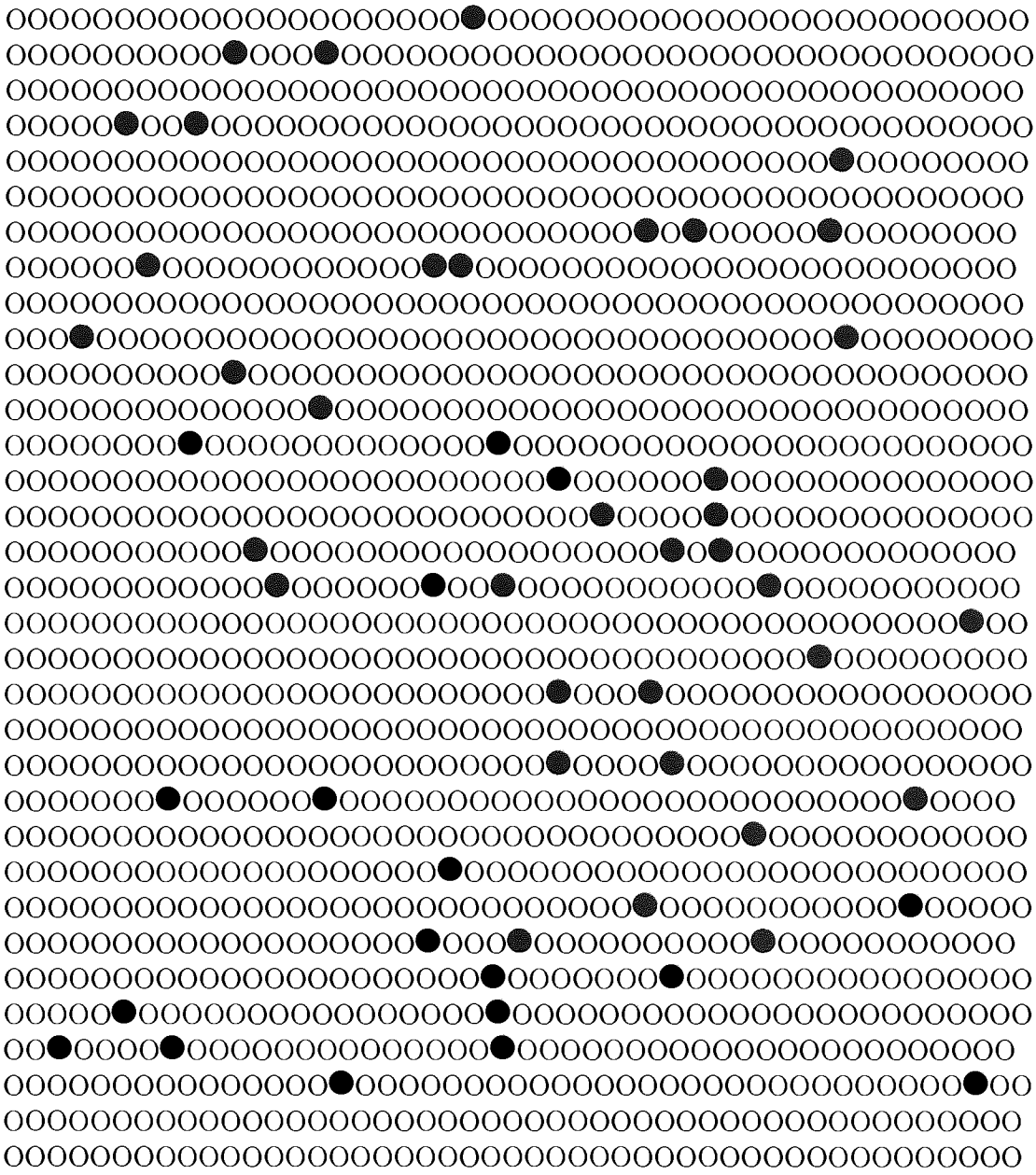

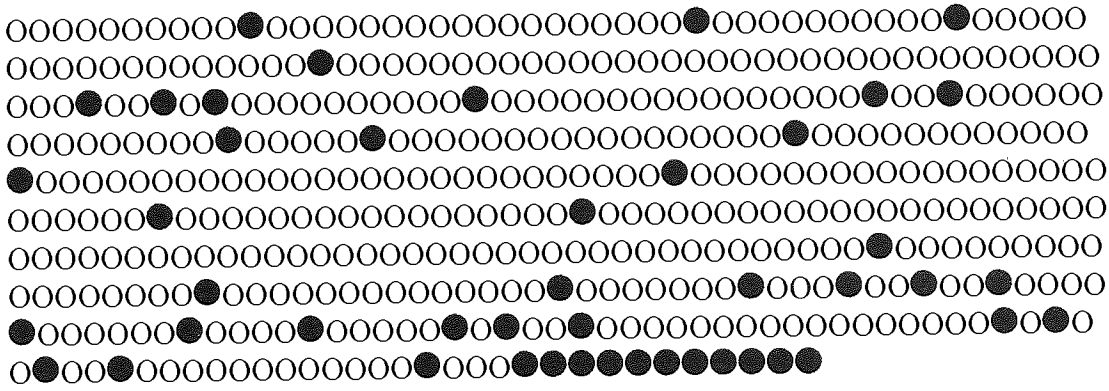

The simulated copolymer contains 1900 HEMA units and 100 DMAEMA units

Sequence Distributions:

Length	HEMA	DMAEMA	Length	HEMA	DMAEMA
1	5	87	26	2	0
2	9	1	27	1	0
3	5	0	28	1	0
4	5	0	32	1	0
5	3	0	33	2	0
6	4	0	34	1	0
7	2	0	35	1	0
10	3	0	36	1	0
11	2	1	38	2	0
12	3	0	39	1	0
13	1	0	40	1	0
14	3	0	41	1	0
15	1	0	49	2	0
16	2	0	55	2	0
17	4	0	59	1	0
18	4	0	75	1	0
21	1	0	76	1	0
22	1	0	84	1	0
23	1	0	89	1	0
24	2	0	92	1	0
25	2	0	106	1	0

4. Computer simulated sequence distribution of a HEMA-DMAEMA 80:20 copolymer

80% of Monomer A, HEMA

20% of Monomer B, DMAEMA

r(AB) = 1.86 r(BA) = 0.25

Polymerised to 100% conversion

In the simulated copolymer HEMA is represented by O and DMAEMA is represented by ●:

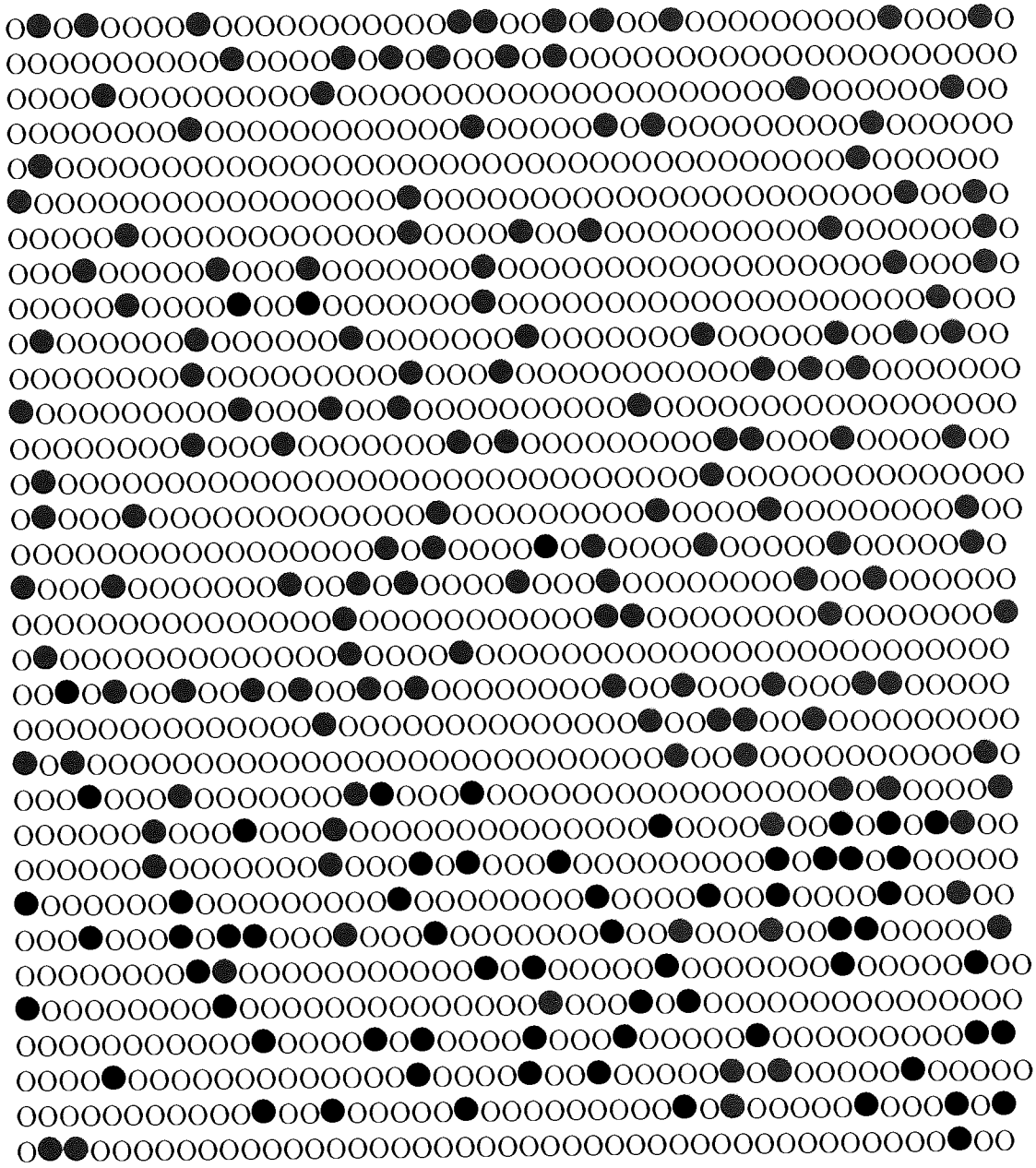

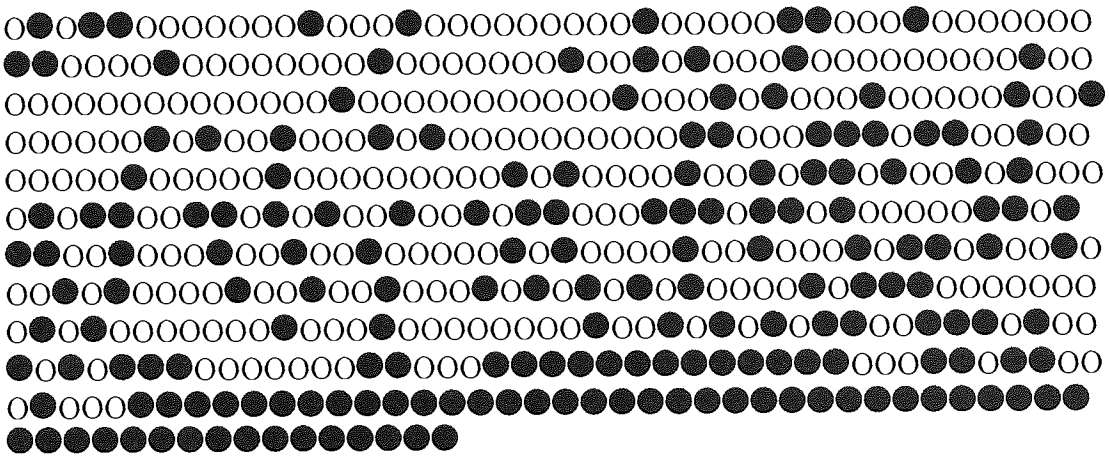

The simulated copolymer contains 1600 HEMA units and 400 DMAEMA units

Sequence Distributions:

Length	HEMA	DMAEMA	Length	HEMA	DMAEMA
1	68	261	16	3	0
2	44	29	17	1	0
3	44	6	18	1	0
4	27	0	19	2	0
5	20	0	20	1	0
6	10	0	21	2	0
7	19	0	22	1	0
8	11	0	25	2	0
9	15	0	26	1	0
10	6	0	27	2	0
11	6	0	30	1	0
12	2	0	37	1	0
13	3	1	40	1	0
14	3	0	50	0	1
15	1	0			

5. Computer simulated sequence distribution of a NNDMA-CHMA-NVI 72:18:10 terpolymer

72% of Monomer A, NNDMA

18% of Monomer B, CHMA

10% of Monomer C, NVI

r(AB) = 0.4 r(AC) = 4.16 r(BA) = 1.73

r(BC) = 5.58 r(CA) = 0.2 r(CB) = 0.06

Polymerised to 100% conversion

In the simulated copolymer NNDMA is represented by O, CHMA is represented by ⊙ and NVI is represented by ●:

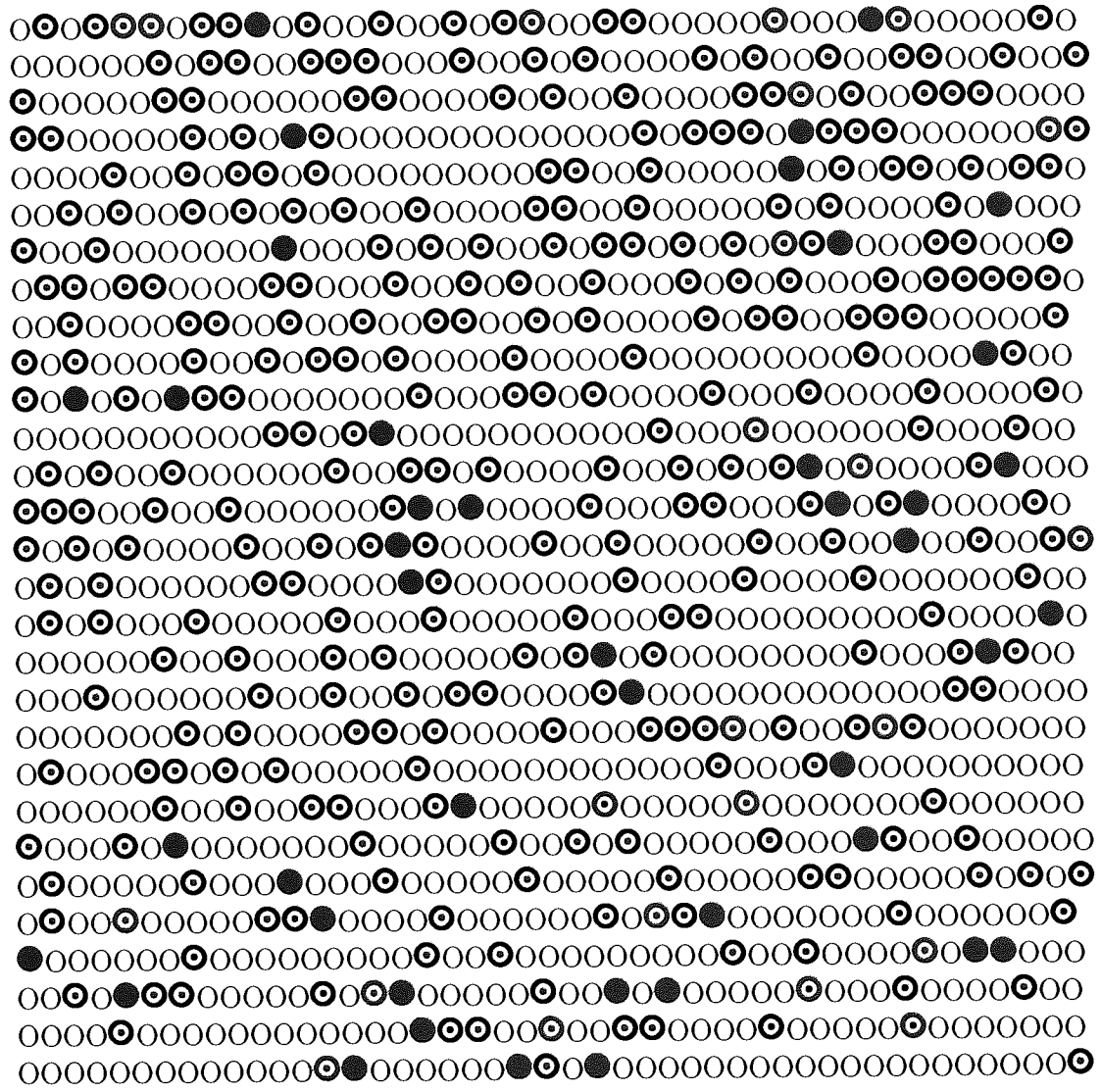

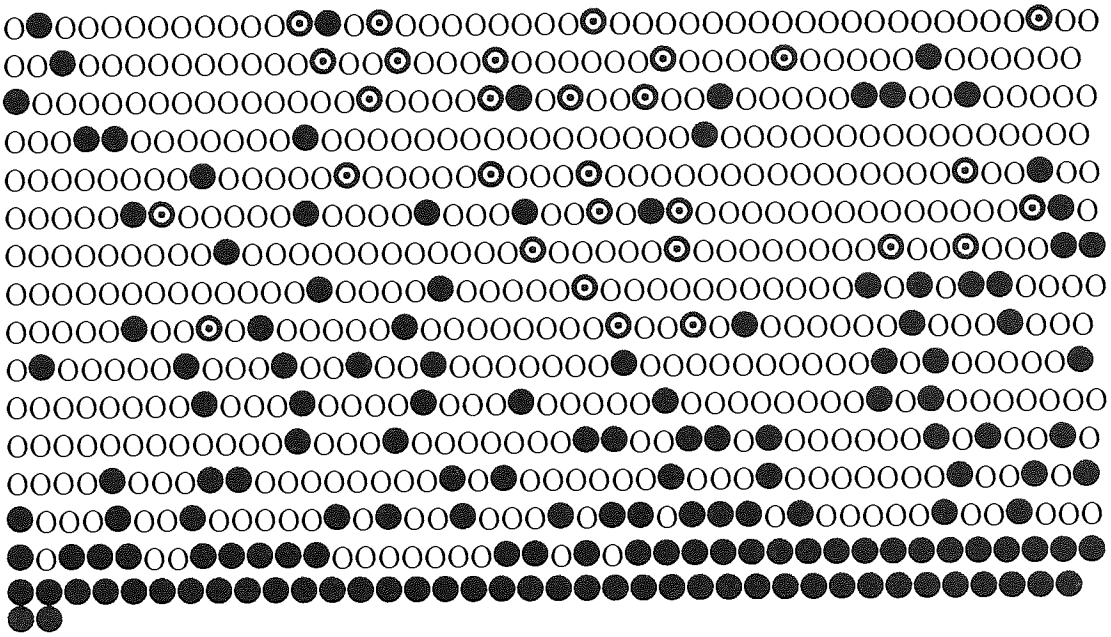

The simulated copolymer contains 1440 NNDMA units, 360 CHMA units and 200 NVI units

Sequence Distributions:

Length	NNDMA	CHMA	NVI	Length	NNDMA	CHMA	NVI
1	103	230	110	12	4	0	0
2	70	47	11	13	3	0	0
3	48	9	2	14	2	0	0
4	41	1	0	15	1	0	0
5	42	1	1	16	2	0	0
6	19	0	0	18	1	0	0
7	15	0	0	19	1	0	0
8	10	0	0	20	2	0	0
9	5	0	0	23	1	0	0
10	4	0	0	57	0	0	1
11	3	0	0				

6. Computer simulated sequence distribution of a NNDMA-CHMA-NVI 63:27:10 terpolymer

63% of Monomer A, NNDMA

27% of Monomer B, CHMA

10% of Monomer C, NVI

r(AB) = 0.4 r(AC) = 4.16 r(BA) = 1.73

r(BC) = 5.58 r(CA) = 0.2 r(CB) = 0.06

Polymerised to 100% conversion

In the simulated copolymer NNDMA is represented by O, CHMA is represented by ⊙ and NVI is represented by ●:

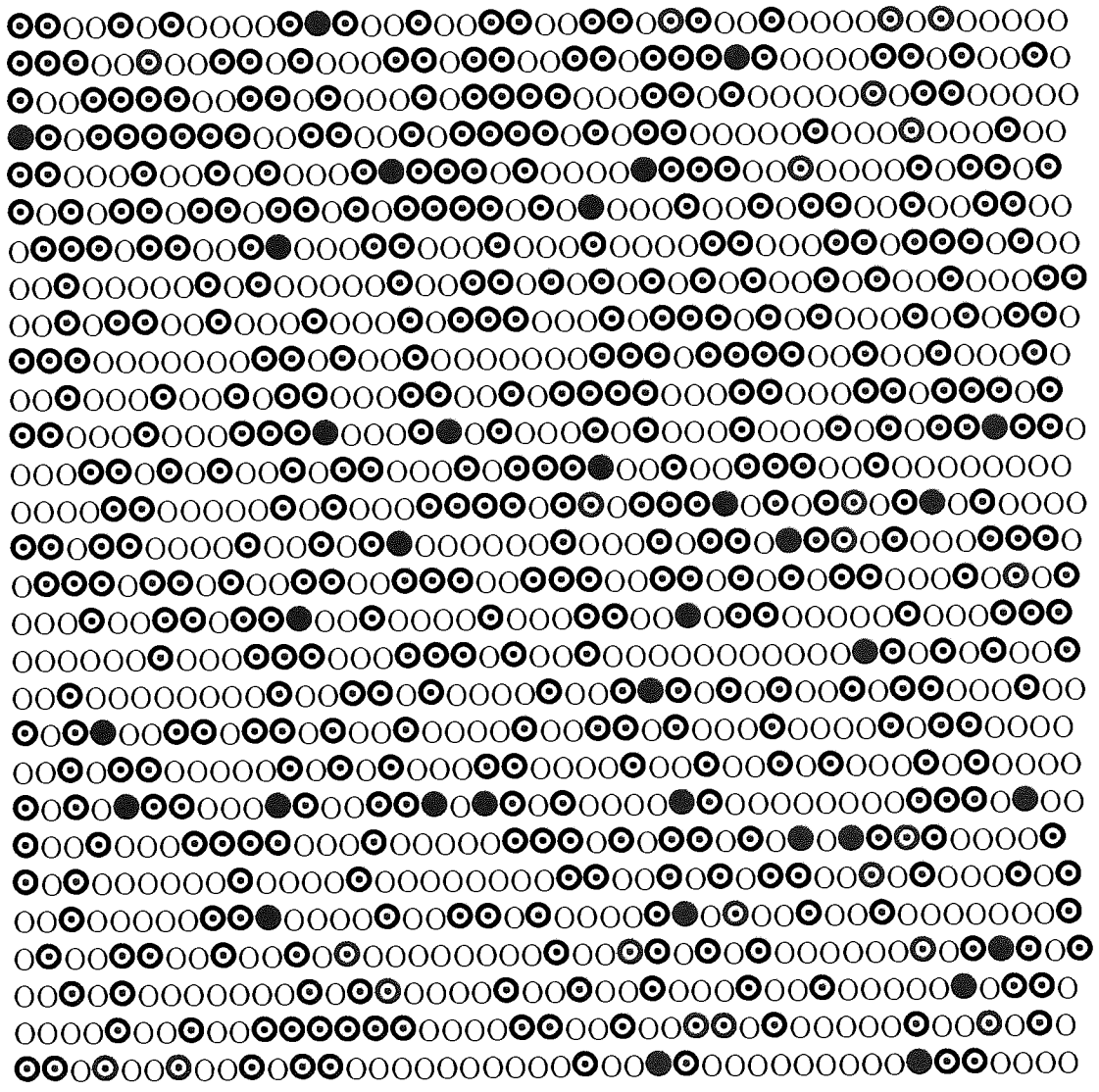

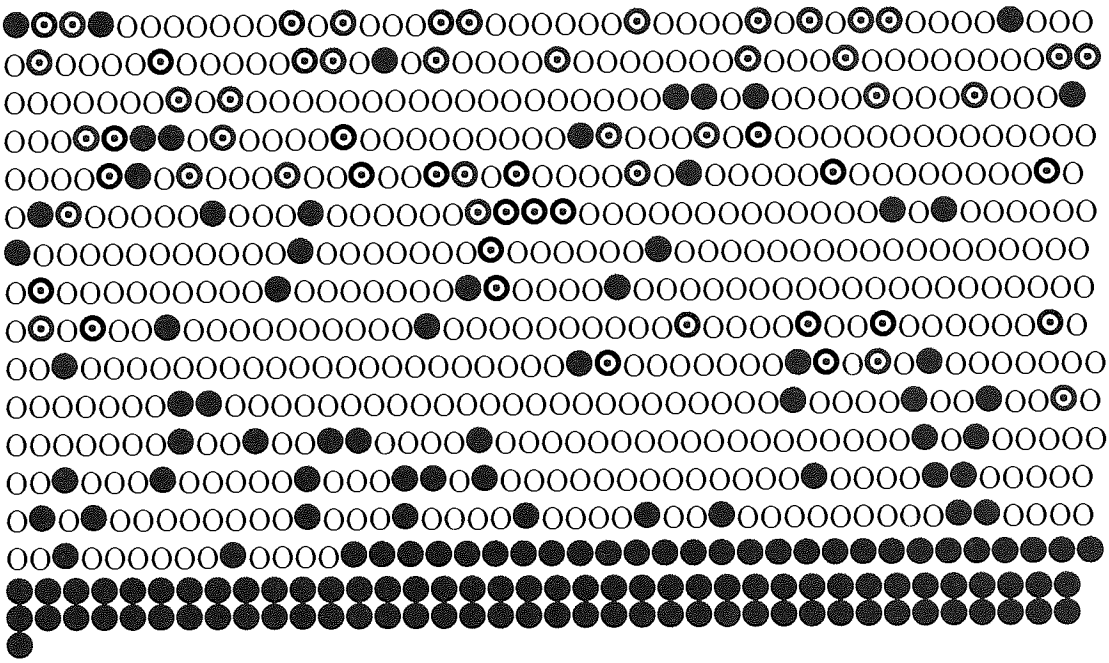

The simulated copolymer contains 1260 NNDMA units, 540 CHMA units and 200 NVI units

Sequence Distributions:

Length	NNDMA	CHMA	NVI	Length	NNDMA	CHMA	NVI
1	149	242	82	11	2	0	0
2	90	86	7	12	1	0	0
3	61	26	0	13	2	0	0
4	40	9	0	14	1	0	0
5	18	0	0	18	3	0	0
6	13	2	0	19	1	0	0
7	11	0	0	21	2	0	0
8	8	0	0	24	1	0	0
9	4	0	0	104	0	0	1
10	3	0	0				

7. Computer simulated sequence distribution of a NNDMA-CHMA-DMAEMA 72:18:10 terpolymer

72% of Monomer A, NNDMA

18% of Monomer B, CHMA

10% of Monomer C, DMAEMA

r(AB) = 0.4 r(AC) = 0.5 r(BA) = 1.73

r(BC) = 1.35 r(CA) = 1.16 r(CB) = 0.73

Polymerised to 100% conversion

In the simulated copolymer NNDMA is represented by O, CHMA is represented by ⊙ and DMAEMA is represented by ●:

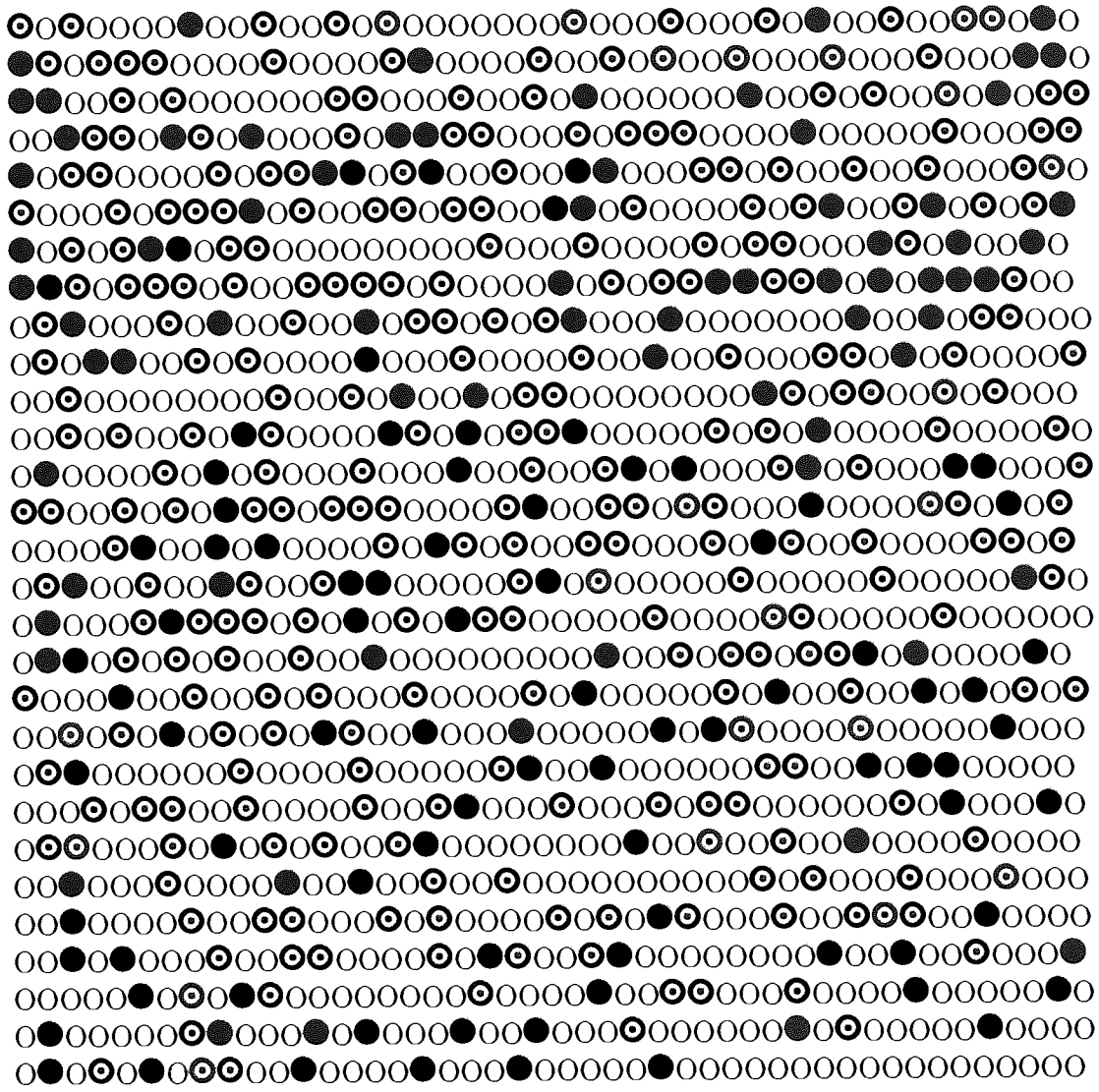

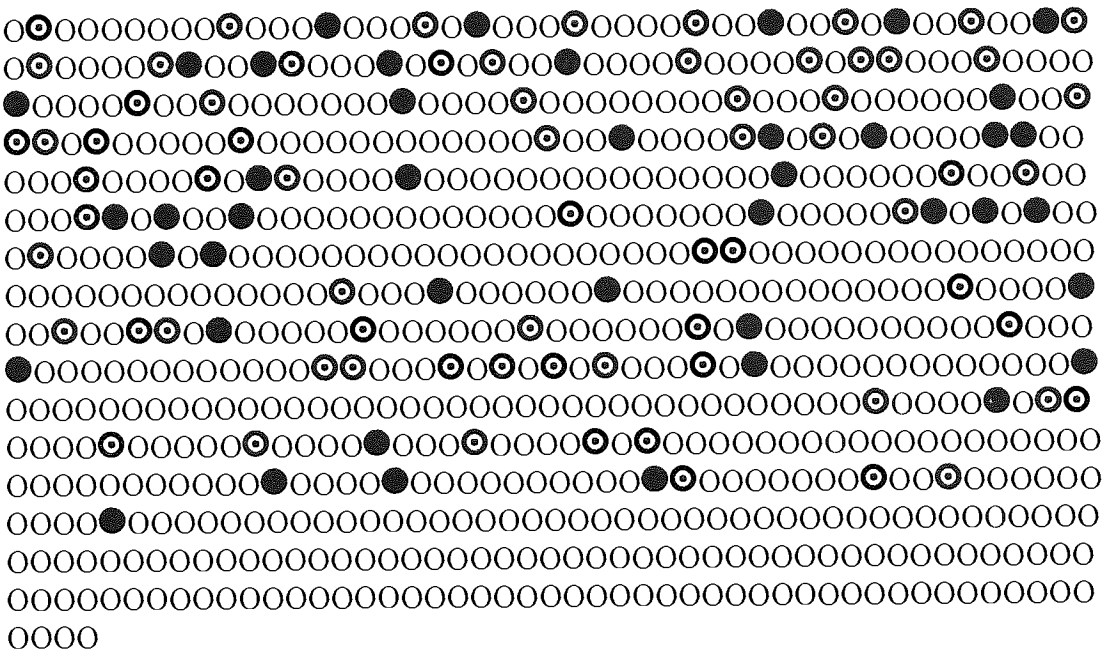

The simulated copolymer contains 1440 NNDMA units, 360 CHMA units and 200 NVI units

Sequence Distributions:

Length	NNDMA	CHMA	DMAEMA	Length	NNDMA	CHMA	DMAEMA
1	143	239	165	12	2	0	0
2	89	45	16	13	2	0	0
3	58	9	1	14	1	0	0
4	55	1	0	15	1	0	0
5	26	0	0	19	1	0	0
6	13	0	0	20	1	0	0
7	7	0	0	29	1	0	0
8	7	0	0	30	1	0	0
9	2	0	0	37	1	0	0
10	4	0	0	140	1	0	0

8. Computer simulated sequence distribution of a NNDMA-CHMA-DMAEMA 63:27:10 terpolymer

63% of Monomer A, NNDMA

27% of Monomer B, CHMA

10% of Monomer C, DMAEMA

r(AB) = 0.4	r(AC) = 0.5	r(BA) = 1.73
r(BC) = 1.35	r(CA) = 1.16	r(CB) = 0.73

Polymerised to 100% conversion

In the simulated copolymer NNDMA is represented by O, CHMA is represented by ⊙ and DMAEMA is represented by ●:

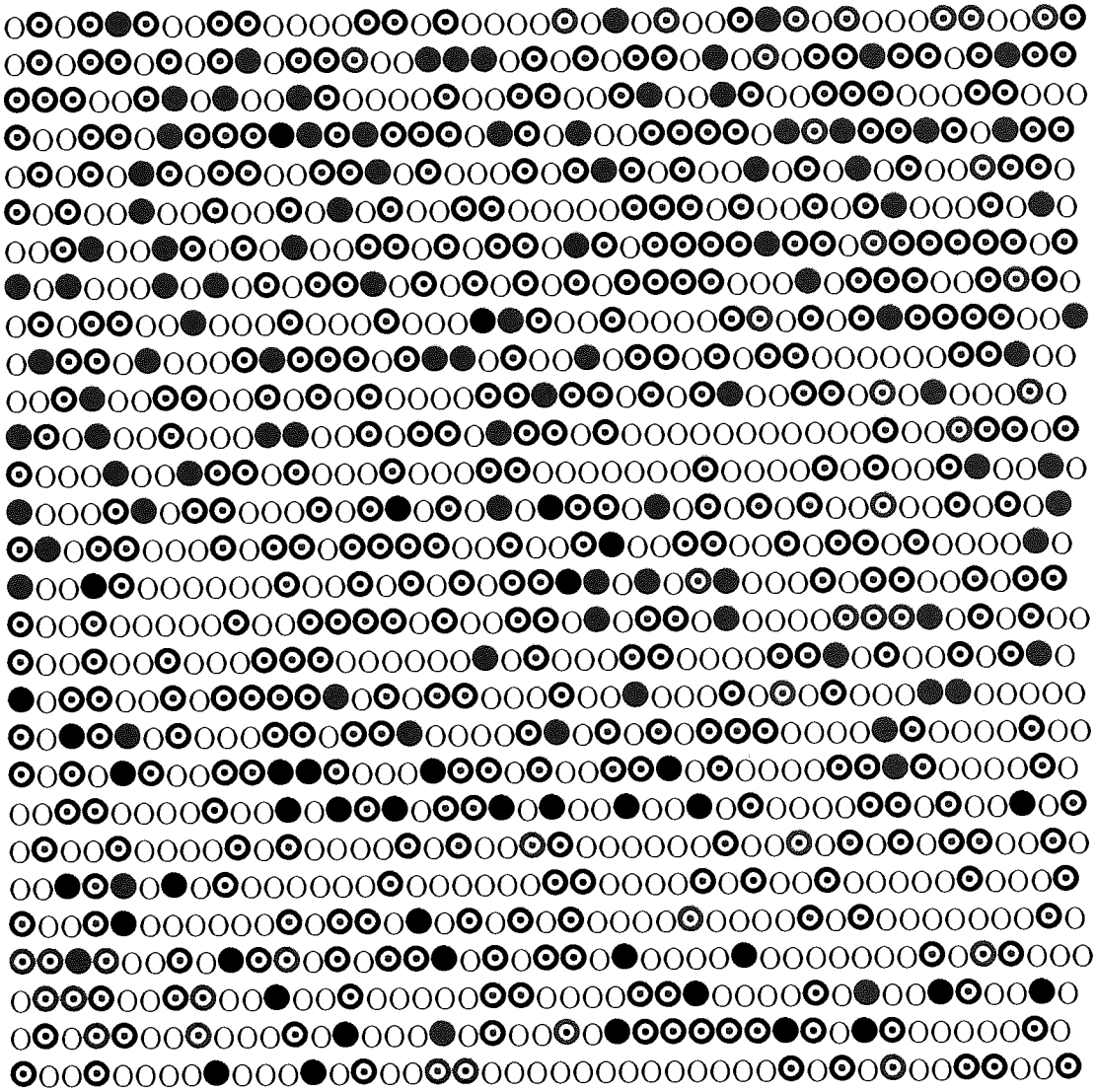

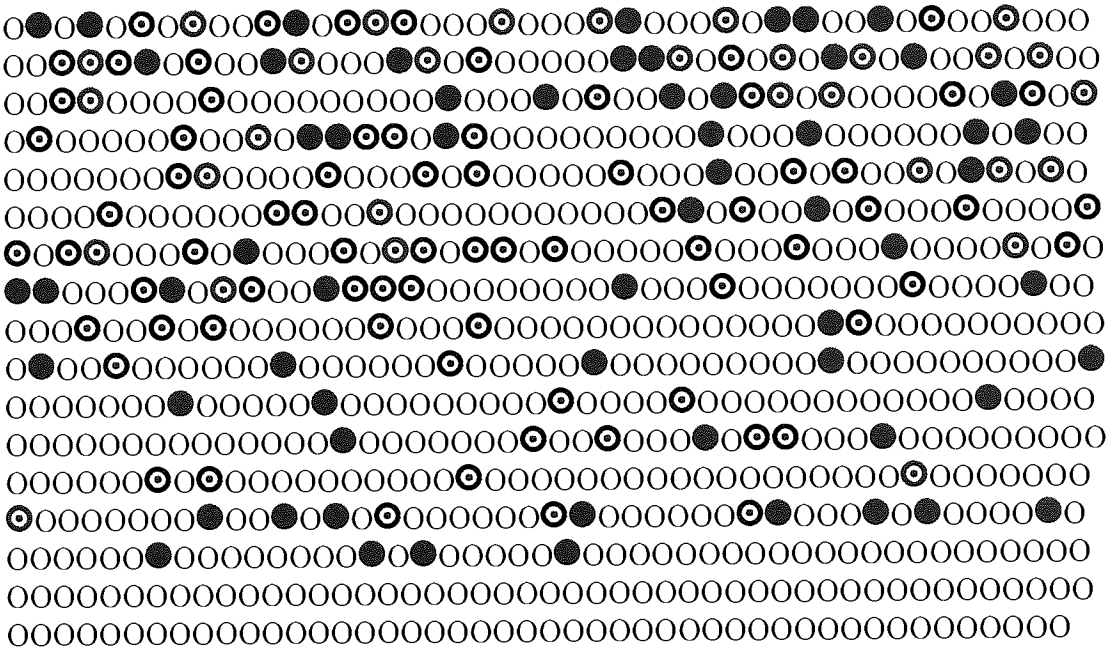

The simulated copolymer contains 1260 NNDMA units, 540 CHMA units and 200 DMAEMA units

Sequence Distributions:

Length	NNDMA	CHMA	DMAEMA	Length	NNDMA	CHMA	DMAEMA
1	217	272	175	10	2	0	0
2	97	85	11	11	3	0	0
3	53	18	1	12	1	0	0
4	36	7	0	13	1	0	0
5	16	2	0	14	1	0	0
6	14	1	0	15	1	0	0
7	9	0	0	18	2	0	0
8	2	0	0	115	1	0	0
9	5	0	0				

9. Computer simulated sequence distribution of a AMO-CHMA-NVI 72:18:10 terpolymer

72% of Monomer A, AMO

18% of Monomer B, CHMA

10% of Monomer C, NVI

r(AB) = 0.45	r(AC) = 3.34	r(BA) = 2.05
r(BC) = 5.58	r(CA) = 0.17	r(CB) = 0.06

Polymerised to 100% conversion

In the simulated copolymer AMO is represented by O, CHMA is represented by ⊙ and NVI is represented by ●:

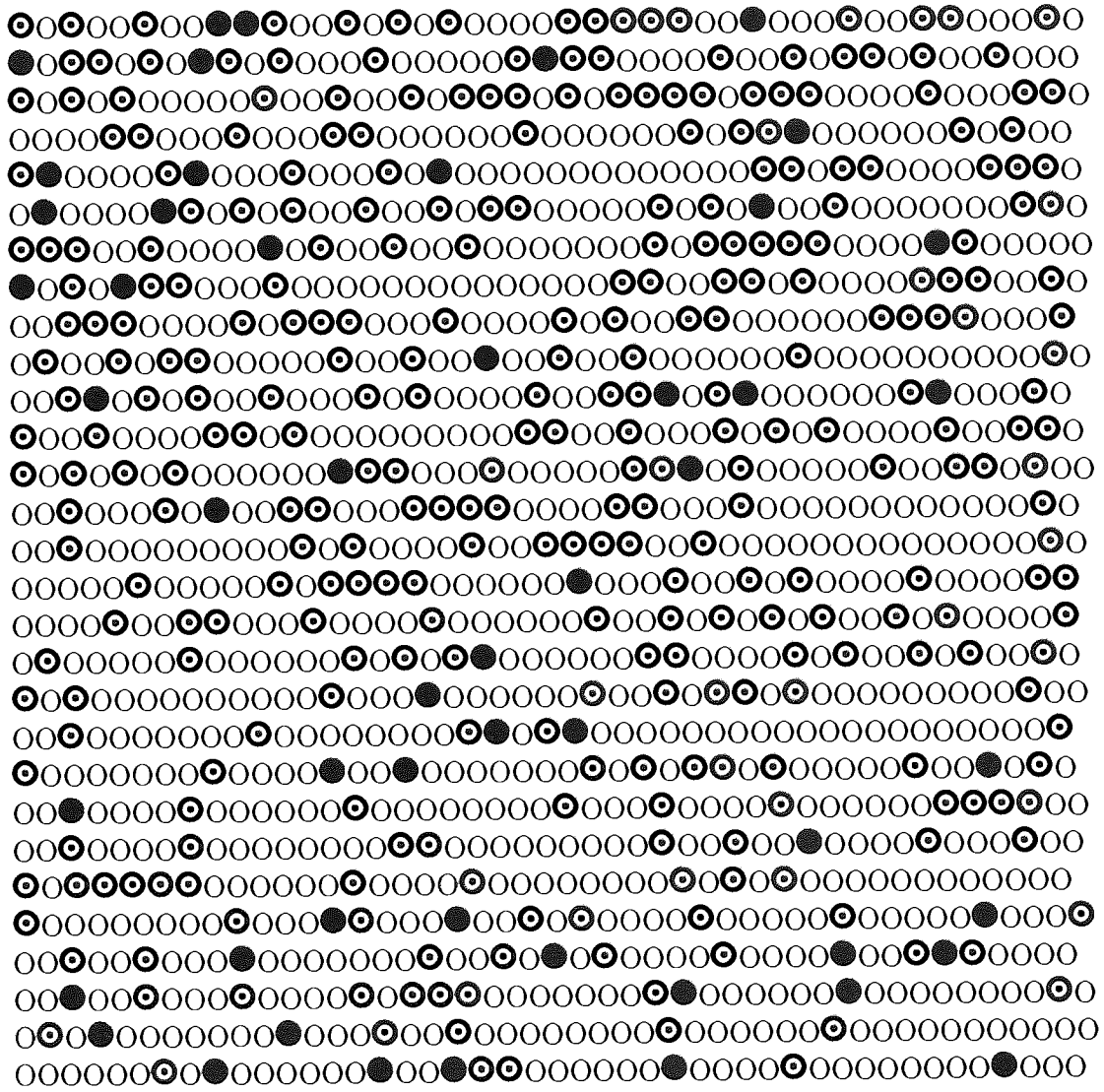

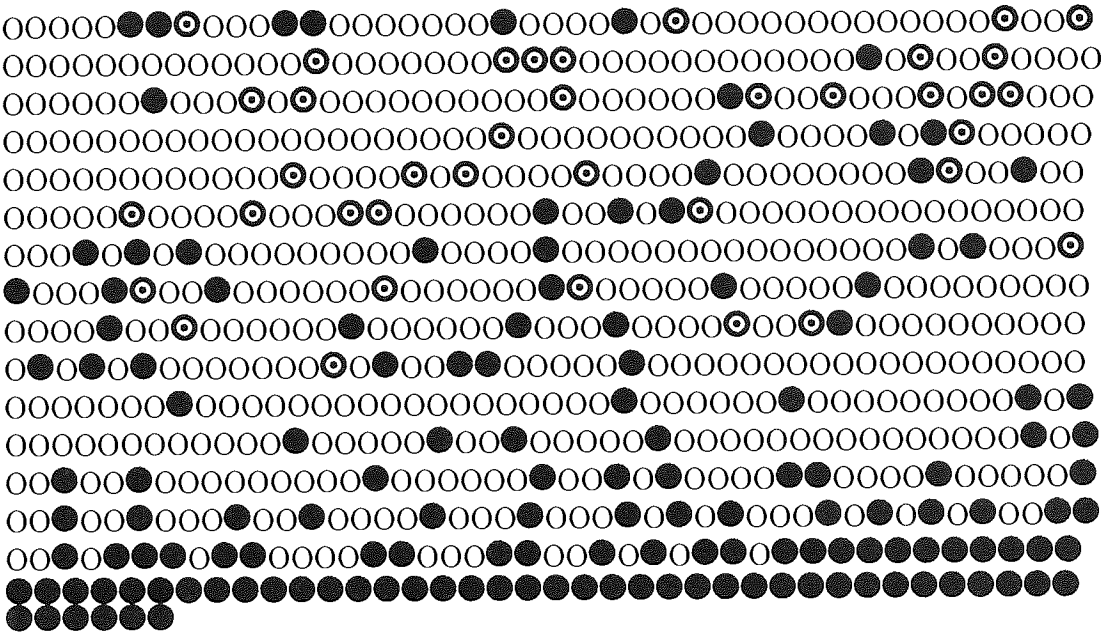

The simulated copolymer contains 1440 AMO units, 360 CHMA units and 200 NVI units

Sequence Distributions:

Length	AMO	CHMA	NVI	Length	AMO	CHMA	NVI
1	106	222	122	12	4	0	0
2	74	36	10	13	4	0	0
3	46	9	1	14	2	0	0
4	48	6	0	15	2	0	0
5	19	3	0	17	2	0	0
6	29	0	0	18	1	0	0
7	12	0	0	19	1	0	0
8	10	0	0	20	1	0	0
9	7	0	0	24	1	0	0
10	5	0	0	26	1	0	0
11	1	0	0	55	0	0	1

10. Computer simulated sequence distribution of a AMO-CHMA-NVI 63:27:10 terpolymer

63% of Monomer A, AMO

27% of Monomer B, CHMA

10% of Monomer C, NVI

r(AB) = 0.45	r(AC) = 3.34	r(BA) = 2.05
r(BC) = 5.58	r(CA) = 0.17	r(CB) = 0.06

Polymerised to 100% conversion

In the simulated copolymer AMO is represented by O, CHMA is represented by ⊙ and NVI is represented by ●:

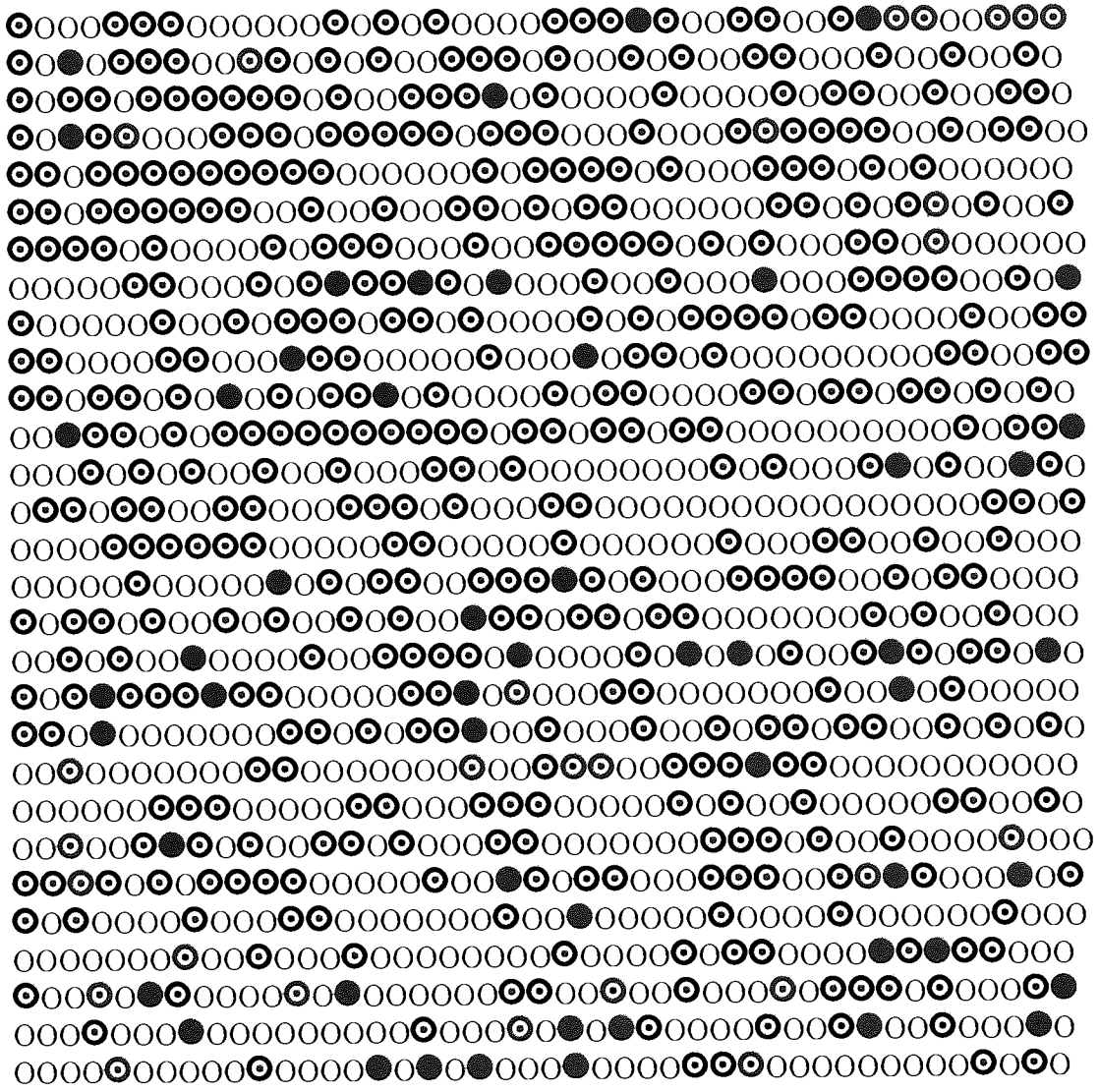

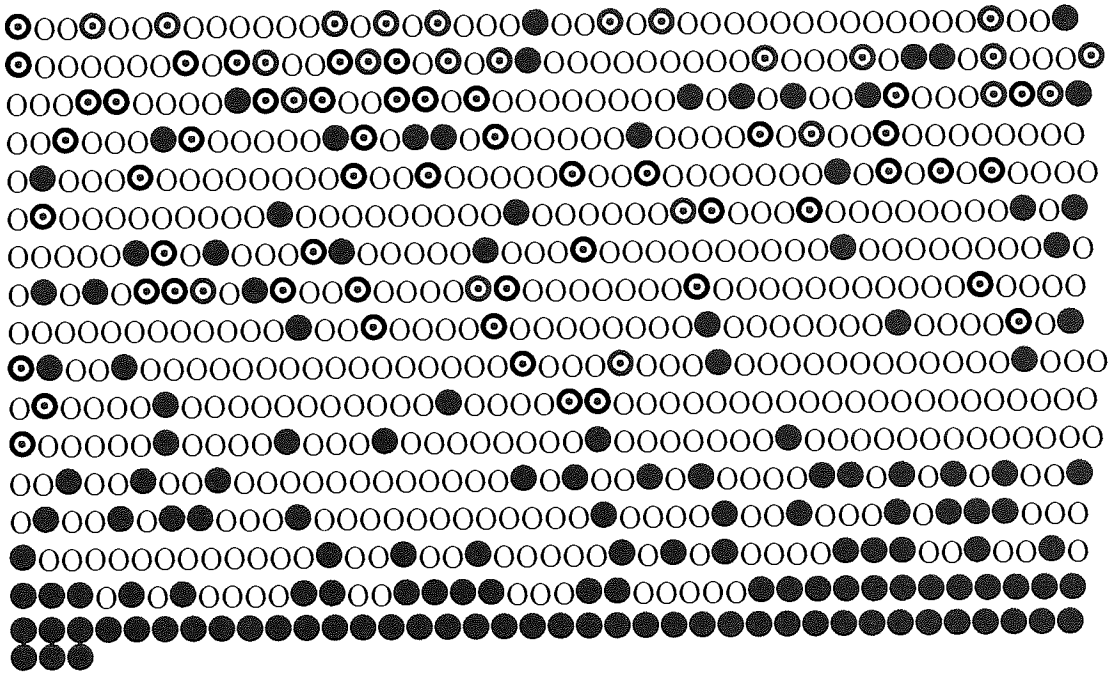

The simulated copolymer contains 1260 AMO units, 540 CHMA units and 200 NVI units

Sequence Distributions:

Length	AMO	CHMA	NVI	Length	AMO	CHMA	NVI
1	156	213	124	10	3	1	0
2	86	77	6	11	3	0	0
3	57	25	3	12	4	0	0
4	36	10	1	13	1	0	0
5	25	3	0	15	1	0	0
6	10	4	0	16	3	0	0
7	12	0	0	17	2	0	0
8	8	0	0	51	0	0	1
9	7	1	0				

11. Computer simulated sequence distribution of a AMO-CHMA-DMAEMA 72:18:10 terpolymer

72% of Monomer A, AMO

18% of Monomer B, CHMA

10% of Monomer C, DMAEMA

r(AB) = 0.45	r(AC) = 0.59	r(BA) = 2.05
r(BC) = 1.35	r(CA) = 1.44	r(CB) = 0.73

Polymerised to 100% conversion

In the simulated copolymer AMO is represented by O, CHMA is represented by ⊙ and DMAEMA is represented by ●:

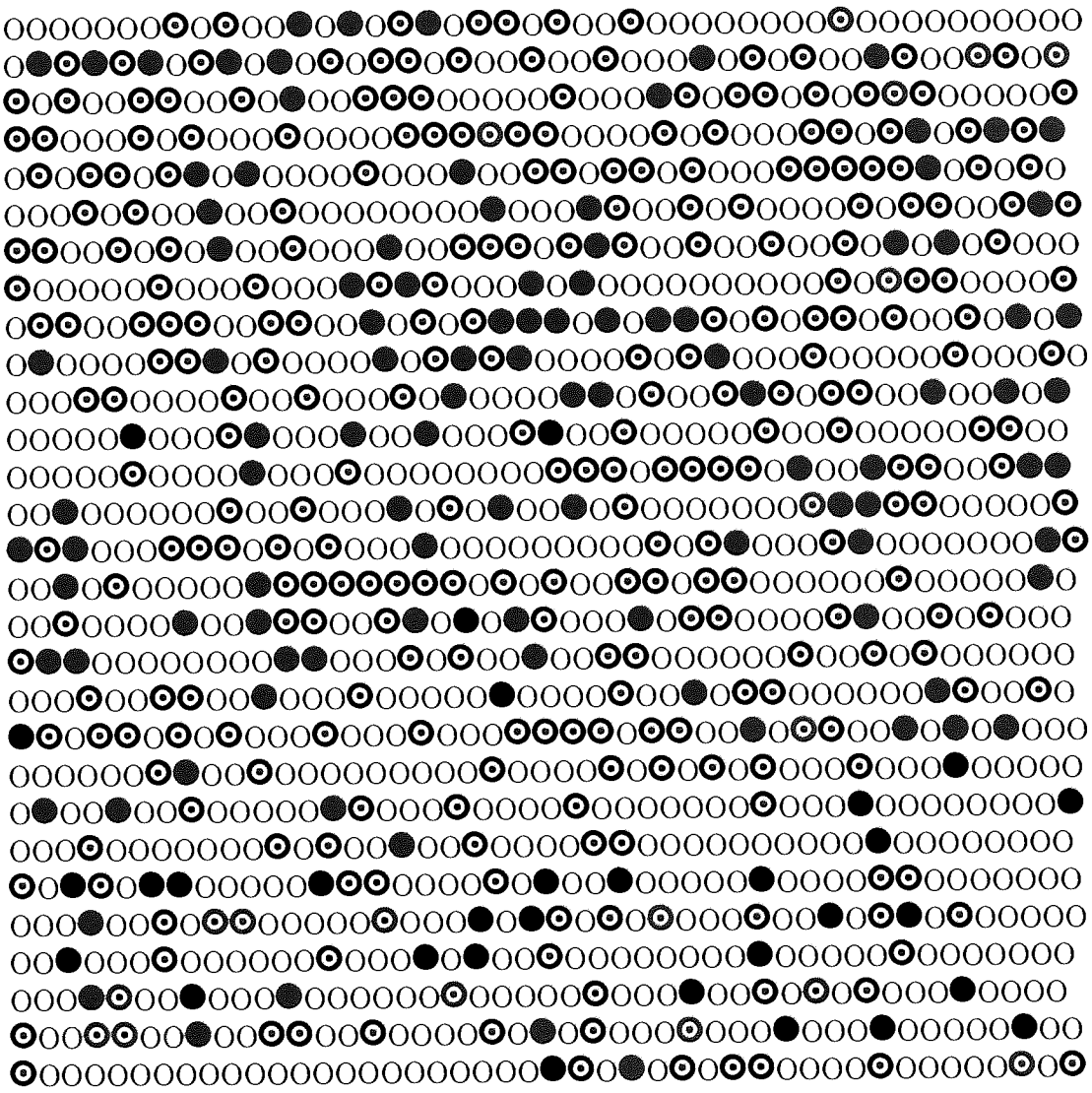

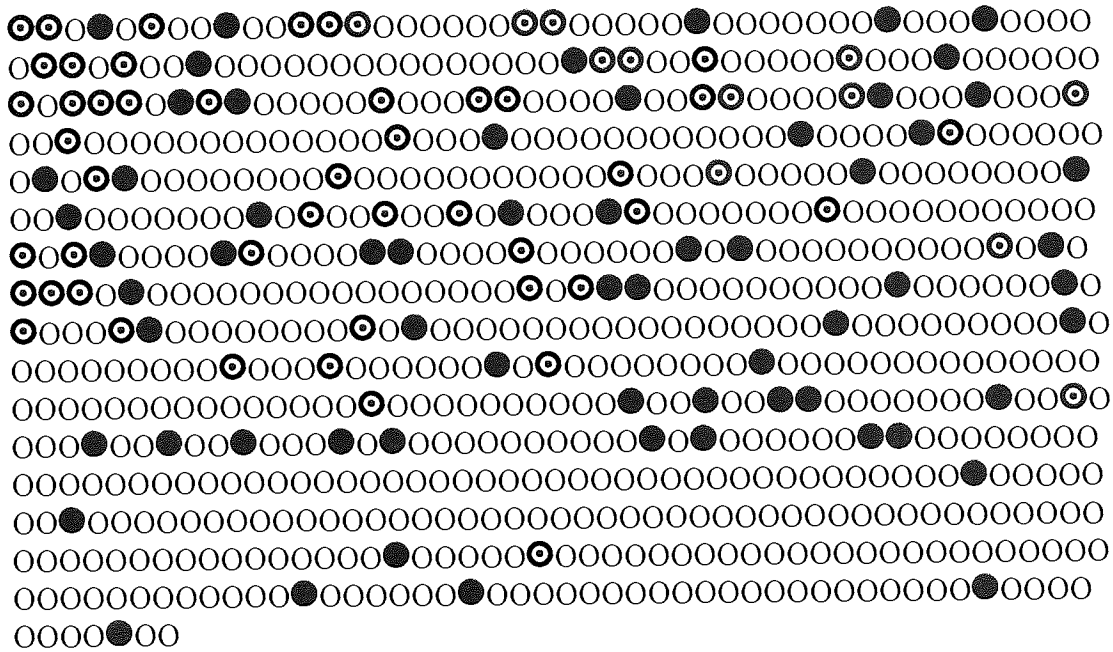

The simulated copolymer contains 1440 AMO units, 360 CHMA units and 200 DMAEMA units

Sequence Distributions:

Length	AMO	CHMA	DMAEMA	Length	AMO	CHMA	DMAEMA
1	127	211	175	12	1	0	0
2	81	42	11	13	1	0	0
3	58	13	1	15	1	0	0
4	31	2	0	16	1	0	0
5	25	1	0	17	1	0	0
6	14	1	0	21	1	0	0
7	13	1	0	22	1	0	0
8	12	0	0	29	1	0	0
9	5	0	0	36	1	0	0
10	9	0	0	48	1	0	0
11	3	0	0	60	1	0	0

12. Computer simulated sequence distribution of a AMO-CHMA-DMAEMA 63:27:10 terpolymer

63% of Monomer A, AMO

27% of Monomer B, CHMA

10% of Monomer C, DMAEMA

r(AB) = 0.45	r(AC) = 0.59	r(BA) = 2.05
r(BC) = 1.35	r(CA) = 1.44	r(CB) = 0.73

Polymerised to 100% conversion

In the simulated copolymer AMO is represented by O, CHMA is represented by ⊙ and DMAEMA is represented by ●:

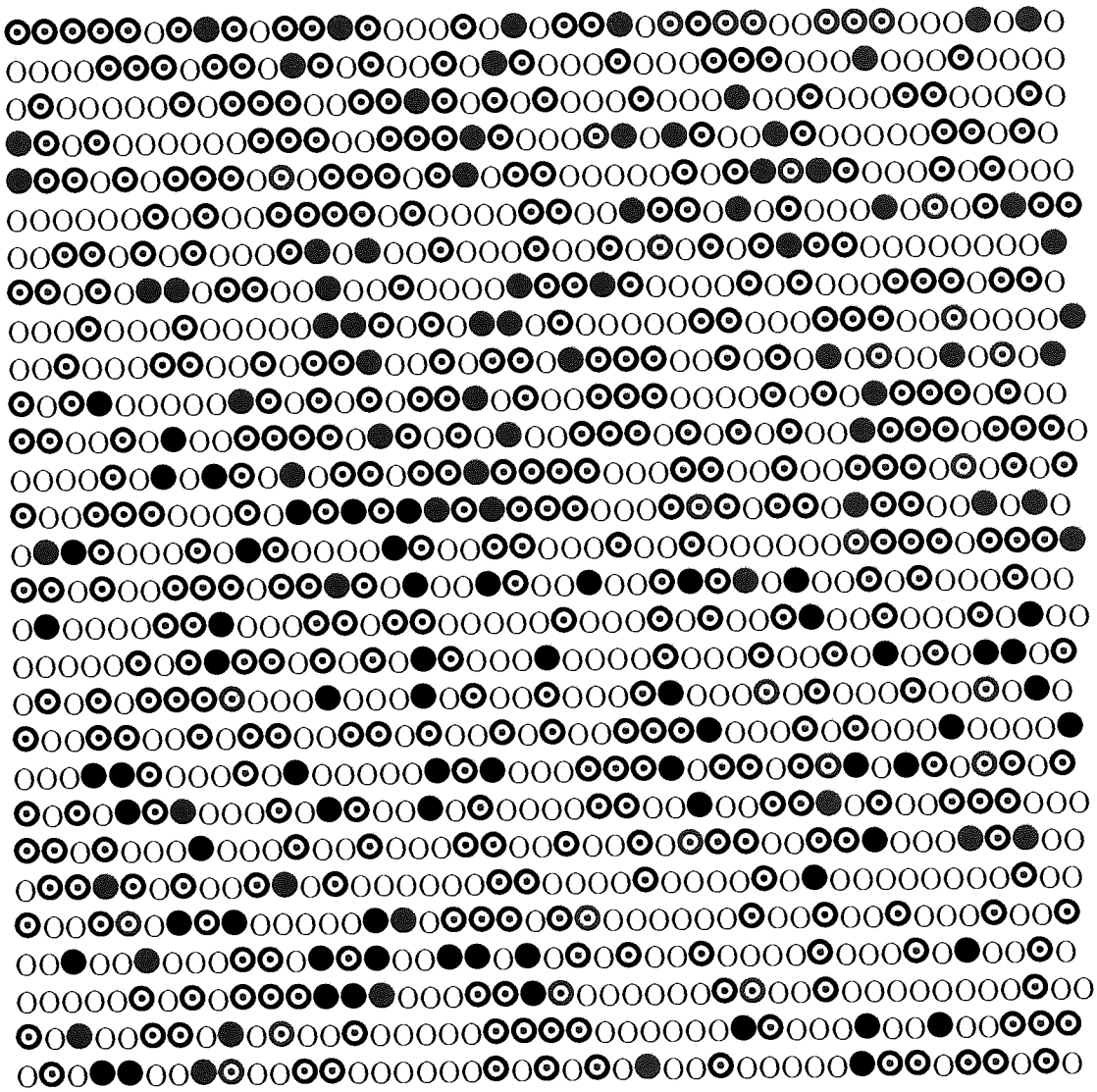

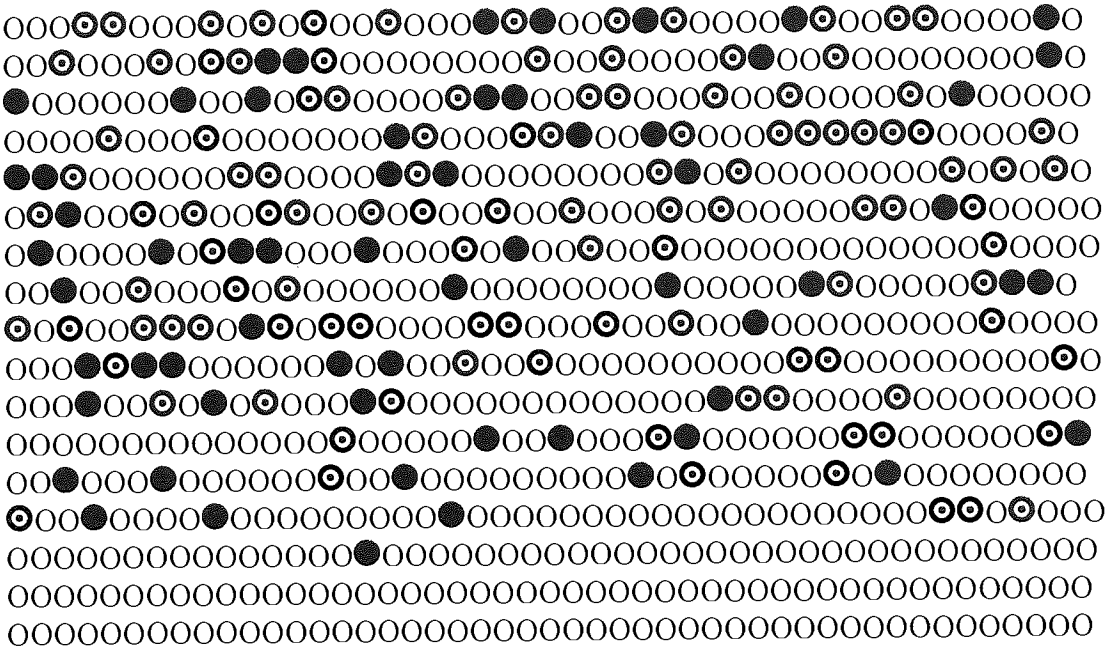

The simulated copolymer contains 1260 AMO units, 540 CHMA units and 200 DMAEMA units

Sequence Distributions:

Length	AMO	CHMA	DMAEMA	Length	AMO	CHMA	DMAEMA
1	174	263	165	9	6	0	0
2	103	74	16	10	1	0	0
3	69	30	1	13	2	0	0
4	27	7	0	18	1	0	0
5	19	1	0	20	1	0	0
6	17	1	0	22	1	0	0
7	3	0	0	125	1	0	0
8	9	0	0				

APPENDIX 2

Water Binding Data for Hydrogel Materials

Copolymer Hydrogel Composition	Equilibrium Water Content (%)	Freezing Water Content (%)	Non-Freezing Water Content (%)	Total Grams of Water / Gram of Polymer	Grams of Freezing Water / Gram of Polymer	Grams of Non-Freezing Water / Gram of Polymer
poly HEMA	34.6	13.5	21.1	0.53	0.21	0.32
HEMA-NVI 95:5	36.1	9.9	26.2	0.56	0.15	0.41
HEMA-NVI 90:10	35.1	5.3	29.8	0.54	0.08	0.46
HEMA-NVI 85:15	33.6	5.5	28.1	0.51	0.08	0.42
HEMA-NVI 80:20	34.0	3.8	30.2	0.52	0.06	0.46
poly HEMA	37.1	16.3	20.8	0.59	0.26	0.33
HEMA-DMAEMA 95:5	37.1	14.2	22.9	0.59	0.23	0.36
HEMA-DMAEMA 90:10	37.1	10.8	26.3	0.59	0.17	0.42
HEMA-DMAEMA 85:15	38.1	14.2	23.9	0.62	0.23	0.39
HEMA-DMAEMA 80:20	38.4	13.9	24.5	0.62	0.23	0.40
NNDMA-CHMA 80:20	64.1	35.7	28.4	1.79	0.99	0.79
NNDMA-CHMA-NVI 76:19:5	61.8	36.1	25.7	1.62	0.95	0.67
NNDMA-CHMA-NVI 72:18:10	66.3	38.4	27.9	1.97	1.14	0.83
NNDMA-CHMA-NVI 68:17:15	65.5	40.2	25.3	1.90	1.16	0.73
NNDMA-CHMA-NVI 64:16:20	70.7	43.9	26.8	2.41	1.50	0.91
NNDMA-CHMA 70:30	48.1	14.7	33.4	0.93	0.28	0.64
NNDMA-CHMA-NVI 66.5:28.5:5	49.6	16.3	33.3	0.98	0.32	0.66
NNDMA-CHMA-NVI 63:27:10	51.2	20.7	30.5	1.05	0.42	0.63
NNDMA-CHMA-NVI 59.5:25.5:15	52.0	22.8	29.2	1.08	0.48	0.61
NNDMA-CHMA-NVI 56:24:20	54.9	21.5	33.4	1.22	0.48	0.74

Copolymer Hydrogel Composition	Equilibrium Water Content (%)	Freezing Water Content (%)	Non-Freezing Water Content (%)	Total Grams of Water / Gram of Polymer	Grams of Freezing Water / Gram of Polymer	Grams of Non-Freezing Water / Gram of Polymer
NNDMA-CHMA 80:20	57.5	35.4	22.1	1.35	0.83	0.52
NNDMA-CHMA-DMAEMA 76:19:5	61.5	40.3	21.2	1.59	1.05	0.55
NNDMA-CHMA-DMAEMA 72:18:10	65.8	40.5	25.3	1.92	1.18	0.74
NNDMA-CHMA-DMAEMA 68:17:15	64.7	41.1	23.6	1.83	1.16	0.67
NNDMA-CHMA-DMAEMA 64:16:20	67.9	41.8	26.1	2.12	1.30	0.81
NNDMA-CHMA 70:30	52.9	23.2	29.7	1.12	0.49	0.63
NNDMA-CHMA-DMAEMA 66.5:28.5:5	52.3	22.4	29.9	1.10	0.47	0.63
NNDMA-CHMA-DMAEMA 63:27:10	52.9	19.2	33.7	1.12	0.41	0.72
NNDMA-CHMA-DMAEMA 59.5:25.5:15	52.2	21.1	31.1	1.09	0.44	0.65
NNDMA-CHMA-DMAEMA 56:24:20	54.4	26.5	27.9	1.19	0.58	0.61
AMO-CHMA 80:20	35.5	11.5	24.0	0.55	0.18	0.37
AMO-CHMA-NVI 76:19:5	41.2	19.0	22.2	0.70	0.32	0.38
AMO-CHMA-NVI 72:18:10	44.2	22.5	21.7	0.79	0.40	0.39
AMO-CHMA-NVI 68:17:15	45.4	19.2	26.2	0.83	0.35	0.48
AMO-CHMA-NVI 64:16:20	46.0	21.7	24.3	0.85	0.40	0.45
AMO-CHMA 70:30	18.4	1.6	16.8	0.23	0.02	0.21
AMO-CHMA-NVI 66.5:28.5:5	23.0	3.6	19.4	0.30	0.05	0.25
AMO-CHMA-NVI 63:27:10	28.7	6.9	21.8	0.40	0.09	0.31
AMO-CHMA-NVI 59.5:25.5:15	28.6	6.9	21.7	0.40	0.10	0.30
AMO-CHMA-NVI 56:24:20	28.8	8.6	20.2	0.40	0.12	0.28

Copolymer Hydrogel Composition	Equilibrium Water Content (%)	Freezing Water Content (%)	Non-Freezing Water Content (%)	Total Grams of Water / Gram of Polymer	Grams of Freezing Water / Gram of Polymer	Grams of Non-Freezing Water / Gram of Polymer
AMO-CHMA 80:20	35.2	15.7	19.5	0.54	0.24	0.30
AMO-CHMA-DMAEMA 76:19:5	42.4	22.5	19.9	0.74	0.39	0.35
AMO-CHMA-DMAEMA 72:18:10	45.5	25.7	19.8	0.83	0.47	0.36
AMO-CHMA-DMAEMA 68:17:15	46.9	28.8	18.1	0.88	0.54	0.34
AMO-CHMA-DMAEMA 64:16:20	51.9	31.9	20.0	1.08	0.66	0.42
AMO-CHMA 70:30	24.9	1.6	23.3	0.33	0.02	0.31
AMO-CHMA-DMAEMA 66.5:28.5:5	26.1	3.3	22.8	0.35	0.04	0.31
AMO-CHMA-DMAEMA 63:27:10	30.7	6.1	24.6	0.44	0.09	0.35
AMO-CHMA-DMAEMA 59.5:25.5:15	30.8	5.9	24.9	0.45	0.09	0.36
AMO-CHMA-DMAEMA 56:24:20	34.6	9.5	25.1	0.53	0.15	0.38

APPENDIX 3

Tensile Data for Hydrogel Materials

Copolymer Hydrogel Composition	E.W.C. (%)	Tensile Strength (MPa)	Elongation to Break (%)	Youngs Modulus (MPa)
poly HEMA	34.6	0.615	117.9	0.571
HEMA-NVI 95:5	36.1	0.616	125.0	0.540
HEMA-NVI 90:10	35.1	0.633	137.9	0.538
HEMA-NVI 85:15	33.6	0.659	156.9	0.536
HEMA-NVI 80:20	34.0	0.875	189.8	0.461
poly HEMA	37.1	0.625	128.1	0.545
HEMA-DMAEMA 95:5	37.1	0.712	126.3	0.567
HEMA-DMAEMA 90:10	37.1	0.853	125.0	0.561
HEMA-DMAEMA 85:15	38.1	0.864	120.6	0.581
HEMA-DMAEMA 80:20	38.4	0.884	102.5	0.581
NNDMA-CHMA 80:20	64.1	0.832	236.0	0.400
NNDMA-CHMA-NVI 76:19:5	61.8	0.752	186.7	0.349
NNDMA-CHMA-NVI 72:18:10	66.3	0.628	166.0	0.269
NNDMA-CHMA-NVI 68:17:15	65.5	0.554	175.0	0.296
NNDMA-CHMA-NVI 64:16:20	70.7	0.439	172.7	0.250
NNDMA-CHMA 70:30	48.1	4.180	138.1	8.923
NNDMA-CHMA-NVI 66.5:28.5:5	49.6	3.050	139.0	5.230
NNDMA-CHMA-NVI 63:27:10	51.2	3.050	140.6	4.250
NNDMA-CHMA-NVI 59.5:25.5:15	52.0	2.410	141.7	2.540
NNDMA-CHMA-NVI 56:24:20	54.9	2.316	152.7	1.655

Copolymer Hydrogel Composition	E.W.C. (%)	Tensile Strength (MPa)	Elongation to Break (%)	Youngs Modulus (MPa)
NNDMA-CHMA 80:20	57.5	0.812	255.0	0.402
NNDMA-CHMA-DMAEMA 76:19:5	61.5	0.500	234.0	0.279
NNDMA-CHMA-DMAEMA 72:18:10	65.8	0.451	208.6	0.207
NNDMA-CHMA-DMAEMA 68:17:15	64.7	0.389	190.0	0.184
NNDMA-CHMA-DMAEMA 64:16:20	67.9	0.348	185.5	0.201
NNDMA-CHMA 70:30	52.9	3.700	149.5	8.933
NNDMA-CHMA-DMAEMA 66.5:28.5:5	52.3	3.370	189.0	6.365
NNDMA-CHMA-DMAEMA 63:27:10	52.9	2.420	281.0	2.528
NNDMA-CHMA-DMAEMA 59.5:25.5:15	52.2	2.009	255.0	1.440
NNDMA-CHMA-DMAEMA 56:24:20	54.4	1.479	318.0	0.644
AMO-CHMA 80:20	35.5	2.110	314.0	0.854
AMO-CHMA-NVI 76:19:5	41.2	1.975	280.3	0.477
AMO-CHMA-NVI 72:18:10	44.2	1.652	257.0	0.332
AMO-CHMA-NVI 68:17:15	45.4	0.918	275.0	0.304
AMO-CHMA-NVI 64:16:20	46.0	1.024	249.0	0.281
AMO-CHMA 70:30	18.4	7.820	71.8	25.600
AMO-CHMA-NVI 66.5:28.5:5	23.0	7.110	79.2	23.100
AMO-CHMA-NVI 63:27:10	28.7	6.690	80.7	20.300
AMO-CHMA-NVI 59.5:25.5:15	28.6	4.310	98.3	19.800
AMO-CHMA-NVI 56:24:20	28.8	4.600	112.4	19.600

Copolymer Hydrogel Composition	E.W.C. (%)	Tensile Strength (MPa)	Elongation to Break (%)	Youngs Modulus (MPa)
AMO-CHMA 80:20	35.2	1.940	302.0	0.896
AMO-CHMA-DMAEMA 76:19:5	42.4	1.108	289.0	0.548
AMO-CHMA-DMAEMA 72:18:10	45.5	0.662	284.0	0.268
AMO-CHMA-DMAEMA 68:17:15	46.9	0.550	241.0	0.199
AMO-CHMA-DMAEMA 64:16:20	51.9	0.500	241.0	0.181
AMO-CHMA 70:30	24.9	7.520	83.2	25.461
AMO-CHMA-DMAEMA 66.5:28.5:5	26.1	4.280	98.8	19.880
AMO-CHMA-DMAEMA 63:27:10	30.7	3.880	137.0	9.730
AMO-CHMA-DMAEMA 59.5:25.5:15	30.8	2.950	150.3	8.001
AMO-CHMA-DMAEMA 56:24:20	34.6	2.473	213.0	2.317

APPENDIX 4

Measured Surface Energies

for Hydrated and Dehydrated Hydrogel Materials

Copolymer Hydrogel Composition (Hydrated)	Air Contact Angle	n-Octane Contact Angle	Dispersive Component of Surface Free Energy (mN/m)	Polar Component of Surface Free Energy (mN/m)	Total Surface Free Energy (mN/m)
poly HEMA	39.5	145	15.1	42.2	57.3
HEMA-NVI 95:5	34	146	18.3	42.7	61.0
HEMA-NVI 90:10	30	145	21.4	42.2	63.6
HEMA-NVI 85:15	35	142	19.6	40.8	60.4
HEMA-NVI 80:20	33	140	22.1	39.8	61.9
poly HEMA	39.5	145	15.1	42.2	57.3
HEMA-DMAEMA 95:5	39	141	17.3	40.2	57.6
HEMA-DMAEMA 90:10	36	139	20.5	39.3	59.8
HEMA-DMAEMA 85:15	36	140	19.9	39.8	59.7
HEMA-DMAEMA 80:20	37	140	19.2	39.8	59.0
NNDMA-CHMA 80:20	33	143	20.5	41.2	61.7
NNDMA-CHMA-NVI 76:19:5	33	141	21.6	40.2	61.8
NNDMA-CHMA-NVI 72:18:10	33	136	24.5	37.7	62.2
NNDMA-CHMA-NVI 68:17:15	35	133	25.1	36.1	61.1
NNDMA-CHMA-NVI 64:16:20	36	139	20.5	39.3	59.8
NNDMA-CHMA 70:30	38	134	22.1	36.6	58.7
NNDMA-CHMA-NVI 66.5:28.5:5	37	138	20.4	38.7	59.1
NNDMA-CHMA-NVI 63:27:10	36	141	19.5	40.2	59.7
NNDMA-CHMA-NVI 59.5:25.5:15	35	137	22.4	38.2	60.7
NNDMA-CHMA-NVI 56:24:20	36	140	19.9	39.8	59.7

Copolymer Hydrogel Composition (Hydrated)	Air Contact Angle	n-Octane Contact Angle	Dispersive Component of Surface Free Energy (mN/m)	Polar Component of Surface Free Energy (mN/m)	Total Surface Free Energy (mN/m)
NNDMA-CHMA 80:20	33	143	20.5	41.2	61.7
NNDMA-CHMA-DMAEMA 76:19:5	30	148	19.9	43.6	63.5
NNDMA-CHMA-DMAEMA 72:18:10	29	142	23.6	40.8	64.4
NNDMA-CHMA-DMAEMA 68:17:15	29	143	23.1	41.2	64.3
NNDMA-CHMA-DMAEMA 64:16:20	32	143	21.2	41.2	62.4
NNDMA-CHMA 70:30	38	140	18.5	39.8	58.3
NNDMA-CHMA-DMAEMA 66.5:28.5:5	32	147	19.1	43.1	62.3
NNDMA-CHMA-DMAEMA 63:27:10	33	146	19.0	42.7	61.6
NNDMA-CHMA-DMAEMA 59.5:25.5:15	36	146	17.0	42.7	59.7
NNDMA-CHMA-DMAEMA 56:24:20	35	148	16.8	43.6	60.4
AMO-CHMA 80:20	32	142	21.6	40.8	62.4
AMO-CHMA-NVI 76:19:5	38	146	15.7	42.7	58.3
AMO-CHMA-NVI 72:18:10	30	143	22.5	41.2	63.7
AMO-CHMA-NVI 68:17:15	31	146	20.2	42.7	62.9
AMO-CHMA-NVI 64:16:20	29	147	21.0	43.1	64.1
AMO-CHMA 70:30	37	143	17.8	41.2	59.0
AMO-CHMA-NVI 66.5:28.5:5	34	149	17.1	44.0	61.0
AMO-CHMA-NVI 63:27:10	33	148	18.0	43.6	61.6
AMO-CHMA-NVI 59.5:25.5:15	34	140	21.4	39.8	61.2
AMO-CHMA-NVI 56:24:20	30	143	22.5	41.2	63.7

Copolymer Hydrogel Composition (Hydrated)	Air Contact Angle	n-Octane Contact Angle	Dispersive Component of Surface Free Energy (mN/m)	Polar Component of Surface Free Energy (mN/m)	Total Surface Free Energy (mN/m)
AMO-CHMA 80:20	32	142	21.6	40.8	62.4
AMO-CHMA-DMAEMA 76:19:5	37	146	16.3	42.7	59.0
AMO-CHMA-DMAEMA 72:18:10	30	145	21.4	42.2	63.6
AMO-CHMA-DMAEMA 68:17:15	34	146	18.3	42.7	61.0
AMO-CHMA-DMAEMA 64:16:20	31	148	19.3	43.6	62.9
AMO-CHMA 70:30	37	143	17.8	41.2	59.0
AMO-CHMA-DMAEMA 66.5:28.5:5	31	150	18.5	44.4	62.9
AMO-CHMA-DMAEMA 63:27:10	33	154	15.8	45.9	61.8
AMO-CHMA-DMAEMA 59.5:25.5:15	30	151	18.7	44.8	63.5
AMO-CHMA-DMAEMA 56:24:20	32	150	17.8	44.4	62.3

Copolymer Hydrogel Composition (Dehydrated)	Water Contact Angle	Methylene Iodide Contact Angle	Dispersive Component of Surface Free Energy (mN/m)	Polar Component of Surface Free Energy (mN/m)	Total Surface Free Energy (mN/m)
poly HEMA	62	36	33.5	13.8	47.3
HEMA-NVI 95:5	63	35	34.3	12.9	47.2
HEMA-NVI 90:10	61	35	33.8	14.2	48.0
HEMA-NVI 85:15	63	40	31.7	14.0	45.7
HEMA-NVI 80:20	66	40	32.4	12.0	44.4
poly HEMA	62	36	33.5	13.8	47.3
HEMA-DMAEMA 95:5	62	38	32.5	14.2	46.7
HEMA-DMAEMA 90:10	63	43	30.0	14.7	44.7
HEMA-DMAEMA 85:15	64	42	30.8	13.8	44.6
HEMA-DMAEMA 80:20	66	40	32.4	12.0	44.4
NNDMA-CHMA 80:20	75	39	35.1	6.5	41.6
NNDMA-CHMA-NVI 76:19:5	79	41	35.1	4.9	40.0
NNDMA-CHMA-NVI 72:18:10	79	41	35.1	4.9	40.0
NNDMA-CHMA-NVI 68:17:15	79	38	36.8	4.5	41.3
NNDMA-CHMA-NVI 64:16:20	79	36	37.8	4.2	42.0
NNDMA-CHMA 70:30	78	42	34.2	5.5	39.7
NNDMA-CHMA-NVI 66.5:28.5:5	75	38	35.7	6.3	42.0
NNDMA-CHMA-NVI 63:27:10	76	40	34.8	6.2	41.0
NNDMA-CHMA-NVI 59.5:25.5:15	76	38	36.0	5.9	41.9
NNDMA-CHMA-NVI 56:24:20	74	39	34.9	7.0	41.9

Copolymer Hydrogel Composition (Dehydrated)	Water Contact Angle	Methylene Iodide Contact Angle	Dispersive Component of Surface Free Energy (mN/m)	Polar Component of Surface Free Energy (mN/m)	Total Surface Free Energy (mN/m)
NNDMA-CHMA 80:20	75	39	35.1	6.5	41.6
NNDMA-CHMA-DMAEMA 76:19:5	81	37	37.9	3.6	41.5
NNDMA-CHMA-DMAEMA 72:18:10	82	38	37.6	3.3	40.9
NNDMA-CHMA-DMAEMA 68:17:15	83	39	37.3	3.0	40.3
NNDMA-CHMA-DMAEMA 64:16:20	82	39	37.0	3.4	40.4
NNDMA-CHMA 70:30	78	42	34.2	5.5	39.7
NNDMA-CHMA-DMAEMA 66.5:28.5:5	77	37	36.8	5.2	42.0
NNDMA-CHMA-DMAEMA 63:27:10	81	38	37.3	3.7	41.0
NNDMA-CHMA-DMAEMA 59.5:25.5:15	80	42	34.7	4.6	39.3
NNDMA-CHMA-DMAEMA 56:24:20	76	42	33.7	6.5	40.2
AMO-CHMA 80:20	78	34	38.6	4.4	43.0
AMO-CHMA-NVI 76:19:5	77	29	40.8	4.3	45.1
AMO-CHMA-NVI 72:18:10	78	33	39.1	4.3	43.4
AMO-CHMA-NVI 68:17:15	75	33	38.3	5.7	44.0
AMO-CHMA-NVI 64:16:20	76	37	36.5	5.7	42.2
AMO-CHMA 70:30	79	35	38.4	4.1	42.5
AMO-CHMA-NVI 66.5:28.5:5	75	33	38.3	5.7	44.0
AMO-CHMA-NVI 63:27:10	78	39	35.9	5.1	41.0
AMO-CHMA-NVI 59.5:25.5:15	74	34	37.5	6.3	43.8
AMO-CHMA-NVI 56:24:20	78	33	39.1	4.3	43.4

Copolymer Hydrogel Composition (Dehydrated)	Water Contact Angle	Methylene Iodide Contact Angle	Dispersive Component of Surface Free Energy (mN/m)	Polar Component of Surface Free Energy (mN/m)	Total Surface Free Energy (mN/m)
AMO-CHMA 80:20	78	34	38.6	4.4	43.0
AMO-CHMA-DMAEMA 76:19:5	79	34	38.9	4.0	42.9
AMO-CHMA-DMAEMA 72:18:10	78	32	39.6	4.2	43.8
AMO-CHMA-DMAEMA 68:17:15	77	33	38.9	4.7	43.6
AMO-CHMA-DMAEMA 64:16:20	79	37	37.3	4.4	41.7
AMO-CHMA 70:30	79	35	38.4	4.1	42.5
AMO-CHMA-DMAEMA 66.5:28.5:5	77	35	37.8	5.0	42.8
AMO-CHMA-DMAEMA 63:27:10	77	38	36.2	5.4	41.6
AMO-CHMA-DMAEMA 59.5:25.5:15	77	36	37.3	5.1	42.4
AMO-CHMA-DMAEMA 56:24:20	77	37	36.8	5.2	42.0

APPENDIX 5

Results from *in vitro* Spoilation Model for Hydrogel Materials

Copolymer Hydrogel Composition	Time (Days)	Lipid 360nm (%) (transmission)	Protein 280nm (%) (transmission)	Lipid 280nm (%) (transmission)	Spoilation Factor (%)
polyHEMA	4	1.30	0.30	0.00	0.53
	7	1.90	0.90	0.30	1.03
	10	2.20	1.30	0.30	1.27
	14	2.50	1.60	0.60	1.57
	17	2.50	1.60	0.60	1.57
	21	2.80	2.20	1.10	2.03
	24	3.10	3.70	1.30	2.70
	28	3.40	4.70	1.60	3.23
HEMA 99% NVI 1%	4	1.20	1.20	0.00	0.80
	7	1.90	1.20	0.60	1.23
	10	2.50	1.90	0.60	1.67
	14	2.50	1.90	0.60	1.67
	17	2.50	1.90	0.60	1.67
	21	2.50	1.90	0.60	1.67
	24	4.90	1.90	1.20	2.67
	28	6.80	1.90	3.10	3.93
HEMA 98% NVI 2%	4	0.60	0.60	0.60	0.60
	7	0.60	0.60	0.60	0.60
	10	1.20	0.60	0.60	0.80
	14	1.90	1.20	0.60	1.23
	17	2.50	1.90	1.20	1.87
	21	3.10	3.10	1.90	2.70
	24	3.10	3.70	1.90	2.90
	28	3.10	4.30	2.50	3.30
HEMA 97% NVI 3%	4	1.20	0.00	0.60	0.60
	7	1.20	1.20	0.60	1.00
	10	1.90	1.20	0.60	1.23
	14	3.10	1.20	0.60	1.63
	17	3.10	1.90	1.20	2.07
	21	3.70	1.90	1.20	2.27
	24	3.70	1.90	1.20	2.27
	28	6.20	2.50	1.20	3.30
HEMA 96% NVI 4%	4	0.60	1.20	0.60	0.80
	7	1.90	1.20	0.60	1.23
	10	1.90	1.90	0.60	1.47
	14	1.90	1.90	1.20	1.67
	17	2.50	1.90	1.20	1.87
	21	3.10	1.90	1.20	2.07
	24	3.10	1.90	1.20	2.07
	28	3.70	3.10	1.20	2.67

Copolymer Hydrogel Composition	Time (Days)	Lipid 360nm (%) (transmission)	Protein 280nm (%) (transmission)	Lipid 280nm (%) (transmission)	Spoilation Factor (%)
HEMA 95% NVI 5%	4	1.20	0.60	0.60	0.80
	7	1.20	1.20	0.60	1.00
	10	1.90	1.20	0.60	1.23
	14	1.90	1.20	1.20	1.43
	17	2.50	1.90	1.20	1.87
	21	3.10	1.90	1.20	2.07
	24	3.70	2.50	1.90	2.70
	28	3.70	3.70	1.90	3.10
polyHEMA	4	1.30	0.30	0.00	0.53
	7	1.90	0.90	0.30	1.03
	10	2.20	1.30	0.30	1.27
	14	2.50	1.60	0.60	1.57
	17	2.50	1.60	0.60	1.57
	21	2.80	2.20	1.10	2.03
	24	3.10	3.70	1.30	2.70
	28	3.40	4.70	1.60	3.23
HEMA 99% DMAEMA 1%	4	1.20	0.00	0.00	0.40
	7	1.20	0.60	0.60	0.80
	10	1.20	1.90	0.60	1.23
	14	1.90	1.90	1.20	1.67
	17	2.50	2.90	1.20	2.20
	21	2.50	3.70	1.20	2.47
	24	2.50	3.70	1.90	2.70
	28	2.50	3.70	1.90	2.70
HEMA 98% DMAEMA 2%	4	0.60	0.60	0.00	0.40
	7	0.60	0.60	0.60	0.60
	10	0.60	0.60	0.60	0.60
	14	1.20	0.60	0.60	0.80
	17	1.90	0.60	0.60	1.03
	21	2.50	1.20	0.60	1.43
	24	3.10	1.20	0.60	1.63
	28	3.70	3.10	1.20	2.67
HEMA 97% DMAEMA 3%	4	1.20	0.00	0.00	0.40
	7	1.90	0.60	0.60	1.03
	10	1.90	0.60	0.60	1.03
	14	2.50	0.60	0.60	1.23
	17	3.10	1.20	0.60	1.63
	21	3.10	1.20	0.60	1.63
	24	3.70	1.20	0.60	1.83
	28	3.70	1.20	1.20	2.03

Copolymer Hydrogel Composition	Time (Days)	Lipid 360nm (%) (transmission)	Protein 280nm (%) (transmission)	Lipid 280nm (%) (transmission)	Spoilation Factor (%)
HEMA 96%	4	0.60	0.00	0.00	0.20
DMAEMA 4%	7	0.60	0.60	0.00	0.40
	10	1.20	0.60	0.60	0.80
	14	1.90	0.60	0.60	1.03
	17	1.90	1.20	0.60	1.23
	21	2.50	1.90	0.60	1.67
	24	2.50	1.90	2.50	2.30
	28	3.70	1.90	3.10	2.90
HEMA 95%	4	1.20	0.00	0.00	0.40
DMAEMA 5%	7	1.20	0.60	0.60	0.80
	10	1.20	0.60	0.60	0.80
	14	1.90	0.60	1.20	1.23
	17	1.90	1.90	1.20	1.67
	21	2.50	1.90	1.90	2.10
	24	3.10	1.90	1.90	2.30
	28	3.70	3.70	1.90	3.10
HEMA 94%	4	0.60	0.00	0.00	0.20
NVI 5%	7	1.20	0.60	0.60	0.80
MAA 1%	10	1.90	0.60	0.60	1.03
	14	1.90	1.20	0.60	1.23
	17	2.50	1.90	1.20	1.87
	21	2.50	1.90	1.20	1.87
	24	3.70	3.10	1.90	2.90
	28	9.90	4.90	1.90	5.57
HEMA 93%	4	1.90	0.00	0.60	0.83
NVI 5%	7	1.90	0.60	0.60	1.03
MAA 2%	10	3.10	1.20	0.60	1.63
	14	3.10	1.90	1.20	2.07
	17	3.10	1.90	1.20	2.07
	21	4.90	3.70	1.90	3.50
	24	6.20	4.30	1.90	4.13
	28	6.20	5.60	1.90	4.57
HEMA 92%	4	1.20	0.00	0.00	0.40
NVI 5%	7	1.20	0.60	0.60	0.80
MAA 3%	10	1.90	1.20	1.20	1.43
	14	2.50	1.20	1.20	1.63
	17	3.10	1.90	1.20	2.07
	21	3.10	2.50	1.90	2.50
	24	5.60	3.70	3.10	4.13
	28	6.80	5.60	3.10	5.17

Copolymer Hydrogel Composition	Time (Days)	Lipid 360nm (%) (transmission)	Protein 280nm (%) (transmission)	Lipid 280nm (%) (transmission)	Spoilation Factor (%)
HEMA 91%	4	0.60	0.60	0.60	0.60
NVI 5%	7	1.20	0.60	0.60	0.80
MAA 4%	10	1.90	1.20	1.20	1.43
	14	4.90	1.90	1.20	2.67
	17	6.20	3.70	1.20	3.70
	21	5.20	4.30	1.90	3.80
	24	6.20	4.90	1.90	4.33
	28	6.20	5.60	2.50	4.77
HEMA 90%	4	0.60	0.60	0.60	0.60
NVI 5%	7	0.60	0.60	0.60	0.60
MAA 5%	10	1.20	1.20	0.60	1.00
	14	1.90	1.20	1.20	1.43
	17	3.70	3.10	1.20	2.67
	21	4.30	3.70	1.90	3.30
	24	4.90	4.30	1.90	3.70
	28	5.60	6.20	2.50	4.77
HEMA 91%	4	0.60	0.60	0.60	0.60
NVI 4%	7	0.60	1.20	0.60	0.80
MAA 5%	10	2.50	1.20	0.60	1.43
	14	3.10	1.90	1.20	2.07
	17	3.70	2.50	1.20	2.47
	21	6.20	4.30	1.90	4.13
	24	6.20	4.90	2.50	4.53
	28	8.00	5.60	3.10	5.57
HEMA 92%	4	0.60	0.60	0.60	0.60
NVI 3%	7	0.60	0.60	0.60	0.60
MAA 5%	10	1.20	1.20	1.20	1.20
	14	2.50	2.50	1.20	2.07
	17	4.90	2.50	1.90	3.10
	21	4.90	2.50	2.50	3.30
	24	6.20	3.10	2.50	3.93
	28	6.80	3.70	2.50	4.33
HEMA 93%	4	0.60	0.60	0.60	0.60
NVI 2%	7	1.20	0.60	0.60	0.80
MAA 5%	10	1.90	1.20	1.20	1.43
	14	1.90	1.90	1.20	1.67
	17	3.10	1.90	1.20	2.07
	21	3.70	2.50	1.90	2.70
	24	6.20	3.10	1.90	3.73
	28	6.20	3.70	2.50	4.13

Copolymer Hydrogel Composition	Time (Days)	Lipid 360nm (%) (transmission)	Protein 280nm (%) (transmission)	Lipid 280nm (%) (transmission)	Spoilation Factor (%)
HEMA 94%	4	0.60	1.20	0.60	0.80
NVI 1%	7	1.20	1.20	0.60	1.00
MAA 5%	10	1.90	1.20	0.60	1.23
	14	3.10	1.90	0.60	1.87
	17	3.70	1.80	0.60	2.03
	21	4.30	2.50	1.20	2.67
	24	9.30	3.10	1.20	4.53
	28	9.30	3.70	1.20	4.73
NNDMA 80%	4	1.10	0.80	0.60	0.83
CHMA 20%	7	1.40	1.40	0.60	1.13
	10	1.60	1.70	0.80	1.37
	14	2.20	2.40	0.80	1.80
	17	2.80	2.80	1.20	2.27
	21	2.80	3.30	1.20	2.43
	24	4.10	4.90	1.40	3.47
	28	5.70	5.80	2.70	4.73
NNDMA 76%	4	0.90	1.20	0.60	0.90
CHMA 19%	7	1.20	2.20	0.60	1.33
NVI 5%	10	2.20	2.20	0.90	1.77
	14	3.10	2.20	1.60	2.30
	17	4.30	3.10	1.60	3.00
	21	4.30	3.10	1.60	3.00
	24	5.30	3.40	1.60	3.43
	28	5.90	4.30	1.60	3.93
NNDMA 72%	4	1.20	0.60	0.60	0.80
CHMA 18%	7	1.40	0.60	0.60	0.87
NVI 10%	10	1.90	1.30	0.90	1.37
	14	2.50	2.50	1.20	2.07
	17	3.10	2.70	1.20	2.33
	21	4.00	3.10	1.60	2.90
	24	4.50	3.40	1.60	3.17
	28	6.80	4.90	1.90	4.53
NNDMA 68%	4	1.60	1.20	0.60	1.13
CHMA 17%	7	2.50	1.20	0.60	1.43
NVI 15%	10	2.80	1.90	1.20	1.97
	14	3.10	2.80	1.20	2.37
	17	3.10	2.80	1.60	2.50
	21	4.60	3.10	2.50	3.40
	24	5.60	3.70	2.50	3.93
	28	6.20	3.70	2.50	4.13

Copolymer Hydrogel Composition	Time (Days)	Lipid 360nm (%) (transmission)	Protein 280nm (%) (transmission)	Lipid 280nm (%) (transmission)	Spoilation Factor (%)
NNDMA 64%	4	1.20	0.60	0.60	0.80
CHMA 16%	7	1.20	1.20	1.20	1.20
NVI 20%	10	1.60	2.50	1.60	1.90
	14	2.20	3.40	1.60	2.40
	17	2.50	3.70	1.60	2.60
	21	3.70	4.30	1.60	3.20
	24	4.00	4.70	2.50	3.73
	28	7.70	5.60	2.80	5.37
NNDMA 70%	4	1.90	1.50	1.20	1.53
CHMA 30%	7	1.90	1.90	1.20	1.67
	10	3.10	1.90	1.20	2.07
	14	3.70	3.70	1.20	2.87
	17	3.70	4.00	1.90	3.20
	21	4.00	4.90	1.90	3.60
	24	4.30	6.20	2.50	4.33
	28	8.60	6.20	2.50	5.77
NNDMA 66.5%	4	2.50	1.20	0.30	1.33
CHMA 28.5%	7	3.10	1.20	0.60	1.63
NVI 5%	10	3.70	2.50	1.20	2.47
	14	4.30	2.50	1.90	2.90
	17	6.20	2.50	2.50	3.73
	21	6.20	2.50	2.50	3.73
	24	6.20	3.10	4.30	4.53
	28	8.00	2.50	6.20	5.57
NNDMA 63%	4	3.10	0.30	0.30	1.23
CHMA 27%	7	3.10	1.20	0.30	1.53
NVI 10%	10	3.10	1.50	0.30	1.63
	14	3.70	1.80	0.30	1.93
	17	4.30	1.90	0.30	2.17
	21	6.20	1.90	0.60	2.90
	24	6.80	3.10	0.60	3.50
	28	8.00	3.70	1.90	4.53
NNDMA 59.5%	4	3.10	0.30	0.60	1.33
CHMA 25.5%	7	3.10	1.20	0.60	1.63
NVI 15%	10	3.70	1.20	0.60	1.83
	14	3.70	1.20	1.20	2.03
	17	4.30	1.20	1.20	2.23
	21	6.80	1.90	1.90	3.53
	24	6.80	3.10	1.90	3.93
	28	9.90	3.10	1.90	4.97

Copolymer Hydrogel Composition	Time (Days)	Lipid 360nm (%) (transmission)	Protein 280nm (%) (transmission)	Lipid 280nm (%) (transmission)	Spoilation Factor (%)
NNDMA 56% CHMA 24% NVI 20%	4	3.10	0.30	0.30	1.23
	7	3.10	0.30	0.60	1.33
	10	4.30	0.30	1.20	1.93
	14	4.30	0.30	1.20	1.93
	17	4.30	1.20	1.20	2.23
	21	4.90	2.50	1.90	3.10
	24	6.20	3.10	1.90	3.73
	28	9.90	4.90	1.90	5.57
NNDMA 80% CHMA 20%	4	1.10	0.80	0.60	0.83
	7	1.40	1.40	0.60	1.13
	10	1.60	1.70	0.80	1.37
	14	2.20	2.40	0.80	1.80
	17	2.80	2.80	1.20	2.27
	21	2.80	3.30	1.20	2.43
	24	4.10	4.90	1.40	3.47
	28	5.70	5.80	2.70	4.73
NNDMA 76% CHMA 19% DMAEMA 5%	4	0.60	0.60	0.60	0.60
	7	1.20	1.20	0.60	1.00
	10	1.20	1.20	1.20	1.20
	14	2.50	1.90	1.20	1.87
	17	2.50	1.90	1.20	1.87
	21	3.10	1.90	1.20	2.07
	24	3.70	3.70	1.90	3.10
	28	6.20	6.20	3.10	5.17
NNDMA 72% CHMA 18% DMAEMA 10%	4	0.60	0.60	0.60	0.60
	7	1.90	0.60	0.60	1.03
	10	1.90	0.60	0.60	1.03
	14	1.90	1.90	0.60	1.47
	17	1.90	1.90	1.20	1.67
	21	1.50	1.90	1.20	1.53
	24	3.10	2.50	1.20	2.27
	28	4.90	6.20	2.50	4.53
NNDMA 68% CHMA 17% DMAEMA 15%	4	0.60	0.60	0.60	0.60
	7	0.60	2.50	0.60	1.23
	10	0.60	2.50	0.60	1.23
	14	1.20	3.10	0.60	1.63
	17	2.50	3.10	0.60	2.07
	21	3.70	3.10	1.20	2.67
	24	4.30	4.30	1.20	3.27
	28	6.20	4.90	1.20	4.10

Copolymer Hydrogel Composition	Time (Days)	Lipid 360nm (%) (transmission)	Protein 280nm (%) (transmission)	Lipid 280nm (%) (transmission)	Spoilation Factor (%)
NNDMA 64% CHMA 16% DMAEMA 20%	4	0.60	0.60	0.60	0.60
	7	1.20	1.20	1.20	1.20
	10	1.20	1.20	1.20	1.20
	14	1.90	1.90	1.20	1.67
	17	2.50	1.90	1.20	1.87
	21	3.70	1.90	1.20	2.27
	24	3.70	1.90	1.20	2.27
	28	6.80	6.20	1.90	4.97
NNDMA 70% CHMA 30%	4	1.90	1.50	1.20	1.53
	7	1.90	1.90	1.20	1.67
	10	3.10	1.90	1.20	2.07
	14	3.70	3.70	1.20	2.87
	17	3.70	4.00	1.90	3.20
	21	4.00	4.90	1.90	3.60
	24	4.30	6.20	2.50	4.33
	28	8.60	6.20	2.50	5.77
NNDMA 66.5% CHMA 28.5% DMAEMA 5%	4	1.60	0.30	0.30	0.73
	7	2.20	0.60	0.30	1.03
	10	2.20	0.60	0.60	1.13
	14	2.90	1.20	0.60	1.57
	17	3.50	1.20	0.60	1.77
	21	4.10	1.20	1.20	2.17
	24	4.70	3.10	1.90	3.23
	28	7.20	5.90	2.90	5.33
NNDMA 63% CHMA 27% DMAEMA 10%	4	1.80	0.30	0.30	0.80
	7	2.90	0.60	0.60	1.37
	10	2.90	0.60	0.60	1.37
	14	3.10	1.20	1.20	1.83
	17	3.50	1.90	1.20	2.20
	21	4.50	1.90	1.20	2.53
	24	5.10	2.10	1.90	3.03
	28	6.80	4.50	2.50	4.60
NNDMA 59.5% CHMA 25.5% DMAEMA 15%	4	2.60	0.60	0.60	1.27
	7	2.60	0.60	0.60	1.27
	10	2.60	1.20	0.60	1.47
	14	3.20	1.90	0.60	1.90
	17	3.50	2.50	0.60	2.20
	21	4.10	2.50	0.60	2.40
	24	5.30	3.10	1.20	3.20
	28	8.20	4.30	1.20	4.57

Copolymer Hydrogel Composition	Time (Days)	Lipid 360nm (%) (transmission)	Protein 280nm (%) (transmission)	Lipid 280nm (%) (transmission)	Spoilation Factor (%)
NNDMA 56%	4	2.60	0.60	0.60	1.27
CHMA 24%	7	3.20	0.60	0.60	1.47
DMAEMA 20%	10	3.50	0.60	0.60	1.57
	14	3.50	1.20	1.20	1.97
	17	4.10	1.20	1.20	2.17
	21	4.50	1.90	1.20	2.53
	24	5.20	2.50	1.20	2.97
	28	8.00	4.20	1.90	4.70
AMO 80%	4	1.30	0.50	0.50	0.75
CHMA 20%	7	3.40	1.90	3.40	2.90
	10	4.30	2.20	3.70	3.40
	14	5.90	2.50	4.00	4.13
	17	6.20	3.10	4.00	4.43
	21	6.50	3.70	4.00	4.73
	24	7.80	3.70	4.00	5.17
	28	9.30	5.90	4.40	6.53
AMO 76%	4	1.20	0.30	0.30	0.60
CHMA 19%	7	1.90	0.30	0.60	0.93
NVI 5%	10	2.50	0.30	2.50	1.77
	14	3.10	0.60	2.50	2.07
	17	4.90	1.20	3.10	3.07
	21	5.60	3.10	4.30	4.33
	24	7.40	3.70	10.50	7.20
	28	9.30	4.90	10.50	8.23
AMO 72%	4	1.90	0.30	0.30	0.83
CHMA 18%	7	3.10	0.30	0.60	1.33
NVI 10%	10	3.10	0.30	1.20	1.53
	14	3.10	0.30	1.20	1.53
	17	4.30	1.20	1.20	2.23
	21	6.20	1.20	3.10	3.50
	24	6.80	1.20	6.20	4.73
	28	11.70	3.10	6.80	7.20
AMO 68%	4	0.30	0.30	0.30	0.30
CHMA 17%	7	1.20	0.30	0.30	0.60
NVI 15%	10	2.50	0.30	0.30	1.03
	14	3.10	0.30	0.30	1.23
	17	3.70	0.30	0.30	1.43
	21	4.30	1.20	0.60	2.03
	24	4.90	1.20	1.90	2.67
	28	4.90	1.20	4.30	3.47

Copolymer Hydrogel Composition	Time (Days)	Lipid 360nm (%) (transmission)	Protein 280nm (%) (transmission)	Lipid 280nm (%) (transmission)	Spoilation Factor (%)
AMO 64%	4	3.10	0.30	3.10	2.17
CHMA 16%	7	3.70	0.60	2.50	2.27
NVI 20%	10	4.90	2.50	2.50	3.30
	14	4.90	2.50	2.50	3.30
	17	5.60	2.50	4.30	4.13
	21	6.20	3.10	4.90	4.73
	24	9.30	3.70	4.90	5.97
	28	9.30	4.30	4.90	6.17
AMO 70%	4	0.30	0.30	0.60	0.40
CHMA 30%	7	0.60	0.30	0.60	0.50
	10	2.50	1.20	0.60	1.43
	14	2.50	2.50	0.60	1.87
	17	2.50	3.10	0.60	2.07
	21	2.50	3.70	0.60	2.27
	24	3.10	6.20	1.20	3.50
	28	5.60	7.40	1.90	4.97
AMO 66.5%	4	1.20	0.30	0.60	0.70
CHMA 28.5%	7	3.10	0.30	1.90	1.77
NVI 5%	10	3.70	0.30	3.10	2.37
	14	3.70	0.30	3.10	2.37
	17	3.70	0.30	4.30	2.77
	21	4.90	0.30	5.60	3.60
	24	4.90	1.20	6.20	4.10
	28	6.20	3.10	4.30	4.53
AMO 63%	4	2.50	0.60	1.90	1.67
CHMA 27%	7	3.10	1.20	1.90	2.07
NVI 10%	10	3.10	1.20	2.50	2.27
	14	4.30	1.90	3.10	3.10
	17	6.20	3.70	4.90	4.93
	21	6.20	3.10	4.90	4.73
	24	6.20	3.10	6.20	5.17
	28	11.10	3.10	6.80	7.00
AMO 59.5%	4	1.90	0.30	0.30	0.83
CHMA 25.5%	7	1.90	0.60	0.60	1.03
NVI 15%	10	3.10	1.90	1.90	2.30
	14	3.70	1.90	4.30	3.30
	17	4.20	1.90	4.90	3.67
	21	4.90	1.90	6.20	4.33
	24	6.80	1.90	6.20	4.97
	28	9.30	3.10	9.90	7.43

Copolymer Hydrogel Composition	Time (Days)	Lipid 360nm (%) (transmission)	Protein 280nm (%) (transmission)	Lipid 280nm (%) (transmission)	Spoilation Factor (%)
AMO 56% CHMA 24% NVI 20%	4	3.70	1.90	1.90	2.50
	7	3.70	2.50	4.30	3.50
	10	4.90	3.10	3.70	3.90
	14	4.90	3.10	4.90	4.30
	17	6.80	3.10	4.90	4.93
	21	7.40	3.10	6.20	5.57
	24	7.40	3.70	6.20	5.77
	28	9.30	3.70	12.30	8.43
AMO 80% CHMA 20%	4	1.30	0.50	0.50	0.75
	7	3.40	1.90	3.40	2.90
	10	4.30	2.20	3.70	3.40
	14	5.90	2.50	4.00	4.13
	17	6.20	3.10	4.00	4.43
	21	6.50	3.70	4.00	4.73
	24	7.80	3.70	4.00	5.17
	28	9.30	5.90	4.40	6.53
AMO 76% CHMA 19% DMAEMA 5%	4	0.60	0.60	0.60	0.60
	7	1.20	1.20	1.20	1.20
	10	1.20	1.20	1.20	1.20
	14	1.20	1.90	1.20	1.43
	17	1.20	2.50	1.20	1.63
	21	1.90	3.70	1.20	2.27
	24	2.50	6.20	1.90	3.53
	28	3.10	6.20	1.90	3.73
AMO 72% CHMA 18% DMAEMA 10%	4	0.60	0.60	0.60	0.60
	7	1.20	1.90	0.60	1.23
	10	1.20	1.90	0.60	1.23
	14	1.90	3.10	1.20	2.07
	17	1.90	3.10	1.90	2.30
	21	2.50	3.10	1.90	2.50
	24	3.10	3.70	1.90	2.90
	28	3.70	5.60	2.50	3.93
AMO 68% CHMA 17% DMAEMA 15%	4	0.60	0.60	0.60	0.60
	7	1.90	1.90	0.60	1.47
	10	1.90	1.90	0.60	1.47
	14	3.10	1.90	1.20	2.07
	17	3.10	2.50	1.20	2.27
	21	3.10	2.50	1.90	2.50
	24	3.70	4.30	1.90	3.30
	28	4.90	4.30	2.50	3.90

Copolymer Hydrogel Composition	Time (Days)	Lipid 360nm (%) (transmission)	Protein 280nm (%) (transmission)	Lipid 280nm (%) (transmission)	Spoilation Factor (%)
AMO 64%	4	0.60	0.60	0.60	0.60
CHMA 16%	7	1.20	1.20	0.60	1.00
DMAEMA 20%	10	1.20	1.20	0.60	1.00
	14	1.90	1.90	1.20	1.67
	17	1.90	1.90	1.20	1.67
	21	2.50	1.90	1.90	2.10
	24	3.10	3.10	1.90	2.70
	28	6.20	6.70	2.50	5.13
AMO 70%	4	0.30	0.30	0.60	0.40
CHMA 30%	7	0.60	0.30	0.60	0.50
	10	2.50	1.20	0.60	1.43
	14	2.50	2.50	0.60	1.87
	17	2.50	3.10	0.60	2.07
	21	2.50	3.70	0.60	2.27
	24	3.10	6.20	1.20	3.50
	28	5.60	7.40	1.90	4.97
AMO 66.5%	4	2.60	0.30	0.60	1.17
CHMA 28.5%	7	3.50	0.60	0.60	1.57
DMAEMA 5%	10	3.70	0.60	1.20	1.83
	14	3.90	1.20	1.90	2.33
	17	4.10	1.20	2.50	2.60
	21	4.90	1.90	2.50	3.10
	24	4.90	3.10	3.10	3.70
	28	8.30	4.30	4.10	5.57
AMO 63%	4	2.60	0.60	0.60	1.27
CHMA 27%	7	3.50	0.60	0.60	1.57
DMAEMA 10%	10	3.90	0.60	1.20	1.90
	14	3.90	1.20	1.20	2.10
	17	4.50	1.90	1.90	2.77
	21	4.90	3.50	1.90	3.43
	24	6.30	4.30	1.90	4.17
	28	9.90	5.60	2.50	6.00
AMO 59.5%	4	2.50	0.60	0.60	1.23
CHMA 25.5%	7	2.50	0.60	0.60	1.23
DMAEMA 15%	10	2.60	1.20	0.60	1.47
	14	3.50	1.90	0.60	2.00
	17	3.50	2.50	1.20	2.40
	21	4.90	4.30	1.20	3.47
	24	6.20	4.90	1.90	4.33
	28	8.60	5.20	2.60	5.47

Copolymer Hydrogel Composition	Time (Days)	Lipid 360nm (%) (transmission)	Protein 280nm (%) (transmission)	Lipid 280nm (%) (transmission)	Spoilation Factor (%)
AMO 56%	4	1.90	0.60	0.60	1.03
CHMA 24%	7	3.10	0.60	0.60	1.43
DMAEMA 20%	10	3.10	1.20	0.60	1.63
	14	3.10	1.90	1.20	2.07
	17	3.70	2.50	1.20	2.47
	21	4.90	2.50	1.20	2.87
	24	7.20	4.30	1.90	4.47
	28	9.90	4.60	2.50	5.67
HEMA 90%	4	1.20	1.20	0.30	0.90
NVP 10%	7	1.90	1.90	0.60	1.47
	10	1.90	3.10	0.60	1.87
	14	1.90	3.10	0.60	1.87
	17	2.20	3.70	1.20	2.37
	21	2.50	4.30	1.20	2.67
	24	2.50	8.60	1.20	4.10
	28	3.10	12.30	1.90	5.77
HEMA 80%	4	0.30	1.90	0.60	0.93
NVP 20%	7	1.20	2.50	1.90	1.87
	10	1.20	2.50	1.90	1.87
	14	1.20	3.10	1.90	2.07
	17	1.20	4.90	1.90	2.67
	21	1.90	4.90	1.90	2.90
	24	2.20	5.60	2.00	3.27
	28	3.10	8.00	2.50	4.53
HEMA 70%	4	0.30	2.50	0.60	1.13
NVP 30%	7	0.60	2.50	0.60	1.23
	10	0.60	3.10	0.60	1.43
	14	0.60	3.70	0.60	1.63
	17	2.50	4.30	1.20	2.67
	21	2.50	4.90	2.50	3.30
	24	3.10	12.90	3.10	6.37
	28	3.70	12.90	7.40	8.00
HEMA 60%	4	0.60	1.20	0.30	0.70
NVP 40%	7	0.60	2.50	0.60	1.23
	10	0.60	3.10	0.60	1.43
	14	0.60	3.10	0.60	1.43
	17	BROKE			
	21				
	24				
	28				

Copolymer Hydrogel Composition	Time (Days)	Lipid 360nm (%) (transmission)	Protein 280nm (%) (transmission)	Lipid 280nm (%) (transmission)	Spoilation Factor (%)
HEMA 50% NVP 50%	4 7 10 14 17 21 24 28	0.30 0.30 0.60 0.60 1.90 2.20 BROKE	1.20 1.90 2.80 3.10 4.90 5.60	0.60 0.60 0.90 0.90 0.90 0.90	0.70 0.93 1.43 1.53 2.57 2.90
HEMA 90% NNDMA 10%	4 7 10 14 17 21 24 28	0.60 1.20 1.90 1.90 2.20 2.50 2.80 5.60	0.60 2.20 3.10 4.30 6.20 6.80 6.80 11.40	0.60 0.60 1.20 1.50 1.50 1.90 1.90 2.20	0.60 1.33 2.07 2.57 3.30 3.73 3.83 6.40
HEMA 80% NNDMA 20%	4 7 10 14 17 21 24 28	0.60 0.60 1.20 1.20 1.90 1.90 2.50 4.30	1.20 2.50 3.70 3.70 4.90 7.40 12.30 13.60	0.60 0.60 0.90 0.90 1.20 1.50 2.50 2.50	0.80 1.23 1.93 1.93 2.67 3.60 5.77 6.80
HEMA 70% NNDMA 30%	4 7 10 14 17 21 24 28	0.30 0.60 1.20 1.90 1.90 1.90 2.50 3.40	1.90 2.50 3.10 3.70 3.70 6.80 8.60 9.60	0.30 0.60 0.90 1.20 1.20 1.90 1.90 2.50	0.83 1.23 1.73 2.27 2.27 3.53 4.33 5.17
HEMA 60% NNDMA 40%	4 7 10 14 17 21 24 28	0.30 0.60 1.90 2.50 3.70 4.90 BROKE	1.20 1.90 2.50 4.90 5.60 8.60	0.30 0.60 0.60 1.20 1.20 1.50	0.60 1.03 1.67 2.87 3.50 5.00

Copolymer Hydrogel Composition	Time (Days)	Lipid 360nm (%) (transmission)	Protein 280nm (%) (transmission)	Lipid 280nm (%) (transmission)	Spoilation Factor (%)
HEMA 50% NNDMA 50%	4 7 10 14 17 21 24 28	0.30 0.60 0.60 BROKE	1.90 2.50 2.50	0.60 0.60 0.60	0.93 1.23 1.23
HEMA 90% AMO 10%	4 7 10 14 17 21 24 28	0.30 0.60 0.60 1.20 1.90 1.90 2.50 3.10	1.20 1.20 1.90 1.90 1.90 2.50 3.10 6.20	0.30 0.60 0.60 0.90 1.20 1.20 1.20 1.20	0.60 0.80 1.03 1.33 1.67 1.87 2.27 3.50
HEMA 80% AMO 20%	4 7 10 14 17 21 24 28	0.30 0.60 0.60 0.60 0.90 2.50 2.50 3.40	0.30 0.60 0.60 1.90 2.50 2.50 3.40 4.90	0.30 0.60 0.60 0.90 0.90 0.90 1.20 1.50	0.30 0.60 0.60 1.13 1.43 1.97 2.37 3.27
HEMA 70% AMO 30%	4 7 10 14 17 21 24 28	0.30 0.60 0.60 0.90 0.90 1.20 1.90 2.50	0.60 0.90 0.90 1.90 1.90 2.50 3.10 5.20	0.60 0.60 0.60 0.60 0.60 0.60 0.60 0.60	0.50 0.70 0.70 1.13 1.13 1.43 1.87 2.77
HEMA 60% AMO 40%	4 7 10 14 17 21 24 28	0.30 0.60 0.60 0.90 1.20 1.90 1.90 BROKE	0.60 0.90 0.90 1.20 4.30 4.90 5.60	0.30 0.60 0.60 0.60 1.20 1.20 1.50	0.40 0.70 0.70 0.90 2.23 2.67 3.00

Copolymer Hydrogel Composition	Time (Days)	Lipid 360nm (%) (transmission)	Protein 280nm (%) (transmission)	Lipid 280nm (%) (transmission)	Spoilation Factor (%)
HEMA 50%	4	0.30	0.90	0.30	0.50
AMO 50%	7	0.30	0.90	0.60	0.60
	10	0.60	1.20	0.60	0.80
	14	0.60	2.20	0.60	1.13
	17	0.90	2.50	0.60	1.33
	21	1.50	3.10	0.60	1.73
	24	BROKE			
	28				

APPENDIX 6

FTIR and NMR Spectra

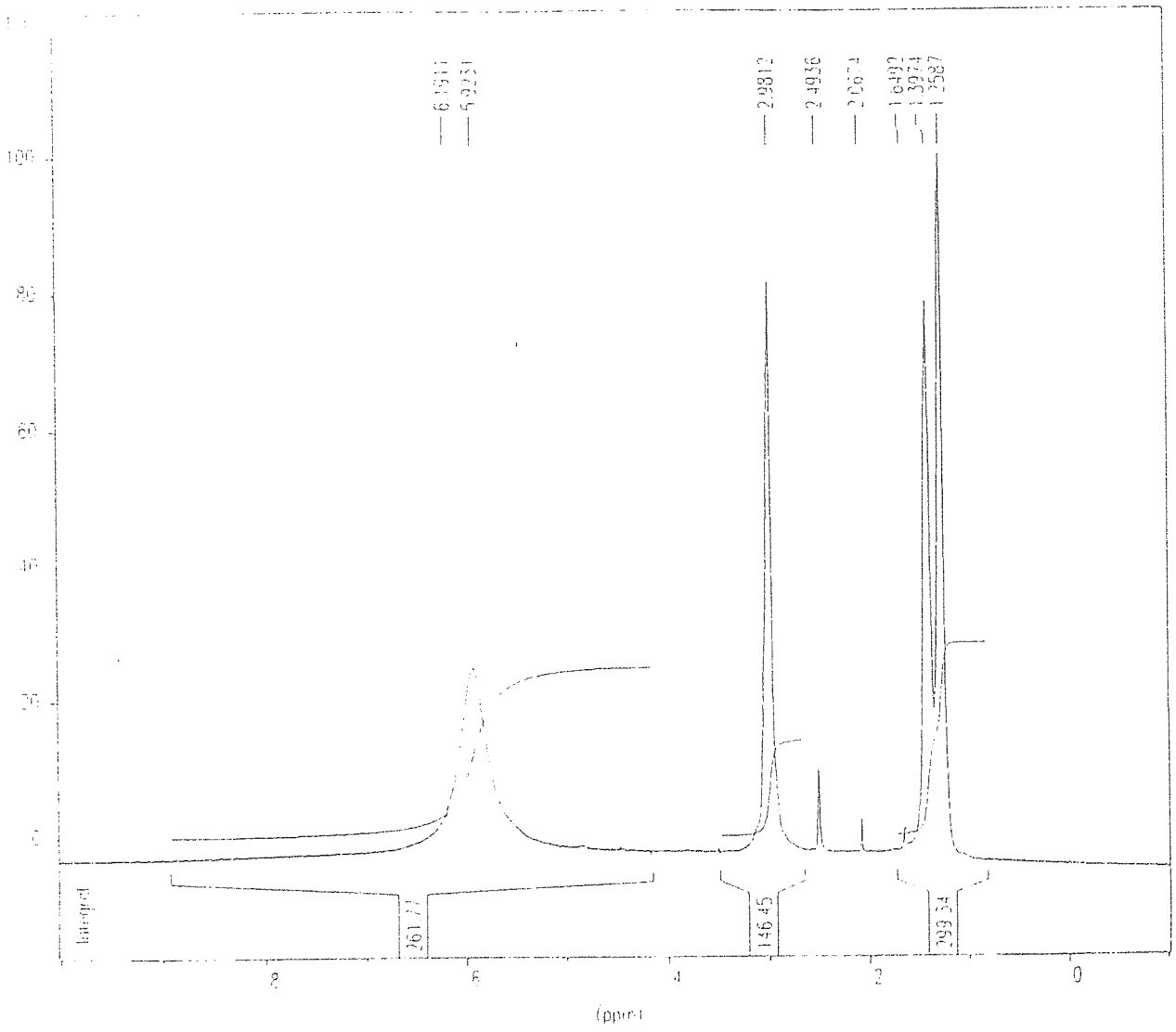

1) ^{1}H NMR Spectrum of vantocil IB

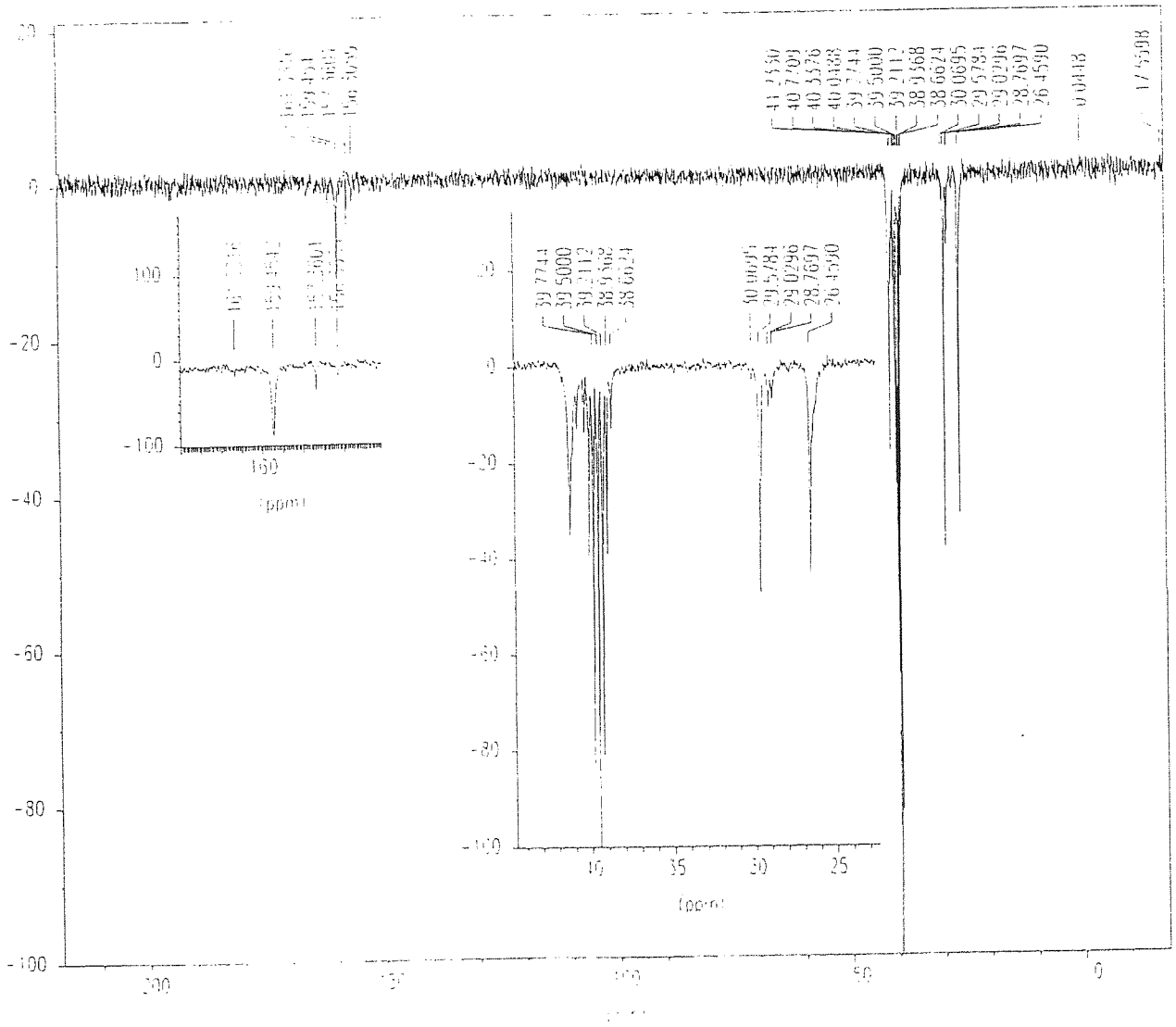

2) ^{13}C NMR Spectrum of vantocil IB

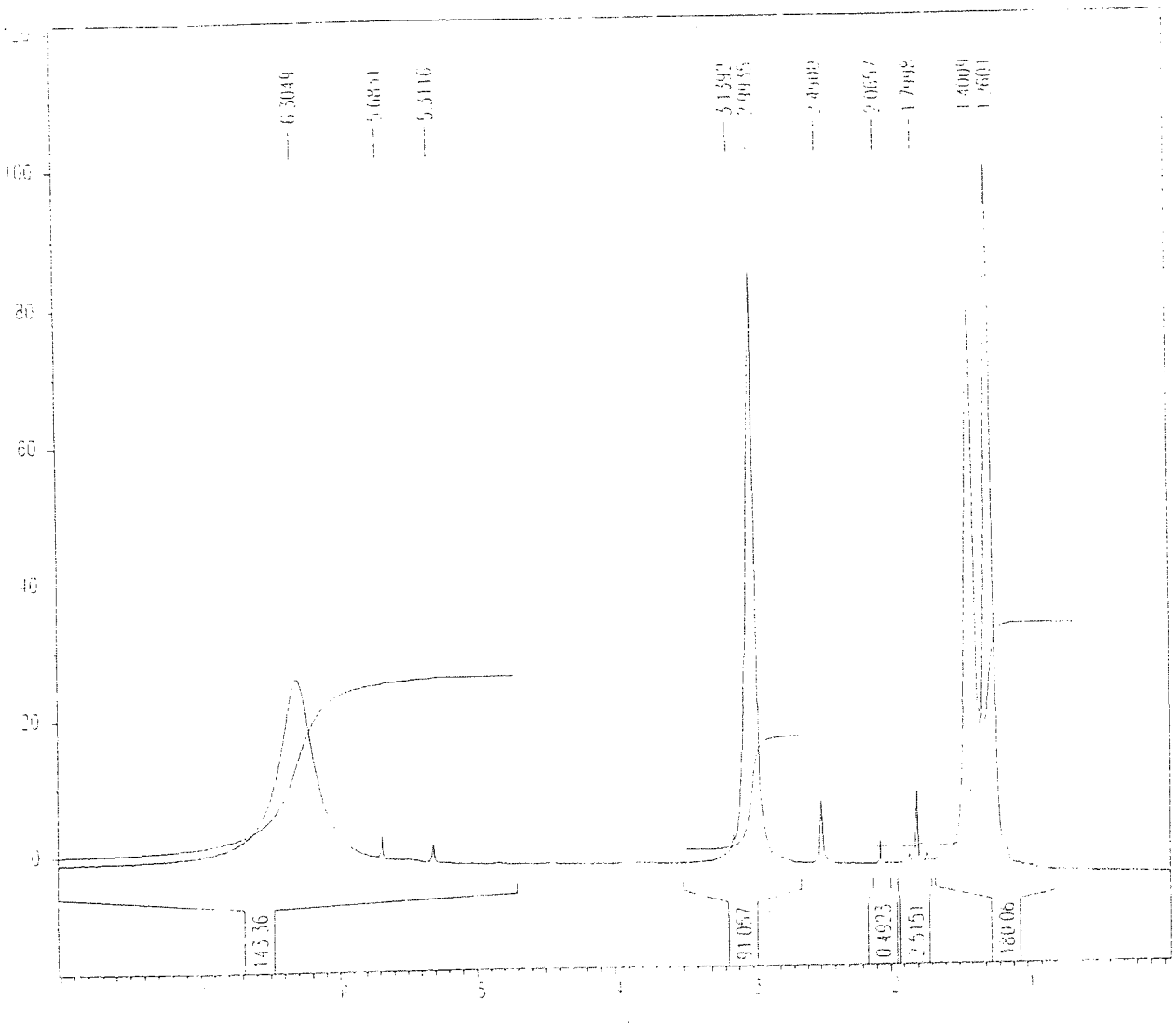

3) ^{1}H NMR Spectrum of the reaction product of vantocil IB and methacryoyl isocyanate

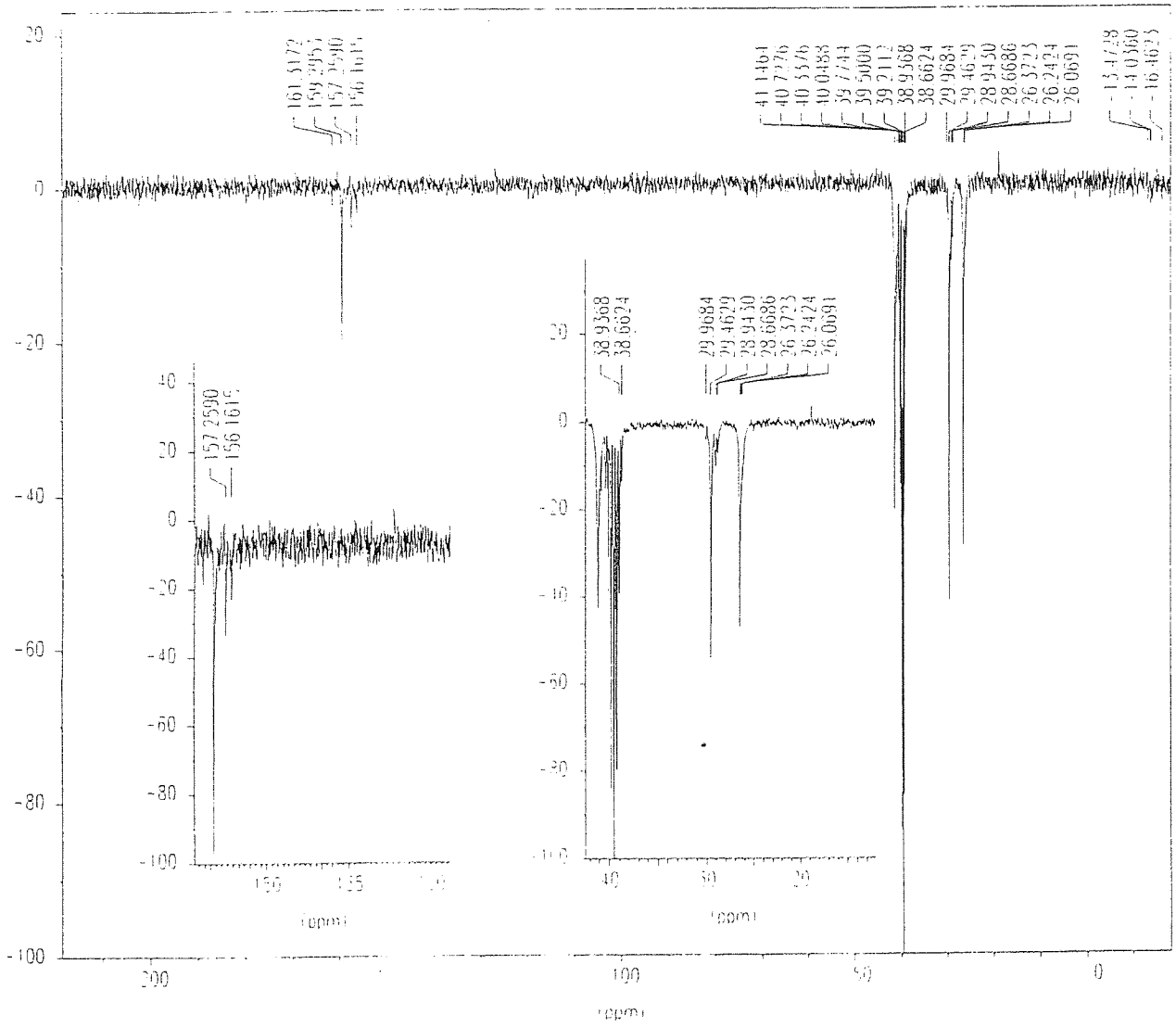

4) ^{13}C NMR Spectrum of the reaction product of vantocil IB and methacryoyl isocyanate

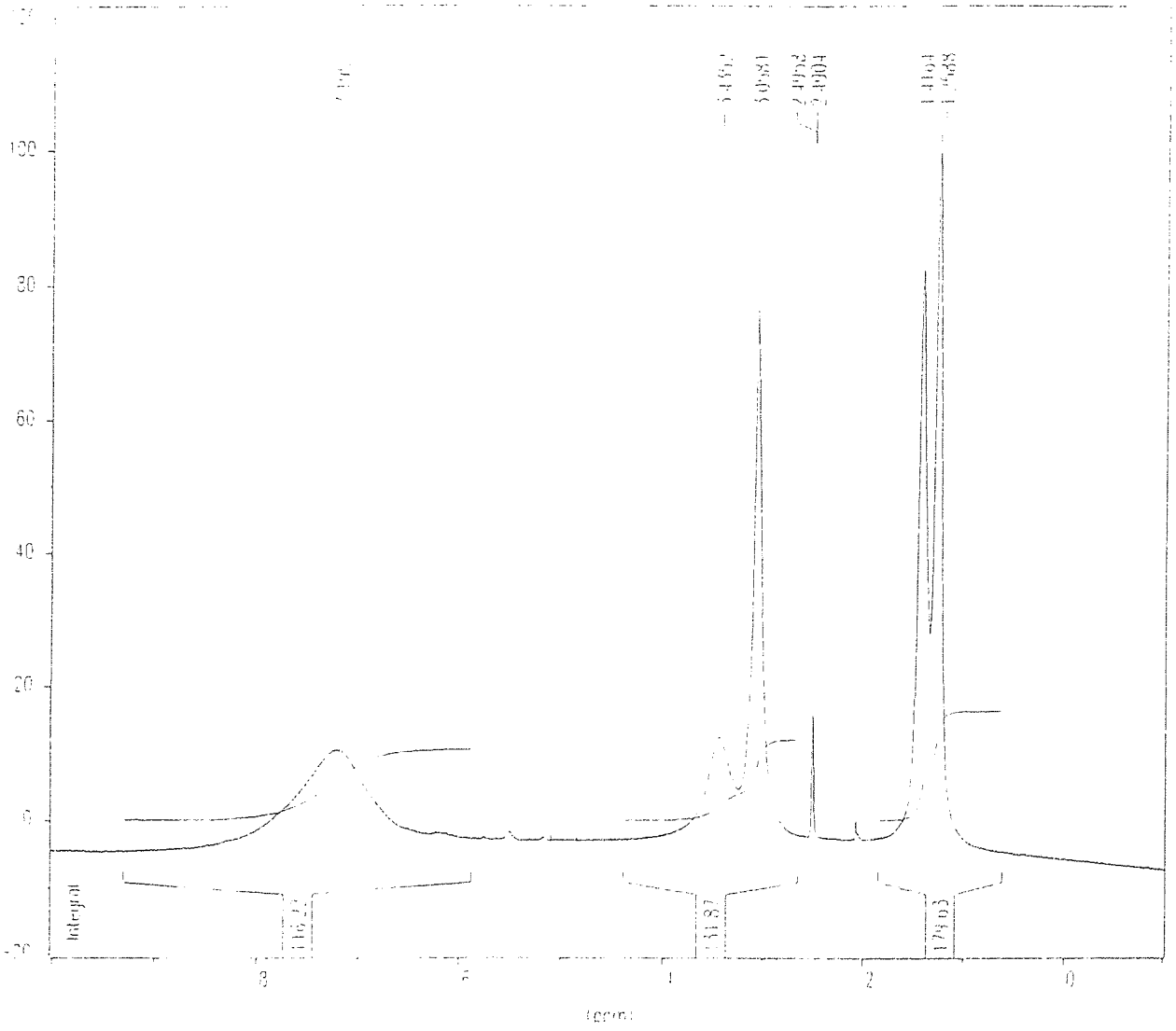

5) ^{1}H NMR Spectrum of the reaction product of vantocil IB and itaconyl chloride

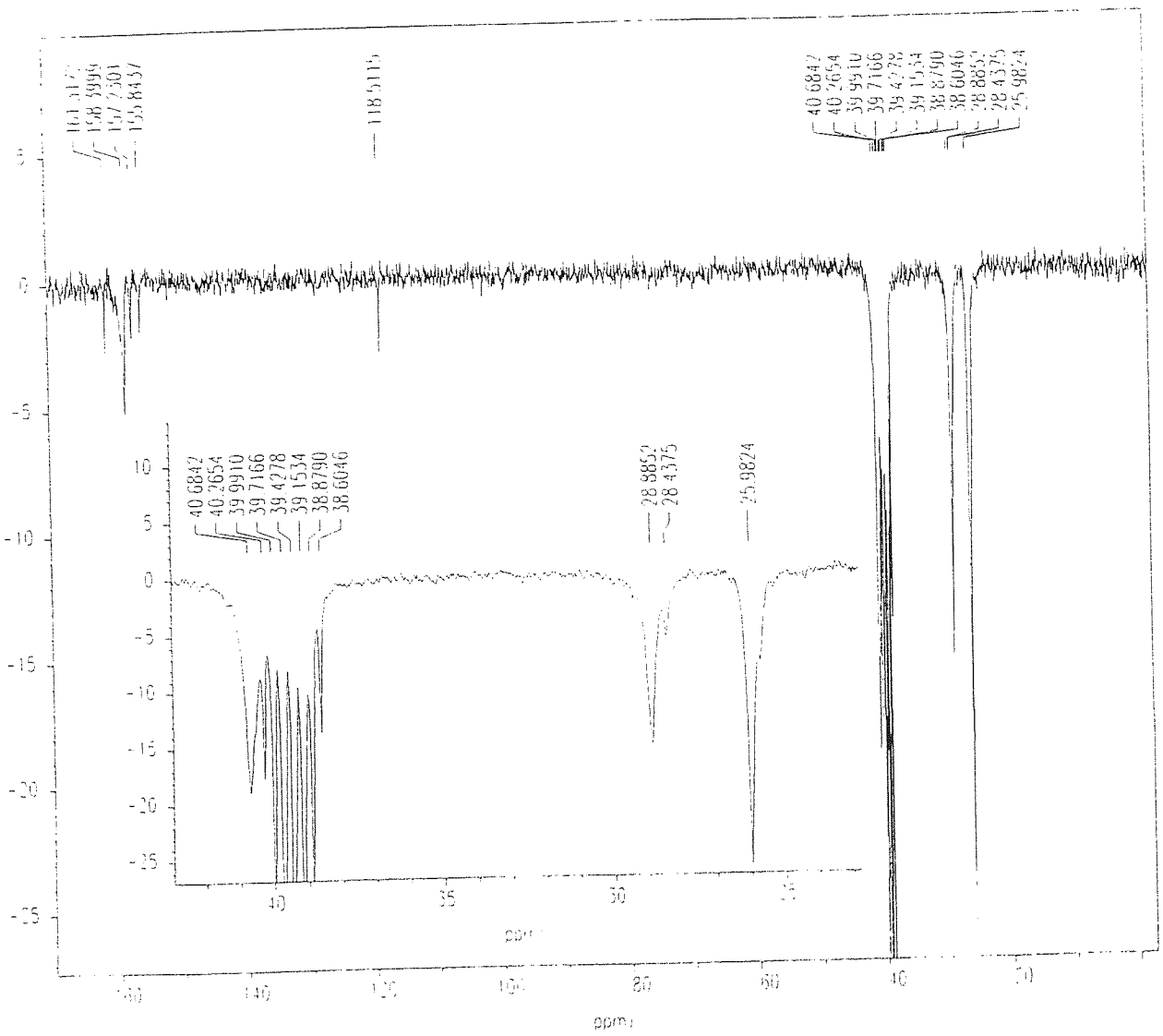

6) ^{13}C NMR Spectrum of the reaction product of vantocil IB and itaconyl chloride

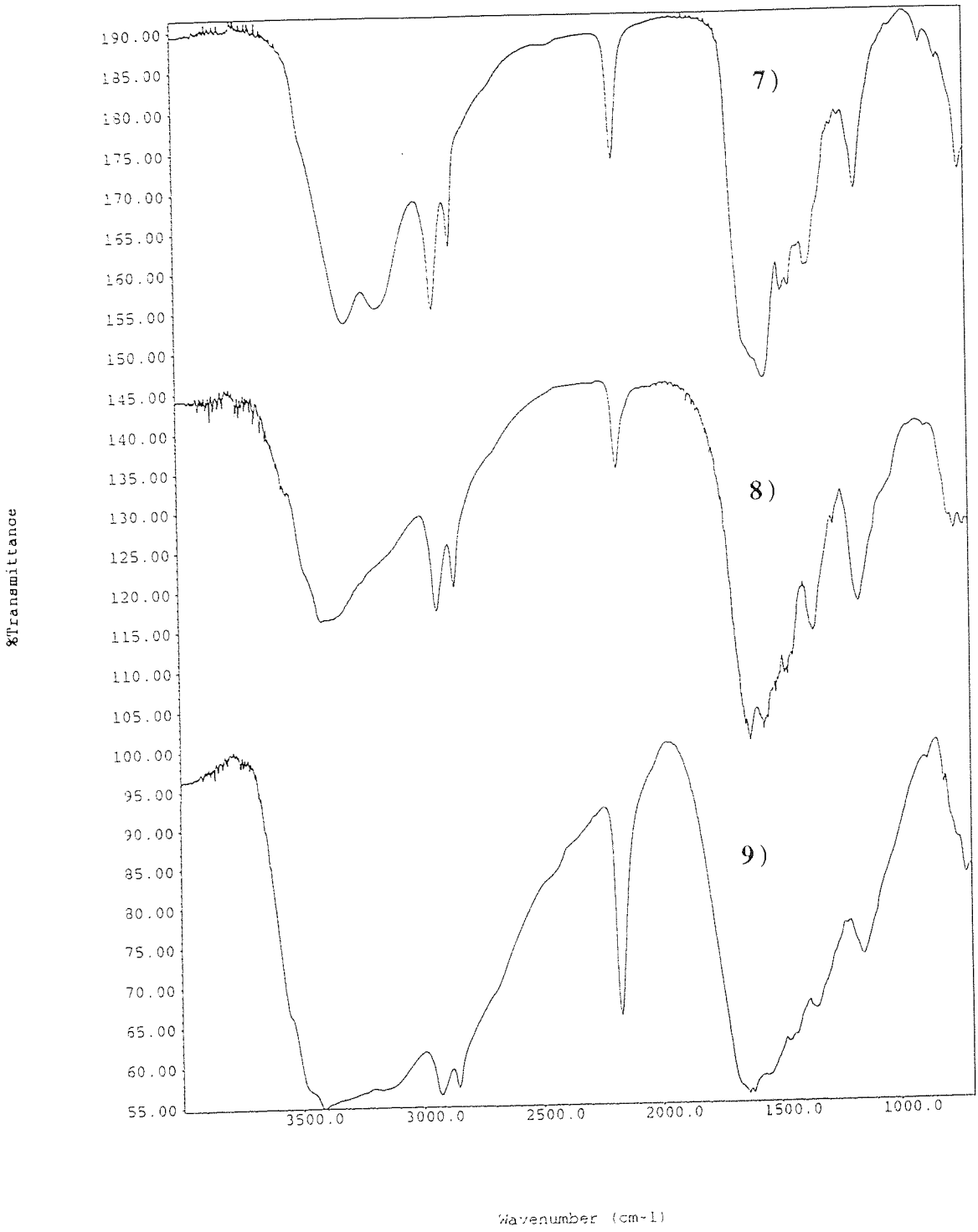

7) FT-IR Spectrum of vantocil IB

8) FT-IR Spectrum of the reaction product of vantocil IB and methacryloyl isocyanate

9) FT-IR Spectrum of the reaction product of vantocil IB and itaconyl chloride

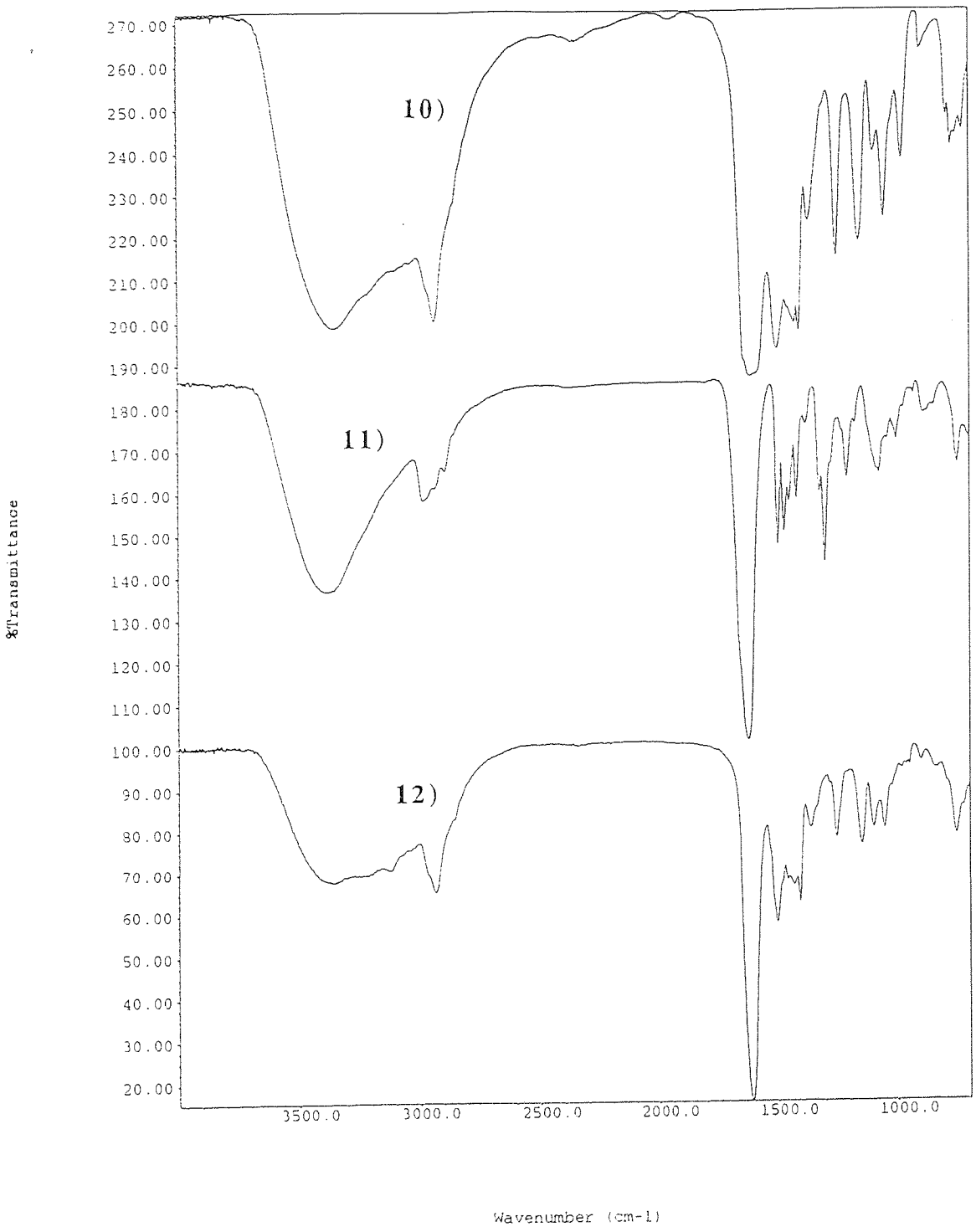

10) FT-IR spectrum of the reaction product of 50%(w/w) indene and 50%(w/w) NNDMA

11) FT-IR spectrum of the reaction product of 50%(w/w) indene and 50%(w/w) NVP

12) FT-IR spectrum of the reaction product of 45%(w/w) indene, 45%(w/w) NNDMA and 10%(w/w) NVI

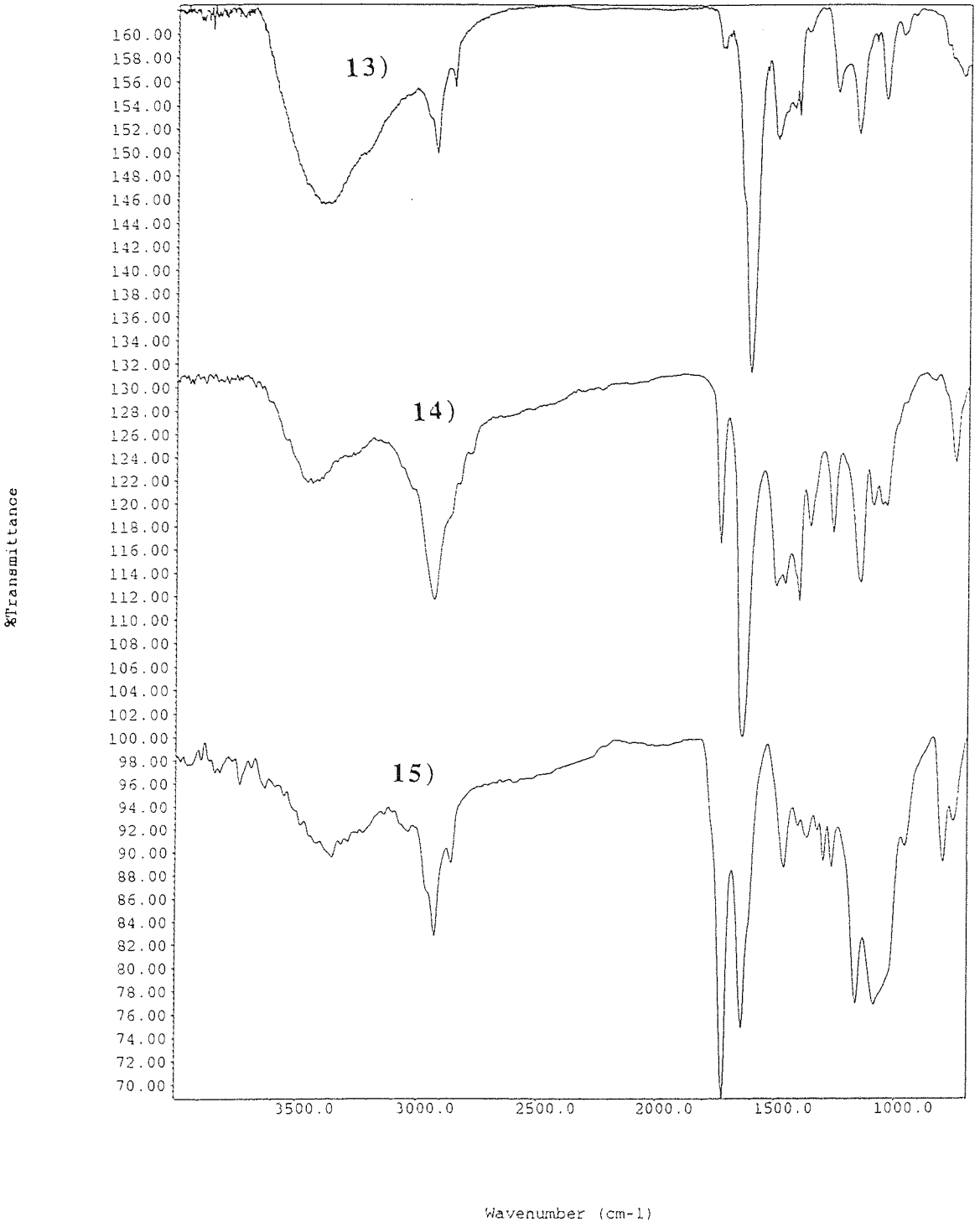

13) FT-IR spectrum of the reaction product of 45%(w/w) indene, 45%(w/w) NNDMA and 10%(w/w) SPE

14) FT-IR spectrum of the reaction product of 26%(w/w) CHMA, 45%(w/w) NNDMA and 28%(w/w) DMAEMA

15) FT-IR spectrum of the reaction product of 45%(w/w) indene, 45%(w/w) NNDMA and 10%(w/w) DMAEMA